VOLUME 86 NO. HY9
NOVEMBER 1960
PART 1

JOURNAL of the

Hydraulics Division

PROCEEDINGS OF THE
AMERICAN SOCIETY
OF CIVIL ENGINEERS

BASIC REQUIREMENTS FOR MANUSCRIPTS

Original papers and discussions of current papers should be submitted to the Manager of Technical Publications, ASCE. Authors should indicate the technical division to which the paper is referred. The final date on which a discussion should reach the Society is given as a footnote with each paper. Those who are planning to submit material will expedite the review and publication procedures by complying with the following basic requirements:

1. Titles must have a length not exceeding 50 characters and spaces.

2. A 50-word summary must accompany the paper, a 300-word synopsis must precede it, and a conclusion must end it.

3. The manuscript (an original and two duplicate copies) should be double-spaced on one side of 8½-inch by 11-inch paper. Three copies of all illustrations, tables, etc., must be included.

4. The author's full name, Society membership grade, and footnote reference stating present employment must appear on the first page of the paper.

5. Mathematics are recomposed from the copy that is submitted. Because of this, it is necessary that letters be drawn carefully, and that special symbols be properly identified.

6. Tables should be typed (an original and two duplicate copies) on one side of 8½-inch by 11-inch paper. Specific illustrations and explanation must be made in the text for each table.

7. Illustrations must be drawn in black ink on one side of 8½-inch by 11-inch paper. Because illustrations will be reproduced with a width of between 3 inches and 4½ inches, the lettering must be large enough to be legible at this width. Photographs should be submitted as glossy prints. Explanations and descriptions must be made within the text for each illustration.

8. Papers should average about 12,000 words in length and must be no longer than 18,000 words. As an approximation, each full page of typed text, tables, or illustrations is the equivalent of 300 words.

9. Technical papers intended for publication must be written in the third person.

10. If letter symbols are used in the paper they should be defined where they first appear, in the illustrations or in the text, and arranged alphabetically in an appendix.

This Journal is published monthly by the American Society of Civil Engineers. Publication office is at 2500 South State Street, Ann Arbor, Michigan. Editorial and General Offices are at 33 West 39 Street, New York 18, New York. [illegible] of a member's dues are applied as a subscription to this Journal. Second-class postage paid at Ann Arbor, Michigan.

The index for [illegible] was published as ASCE Publication 1960-10 (list price $2.00); indexes for previous years are also available.

Journal of the

HYDRAULICS DIVISION

Proceedings of the American Society of Civil Engineers

CONTENTS

November, 1960

Papers

(over)

Note.—Part 2 of this Journal is the 39, 1960 Newsletter of the Hydraulics Division.

DISCUSSION

(over)

Journal of the
HYDRAULICS DIVISION
Proceedings of the American Society of Civil Engineers

FLOOD-FREQUENCY RELATIONSHIPS IN THE PACIFIC NORTHWEST

By George L. Bodhaine,[1] M. ASCE

SYNOPSIS

This paper describes, in general terms, a method of determining the magnitude and frequency of expected floods that is applicable to any area in the Pacific Northwest of the United States. The development of a composite frequency curve applicable to any site in a large homogeneous region is examined, and the effect of mean elevation and size of drainage area on the shape of the frequency curves in designated parts of the Pacific Northwest is demonstrated. A formula for determining the mean annual flood for any site on the west side of the Cascade Range in Washington is shown, and the drainage-basin characteristics used in its derivation are listed. A flood-frequency curve can be drawn for any given site in the Pacific Northwest by combining the results obtained from the mean annual flood formula and the composite frequency curve that are both applicable to that site. Comments about limitations on the use of results obtained by this method are included.

INTRODUCTION

The purpose of this paper is to present a method of correlating streamflow data and basin characteristics to obtain information relative to the magnitude and frequency of flood discharges in the Pacific Northwest. The method reflects the latest developments based on a continuing study of the subject by engineers of the United States Geological Survey, Dept. of the

Note.—Discussion open until April 1, 1961. To extend the closing date one month, a written request must be filed with the Executive Secretary, ASCE. This paper is part of the copyrighted Journal of the Hydraulics Division, Proceedings of the American Society of Civil Engineers, Vol. 86, No. HY 9, November, 1960.

[1] Flood Specialist, U. S. Geological Survey, Tacoma, Washington.

Interior (USGS). It is expected that the method will be revised from time to time as new ideas are conceived and tested.

The discharge records collected by the USGS and others are the data on which flood-frequency studies are based. The records from about 800 gaging stations in the Pacific Northwest were of sufficient length to furnish data for deriving the flood-frequency curves. A curve based on a gaging-station record, however, applies only to that one particular site, whereas, generally, the information is desired at an ungaged point, frequently on an ungaged stream. The two parts to the problem are (1) computation of flood frequency at a point, and (2) adaption of the point data to apply over a basin or a region.

In general, the needs of most engineering studies are met by information concerning floods with average recurrence intervals of 10 yr, 25 yr, 50 yr and 100 yrs. For example, some states' Highway Departments design their primary highway drainage structures to withstand floods that are expected to occur, on the average, once in 50 yrs whereas their secondary highway structures are designed to withstand floods that are expected to occur, on the average, once in 25 yr.

The Pacific Northwest is defined as the Columbia River basin and the western slope of the Cascade Range in Washington and Oregon. This area is designated as Parts 12, 13, and 14 by the USGS.

FLOOD FREQUENCY AT A GAGING STATION

The first step in a flood compilation is to select the gaging stations to be included. There should be at least 10 yr of record at each station, although records as short as 5 yr are used when no others are available. Adjustments should be made for storage, or other artificial factors, that, tend to modify flood discharges significantly, or the record should not be used.

Flood Series.—There are two kinds of flood series to be considered in plotting frequency curves, the annual-flood series and the partial-duration series. The two methods give essentially the same results for recurrence intervals greater than 10 yr. A relationship between the two series has been derived by Langbein[2], of the USGS, so that, when necessary, the annual-flood curve can be converted to the partial-duration series. For example, a flood having a recurrence interval of 2.0 yr in the annual-flood series would have a recurrence interval of 1.45 yr in the partial-duration series. At a recurrence interval of 10.5 yr the comparative value would be 10.0 yr and at 50.5 yr, 50.0 yr. The annual-flood method is used in these studies because of its simplicity.

Plotting Procedure.—Recurrence intervals are computed from the formula

$$T = (N + 1)/M \qquad (1)$$

in which T is recurrence interval in years, N is the number of years of record, and M is the relative magnitude of the event beginning with the highest as 1.

Annual floods are plotted on a special form developed for analysis of flood frequencies by the Gumbel[3] method. Discharge is plotted as ordinate and time

---

[2] "Annual Floods and the Partial-Duration Flood Series," by W. B. Langbein, American Geophysical Union Transactions, Vol. 30, 1949, pp. 879-881.

[3] "Floods Estimated by the Probability Method," by E. J. Gumbel, Engineering News Record, June 14, 1945.

as abcissa. Both linear and logarithmic ordinate scales are used, depending on which plot more nearly approximates a straight line. An example of each kind of plot is shown in Fig. 1. The same data are plotted here to show the characteristic difference in the shape of the final curves.

Fitting Frequency Graphs.—After the annual floods are plotted on a frequency diagram, a curve is fitted to the data. Considering the fact that most

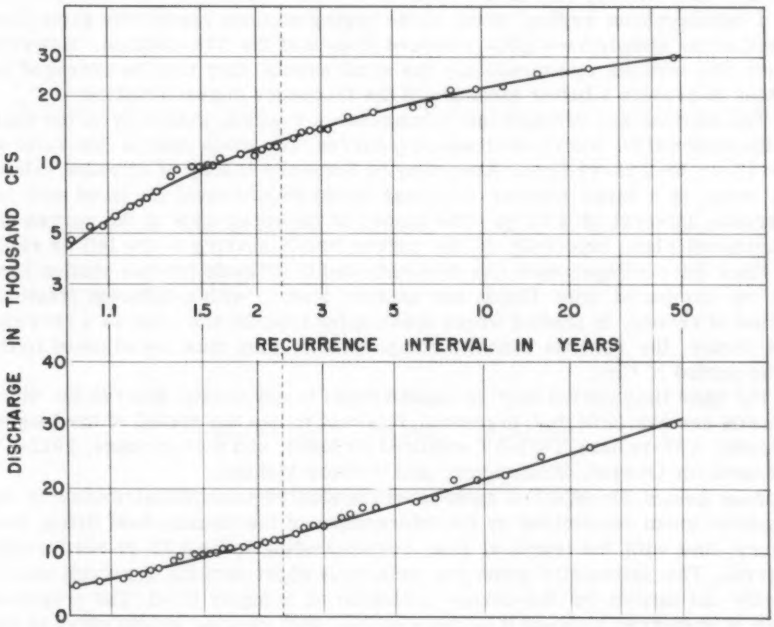

FIG. 1.—MAGNITUDE AND FREQUENCY OF ANNUAL FLOODS.

streamflow records are less than 35 yr in length, and analytically fitted function has little value. Therefore, graphical treatment only is applied, and a simple curve of visual best-fit is drawn.

REGIONAL DISTRIBUTION

Flood-frequency compilations, prepared in accordance with procedures described, result in a curve of flood magnitude versus recurrence intervals for each station studied. The curve is not applicable directly to ungaged areas. In most instances, the flood records are short and time-sampling errors may be large. That is, the flows sampled by the period of record may not be representative of conditions for long periods. Also, the records are, generally, for different periods of time. By combining the records for all stations in a drainage basin or a larger region, time-sampling and areal-sampling errors are reduced, and the resulting composite curves are applicable to ungaged areas. However, these curves simply show floods of

various recurrence intervals in terms of mean annual flood, so the latter must be computed before the composite curve can be applied to an ungaged area. That can be accomplished by relating the mean annual flood to measurable characteristics of the drainage basin.

Combining Records.—If the flood data for gaging stations at which only records of short length have been collected could be added together to make long records, than five records each 20 yr long would provide a 100-yr record. Unfortunately, this cannot be done because the data are not independent. In a homogeneous region, many of the gaging stations record the same flood event so we simply have a 20-yr record at each of the five stations. However, since the stations are measuring the same events, they may be averaged together to provide a better measure of the frequency characteristics.

The stations are grouped into homogeneous regions, generally on the basis of the slopes of the individual frequency curves. The slope used is the ratio of the 10-yr to 2.33-yr flood. According to Gumbel's theory of extreme values, the mean of a large number of annual floods should equal the flood with recurrence interval of 2.33 yr. The slopes of the upper ends of the curves are considered also, especially if the curves break sharply to the left or right.

Time Base.—Experience has demonstrated that floods for one station cannot be compared with floods for another station with a different length or period of record. In studies where mean annual floods are used as a correlation factor, the records must be comparable so they must be adjusted to the same period of time.

The base time period may be chosen equal to any period desired for which records are available, but, in general, it is best to use the period of the longest records. A 37-yr base, 1921-57, was used for Idaho, and a 46-yr base, 1912-57, was used for Oregon, Washington, and western Montana.

Mean Annual Flood.—The mean used for each frequency distribution is the graphical mean determined by the intersection of the visually best fitting frequency line with the vertical line corresponding to the 2.33-yr recurrence interval. The arithmetic mean for relatively short periods of record can be greatly influenced by the chance inclusion of a major flood. The graphical mean is preferred because it is more stable, with greater weight given to the medium floods than to the extreme floods.

Composite Frequency Curve.—All homogeneous stations are grouped for the purpose of computing an average frequency curve applicable to that region. For each station, the flood discharges for several recurrence intervals are determined from the individual frequency curves. These discharges are divided by the mean annual flood in order to place them on a dimensionless basis. The medium value of the ratios is then determined for each of the selected recurrence intervals. Each median flood ratio is plotted to its corresponding recurrence interval on a frequency chart, and a frequency curve is drawn. This curve, showing discharge in ratio to the mean annual flood versus recurrence interval in years, is based on all significant discharge records available and may be considered as representing the most likely flood-frequency values for all places in the region. (See Fig. 2).

Adjustments to Composite Curves.—Recent studies of streams in Idaho have shown that, in some areas, the shape of the curve changes with elevation. Also, some investigators have found that the size of the drainage area has an effect on the shape of the frequency curve, and that the effect increases with increase in recurrence interval.

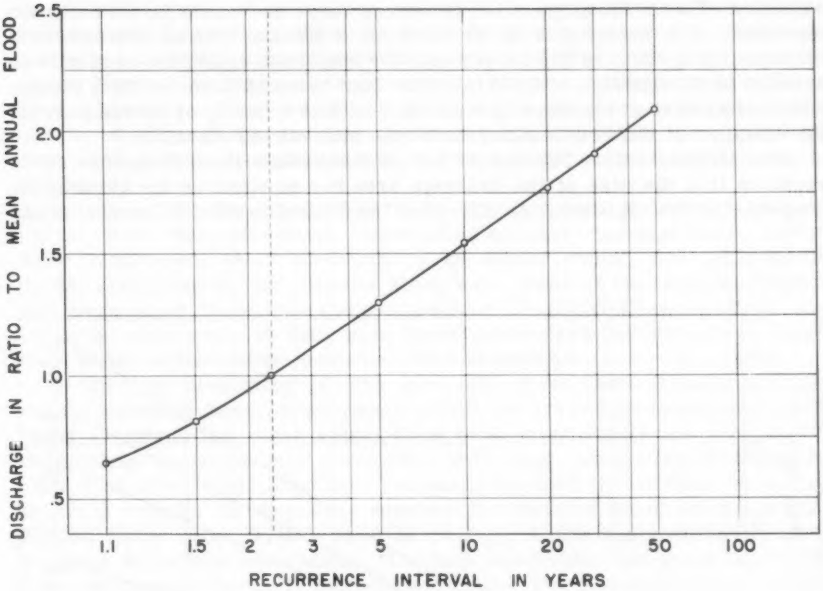

FIG. 2.—FREQUENCY OF ANNUAL FLOODS.

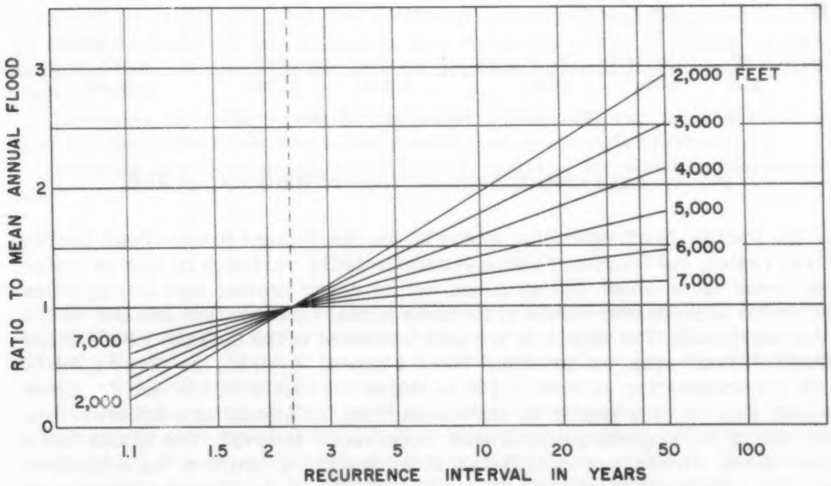

FIG. 3.—VARIATION OF FLOOD RATIO WITH RECURRENCE INTERVAL AND ELEVATION.

Elevation Adjustments.—In certain areas, such as the Clearwater River basin in Idaho, there is a definite relationship between flood discharge and elevation. There, the slope of the frequency curve decreases as the elevation increases. For example, a 50-yr flood for a stream, with an average basin elevation of 2,000 ft is 36% larger than for one of the same size area with an average basin elevation of 4,000 ft, and is about twice as large as for a stream with this area at an elevation of 6,000 ft. Fig. 3 is a family of curves showing the variation of flood ratio with recurrence interval and elevation.

Area Adjustments.—The use of the dimensionless flood-frequency curve assumes that the size of the drainage area has no effect on the slope of the frequency curve. However, an effect has been found to exist in several areas

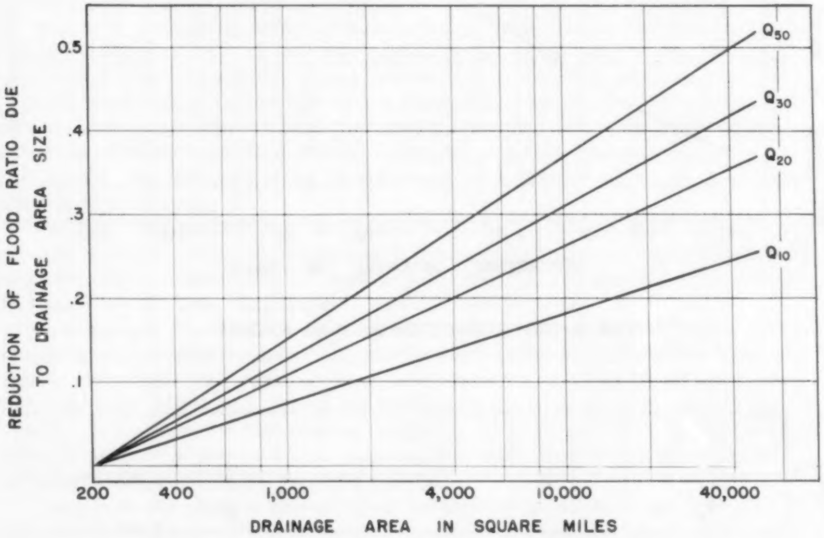

FIG. 4.—AREA CORRECTION FACTORS TO REGIONAL CURVE.

in the Pacific Northwest. For example, in the Spokane River—Pend Oreille River region, the frequency curve is not affected by variation in size of drainage areas up to about 200 sq miles, but for areas greater than 200 sq miles the ratios of the larger floods to the mean annual flood become smaller as the area increases. The effect is not as pronounced in the Spokane River—Pend Oreille River area as in some other regions. Even so, the 50-yr ratio of 2.05 determined for an area of 200 sq miles is reduced to 1.62 for 20,000 sq miles. Fig. 4 is a family of curves showing the amount of correction with respect to both drainage area and recurrence interval. The values taken from these curves are subtracted from the flood ratios of the composite curve to obtain flood ratios that are applicable to the size area being considered.

Derivation of Formula for Mean Annual Flood.— A plot of drainage area against mean annual flood in any region usually results in a graph in which the standard error of the plotted points about the regression line is large, sometimes 100% or more. Such a large standard error indicates that drainage-basin characteristics other than drainage area may effect the size of the mean annual flood. Sometimes, it is possible to obtain a satisfactory correlation by dividing the region into hydrologic zones in which the runoff per square mile is similar. If the standard error of the plotted points for a hydrologic zone still seems excessive, other drainage basin characteristics must be considered.

In this study, the standard error of drainage area plotted against mean annual flood was excessive, about 90%, so other drainage-basin factors were considered. Mean elevation, mean annual runoff, area of lages and ponds, precipitation, and channel slope were some of the additional factors that were found to improve the correlations. Graphical-linear-multiple correlations were made to determine those parameters that were most significant before entering into mathematical correlations.

In the area designated as "the west side of the Cascade Range in Washington" drainage area, mean annual runoff and area of lakes and ponds were found to affect the mean annual flood most significantly and were used as independent variables in a correlation with mean annual flood. Residual deviation of about equal magnitude remaining in these correlations were found to group areally, so they were assumed to represent the effect of some undefined basin characteristic such as geology. A map was prepared on which residual deviations were shown. The map was divided into areas by drawing lines enveloping residuals of about equal size. The median residual for each area was used to represent a geographical factor for that area.

The standard error of the multiple correlation, before introducing geographical factors, was about 46%, and the coefficient of correlation was about 0.97. After assigning values for geographical location and reducing the degrees of freedom by one for each zone used, the standard error was reduced to about 24%, and the coefficient of correlation increased to 0.99. A standard error of 24% indicates that about two-thirds of the time a mean annual flood computed by the method described should be within 24% of the correct value.

Formulas for other areas in the Pacific Northwest, such as western Oregon and the Snake River basin, were developed in a similar manner.

Formula and Nomograph.—The formula derived for western Washington is

$$Q = 0.638\, A^{0.89}\, R^{1.14}\, L^{-.04}\, G \qquad \text{(2)}$$

in which Q refers to the mean annual flood in cubic feet per second, A denotes the drainage area in square miles, R is the mean annual runoff in inches for period 1930-57, L refers to the area of lakes and ponds in percent of drainage area, and G is the geographical factor.

Eq. 2 may be solved by use of logarithms or by slide rule, but it is also presented in nomograph form for ease of application. Two nomographs were designed for the above formula, one for drainage areas of 0.1 to 10 sq miles and another for areas of 10 to 1,000 sq miles. The nomograph for small areas is shown in Fig. 5.

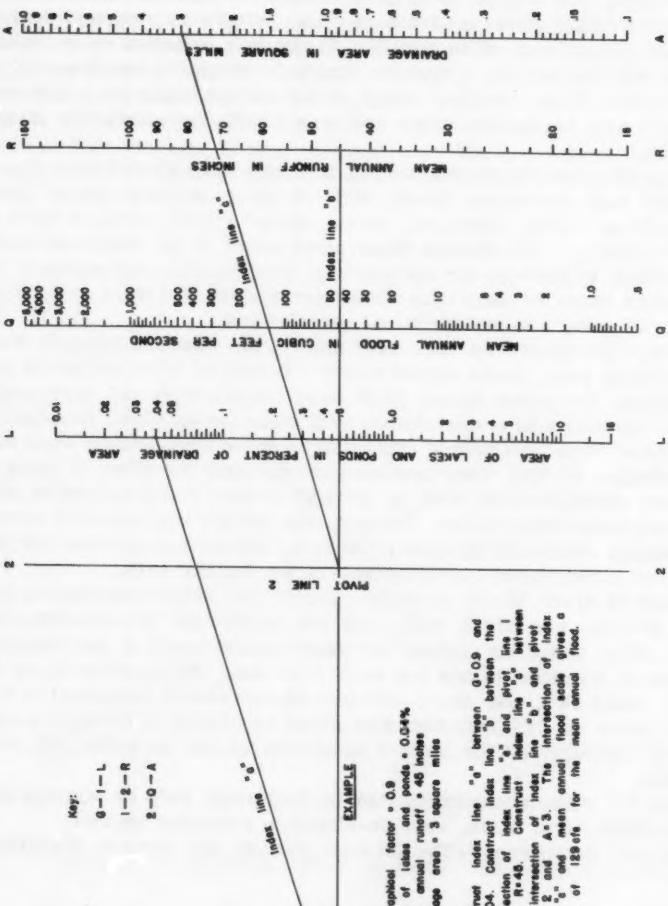

FIG. 5.—NOMOGRAPH FOR COMPUTING MEAN ANNUAL FLOOD FOR DRAINAGE AREAS OF 0.1 TO 10 SQUARE MILES WEST OF THE CASCADE MOUNTAINS.

Derivation of Frequency Curve for Any Site.—The procedure for deriving a flood-frequency curve for any site in a region is as follows: (1) Obtain the drainage area, mean annual runoff, area of lakes and ponds, and other characteristics, as necessary, from appropriate maps (Mean annual runoff is obtained from a map showing isopleths based on gaging-station records.); (2) use the nomograph or formula to determine the mean annual flood; (3) select the proper flood-ratio curve and determine ratios to mean annual flood for selected recurrence intervals up to 50 yr; and (4) multiply these ratios by the mean annual flood computed in step 2 and plot against recurrence intervals to define the frequency curve.

LIMITATIONS

The methods described may be used to predict the magnitude of floods of given return intervals on streams in the Pacific Northwest. However, they must be used with full knowledge of their limitations.

1. The term "return interval", when considering annual floods, represents the average length of time, in years, between the individual occurrences of flood peaks of a given magnitude over a very long period. It does not indicate that the flood will occur on a specific time schedule, 50-yr flood is one that has a 2% chance of occurring in any year.
2. The relationships shown in this report were developed from data gathered on the natural flows of representative streams, and should not be applied to streams on which the flood-flow potential has been altered by the works of man, or to streams with unique drainage-basin characteristics. Many of the smaller streams in the semiarid areas of eastern Washington and Oregon are essentially dry except when they experience flash floods caused by local thunderstorms. This type of stream does not lend itself to the methods of analysis presented herein but will require special studies.
3. Extrapolation beyond the areal limits of the basic data is not advised. The mean annual flood formulas should not be applied to drainage areas outside the regions for which they were derived.
4. The length of existing gaging-station records does not justify extending the frequency curves beyond the 50-yr recurrence interval. Extrapolation of the curves beyond this limit may introduce considerable error. However, such extrapolation may provide the best available estimate.
5. The confidence that may be placed in the accuracy of the results obtained by using these data is related to the areal density of the basic data used. The denser the gaging sites, the more confidently the frequency curves can be defined, and the more accurately the geographical and runoff factors for the flood formulas can be determined.
6. Use of the methods outlined in this paper will facilitate design of structures commonly built in or along stream channels. Where design requires consideration of recurrence intervals greater than 50 yr, or the design is for a site otherwise outside the limitations stated, a special study should be made.

SUMMARY AND CONCLUSIONS

A method has been presented for determining the magnitude and frequency of floods to be expected at any site in the Pacific Northwest, with exceptions

as noted in item 2 of the limitations. Flood-frequency curves for individual stations are combined into several regional flood-frequency curves. The regions include stations for which slopes of individual flood-frequency curves are similar. The regional curves show flood magnitudes in terms of mean annual floods. To obtain the frequency curve for an ungaged site, it is only necessary to compute the mean annual flood for that site and convert the appropriate regional frequency curve to flow in cubic feet per second by multiplying the ordinates of that curve by the mean annual flood.

Magnitudes of mean annual floods have significant correlations with drainage area, mean annual runoff, area of lakes and ponds and in some places with elevation. After all these factors are taken into account in multiple correlations, large residual standard errors still exist. These residuals tend to be of about equal magnitude in given geographical areas, suggesting that a factor such as geology of the area has a significant effect. So-called geographic factors based on residual errors are developed.

The formula for mean annual floods in western Washington is expressed in terms of drainage area, area of lakes and ponds, mean annual runoff, and the geographical factor. Similar equations have been developed for other areas in the Pacific Northwest. Drainage area and area of lakes and ponds are easily obtained from topographic maps. Mean-annual runoff is obtained from an isopleth map based on gaging-station records. Geographical factors are obtained from a map that has been divided into areas having residual errors of similar magnitude. The geographical factor is based on the median residual error for that area. Because all of these factors are readily available, the formula is easily applied.

The methods presented herein are subject to limitations. They cannot be applied to streams in which the regimen has been so altered by the works of man that satisfactory adjustments for such cannot be applied. Nor can such adjustments be applied to certain small streams in semi-arid eastern Washington and Oregon in which practically the sole sources of runoff are local thunderstorms. Extensions of frequency curves beyond the 50-yr recurrence interval are not justified, and extrapolation beyond that limit should be a computed risk taken only when no better estimate is available.

Journal of the
HYDRAULICS DIVISION
Proceedings of the American Society of Civil Engineers

PERIODICAL GRAVITY WAVE ON A DISCONTINUITY

By Bernard Le Méhauté[1]

SYNOPSIS

A general theory is presented to study the transmission and reflection of gravity waves on a discontinuity to the first order of approximation.

Particular attention is given to the cases of an obstruction, a change of width, and a change of depth. In the latter case only, the gravity wave arriving at an angle is studied.

INTRODUCTION

In harbors, the study of wave motion, caused by the action of incident waves from the open sea, is generally a difficult theoretical problem. The complexity of wave patterns is increased by successive reflections within the harbor.

Some authors[2,3,4] gave linear solutions for some simple cases, assuming that there were no energy losses in the harbor, that is no beach or wave-trap. Thus, the solutions for circular,[2] square[2,3] and sector harbors[4] connected to the open sea by a small opening are known. The general method consisted in finding a potential function ϕ, satisfying the usual free-surface, bottom and limit conditions for the harbor, and combining this with the potential function at sea.

Note.—Discussion open until April 1, 1961. To extend the closing date one month, a written request must be filed with the Executive Secretary, ASCE. This paper is part of the copyrighted Journal of the Hydraulics Division, Proceedings of the American Society of Civil Engineers, Vol. 86, No. HY 9, November, 1960.

1 Ingénieur-Docteur, Special Lecturer in Graduate Studies and Research Associate at Queen's Univ., Kingston, Ontario.

2 "Sur l'entretion des oscillations des eaux portuaires," by Mc Known, Publications du Ministre de l'air, No. 278, 1953.

3 "Quelques recherches sur les oscillations des eaux portuaires," by Kravtchenko, and Santon, 6th Congress, AIRH, La Haye, 1955.

4 "Agitation dans les ports a jetées convergentes," by Bernard Le Méhauté, L'ingénieur, Hiver, No. 176, Canada, 1958.

Unfortunately such a potential function ϕ is always complicated if there are singularities in the limits. (The reader can see, for example, the very simple case, studied by Ursell,[5] of the wave transmission in infinite depth under a vertical wall.)

Therefore, this kind of solution would not be expected to be of practical importance in harbor engineering. Furthermore, the solutions of many practical cases are still quantitatively unknown. In particular, the effects of the harbor neighborhood shapes, and of the beaches inside the basins, are usually ignored.

As far as the motion can be considered approximately two dimensional, there now exist linear computation methods more simple than the potential function method.

F. Biesel and the author used the complex number computation method to study[5,6,7] wave transmission and reflection on symmetrical obstacles and applied these results to study agitation between a combination of these obstacles, that is, in simple shape basins. In the Sogreah laboratory in France, more complicated shape basins that had not been theoretically analyzed were investigated. The results of these experiments are available.[7,8]

The purpose of this paper is to present a more general wave theory for non-symmetrical discontinuities using a similar method of computation. These theoretical results can be applied to establish a general formula of the agitation value, in a basin subjected to ocean waves, that will verify all the previously published experimental results. Furthermore, this theory allows one to generalize the experimental results and to analyze, quantitatively, the effect of a beach in a harbor.

Perhaps the calculus hypotheses may seem too simple for a rigourous logical mind, but the relative simplicity of established formulas allows engineers to use them in practice. Above all, the assumptions are justified by close agreement between theoretical and experimental values.

Notation.—The letter symbols adopted for use in this paper are defined where they first appear, in the illustrations or in the text, and are arranged alphabetically, for convenience of reference, in Appendix II.

LIMITS OF STUDIED PROBLEMS

The study is limited to periodical irrotational gravity waves. It is assumed that the fluid is ideal (except when specified otherwise), and any terms of the second or higher power of the wave steepness are neglected; that is, the square of the velocity (that is valid if the product of the steepness of the wave and the cube of the inverse of the relative depth is small—$\left(\frac{2\,a}{L}\right)\left(\frac{L}{h}\right)^3$)

The motion is mainly two dimensional and will be treated as such. If there exists a third dimensional component, it must have secondary effects, and only

---

5 "The Effect of a Vertical Barrier on Waves in Deep Water," by Ursell, Admiralty Research Lab., Teddington, December, 1945.

6 "Theoretical Study of the Reflection of Waves from Different Types of Obstacles," by Biesel and Le Méhauté, La Houille Blanche, No. 2, 1955.

7 "Two Dimensional Resonant Motion in Basin Subjected to Incident Waves," by Biesel and Le Méhauté, La Houille Blanche, No. 3, Juillet, 1956.

8 "Two Dimensional Seiche in a Basin Subjected to Incident Waves," by Le Méhauté, Coastal Engineering, September, 1954.

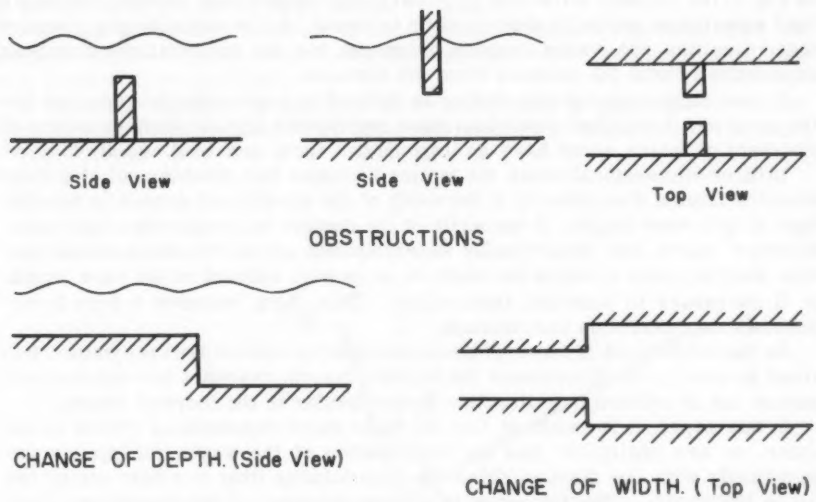

FIG. 1.—DIFFERENT TYPES OF DISCONTINUITIES.

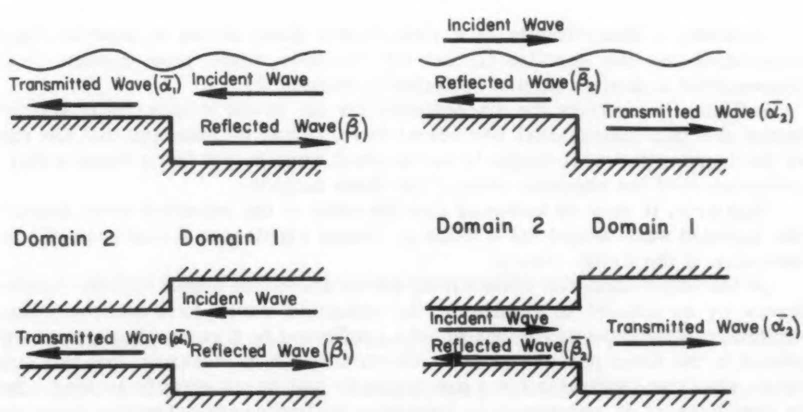

FIG. 2.—COEFFICIENTS OF TRANSMISSION $\bar{\alpha}$ AND REFLECTION $\bar{\beta}$.

the main two dimensional components are analyzed. Finally, some details on three dimensional motion will be given.

When a wave arrives on a two or three dimensional discontinuity, as shown in Fig. 1, the incident wave energy is partially transmitted, partially reflected (and sometimes partially destroyed by friction). In the close neighborhood of discontinuities, the waves become deformed, but the deformations disappear exponentially with the distance from the obstacle.

In two-dimensional cases, motion is defined by a potential function that has the form of a linearized sum of constant coefficients (generalized constants of Fourier) of which some have an exponential form and tend rapidly to zero.

In three-dimensional cases, the motion becomes two-dimensional at a short distance from a discontinuity if the width of the considered domain is smaller than a half wave length. If the width of the domain is greater than this value, Jeffreys' waves are theoretically superimposed on the two-dimensional motion. Only in cases in which the width is large with respect to the wave length, is it necessary to consider their effect. This, then, becomes a pure three-dimensional diffraction phenomenon.

On the other hand, if three-dimensional discontinuities are not symmetrical about an axis in the direction of the incident waves, resonant two-dimensional motion can be excited in a direction perpendicular to the incident waves.

In this paper, it is assumed that all these three-dimensional effects do not occur, or are negligible, and the deformation of the waves disappears exponentially with the distance from the discontinuity (that is within one or two times the depth). The following is a consideration of the two-dimensional periodical wave motion.

DEFINITIONS

Consider a discontinuity in a wave flume (such as one of those in Fig. 2) separating the two domains (1) and (2). Incident waves from domain (1) are transmitted to domain (2) and reflected in domain (1).

Sufficiently far from the discontinuity for the waves to have the characteristics of a two-dimensional periodical wave, it may be assumed that the ratio of the transmitted wave height to the incident wave height has a value α that is independent of the absolute value of the wave heights.

Similarly, it may be assumed that the ratio of the reflected wave height to the incident wave height has a value β. These hypotheses follow from the assumption of the linear theory.

On the other hand, the transmitted waves are out of phase with the incident waves by an amount $\hat{\alpha}$. Similarly, the reflected waves have a certain phase difference $\hat{\beta}$ from the waves that would be reflected by a perfectly vertical wall placed in the same position as the discontinuity. It is assumed that this previous result is applicable for a discontinuity that is not strictly located. But, in this case, it is necessary to introduce an imaginary reflecting reference plane related to the discontinuity. It is then possible to designate the phase of the waves as being that of their vertical amplitude in front of this reference plane, whatever their direction of propagation. For a theoretical plane barrier, it is natural to choose it as the reference plane. When the discontinuity possesses a plane of vertical symmetry perpendicular to the wave direction, this plane would be chosen as the reference plane.

Consequently, the motion of the free surface at any point can be represented by a vector running in the plane of imaginaries (Fig. 3), analogous to that used

in the study of alternating currents in electricity. Therefore, we can represent the coefficients of transmission and reflection by vectors, that is by the complex numbers $\bar{\alpha}$ and $\bar{\beta}$, representing these coefficients both by their arguments: ($\hat{\alpha}$ and $\hat{\beta}$) and by their moduli (α and β).

When the phase and amplitude of the incident waves are represented by the complex number: $\bar{1}$ A, the transmitted and reflected waves will be represented by $\bar{\alpha}$ A and $\bar{\beta}$ A, respectively.

If the discontinuity is symmetrical about a plane that is perpendicular to the wave direction and separates two identical domains, it is clear that the value

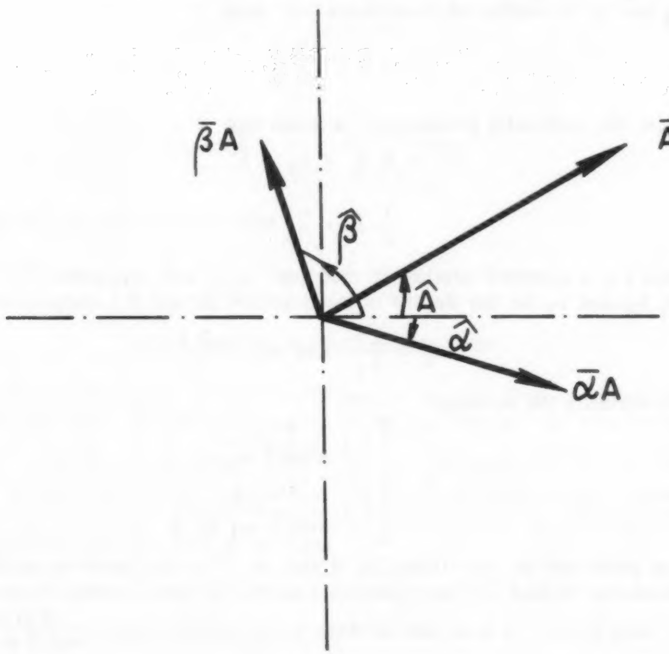

FIG. 3.—VECTORIAL REPRESENTATION OF A PERIODICAL GRAVITY WAVE.

of the coefficients $\bar{\alpha}$ and $\bar{\beta}$ are independent of the side from which the incident waves arrive.

However, in the general case, $\bar{\alpha}$ and $\bar{\beta}$ are probably different for the two directions of incident waves. Therefore, we have to consider two transmission coefficients $\bar{\alpha}_1$ and $\bar{\alpha}_2$, and two reflection coefficients $\bar{\beta}_1$ and $\bar{\beta}_2$.

Consequently, a discontinuity is characterized by eight parameters: Transmission coefficient in domain (2)—$\bar{\alpha}_1 \begin{cases} \alpha_1 \\ \hat{\alpha}_1 \end{cases}$; Reflection coefficient in domain (1)—$\bar{\beta}_1 \begin{cases} \beta_1 \\ \hat{\beta}_1 \end{cases}$; Transmission coefficient in domain (1)—$\bar{\alpha}_2 \begin{cases} \alpha_2 \\ \hat{\alpha}_2 \end{cases}$; Reflection coefficient in domain (2)—$\bar{\beta}_2 \begin{cases} \beta_2 \\ \hat{\beta}_2 \end{cases}$.

From the continuity and energy conservation principles, relationships between these eight parameters will be established. The reader who wishes to use directly the results of this study will refer to Tables 1 through 5 in which the practical results of this study are given for a number of common cases.

THEORETICAL RELATIONSHIPS

All the mathematical developments and demonstrations are given in Appendix I.

Let L_2 and L_1 be the wave lengths in the domains (2) and (1) respectively, and l_2 and l_1 the widths of these domains. Also,

$$Z = \frac{L_2\, l_2}{L_1\, l_1} \qquad (1)$$

From the continuity principle it is found that:

$$Z\, \bar{\alpha}_1 + \bar{\beta}_1 = \bar{i} \qquad (2a)$$

and

$$\frac{1}{Z}\, \bar{\alpha}_2 + \bar{\beta}_2 = \bar{i} \qquad (2b)$$

in which $\bar{i}$ is a complex number of modulus: $i = 1$ and argument: $\hat{i} = 0$

Let h_2 and h_1 be the depths of the domains (2) and (1), respectively, and:

$$m_2 = \frac{2\pi}{L_2} \text{ and } m_1 = \frac{2\pi}{L_1} \qquad (3)$$

and, to simplify the writing

$$A = \left[\frac{1 + \dfrac{2\, m_2\, h_2}{\sinh 2\, m_2\, h_2}}{1 + \dfrac{2\, m_1\, h_1}{\sinh 2\, m_1\, h_1}}\right] \qquad (4)$$

It is pertinent to note from Eq. 4 that $A = 1$ in the cases in which (1) the two domains, (1) and (2), have the same depth, (2) there exists shallow water, since: $\sinh 2\, m\, h \cong 2\, m\, h$, and (3) deep water exists, since $\dfrac{2\, m\, h}{\sinh 2\, m\, h}$ tends to zero.

The conservation of energy principle leads successively to the equalities

$$A\, Z\, \alpha_1^2 + \beta_1^2 = 1 \qquad (5)$$

$$\frac{1}{A\, Z}\, \alpha_2^2 + \beta_2^2 = 1 \qquad (6)$$

and

$$\hat{\alpha}_2 - \hat{\beta}_2 = -\left(\hat{\alpha}_1 - \hat{\beta}_1\right) + \pi\, (+\, 2\, n\, \pi) \qquad (7)$$

in which $n = 0, 1, 2 \ldots$

The two vectorial equalities, Eqs. 2a and 2b, equivalent to four algebraic equalities, form with Eqs. 5, 6, and 7 a system of seven independent equations with eight unknowns.

Hence, we are able to express the values of seven parameters as functions of only one, α_1, and the factors Z and A, that characterize the two domains

and do not depend on the exact shape of the considered discontinuity. Consequently, it is sufficient to know the exact value of α_1 as a function of this shape, in order to know the others from the following theoretical formulas $\left[f(A_1 Z_1 \alpha)\right]$:

$$\alpha_2 = A Z \alpha_1 \quad (8)$$

$$\beta_1 = \beta_2 = \left(1 - A Z \alpha_1^2\right)^{1/2} \quad (9)$$

$$\cos \hat{\alpha}_1 = \cos \hat{\alpha}_2 = \frac{\alpha_1}{2} (A + Z) \quad (10)$$

$$\cos \hat{\beta}_1 = \frac{2 - Z \alpha_1^2 (A + Z)}{2\left(1 - A Z \alpha_1^2\right)^{1/2}} \quad (11)$$

and

$$\cos \hat{\beta}_2 = \frac{2 - \alpha_1^2 (A + Z)}{2\left(1 - A Z \alpha_1^2\right)^{1/2}} \quad (12)$$

Furthermore, it may be shown that

$$\hat{\alpha}_1 = \hat{\alpha}_2 = \frac{\hat{\beta}_1 + \hat{\beta}_2}{2} + \frac{\pi}{2} \; (+ n\pi) \quad (13)$$

GRAPHICAL REPRESENTATION

Assuming α_1 is known, we can easily derive Eq. 10. Now consider the half circle of diameter $\overline{AB}$ (equal to unity) shown in Fig. 4. On this circle, we draw $\overline{BC} = \cos \hat{\alpha}_1$, or the angle $\widehat{ABC} = \hat{\alpha}_1$. On the segment $\overline{BC}$, we plot the point D, so that $\overline{BD} = A\,Z\,\alpha_1$ and draw the circle of center A and radius AD, intersecting CD at the point E. It is easy to verify that this sketch satisfies all the above conditions. Thus, we have

$$\widehat{ABD} = \hat{\alpha}_1 = \hat{\alpha}_2 \quad (14a)$$

$$\widehat{BAD} = \hat{\beta}_1 \quad (14b)$$

$$\widehat{BAE} = \hat{\beta}_2 \quad (14c)$$

$$\widehat{BAC} = \frac{\hat{\beta}_1 + \hat{\beta}_2}{2} \quad (14d)$$

$$\overline{AB} = 1 \quad (14e)$$

$$\overline{AD} = \beta_1 \quad (14f)$$

$$\overline{AE} = \beta_2 \quad (14g)$$

$$\overline{DB} = Z\,\alpha_1 = \frac{1}{A}\,\alpha_2 \quad (14h)$$

$$\overline{EB} = \frac{1}{Z}\,\alpha_2 = A\,\alpha_1 \quad (14i)$$

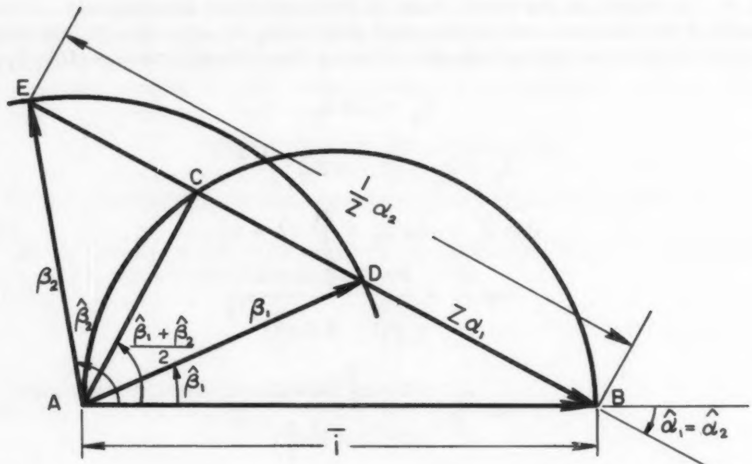

FIG. 4.—VECTORIAL GRAPHICAL REPRESENTATION WITHOUT LOSS OF ENERGY.

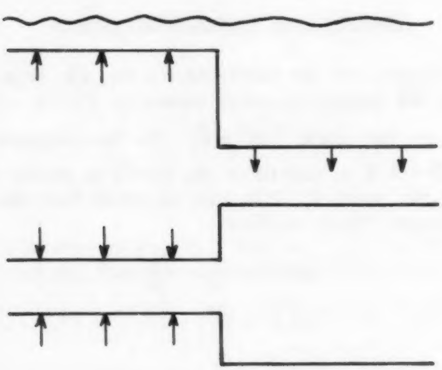

FIG. 5.—LIMIT CASE: ONE OF THE DOMAINS TENDS TO ZERO.

FIG. 6.—A DYSSMMETRICAL DISCONTINUITY.

and

$$\overline{CB} = \frac{A\,\alpha_1 + \frac{1}{A}\,\alpha_2}{2} = \frac{Z\,\alpha_1 + \frac{1}{Z}\,\alpha_2}{2} = \frac{\alpha_1}{2}\,(A + Z) \quad \text{(14j)}$$

or more simply

$$\overrightarrow{AD} = \overrightarrow{\beta_1} \quad \text{(15a)}$$

$$\overrightarrow{DB} = Z\,\overrightarrow{\alpha_1} = \overrightarrow{\alpha_2} \quad \text{(15b)}$$

$$\overrightarrow{AE} = \frac{1}{Z}\,\overrightarrow{\alpha_2} = \overrightarrow{\alpha_1} \quad \text{(15c)}$$

$$\overrightarrow{AC} = \frac{\overrightarrow{\beta_1} + \overrightarrow{\beta_2}}{2} \quad \text{(15d)}$$

$$\overrightarrow{CB} = \frac{A\,\overrightarrow{\alpha_1} + \frac{1}{A}\,\overrightarrow{\alpha_2}}{2} = \frac{Z\,\overrightarrow{\alpha_1} + \frac{1}{Z}\,\overrightarrow{\alpha_2}}{2} = \frac{\overrightarrow{\alpha_1}}{2}\,(A + Z). \quad \text{(15e)}$$

One can see also, without further computation, the following noticeable relationships:

$$A\,\bar{\alpha}_1 + \bar{\beta}_2 = \bar{i} \quad \text{(16)}$$

$$\frac{\bar{\alpha}_2}{A} + \bar{\beta}_1 = \bar{i} \quad \text{(17)}$$

and

$$\left(\frac{A\,\alpha_1 + \frac{1}{A}\,\alpha_2}{2}\right)^2 + \left|\frac{\bar{\beta}_1 + \bar{\beta}_2}{2}\right|^2 = 1 \quad \text{(18)}$$

SOME PARTICULAR CASES

The relative variations of each coefficient are easily studied by means of Fig. 5. When A Z is greater than 1, D and E, β_1 and β_2, $\hat{\beta}_1$ and $\hat{\beta}_2$ . . . are reversed. (a) If A, Z tend to 0, either by a reduction of domain (2), or by an increase of domain (1), as shown in Fig. 5, then, according to the sketch for the wave moving from the domain (1) to the domain (2)

$$\beta_1 \to 1 \qquad \hat{\beta}_1 \to 0$$

$$\alpha_1 \to 0 \qquad \hat{\alpha}_1 \to 0$$

that is, there is total reflection without change of sign (as in a closed acoustic pipe); for the wave moving from the domain (2) to the domain (1), the sketch shows

$$\beta_2 \to 1 \qquad \hat{\beta}_2 \to \pi$$

$$\alpha_2 \to 0 \qquad \hat{\alpha}_2 \to 0$$

There is also total reflection with change of sign, (as in an open acoustic pipe).

(b) If AZ tends to 1, that is, if the domains (1) and (2) are identical, the results previously published are found, that is

$$\bar{\alpha}_1 = \bar{\alpha}_2$$

$$\bar{\beta}_1 = \bar{\beta}_2$$

Even if the discontinuity has an unsymmetrical shape (Fig. 6), the effects on waves are symmetrical. (This is due to the assumption that the discontinuity is local, and that the linear theory is used.)

However, this result is also true when domains (1) and (2) are different, with A, Z = 1, (for example, as in the case shown in Fig. 7. But A, Z can be equal to unity for only one value of the wave period.

(c) If α_1 tends to 0 (by obstruction), A, Z being constant

$$\alpha_2 \rightarrow 0$$

$$\hat{\alpha}_1 \text{ and } \hat{\alpha}_2 \rightarrow \frac{\pi}{2}$$

$$\beta_1 \text{ and } \beta_2 \rightarrow 1$$

and

$$\hat{\beta}_1 \text{ and } \hat{\beta}_1 \rightarrow 0$$

There is total reflection in the two domains without change of sign, that is there is total obstruction.

VALUES OF $\overline{A}$ AND $\overline{B}$ AS FUNCTIONS OF THE SHAPE OF THE DISCONTINUITIES: EMPIRICAL FORMULA

It has been seen that all the coefficients $\overline{\alpha}$ and $\overline{\beta}$ are known when we are able to express only one (for instance α_1) as a function of the shape of the discontinuity. This value has been obtained with the help of theory, physical considerations, and experimental results, some of which have been previously published.[7,8] (However, the formula obtained can be modified after other complementary tests or further theory.)

Consider the most general possible shape of discontinuity frequently met with at the mouth of harbors (Fig. 8).

The coefficient α_1 is given by the empirical formula (N)

$$\alpha_1 = \left(\frac{b}{l_2}\right)^{1/2} \left(\frac{l_1}{l_2}\right)^{1/4} \frac{2}{1 + A\,\dfrac{L_2}{L_1}} \quad \ldots\ldots\ldots\ldots (19)$$

in which b is the opening between domains (1) and (2). However, this empirical equation could be justified by a number of theoretical and physical considerations.

(a) It is easy to verify that, if we apply the theoretical formula of Eq. 8 we find

$$\alpha_2 = \left(\frac{b}{l_1}\right)^{1/2} \left(\frac{l_2}{l_1}\right)^{1/4} \frac{2}{1 + \dfrac{1}{A}\,\dfrac{L_1}{L_2}} \quad \ldots\ldots\ldots\ldots (20)$$

the function α_2 is perfectly symmetrical with respect to α_1. This is physically consistent.

(b) If $l_1 = l_2 = l$, and $h_1 = h_2 = h$, $(L_2 = L_1,\ A\ Z = 1)$ we obtain

$$\alpha_1 = \alpha_2 = \left(\frac{b}{l}\right)^{1/2} = \alpha \quad \ldots\ldots\ldots\ldots\ldots\ldots (21)$$

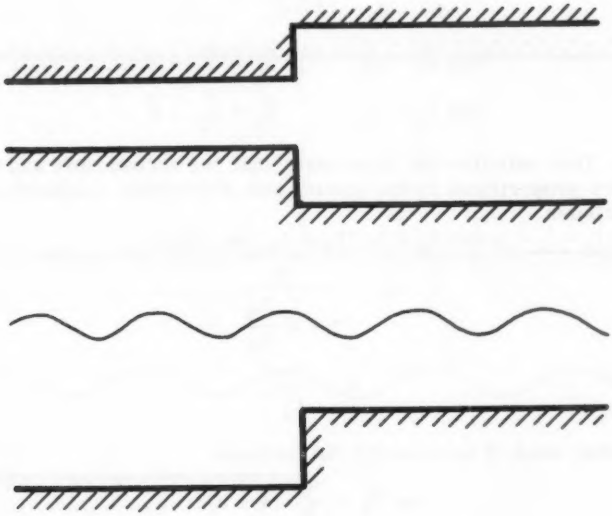

FIG. 7.—A CASE WHERE AZ COULD BE EQUAL TO UNITY DESPITE THE CHANGE OF DEPTH AND WIDTH.

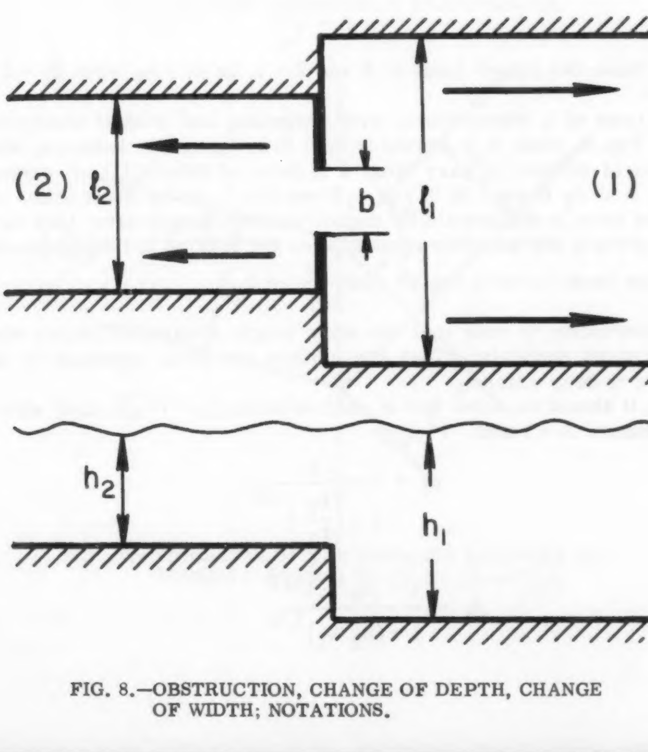

FIG. 8.—OBSTRUCTION, CHANGE OF DEPTH, CHANGE OF WIDTH; NOTATIONS.

$$\beta_1 = \beta_2 = \left(\frac{1 - b}{1}\right)^{1/2} = \beta \qquad (22)$$

$$\cos \hat{\alpha}_1 = \alpha_1 \qquad \hat{\alpha}_1 = \hat{\alpha}_2 = \hat{\alpha} \qquad (23)$$

$$\cos \hat{\beta}_2 = \beta_2 \qquad \hat{\beta}_1 = \hat{\beta}_2 = \hat{\beta} \qquad (24)$$

and so on. This satisfies the hypothesis that the transmitted and reflected energies are proportional to the opening and obstruction, respectively. This is also consistent.

(c) If $l = l_1 = l_2 = b$, and $h_1 \neq h_2$ $(L_2 \neq L_1)$ we obtain

$$\alpha_1 = \frac{2}{1 + A\dfrac{L_2}{L_1}} \qquad (25)$$

and

$$Z = \frac{L_2}{L_1} \qquad (26)$$

On the other hand, if we consider the formula

$$\cos \hat{\alpha}_1 = \frac{\alpha_1}{2}(A + Z) \qquad (27)$$

and the value α_1 in the case of a simple change of depth:

$$\alpha_1 = \frac{2 \cos \hat{\alpha}_1}{A + \dfrac{L_2}{L_1}} \qquad (28)$$

Equating these two values leads to A and Z = 1, or $h_1 = h_2$ when $\hat{\alpha}_1 = 0$ that is consistent.

In the case of a discontinuity with deepening and without obstruction, as shown in Fig. 9, when A Z varies from 0 to 1, that is for instance, when the dimensions of domain (2) vary from 0 to those of domain (1), α_1 varies from 1 to 2, β_1 and β_2 from 1 to 0, and α_2 from 0 to 1, at the same time. Consequently, the wave in the domain (2) cannot have a height greater than twice the height in domain (1), and this occurs when the ratio of the dimensions of the two domains tends to zero; that is when $\dfrac{h_2}{h_1} \to 0$.

It is interesting to note that the wave height always increases when the depth decreases suddenly. That can explain the great agitation of shallow water close to deep water.

Finally, it should be noted that in shallow water $L = T\sqrt{gh}$, and: $\sinh 2\,m\,h \cong 2\,m\,h$. Hence, A = 1 and

$$\alpha_1 = \frac{2}{1 + \left(\dfrac{h_2}{h_1}\right)^{1/2}} \qquad (29a)$$

$$\beta_1 = \frac{1 - (h_2/h_1)^{1/2}}{1 + (h_2/h_1)^{1/2}} \qquad (29b)$$

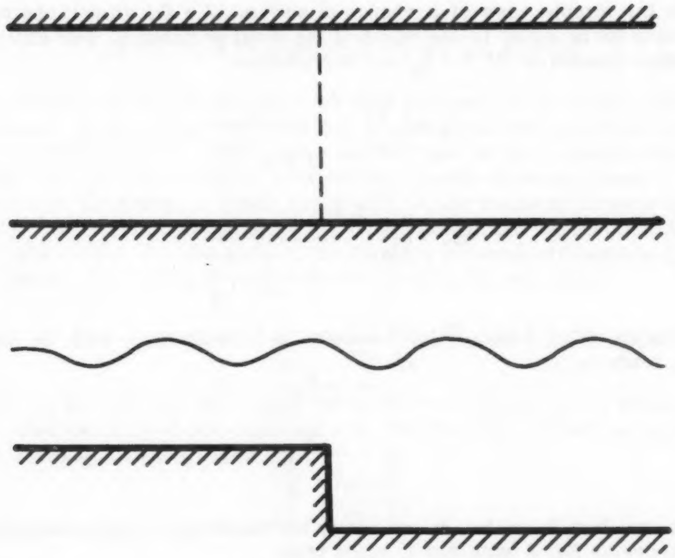

FIG. 9.—A CASE OF MAXIMUM TRANSMISSION.

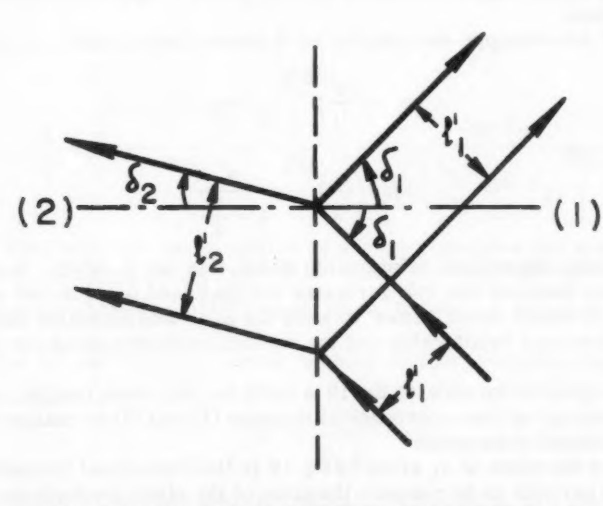

FIG. 10.—VARIATION OF THE DISTANCE BETWEEN ORTHOGONALS FOR A WAVE AT AN ANGLE.

The formulas of this particular case were obtained by Poincare[9] and later by Lamb.[10]

(d) In the simple case of a change of section ($Z \neq 1$), without obstruction, the opening (b) is equal to the width of the smaller domain. For example, if the smaller domain is (2), $b = l_2$, and one obtains

$$\alpha_1 = \left(\frac{l_1}{l_2}\right)^{1/4} \frac{2}{1 + A \dfrac{L_2}{L_1}} \qquad (30a)$$

and

$$\alpha_2 = \left(\frac{l_2}{l_1}\right)^{3/4} \frac{2}{1 + \dfrac{1}{A} \dfrac{L_1}{L_2}} \qquad (30b)$$

Some authors, after Lamb,[10] have adopted a formula that, with the present notation, leads to

$$\alpha_1 = \frac{2}{1 + Z} \qquad (31a)$$

and

$$\alpha_2 = \frac{2}{1 + \dfrac{1}{Z}} \qquad (31b)$$

These two last formulas do not verify the theoretical relationship demonstrated above as Eq. 8 (with $A \neq 1$) holds true.

On the other hand, it is difficult to introduce the effect of an obstruction between the domains (1) and (2), in this formula, without verifying both the theoretical relationship such as Eq. 8, and giving a correct formula for any particular case.

Indeed, if for example, one admits, as it seems logical that

$$\alpha_1 = \left(\frac{b}{l_1}\right)^{1/2} \frac{2}{1 + Z} \qquad (32a)$$

and

$$\alpha_2 = \left(\frac{b}{l_2}\right)^{1/2} \frac{2}{1 + \dfrac{1}{Z}} \qquad (32b)$$

the fundamental theoretical relationship of Eq. 8 is not verified. In practice, the difference between the two formulas for (α_1) (and (α_2)) is not very important, but it would seem better to keep the proposed formulas that satisfy both the theoretical relationship and the physical considerations for any particular case.

Hence, the general formula of Eq. 19 is valid for any case, that is: obstruction without change of characteristics of domains (1) and (2) or change of characteristics without obstruction.

Introducing the value of α_1 given by Eq. 19 in the theoretical formulas (Eqs. 8 through 12) permits us to compute the value of the other coefficients; $\hat{\alpha}_1$, β_1,

9 "Méchanique Céleste," by Poincaré, Torne, 131, p. 87.

10 "Hydrodynamics," by Lamb, 6th ed., p. 263.

$\hat{\beta}_1$, α_2, $\hat{\alpha}_2$, β_2, $\hat{\beta}_2$, in the general case and, in a number of particular cases, as it is shown in Tables 1 through 5.

WAVE ON A DISCONTINUITY AT AN ANGLE

When a periodical gravity wave arrives obliquely at a sudden change of depth, a part of its energy is reflected. The angle of the reflected wave with the line of discontinuity is the same as the angle of the incident wave, as is shown by Fig. 10. The distance between orthogonals does not change.

Because of the change of depth, the velocity of the transmitted wave changes suddenly. Hence, the transmitted wave is refracted, and the distance between orthogonals varies. For example, if the distance between orthogonals l_1' is the deeper domain (1), and l_2' is the shallower domain (2), we obtain

$$\frac{l_2'}{l_1'} = \frac{\cos \delta_2}{\cos \delta_1} \qquad (33)$$

in which δ_1 and δ_2 are the angles of the waves with the line of discontinuity in the domains (1) and (2), respectively. On the other hand, because of the change of velocity of the waves

$$\frac{L_2}{L_1} = \frac{\sin \delta_2}{\sin \delta_1} \qquad (34)$$

Combining these relationships, the value of $\left(\frac{l_2'}{l_1'}\right)$ is obtained as functions of $\left(\frac{L_2}{L_1}\right)$ and one of the angles δ_1 or δ_2, that could be chosen as the angle of the incident wave

$$\frac{l_2'}{l_1'} = \frac{\left[1 - \left(\frac{L_2}{L_1} \sin \delta_1\right)^2\right]^{1/2}}{\cos \delta_1} = \frac{\cos \delta_2}{\left[1 - \left(\frac{L_1}{L_2} \sin \delta_2\right)^2\right]^{1/2}} \qquad (35)$$

If the continuity and conservation of energy principles are applied to this phenomenon, all the previous results are valid, provided that the ratio of distances between orthogonals $\left(\frac{l_2'}{l_1'}\right)$ takes place, instead of the ratio of width of the domains (1) and (2), $\left(\frac{l_2}{l_1}\right)$. Hence, without further computation, introducing the new value

$$Z' = \frac{L_2\, l_2'}{L_1\, l_1'} \qquad (36)$$

all the previously demonstrated theoretical relationships, are valid

$$A\, Z'\, \alpha_1^2 + \beta_1^2 = 1 \qquad (37)$$

$$Z'\, \overline{\alpha}_1 + \overline{\beta}_1 = \overline{1} \qquad (38)$$

and so on . . . giving

$$\alpha_2 = A\,Z'\,\alpha_1 \quad \ldots\ldots\ldots\ldots\ldots\ldots\ldots (39)$$

and so on . . . .

In order to express completely the value of α_1, it will be noticed that a reduction of depth causes an increase of distance between orthogonals. Hence, this case is similar to the case shown by Fig. 7.

Hence, if the domain (2) is assumed to be the shallower domain, the values α_1 and α_2 can be written

$$\alpha_1 = \left(\frac{l_1'}{l_2'}\right)^{3/4} \frac{2}{1 + A\,\dfrac{L_2}{L_1}} \quad \ldots\ldots\ldots\ldots (40a)$$

and

$$\alpha_2 = \left(\frac{l_2'}{l_1'}\right)^{1/4} \frac{2}{1 + \dfrac{1}{A}\cdot\dfrac{L_1}{L_2}} \quad \ldots\ldots\ldots\ldots (40b)$$

Introducing the values $\left(\dfrac{l_2'}{l_1'}\right)$ leads to

$$\alpha_1 = \left[\frac{\cos\delta_1}{\left[1 - \left(\dfrac{L_2}{L_1}\sin\delta_1\right)^2\right]^{1/2}}\right]^{3/4} \frac{2}{1 + A\,\dfrac{L_2}{L_1}} \quad \ldots\ldots\ldots (41a)$$

and

$$\alpha_2 = \left[\frac{\cos\delta_2}{\left[1 - \left(\dfrac{L_1}{L_2}\sin\delta_2\right)^2\right]^{1/2}}\right]^{1/4} \frac{2}{1 + \dfrac{1}{A}\,\dfrac{L_1}{L_2}} \quad \ldots\ldots\ldots (41b)$$

Since the domain (2) is the shallower domain, L_2 is always smaller than L_1, and α_1 always has a definite value. But α_2 tends to be infinite if the wave arrives at an increase of depth at an angle δ_2 such that $(\sin\delta_2)$ tends to $\left(\dfrac{L_2}{L_1}\right)$. In the same time, δ_2 tends to $\frac{\pi}{2}$. If $(\sin\delta_2)$ is greater than $\dfrac{L_2}{L_1}$, that is $\sin\delta_2 > \dfrac{L_2}{L_1}$, there is total reflection at the discontinuity. In practice, such a wave diffracts in the deeper domain. The anology of this phenomena with light arriving at a medium of a different refraction index is evident.[11]

This particular solution has been considered to protect the mouth of a harbor from agitation, but it does not offer a very practical solution because of the cost of maintenance by dredging.

EXPERIMENTAL VERIFICATION

The most complete verification of this theory has been made by studying the agitation in a basin, that is, between two discontinuities. Indeed, a theo-

---

11 "Étude de la houle en profondeur finie-Note sur la réflexion totale," by Carlotti, La Houille Blanche, Mars and Avril, 1947, pp. 112-116.

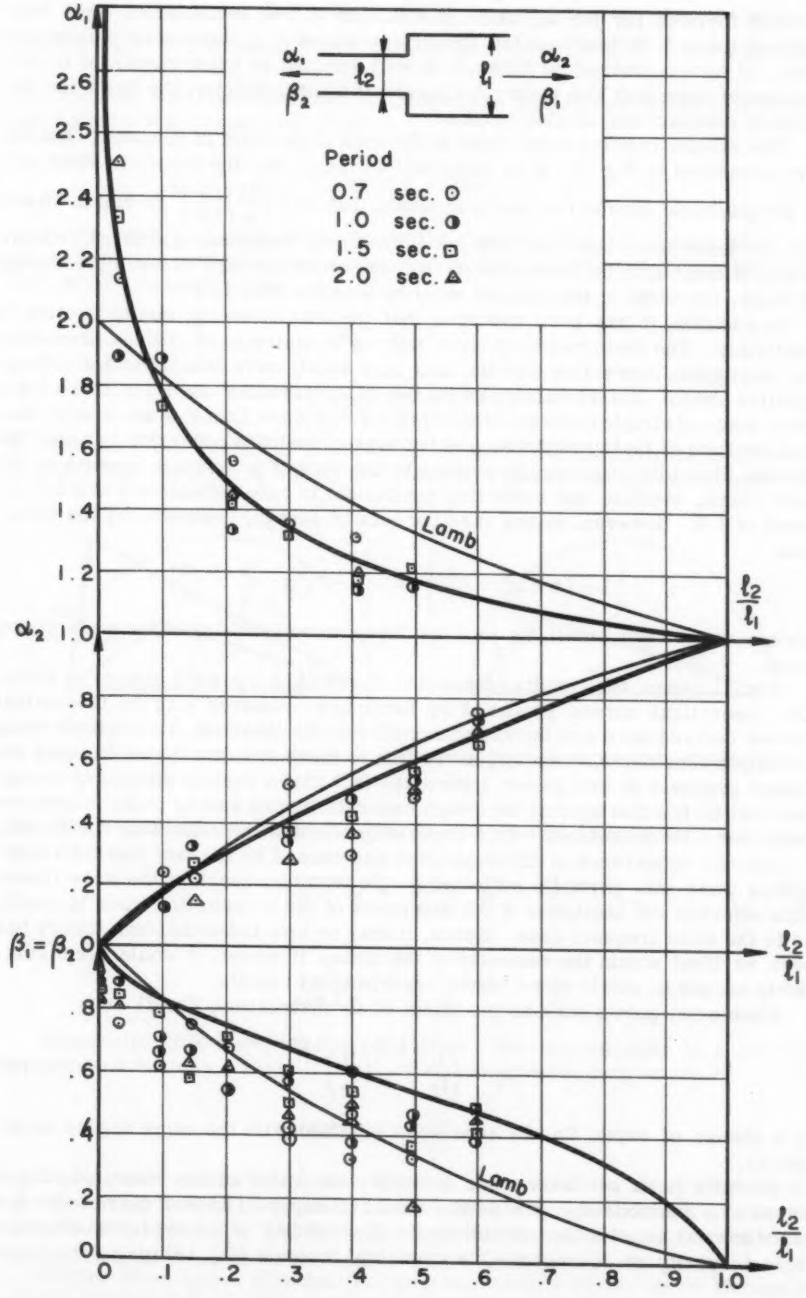

FIG. 11.—EXPERIMENTAL RESULTS IN THE CASE OF A CHANGE OF WIDTH.

retical formula for the agitation in a harbor will be established. This theoretical formula is based on the theory for waves at a discontinuity presented here. If such a theoretical formula is well verified by experiments, it is consequently true that the theory for waves at a discontinuity, the basis for this further computation, is also verified.

The results of some tests made at Queen's University in Kingston, Ontario, are presented in Fig. 11. It is important to recall that the theory is valid only if the quadratic convective inertia is small, that is if $\left(\frac{2a}{L}\right)\left(\frac{L}{h}\right)^3$ is small. Hence all the tests have been carried out with small steepness and large relative depth. It must also be remembered that, except in the case of a simple change of depth, the width of the channel must be smaller than L/2.

In addition, it has been assumed that the loss of energy due to friction is negligible. The main way to achieve this, is to maintain conditions prevailing for negligible convective inertia, that is, a small wave steepness and a large relative depth. Unfortunately, since the discontinuities used for these tests were made of simple concrete blocks placed in a wave flume, some energy was lost because of their roughness and because of the leaks occurring between the blocks. This loss of energy is evident in the case of a complete closure of the wave flume, because the reflection coefficient is only between 0.8 and 0.9 instead of 1.0. However, in any case the loss of energy, computed by the formulas

$$\left[1 - \left(A\, Z\, \alpha_1^2 + \beta_1^2\right)\right] \quad \text{or} \quad \left[1 - \left(\frac{1}{A\, Z}\, \alpha_2^2 + \beta_2^2\right)\right]$$

always stays very small, as long as there is no breaking of the wave at any point.

Fig. 11 shows the results obtained in the case of a simple change of width. The theoretical curves proposed by Lamb are compared with the theoretical curves derived here and the experimental results obtained. Although not being definitely conclusive, it seems, according to these results, better to adopt the values proposed in this paper. Indeed, the fact that a certain amount of energy was lost by friction against the rough concrete blocks and by leaks in between them must be considered. This especially effected the reflection coefficient.

Another occurrence of discrepancies was caused by the fact that the transmitted wave was partially reflected on the terminal beach of the wave flume. This effect is not negligible if the steepness of the transmitted wave is small, as in the most frequent case. Hence, it may be concluded that this theory has been verified within the accuracy of the tests. However, it would seem relatively simple to obtain some better experimental results.

Some other points such as the effect of an obstruction, Eq. 21 or

$$\alpha_1 = \left(\frac{b}{l_2}\right)^{1/2}\left(\frac{l_1}{l_2}\right)^{1/2} \quad \ldots\ldots\ldots\ldots\ldots\ldots (42)$$

or a change of depth, Eq. 25 have been verified with the same degree of accuracy.

No tests have yet been made to verify the value of the theory of oblique waves at a discontinuity. The author would be happy to know if there exist any experimental results that demonstrate the validity of his theory and further tests to verify or to improve his empirical formula (Eq. 19) giving the value of α_1.

It seems that many theoretical results are valid, even when the width is greater than $\frac{L}{2}$; dimensionless factors such as: $\left(\frac{l_1}{L_1}\right), \left(\frac{l_2}{L_2}\right)$ could be taken into account, with the condition that there are no dysymmetrical effects that may cause a transverse resonance.

LOSS OF ENERGY

In the case of a loss of energy at the discontinuity, the relationships obtained from the continuity principle (Eqs. 2a and 2b) are still valid. However, because of the energy loss

$$A\,Z\,\alpha_1^2 + \beta_1^2 < 1$$

$$\frac{1}{A\,Z}\,\alpha_2^2 + \beta_2^2 < 1$$

In this case, the graphical representation has to be modified as is shown by Fig. 12. The theoretical limits are obtained when α_1 and α_2 tend to zero, and

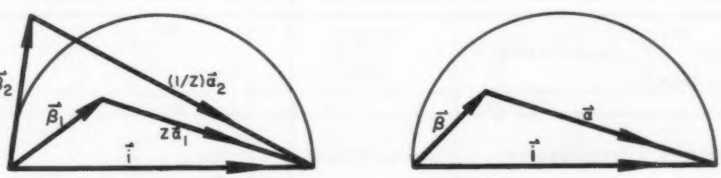

FIG. 12.—VECTORIAL GRAPHICAL REPRESENTATION WITH LOSS OF ENERGY.

the theoretical maximum loss of energy on a located discontinuity is equal to 1/2, when

$$\sqrt{A\,Z}\,\alpha_1 = \frac{1}{2} \qquad \beta_1 = \frac{1}{2} \qquad \text{.......... (43)}$$

or

$$\frac{\alpha_2}{\sqrt{A\,Z}} = \frac{1}{2} \qquad \beta_2 \quad \frac{1}{2} \qquad \text{.......... (44)}$$

Physically, this case could be conceived if the discontinuity is a pervious obstruction such as a rockfill breakwater submitted to long waves.[12]

ACKNOWLEDGMENTS

The author wishes to express his deep appreciation to Mr. F. Biesel, Engineer at Sogreah, in (Grenoble, France) for his advice and help in carrying out the initial study; to Mr. R. J. Kennedy for his encouragement and for his

12 "The Perviousness of Rockfill Breakwater to Gravity Waves," by Le Méhauté, La Houille Blanche, Vol. 12, 1957, p. 903; Vol. 13, 1958, p. 148; Vol. 13, 1958, p. 255.

TABLE 1

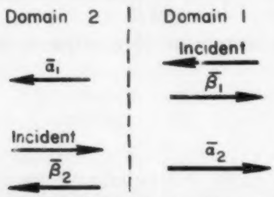	NOTATION	THEORETICAL GENERAL FORMULAE $f(A, Z, \alpha_1)$
Coefficient in case of Change of Depth & Width.	Z	$\frac{L_2 l_2}{L_1 l_1}$
Coefficient in case of Change of Depth.	A	$\frac{1 + \frac{2m_2h_2}{\sinh 2m_2h_2}}{1 + \frac{2m_1h_1}{\sinh 2m_1h_1}}$
Coef of Transmission in Domain 2.	α_1	
Coef. of Transmission in Domain I.	α_2	AZa_1
Phase of Transmission	$\cos a_1 (= \cos a_2)$	$\frac{a_1}{2}(A + Z)$
Coef. of Reflection	$\beta_1 \ (= \beta_2)$	$(1 - AZa_1)^{1/2}$
Phase of Reflection in Domain I.	$\cos \hat{\beta}_1$	$\frac{2 - Za_1^2 \ (A + Z)}{2(1 - AZa_1^2)^{1/2}}$
Phase of Reflection in Domain 2.	$\cos \hat{\beta}_2$	$\frac{2 - a_1^2 (A + Z)}{2(1 - AZa_1^2)^{1/2}}$
GRAPHICAL REPRESENTATION		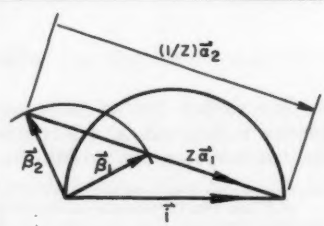

TABLE 2

	Obstruction $\ell_1 = \ell_2 = \ell$ $h_1 = h_2 = h$	Change of Width $b = \ell_2$ $h_1 = h_2 = h$	Obstruction Change of Width $h_1 = h_2 = h$
	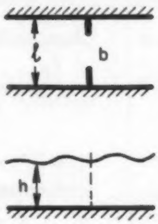	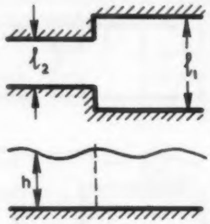	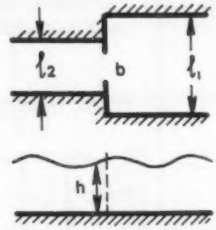
Z	1	$\frac{\ell_2}{\ell_1}$	$\frac{\ell_2}{\ell_1}$
A	1	1	1
a_1	$\left[\frac{b}{\ell}\right]^{1/2}$	$\left[\frac{\ell_1}{\ell_2}\right]^{1/4}$	$\left[\frac{b}{\ell_2}\right]^{1/2}\left[\frac{\ell_1}{\ell_2}\right]^{1/4}$
a_2	$\left[\frac{b}{\ell}\right]^{1/2}$	$\left[\frac{\ell_2}{\ell_1}\right]^{3/4}$	$\left[\frac{b}{\ell_1}\right]^{1/2}\left[\frac{\ell_2}{\ell_1}\right]^{1/4}$
$\cos \hat{a}_1 = \cos \hat{a}_2$	$\left[\frac{b}{\ell}\right]^{1/2}$	$\frac{1}{2}\left[\frac{\ell_1}{\ell_2}\right]^{1/4}\left[1 + \frac{\ell_2}{\ell_1}\right]$	$\frac{1}{2}\left[\frac{b}{\ell_2}\right]^{1/2}\left[\frac{\ell_1}{\ell_2}\right]^{1/4}\left[1 + \frac{\ell_2}{\ell_1}\right]$
$\beta_1 = \beta_2$	$\left[\frac{b-\ell}{\ell}\right]^{1/2}$	$\left[1 - \left\{\frac{\ell_2}{\ell_1}\right\}^{1/2}\right]^{1/2}$	$\left[1 - \frac{b}{(\ell_1 \ell_2)^{1/2}}\right]^{1/2}$
$\cos \hat{\beta}_1$	$\left[\frac{b-\ell}{\ell}\right]^{1/2}$	$\frac{2 - \left[\frac{\ell_2}{\ell_1}\right]^{1/2}\left[1 + \frac{\ell_2}{\ell_1}\right]}{2\beta_1}$	$\frac{2 - \left[\frac{b}{\ell_1}\right]\left[\frac{\ell_2}{\ell_1}\right]^{1/2}\left[1 + \frac{\ell_2}{\ell_1}\right]}{2\beta_1}$
$\cos \hat{\beta}_2$	$\left[\frac{b-\ell}{\ell}\right]^{1/2}$	$\frac{2 - \left[\frac{\ell_1}{\ell_2}\right]^{1/2}\left[1 + \frac{\ell_2}{\ell_1}\right]}{2\beta_1}$	$\frac{2 - \left[\frac{b}{\ell_1}\right]\left[\frac{\ell_1}{\ell_2}\right]^{1/2}\left[1 + \frac{\ell_2}{\ell_1}\right]}{2\beta_1}$
Graph	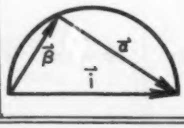	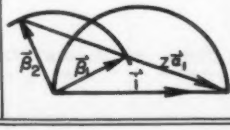	Same as General Case.

TABLE 3

	Change of Depth $b = \ell$ $\ell_1 = \ell_2 = \ell$: any value	Obstruction and Change of Depth $\ell_1 = \ell_2 = \ell$	Change of Width and Depth $b = \ell_2$
	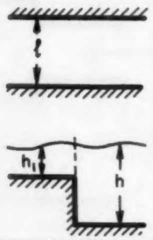	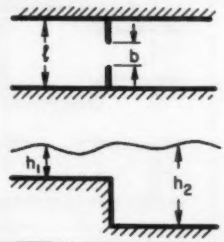	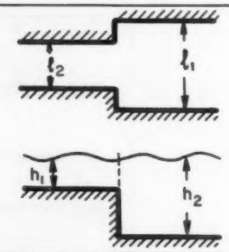
Z	$\frac{L_2}{L_1}$	$\frac{L_2}{L_1}$	$\frac{L_2 \ell_2}{L_1 \ell_1}$
A	$\frac{1 + \frac{2m_2h_2}{\sinh 2m_2h_2}}{1 + \frac{2m_1h_1}{\sinh 2m_1h_1}}$	Same as Previous Case.	Same as Previous Case.
a_1	$\frac{2}{1 + A\frac{L_2}{L}}$	$\left[\frac{b}{\ell}\right]^{1/2} \frac{2}{1 + A\frac{L_2}{L_1}}$	$\left[\frac{\ell_1}{\ell_2}\right]^{1/4} \frac{2}{1 + A\frac{L_2}{L_1}}$
a_2	$\frac{2}{1 + \frac{1}{A}\frac{L_1}{L_2}}$	$\left[\frac{b}{\ell}\right]^{1/2} \frac{2}{1 + \frac{1}{A}\frac{L_1}{L_2}}$	$\left[\frac{\ell_2}{\ell_1}\right]^{3/4} \frac{2}{1 + \frac{1}{A}\frac{L_1}{L_2}}$
$\cos \hat{a}_1$ $(=\cos \hat{a}_2)$	$\hat{a}_1 = \hat{a}_2 = 0$	$\left[\frac{b}{\ell}\right]^{1/2} \frac{A + Z}{1 + A\frac{L_2}{L_1}}$	$\left[\frac{\ell_1}{\ell_2}\right]^{1/4} \frac{2(A + Z)}{1 + A\frac{L_2}{L_1}}$
$\beta_1 = \beta_2$	$\frac{1 - A\frac{L_2}{L_1}}{1 + A\frac{L_2}{L_1}}$	$\left[1 - \frac{b}{\ell} \frac{4AZ}{\left[1 + A\frac{L_2}{L_1}\right]^2}\right]^{1/2}$	$\left[1 - \left[\frac{\ell_1}{\ell_2}\right]^{1/2} \frac{4AZ}{\left[1 + A\frac{L_2}{L_1}\right]^2}\right]^{1/2}$
$\cos \hat{\beta}_1$	$\hat{\beta}_1 = 0$	$\left[1 - \frac{b}{\ell} \frac{2Z(A + Z)}{\left[1 + A\frac{L_2}{L_1}\right]^2}\right] \Big/ \beta_1$	$\frac{2 - Za_1^2(A + Z)}{2\beta_1}$
$\cos \beta_2$	$\beta_2 = \pi$	$\left[1 - \frac{b}{\ell} \frac{2Z(A + Z)}{\left[1 + A\frac{L_2}{L_1}\right]^2}\right] \Big/ \beta_1$	$\frac{2 - a_1^2(A + Z)}{2\beta_1}$
	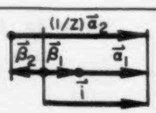	Same as General Case.	Same as General Case.

TABLE 4

	Obstruction Change of Depth and Width	Limit Case $b \to 0$	Limit Cases $\ell_2 \to 0$ $h_2 \to 0$	Pervious Wall $\ell_1 = \ell_2 = \ell$ $h_1 = h_2 = h$
	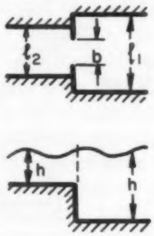	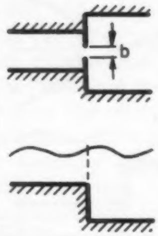	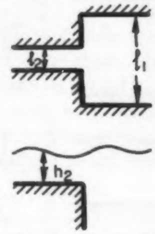	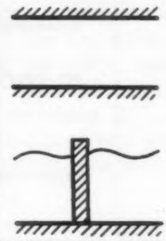
Z	$\frac{L_2 \ell_2}{L_1 \ell_1}$	$\frac{L_2 \ell_2}{L_1 \ell_1}$	$\frac{L_2}{L_1} \to 0$; $\frac{\ell_2}{\ell_1} \to 0$	1
A	$\frac{1 + \frac{2m_2h_2}{\sinh 2m_2h_2}}{1 + \frac{2m_1h_1}{\sinh 2m_1h_1}}$	Same as General Case.	Same as General Case.	1
a_1	$\left[\frac{b}{\ell_2}\right]^{1/2}\left[\frac{\ell_1}{\ell_2}\right]^{1/4}\frac{2}{1+A\frac{L_2}{L_1}}$	$\to 0$	$\to 2$; $\to \infty$ (limit steepness)	$a_1 = a_2 = a$
a_2	$\left[\frac{b}{\ell_1}\right]^{1/2}\left[\frac{\ell_2}{\ell_1}\right]^{1/4}\frac{2}{1+\frac{1}{A}\frac{L_1}{L_2}}$	$\to 0$	$\to 0$	
$\cos \hat{a}_1$ $(=\cos \hat{a}_2)$	$\frac{a_1}{2}(A + Z)$	$a_1 = a_2 \to \frac{\pi}{2}$	$a_1 = a_2 = 0$; $a_1 = a_2 \to 0$	
$\beta_1 = \beta_2$	$\left[1 - AZa_1^2\right]^{1/2}$	$\to 1$ Total Reflection	1 Total Reflection	$\beta_1 = \beta_2 = \beta$
$\cos \hat{\beta}_1$	$\frac{2 - Za_1^2(A+Z)}{2\beta_1}$	$\hat{\beta}_1 \to 0$ with a loop	$\hat{\beta}_1 = 0$ with a loop	$\bar{a} + \bar{\beta} = \bar{1}$ $a^2 + \beta^2 < 1$
$\cos \hat{\beta}_2$	$\frac{2 - a_1^2(A+Z)}{2\beta_1}$	$\hat{\beta}_2 \to 0$ with a loop	$\hat{\beta}_2 = \pi$ with a node	
Graph	Same as General Case.	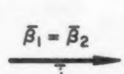	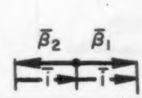	

TABLE 5

	Pervious Wall & Change of Depth & Width	Wave at an Angle Change of Depth $\ell = \infty$	
	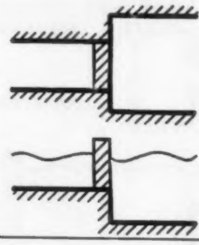	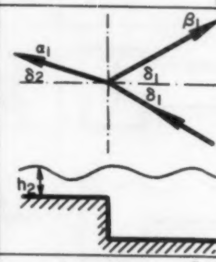	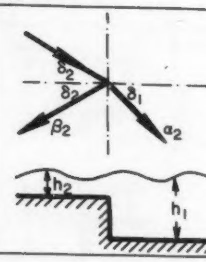
Z	$\frac{L_2 \ell_2}{L_1 \ell_1}$	$\frac{L_2\left[1-\left\{\frac{L_2}{L_1}\sin\delta_1\right\}^2\right]^{1/2}}{L_1\cos\delta_1}$	$= \frac{L_2\cos\delta_2}{L_1\left[1-\left\{\frac{L_1}{L_2}\sin\delta_2\right\}^2\right]^{1/2}}$
A	$\frac{1+\frac{2m_2h_2}{\sinh 2m_2h_2}}{1+\frac{2m_1h_1}{\sinh 2m_1h_1}}$	Same as Previous Case.	
a_1		$\left[\frac{\cos\delta_1}{\left[1-\left\{\frac{L_2}{L_1}\sin\delta_1\right\}^2\right]^{1/2}}\right]^{3/4}\frac{2}{1+A\frac{L_2}{L_1}}$	
a_2		$\left[\frac{\cos\delta_2}{\left[1-\left\{\frac{L_1}{L_2}\sin\delta_2\right\}^2\right]^{1/2}}\right]^{1/4}\frac{2}{1+\frac{1}{A}\frac{L_1}{L_2}}$	
$\cos\alpha_1$ $(=\cos\alpha_2)$		$\frac{a_1}{2}(A+Z')$	
$\beta_1=\beta_2$	$Z\bar{a}_1+\bar{\beta}_1=\bar{1}$	$\left[1-AZ'a_1^2\right]^{1/2}$	If $\sin\delta_2>\frac{L_2}{L_1}$ $\beta_2=1$ Total Reflection
$\cos\beta_1$	$(1/Z)\bar{a}_2+\bar{\beta}_2=\bar{1}$ $AZa_1^2+\beta_1^2<1$	$\frac{2-a_1^2(A+Z)}{2\beta_1}$	
$\cos\beta_2$	$\frac{1}{AZ}a_2^2+\beta_2^2<1$	$\frac{2-Za_1^2(A+Z)}{2\beta_1}$	
	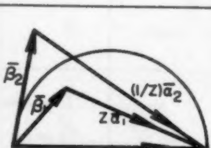	Same as General Case.	

kind permission to use the laboratory facilities of Queen's University, in (Kingston); and to Mr. Trinh Ngoc Quynh of École Polytéchnique of Montreal and Mr. J. I. Collins of Queen's University for their assistance.

APPENDIX I. MATHEMATICAL DEVELOPMENT

Continuity Principle.—We will assume that the discharge of incident and reflected waves in domain (1) is equal to the discharge of the transmitted wave in domain (2) on the discontinuity at any time. It is natural to make this assumption, for if this were not the case, a quantity of water would successively be accumulated near the discontinuity and would issue from it.

The discharge is the product of the velocity times the cross sectional area (depth times width). The velocity μ is a function of the vertical abcissa y. Hence, the discharge could be written

$$l \int_{y=o}^{y=h} u(y)\ dy \quad \ldots\ldots\ldots\ldots\ldots\ldots\ldots \quad (45)$$

in which l is a constant width and h the depth of the considered cross section.

Now assuming that the domains (1) and (2) have constant widths l_1 and l_2, and constant depths h_1 and h_2, respectively, the continuity principle is given by equating the value of the discharge in the two domains at the discontinuity. That is

$$l_1 \int_o^{h_1} u_1(y)\ dy = l_2 \int_o^{h_2} u_2(y)\ dy \quad \ldots\ldots\ldots\ldots \quad (46)$$

Assuming that the motions in domains (1) and (2) are defined by the potential functions ϕ_1 and ϕ_2, respectively, and that the horizontal x-axis origin coincides with the discontinuity, $u_1(y)$ and $u_2(y)$ could be expressed as a function of ϕ_1 or ϕ_2 as follows:

$$u_1(y) = \left(\frac{\partial \phi_1}{\partial x}\right)_{x=o} \quad \ldots\ldots\ldots\ldots\ldots (46a)$$

$$u_2(y) = \left(\frac{\partial \phi_2}{\partial x}\right)_{x=o} \quad \ldots\ldots\ldots\ldots\ldots (46b)$$

Hence, the continuity relationship becomes:

$$l_1 \int_o^{h_1} \left(\frac{\partial \phi_1}{\partial x}\right)_{x=o} dy = l_2 \int_o^{h_2} \left(\frac{\partial \phi_2}{\partial x}\right)_{x=o} dy \ldots \quad (47)$$

The potential function ϕ_1 is given by the sum of the potential function of an incident periodical gravity wave of amplitude 2a travelling towards the discontinuity and the potential function of a reflected wave of amplitude 2a x β_1 travelling seawards and having a difference of phase $\hat{\beta}_1$ at the discontinuity. Hence, ϕ_1 may be written $\left(h = \frac{2\pi}{T},\ m = \frac{2\pi}{L}\right)$

$$\phi_1 = -a \frac{h}{m_1} \cdot \frac{\cosh m_1 (h_1 + y)}{\sinh m_1 h_1} \sin (h t - m_1 \alpha)$$

$$- a \beta_1 \frac{h}{m_1} \cdot \frac{\cosh m_1 (h_1 + y)}{\sinh m_1 h_1} \sin (h t + m_1 \alpha + \hat{\beta}_1) \quad \ldots (48)$$

The potential function ϕ_2 is that of a wave of amplitude 2a x α_1, travelling in the same direction as the incident wave and having a phase difference $\hat{\alpha}_1$ with the incident wave at the discontinuity;

$$\phi_2 = -a \alpha_1 \frac{h}{m_2} \frac{\cosh m_2 (h_2 + y)}{\sinh m_2 h_2} \sin (ht - m_2 \alpha + \hat{\alpha}_1) \quad \ldots\ldots (49)$$

Hence,

$$\left(\frac{\partial \phi_1}{\partial \alpha}\right)_{\alpha=o} = a \frac{\cosh m_1 (h_1 + y)}{\sinh m_1 h_1} \left[\cos ht - \beta_1 \cos (ht + \hat{\beta}_1)\right] \quad \ldots (50)$$

and

$$\left(\frac{\partial \phi_2}{\partial \alpha}\right)_{\alpha=o} = a \frac{\cosh m_2 (h_2 + y)}{\sinh m_2 h_2} \left[\alpha_1 \cos (ht + \hat{\alpha}_1)\right] \quad \ldots\ldots\ldots (51)$$

Introducing these values in Eq. 46 since

$$\int_o^h \frac{\cosh m(h + y)}{\sinh m h} dy = \frac{1}{m} = \frac{L}{2\pi} \quad \ldots\ldots\ldots (52)$$

we obtain

$$l_1 L_1 \left[\cos ht - \beta_1 \cos (ht + \hat{\beta}_1)\right] = l_2 L_2 \alpha_1 \cos (ht + \hat{\alpha}_1)$$

Assuming that h t = 0 and h t = $\frac{\pi}{2}$, successively, leads to

$$l_1 L_1 \left[1 - \beta_1 \cos \hat{\beta}_1\right] = l_2 L_2 \alpha_1 \cos \hat{\alpha}_1 \quad \ldots\ldots\ldots (53a)$$

$$l_1 L_1 \left[0 - \beta_1 \sin \hat{\beta}_1\right] = l_2 L_2 \alpha_1 \sin \hat{\alpha}_1 \quad \ldots\ldots\ldots (53b)$$

or

$$Z \bar{\alpha}_1 + \bar{\beta}_1 = \bar{1} \quad \ldots\ldots\ldots\ldots\ldots\ldots (54)$$

in which

$$Z = \frac{l_2 L_2}{l_1 L_1} \quad \ldots\ldots\ldots\ldots\ldots\ldots (55)$$

Similarly, considering an incident wave from the opposite direction we find

$$\frac{1}{Z} \bar{\alpha}_2 + \bar{\beta}_2 \quad \bar{1} \quad \ldots\ldots\ldots\ldots\ldots\ldots (56)$$

Already, one can see the eight parameters will be functions of the period (included in Z), except in shallow

water, $Z = \frac{l_2}{l_1}\sqrt{\frac{h_2}{h_1}}$, and in infinite depth, or, if the depths of the two domains

are equal $Z = \frac{l_2}{l_1}$

Conservation of Energy.—The transmitted energy of a periodical gravity wave of amplitude 2 a and with a length of crest equal to l is

$$\frac{1}{2} \rho g \frac{L}{T} a^2 l \left(1 + \frac{2 m h}{\sinh 2 m h}\right) \quad \ldots\ldots\ldots\ldots \quad (57)$$

per unit of time.

On the other hand, the most important loss of energy at the discontinuity is due to the convective inertia. Since this force is negligible, one may neglect the loss of energy and equate the incident wave energy to the sum of the reflected energy and the transmitted energy. To simplify the writing we introduce the new symbols

$$A_1 = 1 + \frac{2 m_1 h_1}{\sinh 2 m_1 h_1} \quad \ldots\ldots\ldots\ldots \quad (58a)$$

$$A_2 = 1 + \frac{2 m_2 h_2}{\sinh 2 m_2 h_2} \quad \ldots\ldots\ldots\ldots \quad (58b)$$

The conservation of energy principle may be written as follows

Incident energy = reflected energy + transmitted energy

$$a^2 l_1 L_1 A_1 = (a \beta_1)^2 l_1 L_1 A_1 + (a \alpha_1)^2 l_2 L_2 A_2$$

Dividing by $a^2 l_1 L_1 A_1$ and introducing Z and $A = \frac{A_2}{A_1}$ yields

$$A Z \alpha_1^2 + \beta_1^2 = 1 \quad \ldots\ldots\ldots\ldots \quad (59)$$

Similarly, for a wave from the opposite direction

$$\frac{1}{A Z} \alpha_2^2 + \beta_2^2 = 1 \quad \ldots\ldots\ldots\ldots \quad (60)$$

Now, if we consider two waves of the same period but arriving from the two oppostie directions, with height 2 a_1 and 2 a_2 and with any phase difference, the conservation of energy principle takes the form

$$A_1 l_1 L_1 |\bar{a}_1|^2 + A_2 l_2 L_2 |\bar{a}_2|^2 =$$

$$A_1 l_1 L_1 |\bar{a}_1 \bar{\beta}_1 + \bar{a}_2 \bar{\alpha}_2|^2 + A_2 l_2 L_2 |\bar{a}_1 \bar{\alpha}_1 + \bar{a}_2 \bar{\beta}_2|^2 \quad \ldots\ldots \quad (61)$$

that is

$$A_1 l_1 L_1 |\bar{a}_1|^2 + A_2 l_2 L_2 |\bar{a}_2|^2 =$$

$$a_1^2 \left(A_1 l_1 L_1 \beta_1^2 + A_2 l_2 L_2 \alpha_1^2\right) + a_2^2 \left(A_1 l_1 L_1 \beta_2^2 + A_2 l_2 L_2 \alpha_2^2\right)$$

$$- 2 A_1 l_1 L_1 a_1 a_2 \beta_1 \alpha_2 \cos\left(\widehat{a}_1 + \widehat{\beta}_1 - \widehat{a}_2 - \widehat{\alpha}_2\right)$$

$$- 2 A_2 l_2 L_2 a_1 a_2 \alpha_1 \beta_2 \cos\left(\widehat{a}_1 + \widehat{\alpha}_1 - \widehat{a}_2 - \widehat{\beta}_2\right) \quad \ldots\ldots\ldots \quad (62)$$

that can be written

$$A_1 l_1 L_1 a_1^2 + A_2 l_2 L_2 a_2^2 =$$

$$A_1 l_1 L_1 a_1^2 \left(A Z \alpha_1^2 + \beta_1^2\right) + A_2 l_2 L_2 a_2^2 \left(\frac{1}{A Z} \alpha_2^2 + \beta_2^2\right)$$

$$- 2 a_1 a_2 \left[A_1 l_1 L_1 \alpha_2 \beta_1 \cos\left(\widehat{a}_1 - \widehat{a}_2 + \widehat{\beta}_2 - \widehat{\alpha}_2\right)\right.$$

$$\left. + A_2 l_2 L_2 \alpha_1 \beta_2 \cos\left(\widehat{a}_1 - \widehat{a}_2 + \widehat{\alpha}_1 - \widehat{\beta}_2\right)\right] \ldots\ldots\ldots\ldots \quad (63)$$

Simplifying with respect to Eqs. 58 and 59, we obtain

$$\alpha_2 \beta_1 \cos\left(\widehat{a}_1 - \widehat{a}_2 + \widehat{\beta}_1 - \widehat{\alpha}_2\right) + A Z \alpha_1 \beta_2 \cos\left(\widehat{a}_1 - \widehat{a}_2 + \widehat{\alpha}_1 - \widehat{\beta}_2\right) = 0 \ldots \quad (64)$$

This relationship must be verified for any value, $\left(\widehat{a}_1 - \widehat{a}_2\right)$.

Assuming that $\widehat{a}_1 - \widehat{a}_2 = 0$, $\widehat{a}_1 - \widehat{a}_2 = \frac{\pi}{2}$ successively, we find

$$\widehat{\alpha}_2 - \widehat{\beta}_1 = \widehat{\beta}_2 - \widehat{\alpha}_1 + \pi \; (+ 2 n \pi) \ldots\ldots\ldots\ldots \quad (65a)$$

or

$$\widehat{\alpha}_2 - \widehat{\beta}_2 = -\left(\widehat{\alpha}_1 - \widehat{\beta}_2\right) + \pi \; (+ 2 n \pi) \ldots\ldots\ldots\ldots \quad (65b)$$

(The solution $\widehat{\alpha}_2 - \widehat{\beta}_1 = \widehat{\beta}_2 - \widehat{\alpha}_1 (+ 2 n \pi)$ must be eliminated, α_1, β_1, α_2, β_2 always being positive.) We also obtain

$$\alpha_2 \beta_1 = A Z \alpha_1 \beta_2 \ldots\ldots\ldots\ldots \quad (66a)$$

or

$$\frac{\alpha_2}{\beta_2} = A Z \frac{\alpha_1}{\beta_1} \ldots\ldots\ldots\ldots \quad (66b)$$

The two vectorial equalities, Eqs. 53 and 55 being identical to four algebraic equations, the system formed by Eqs. 53, 55, 58, 59, and 65b gives seven independent equations with eight unknowns. (Indeed, it is easy to demonstrate that Eq. 64b depends on the others.) Therefore, it is possible to express the eight coefficients: α_1, $\widehat{\alpha}_1$, β_1, $\widehat{\beta}_1$, α_2, $\widehat{\alpha}_2$, β_2, $\widehat{\beta}_2$ as a function of only one (for instance α_1), and there exist some other noticeable relations. From the preceding equalities involving energy conservation

$$\frac{\alpha_2}{\beta_2} = A Z \frac{\alpha_1}{\beta_1} \ldots\ldots\ldots\ldots \quad (67)$$

and

$$A Z \alpha_1^2 + \beta_1^2 = \frac{1}{A Z} \alpha_2^2 + \beta_2^2 = 1 \ldots\ldots\ldots\ldots \quad (68)$$

we deduce easily:

$$\alpha_2 = A Z \alpha_1 \ldots\ldots\ldots\ldots \quad (69)$$

and

$$\beta_1 = \beta_2 = \left(1 - A Z \alpha_1^2\right)^{\frac{1}{2}} \ldots\ldots\ldots\ldots \quad (70)$$

Continuity Principle and Energy Conservation Principle.—From the continuity relationship we find, seccessively, for the first incident wave (Fig. (13)

$$Z^2 \alpha_1{}^2 = 1 + \beta_1{}^2 - 2 \beta_1 \cos \hat{\beta_1} \quad \ldots\ldots\ldots\ldots\ldots \quad (71)$$

On inserting Eq. 69, deduced from the conservation of energy principle, this yields

$$\cos \hat{\beta_1} = \frac{2 - Z \alpha_1{}^2 (A + Z)}{2 \left(1 - A Z \alpha_1{}^2\right)^{\frac{1}{2}}} \quad \ldots\ldots\ldots\ldots\ldots\ldots \quad (72)$$

On the other hand

$$\beta_1{}^2 = 1 + Z^2 \alpha_1{}^2 - 2 Z \alpha_1 \cos \hat{\alpha_1} \quad \ldots\ldots\ldots\ldots \quad (73)$$

yields

$$\cos \hat{\alpha_1} = \frac{\alpha_1}{2} (A + Z) \quad \ldots\ldots\ldots\ldots\ldots\ldots\ldots \quad (74)$$

Similarly, for the second incident wave, from Eq. 55 and from the Eqs. 68

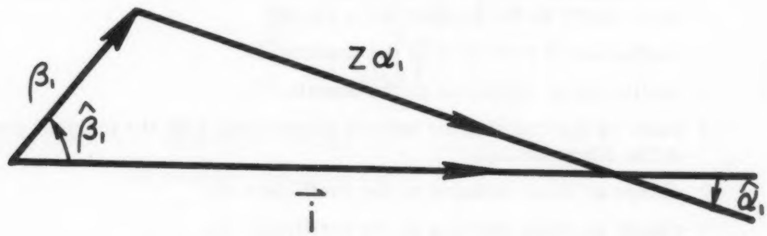

FIG. 13.—VECTORIAL REPRESENTATION OF THE CONTINUTIY PRINCIPLE.

and 69, we find

$$\cos \hat{\beta_2} = \frac{2 - \alpha_1{}^2 (A + Z)}{2 \left(1 - A Z \alpha_1{}^2\right)^{\frac{1}{2}}} \quad \ldots\ldots\ldots\ldots\ldots\ldots \quad (75)$$

and

$$\cos \hat{\alpha_2} = \frac{\alpha_1}{2} (A + Z) \quad \ldots\ldots\ldots\ldots\ldots\ldots\ldots \quad (76)$$

One can see that

$$\cos \hat{\alpha_1} = \cos \hat{\alpha_2} \quad \ldots\ldots\ldots\ldots\ldots\ldots\ldots \quad (77)$$

or that

$$\hat{\alpha_1} = \hat{\alpha_2} \; (+ 2 n \pi) \quad \ldots\ldots\ldots\ldots\ldots\ldots\ldots \quad (78)$$

and Eq. 64b yields

$$\hat{\alpha_1} = \hat{\alpha_2} = \frac{\hat{\beta_1} + \hat{\beta_2}}{2} + \frac{\pi}{2} (+ n \pi) \quad \ldots\ldots\ldots\ldots\ldots \quad (79)$$

The solution $\hat{\alpha}_1 = -\hat{\alpha}_2$ is not possible. Indeed, in this case, Eq. 64b would yield $\hat{\beta}_1 = -\hat{\beta}_2 + \pi\ (+2\,n\,\pi)$ and $\cos\hat{\beta}_1 = -\cos\hat{\beta}_2$. Now, from Eqs. 71 and 74, we could establish a relation between α_1 and Z and A, and all the parameters would be known only as functions of Z and A. This is physically impossible. Indeed, these parameters depend not only on domain characteristics, but also on discontinuity shapes.

APPENDIX II. NOTATION

α : coefficient of transmission at the discontinuity: ratio of transmitted wave height to incident wave height;

α_1 : coefficient of transmission from the domain (1) to the domain (2);

α_2 : coefficient of transmission from the domain (2) to the domain (1);

β : coefficient of reflection at the discontinuity: ratio of the reflected wave height to the incident wave height;

β_1 : coefficient of reflection in the domain (1);

β_2 : coefficient of reflection in the domain (2);

$\hat{\alpha}$: phase of the transmitted wave by comparison with the incident wave at the discontinuity;

$\hat{\alpha}_1$: change of phase relative to the coefficient α_1;

$\hat{\alpha}_2$: change of phase relative to the coefficient α_2;

$\hat{\beta}$: phase of the reflected wave by comparison with the incident wave at the discontinuity;

$\hat{\beta}_1$: relative to the coefficient β_1;

$\hat{\beta}_2$: relative to the coefficient β_2;

$\overline{\alpha}$: complex number of modulus α and argument $\hat{\alpha}$;

$\overline{\beta}$: complex number of modulus β and argument $\hat{\beta}$;

$\overline{1}$: complex number of modulus: $i = 1$, and argument: $\hat{1} = 0$;

$2a_1$: incident wave-height in domain (1);

$\hat{a}_1$: phase of the incident wave in domain (1);

$2a_2$: incident wave-height in domain (2);

$\hat{a}_2$: phase of the incident wave in domain (2);

ϕ_1 : potential function of the motion in the domain (1);

ϕ_2 : potential function of the motion in the domain (2);

0x : horizontal axis;

0y : vertical axis, $y = 0$ at the still water level of the free surface;

$h = \frac{2\pi}{T}$, T : period;

$m = \frac{2\pi}{L}$, L: wave length: $\left(L = \frac{g\,T^2}{2\pi} \tanh \frac{2\,\pi\,h}{L}\right)$;

2a : wave-height of the incident wave;

h : depth of the water;

l : width of the domains;

b : width of the opening of the discontinuity;

l^1 : distance between orthogonals;

δ : angle of oblique wave crest with the line of discontinuity; and

$$Z = \frac{L_2\, l_2}{L_1\, l_1}$$

$$A = \frac{A_2}{A_1} = \left[\frac{1 + \dfrac{2\,m_2\,h_2}{\sinh 2\,m_2\,h_2}}{1 + \dfrac{2\,m_1\,h_1}{\sinh 2\,m_1\,h_1}}\right]$$

subscripts: (1) relative to domain (1)

(2) relative to domain (2)

Journal of the
HYDRAULICS DIVISION
Proceedings of the American Society of Civil Engineers

WATER EDDY FORCES ON OSCILLATING CYLINDERS

By Alan D. K. Laird[1], Charles A. Johnson[2], and Robert W. Walker[3]

SYNOPSIS

Neighboring cylinders may increase drag force on vertical cylinders by 75% or decrease it to mins 20%, and may triple lift forces, for spacing to 3 diameters and cause significant deviations to 10 diameters. Neighboring cylinder eddies cause large force fluctuations.

INTRODUCTION

Recent investigations[4,5] have suggested that eddies formed along piles in ocean waves may make important contributions to wave forces on piling. The present laboratory investigation of these eddy forces is part of a continuing research project being conducted at the University of California in Berkeley.

Note.—Discussion open until April 1, 1961. To extend the closing date one month, a written request must be filed with the Executive Secretary, ASCE. This paper is part of the copyrighted Journal of the Hydraulics Division, Proceedings of the American Society of Civil Engineers, Vol. 86, No. HY 9, November, 1960.

1 Assoc. Prof., Mech. Engrg., Univ. of California, Berkeley, Calif.

2 Research Asst., Inst. of Engrg. Research, Univ. of California, Berkeley, Calif.

3 Research Asst., Inst. of Engrg. Research, Univ. of California, Berkeley, Calif. Presently, Design Engr., Catepillar Tractor Co., Peoria, Ill.

4 "Ocean Wave Forces on Circular Cylindrical Piles," by W. L. Wiegel, K. E. Beebe, and James Moon, Proceedings, ASCE, Vol. 83, April, 1951.

5 "Water Forces on Accelerated Cylinders," by A. D. K. Laird, C. A. Johnson, and R. W. Walker, Proceedings, ASCE, Vol. 85, No. WW 1, March, 1959.

TABLE 1.—RATIOS OF AVERAGED MAXIMUM DRAG FORCES ON TEST CYLINDER WITH PARALLEL NEIGHBORING CYLINDERS, TO MAXIMUM DRAG FORCE ON TEST CYLINDER WITHOUT NEIGHBORS.[a]

(A) Two neighbors symmetrically spaced to left and right of test cylinder (628 runs used).[b,c]

Ahead diameter	To each side, diameter 0.50	0.75	1.00	1.25	1.50	2.00	2.50	3.00	3.50	4.00	4.50	5.00
0.0			1.75	1.47		1.21	1.21	1.21	1.33	1.25	1.27	1.23
0.5		0.46	1.07	1.26	1.17	1.18	1.23	1.31	1.23	1.24	1.47	1.47
1.0	0.41	0.70	0.77	0.96	0.97	1.13	1.18	1.10	1.26	1.10	1.26	1.24
1.5	0.35	0.40	0.79	0.93	0.94	1.08	1.10	1.10	1.33	1.03	1.10	1.17
2.0	0.46	0.86	0.77	1.15	1.08	1.08	1.08	1.08	1.24	1.02	1.15	1.18
2.5	0.55	0.96	0.98	0.74	1.03	0.95	1.03	1.02	1.12	1.02	1.11	1.08
3.0	0.60	0.92	1.11	0.99	0.95	1.11	1.23	1.12	1.20	1.04	1.20	1.09
3.5	0.67	1.14	1.08	0.99	0.88	1.05	1.03	1.03	1.10	1.01	1.17	1.06
4.0	0.72	1.08	1.16	1.12	1.02	1.04	1.07	1.09	1.03	1.09	1.03	1.11
4.5	0.80	0.92	0.99	1.20	0.94	0.94	1.07	1.03	1.09	1.05	1.07	1.05
5.0	0.86	0.94	0.90	1.00	1.19	1.12	1.01	1.08	1.04	1.14	1.02	1.06
5.5	0.86	0.92	1.03	0.88	1.18	0.92	0.92	1.09	1.11	1.07	1.05	1.04
6.0	0.93	0.95	0.79	1.05	0.91	0.98	0.96	1.04	1.11	0.99	0.96	0.99
6.5	0.90	0.97	1.00	0.90	1.03	0.98	1.16	1.00	1.08	1.05	1.08	1.11
7.0	0.92	0.92	0.98	0.91	0.95	0.98	0.99	1.07	1.08	1.01	1.07	1.09
7.5	1.02	1.02	0.95	0.88	1.05	0.96	1.06	1.05	1.12	0.98	1.03	1.04
8.0	0.85	0.91	1.04	0.93	1.00	1.02	1.04	0.98	1.09	1.08	1.05	0.94
8.5	0.93	0.94	0.97	0.90	0.97	0.96	1.04	0.93	1.16	1.06	1.04	1.10
9.0	0.89	0.92	0.95	0.86	0.94	1.04	1.04	1.06	1.12	1.09	0.98	0.98
9.5	0.92	0.90	0.98	0.99	1.02	0.98	0.95	0.96	1.01	1.02	1.00	0.95
10.0	0.99	0.94	0.89	0.88	0.97	1.06	1.05	1.02	1.08	1.03	1.09	0.97
10.5	0.86	0.95	0.91	0.90	0.98	0.97	1.03	0.97	1.03	0.93	1.03	1.03
11.0	0.95	0.95	0.97	0.94	0.90	0.94	0.95	1.04	0.99	1.01	1.04	0.97
11.5	0.85	0.87	0.96	0.98	0.97	0.92	0.85	0.85	1.09	1.03	0.99	0.95
12.0	0.94	0.97	0.93	0.95	1.01	0.99	1.04	0.86	0.97	1.00	0.95	1.04
12.5	0.93	0.96	0.95	0.93	0.99	0.99	1.04	1.11	0.97	1.00	0.96	1.04
13.0	0.85	0.91	0.98	0.96	1.02	1.02	1.06	1.11	1.08	1.01	0.92	0.98

(B) One neighbor (179 runs used).[b,c]

Ahead diameter	To side, diameter 0.0	0.5	.75	1.0	1.25	1.50	2.0	2.5	3.0
0.0				1.44	1.28	1.28	1.30	1.29	
0.5			1.02	0.93	1.20	0.97	1.16	1.07	1.14
1.0	0.38	0.57	1.02	0.85	1.19	0.98	1.13	1.17	1.24
1.5	0.52	0.84	1.01	0.85	1.23	1.07	1.07	1.00	1.17
2.0	0.64	0.98	1.23	1.12	1.31	1.06	0.99	1.10	1.21
2.5	0.81	0.95	1.29	1.00	1.22	1.07	1.03	1.13	1.16
3.0	0.87	1.03	1.26	0.97	1.07	1.01	1.02	0.97	1.12
3.5	0.88	0.90	0.95	0.95	0.97	0.94	1.01	1.05	1.11
4.0	1.00	0.96	0.98	0.93	1.14	0.93	0.94	1.10	1.16
4.5	0.96	0.96	0.96	0.94	0.98	0.96	0.88	0.95	1.07
5.0	1.02	0.96	0.98	1.08	1.10	1.03	1.06	1.09	
5.5	1.00	1.00	1.01	1.12	1.04	1.06	1.15	1.04	1.09
6.0	0.92	1.12	0.87	1.06	1.00	1.04	1.06	1.03	
6.5	0.90	0.98	1.03	1.11	0.97	1.01	1.05	1.07	1.11
7.0	0.93	0.96	1.03	1.02	1.00	1.03	0.97	1.00	1.13
7.5	1.08	1.10	1.07	1.11	1.01	1.15	1.04	1.06	1.04

TABLE 1.—(CONT'D)

(B) One neighbor (179 runs used).[b,c]

Ahead diameter	To side, diameter 0.0	0.5	.75	1.0	1.25	1.50	2.0	2.5	3.0
8.0	0.96								
8.5	0.96								
9.0	0.96								
9.5	0.96								
10.0	1.04								
10.5	0.92								
11.0	0.98								
11.5	0.93								
12.0	0.97								
12.5	1.01								
13.0	0.98								

(C) Two neighbors symmetrically spaced to left and right of test cylinder path (64 runs used).[d,e]

Ahead diameter	To each side, diameter 1	2	4	6	8
0		1.33			
1	0.98		1.09	1.11	
2	1.16	1.17	1.02	1.19	1.16
4	1.21	1.49	1.06	1.26	1.14
6	1.17	1.27	0.97	1.08	1.14
8	1.16		0.96	0.99	1.05
10	0.98	1.02	1.04	1.00	
12	0.97	0.99	0.98	1.02	
14	0.90	1.14			
16		0.99			
18		1.04			

(D) One neighbor (55 runs used).[d,e]

Ahead diameter	To side, diameter 0	1	2	4	6	8
0			1.45	1.17		
1				1.16	1.10	
2	0.48		1.48	0.99	1.14	0.99
4	0.80		1.18	1.01	1.10	1.10
6	0.90		1.32	0.95	1.05	1.09
8	0.89	0.92		0.99	0.98	1.08
10			1.04	1.06	0.99	
12			1.01	1.01	1.02	

[a] Positions of neighbors are given relative to the axis of the test cylinder, in cylinder diameters. Ratios were taken at the bottom of the first swing after release from rest. [b] Cylinder diameter = 2 in. [c] Amplitude of oscillation = 18 in. [d] Cylinder diameter = 1.2 in. [e] Amplitude of oscillation = 6.4 in.

It was the object of this experiment to demonstrate that wave forces on a circular cylinder could be influenced significantly by parallel neighboring cylinders, and particularly by eddies shed by these neighbors.

EXPERIMENTAL EQUIPMENT

The horizontal components of the wave-induced water particle velocities past vertical cylinders were modeled by the motion of the cylinders performing simple harmonic motion in otherwise still water. The heavily weighted four-wire pendulum which was used to produce the motion is shown in Fig. 1 for the

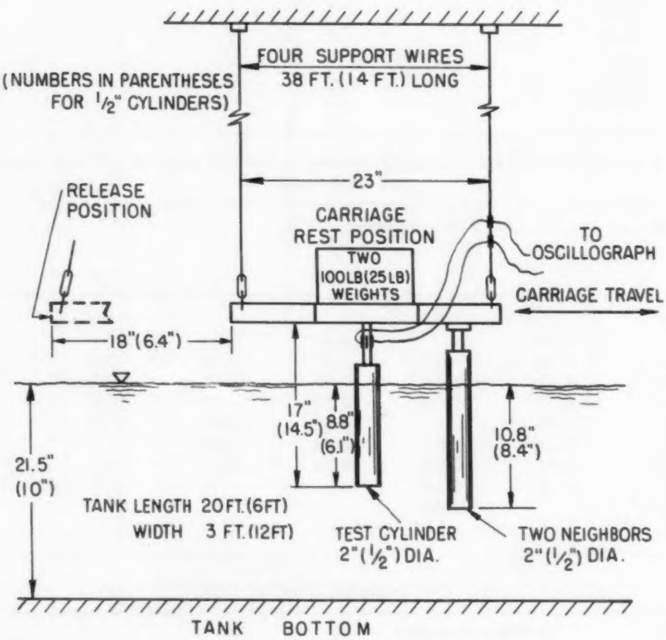

FIG. 1.—APPARATUS DIMENSIONS

1/2-in. and 2-in. cylinders. The test cylinder was mounted on a strain bar at the center of the pendulum frame. As listed in Table 1, the neighboring cylinders of the same diameter as the test cylinder were spaced, with respect to the test cylinder, from touching up to 8 diameters to the side and 18 diameters ahead of the test cylinder in the direction of the first forward swing after release.

For the 1/2-in. cylinder, the strain bar deflections were sensed by a capacity type transducer, and recorded by an oscillograph. Since this strain bar was one-directional, drag and transverse, or lift, forces had to be recorded during different runs by turning the bar through 90°. The forces on the 2-in.

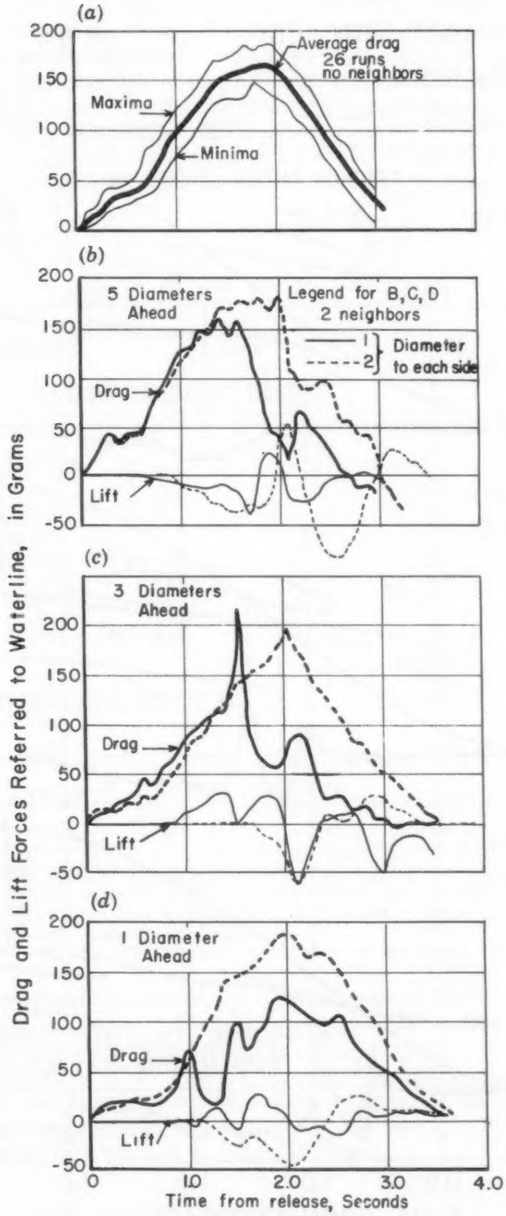

FIG. 2.—RESISTANCE AND LIFT FORCES ON A 2-IN. CYLINDER FOLLOWING TWO NEIGHBORING CYLINDERS FOR COMPARISON WITH SINGLE CYLINDER DRAG FORCES

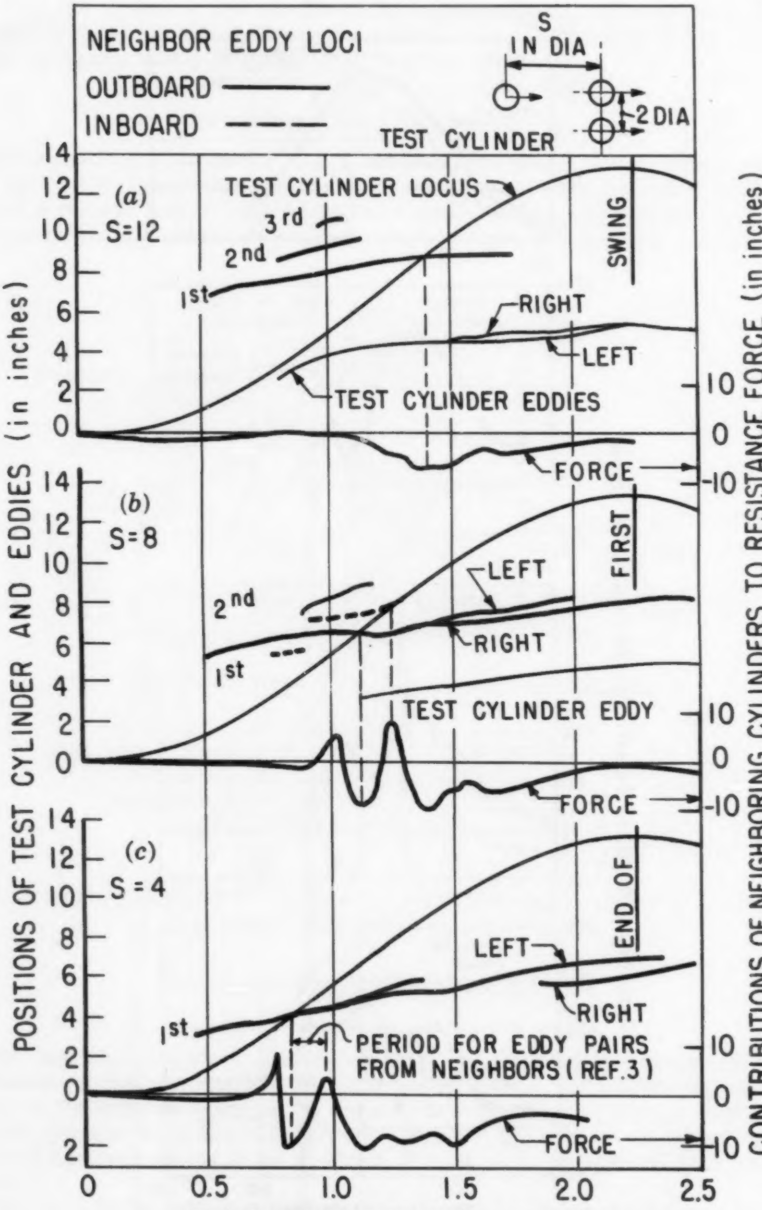

FIG. 3.—TIME POSITION HISTORIES

cylinder were detected by strain gauge bridges and recorded by the oscillograph. Asimultaneous trace from a 2 g accelerometer was recorded with each run of the one-directional bars for both the 1/2-in. and 2-in. test cylinders. About half the runs were taken with a one-directional bar, Introduction of a two-directional strain bar allowed simultaneous recording of drag and transverse forces, but the accelerometer trace was omitted. Calibrations of the strain bars were made before and after each set of runs by applying known forces at the waterline of the test cylinder by means of balanced strings, pulleys, and weights.

TABLE 2.—MAXIMUM FORCES ON 2-IN. TEST CYLINDER, IN GRAMS, REFERRED TO THE WATER LINE.

Two neighbors (spacing in diam.)					
1 1/2 ahead 1 1/2 aside		2 ahead 2 aside		3 1/2 ahead 2 aside	
Drag	Lift	Drag	Lift	Drag	Lift
151	143	167	- 42	204	82
159	- 68	219	-125	197	- 95
166	122	175	91	159	89
181	75	204	31	189	89
182	157	212	- 84	204	94
182	79	212	99	197	84
189	- 88	219	-125	189	- 53
182	99	219	120	212	84
204	-131	233	- 68	241	- 79
175	57	219	79	197	-100
204	-125	219	- 79	204	63
182	- 73	...	...	204	120
204	31	...	...	197	-125
225	-136	...	...	204	47
175	136	...	...	...	...
189	94	...	...	...	...
Average magnitudes					
185	101	208	86	200	86

[a] The two parallel 2-in. neighboring cylinders were spaced symmetrically to left and right of the test cylinder path. Amplitude of oscillation, 18 in. Positive and negative lift forces to opposite sides. Forces are maxima with test cylinder following neighbors, but not necessarily on first swing after release.

To avoid the vibrations caused by suddenly applied accelerations, motion was started from maximum deflection by relaxing the tension in a hand-held cord attached to the center of gravity of the pendulum.

During many runs, a 16 mm camera recorded the motion of the eddies shed by the cylinders, the traces of the magnetic oscillographs, the pendulum position, and a timer. Thus, visual impressions of the action could be checked by viewing the film in slow motion, or frame by frame.

ANALYSIS OF DATA

Since the chief aim of this research was to discover effects of neighboring cylinders on a test cylinder, the forces on the test pile by itself were made the

basis for comparison. The drag force histories for runs without neighbors were averaged from the oscillograph records and the extremes were recorded as shown in Fig. 2(a). The curves were not corrected for velocity variations. The drag difference curves shown in Fig. 3, resulting from subtracting the average force curve from the force curve for the run under consideration, emphasized the effects of the neighboring cylinders. Fig. 3 shows typical time position histories of test cylinders, test cylinder eddies, and eddies from two neighboring cylinders showing comparison with the corresponding time force difference curves (1/2-in. cylinders).

The neighboring cylinders further decreased the velocity and amplitude of the pendulum motion over that caused by the test cylinder alone. For each number of cylinders, the decrement of the amplitude was measured so that the maximum velocity at the bottom of the first swing from release could be computed from the theory of damped simple harmonic motion. A multiplicative correction factor was computed for each of the cases by dividing the square of the computed maximum velocity of the no-neighbor runs, by the square of the computed maximum velocity of the runs with different numbers of neighbors. For one neighboring cylinder this factor was 1.03; for two it was 1.08. Each of the values in the tables has been multiplied by the appropriate correction factor.

The lift forces proved to be non-replicative so they were not averaged. Typical curves are included in Figs. 2(b), (c) and (d), and maximum values are listed in Table 2. From successive frames of the motion picture films, measurements of the positions of the test cylinder, and of the eddies shed by the test cylinder and its neighbors, resulted in curves of cylinder and eddy distances from the release point of the test cylinder as functions of time, such as shown in Fig. 3

RESULTS AND DISCUSSION

It was found that the neighboring cylinders significantly influenced the forces on the test cylinder as shown in Figs. 2, 3, 4, and 5 and Tables 1 and 2. The curves shown in Fig. 4 were not corrected for velocity variations. When the test cylinder was in the wake from its neighbors there was a general decrease in the average drag force to minima of about 20% of single cylinder values at mid-swing. When the test cylinder was not in a wake, there was an increase in mid-swing average drag to maxima of over 150% of single cylinder values. Superimposed on this general increase or decrease of average drag were fluctuating drag and lift forces caused by eddies passing the test cylinder. The largest fluctuations of mid-swing lift and drag forces were over 90% and 150%, respectively, of the maximum drag force on the test cylinder without neighbors. Since the test cylinder experiences increased average drag forces when outside the wake of a neighboring cylinder and maximum lift and fluctuations of drag forces only when it lies within the wake, there is little possibility of complete reinforcement of these effects. Nevertheless, reinforcement did occur, as shown by the highest and lowest recorded drag forces at mid-swing of 1.75 and minus 0.17 times the average mid-swing value for single cylinders.

The average resistance forces on a single 2-in. cylinder are shown in Fig. 2(a) and the envelope enclosing all the corresponding resistance forces measured is shown in Figs. 2(a) and 4. The drag coefficients corrected to infinite

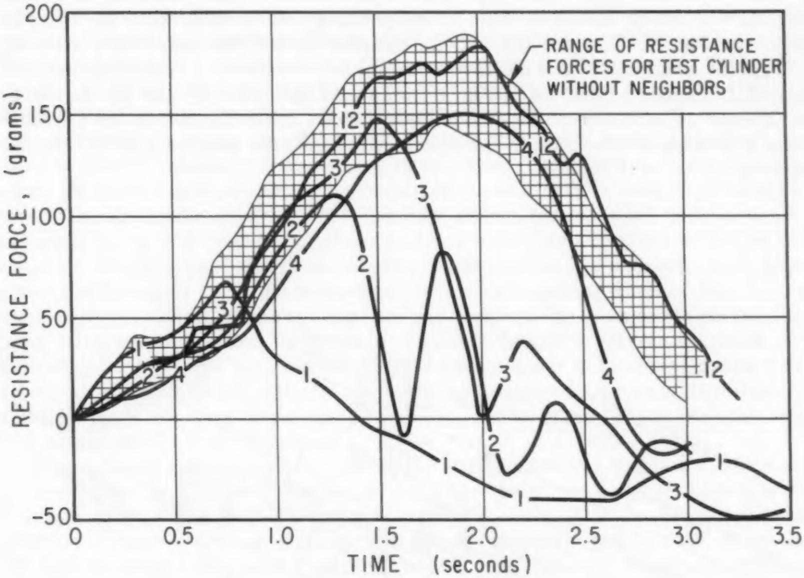

FIG. 4.—RESISTANCE FORCES ON 2-IN. TEST CYLINDER FOLLOWING DIRECTLY BEHIND A 2-IN. NEIGHBOR CYLINDER AT NUMBERS OF DIAMETERS SHOWN ON CURVES

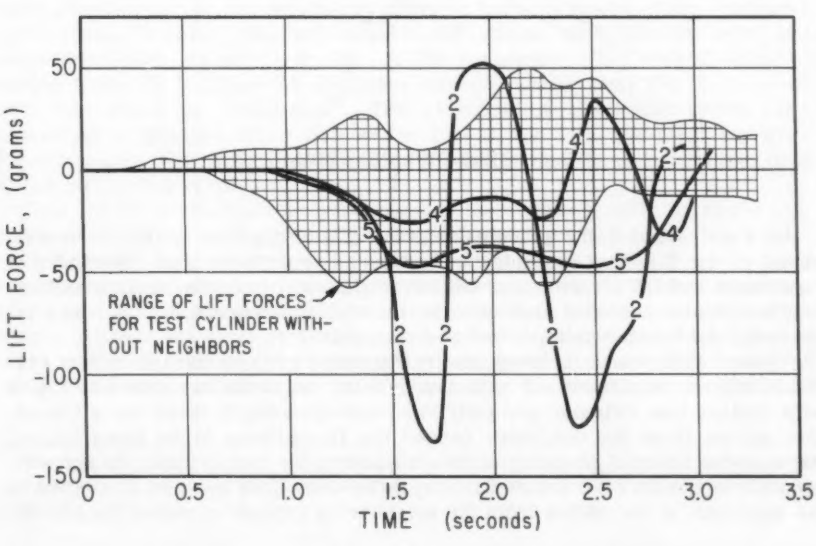

FIG. 5.—LIFT FORCES ON 2-IN. TEST CYLINDER FOR THE RUNS USED IN FIG. 4 HAVING SPACINGS OF 2, 4, AND 5 DIAMETERS

cylinder values were the usual 1.3 to 1.4 for vertical cylinders extending through the water surface. The corresponding lift or side force envelope is shown in Fig. 5. Data for the 1/2-in. cylinders were the same but for scale.

Typical resistance and lift forces on the test cylinder in the company of a pair of neighbors placed as in Fig. 6 make up Figs. 2(b), (c) and (d). In these, significant departures of the resistance forces from those for the cylinder alone are evident. The closer the spacing, the greater and the earlier are the departures.

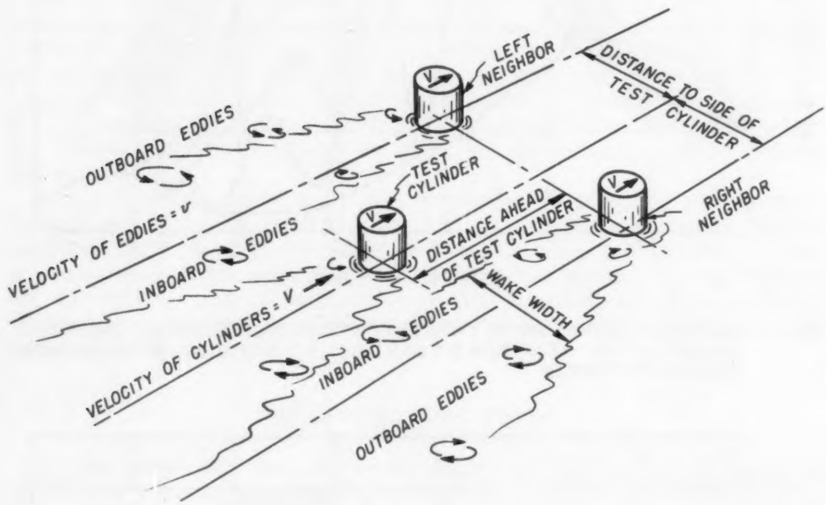

FIG. 6.—CYLINDER AND EDDY MOTION

In Figs. 4 and 5 the principal effects of a single 2-in. neighbor directly ahead of the 2-in test cylinder can be seen as departures from the ranges of resistance and lift forces found without neighbors. Again, the deviations from single cylinder behavior decrease as the distance between the cylinders increases, and become unimportant at 4 diameters.

Typical differences between the resistance forces on the 1/2-in test cylinder without neighbors and with two 1/2-in. neighbors are shown in Fig. 3 with typical test cylinder and eddy loci corresponding to these force traces. The eddies from the neighbors caused the fluctuations in the force traces. Because the times of shedding of the eddies from the test cylinder do not correspond to the force trace deviations, these deviations must be attributed to the approach of the eddies from the neighboring cylinders, rather than to the

shedding of eddies from the test cylinder. It is evident that the closest approach of the first shed outboard eddy pair to the test cylinder coincides with the same point on the first dip of each of the resistance difference curves. These eddies have a direction of rotation that causes a decrease in the velocity of the test cylinder relative to the surrounding water and must therefore be the reason for the negative force contribution. Subsequent outboard eddies cause similar negative contributions. For the run at 8 diameter spacing, two pairs of inboard eddies could be seen on the film. Their loci precede the corresponding outboard pairs and they must, because of their direction of rotation, cause the increase in drag contributions shown before each decrease. Unfortunately, on the films the inboard eddies were very difficult to follow because of the surface disturbances behind the cylinders. As a result, none were clearly defined for the 4 diameter and 12 diameter spacing runs of Fig. 3. One may, however, infer their existence because in all of the runs in which fluctuations of drag force were noticeable the first deviation was an increase. All data support the facts that the shedding of eddies from the test cylinders when alone or with neighbors, caused no significant change in the resistance force, and that large changes were caused when the eddies from the neighboring cylinders passed the test cylinders.

The maximum recorded lift force of 157 gm is shown in Table 2. This force is some 80% of the average single cylinder drag force and about triple the average single cylinder lift force. Lift forces of 50% of the single cylinder drag force were common. Drag forces were often increased by 50%. Thus, the lift and the drag force acting simultaneously may augment the single cylinder force by at least 60% and cause oscillating forces on piling.

Often the motion pictures showed that an eddy was shed almost simultaneously from each side of the test cylinder without causing a lift force. In many cases, the eddy that formed first was not shed first. It sometimes shrank while the opposite eddy grew and was shed. These starts were often followed by ultimate shedding as in the single cylinder von Karman street. When neighbors were close, however, the test cylinder sometimes shed only one eddy, and sometimes none, as shown in Fig. 3. The frequency of shedding shedding of eddies from the neighboring cylinders can be judged, from Fig. 3, to agree with that given by Landweber[6]. The velocities of these shed eddies were measured in this and other figures for 1/2-in. and 2-in. cylinders and were found to agree with Landweber's values for eddies shed by cylinders traveling at the mid-swing velocity.

The lift force fluctuation periods agreed more closely with the single cylinder eddy pair shedding period given by the von Karman vortex street analysis than with the periods for eddy pair shedding from the neighbors as given elsewhere for medium to wide spacing of the cylinders. With these spacings, there was little measured difference between the lift force records and the single cylinder lift force records. It is therefore indicated that the lift forces were caused mostly by the shedding of eddies from the test cylinder with but little effect from neighboring cylinders, unless the neighbors were within 4

---

6 "Flow about a Pair of Adjacent, Parallel Cylinders, Normal to a Stream: Theoretical Analysis, U. S. Navy, The David W. Taylor Model Basin," by L. Landweber, Report 485, July, 1942.

diameters ahead and 3 diameters to the side. The directions in which the lift forces were exerted were not replicative, as shown in Table 2.

CONCLUSIONS

1. The presence of neighboring cylinders may increase the drag force of a cylinder by 75% or decrease it to less than minus 15%.

2. Lift forces of 75% of the single cylinder drag force may result from the presence of neighboring cylinders.

3. The average drag force on a cylinder may be increased by as such as 45% if outside, or decreased by 80% if inside, the wake of close neighbors.

4. Fluctuating drag forces are caused mostly by eddies from neighboring cylinders.

5. One neighbor has approximately the same effect as two.

6. Neighbors more than 10 diameters from a test cylinder cause only minor drag and lift disturbances.

Journal of the
HYDRAULICS DIVISION
Proceedings of the American Society of Civil Engineers

FLUME STUDIES OF FLOW IN STEEP, ROUGH CHANNELS[a]

By Dean F. Peterson,[1] F. ASCE and P. K. Mohanty[2]

SYNOPSIS

Based on observations of both natural streams and flume experiments, three classifications of flow in steep, rough, open channels are proposed: tranquil, tumbling, and rapid. The tranquil and rapid regimes are dominated by subcritical and supercritical flow, respectively. In the tumbling regime the roughness elements induce supercritical flow over their crests followed by individual hydraulic jumps to the tranquil state. The characteristics of flow in each of the proposed regimes are described, and criteria for delineating the regimes are proposed.

INTRODUCTION

Uniform flow is commonly considered to occur when the water surface is parallel to the bed slope. For such flow the depth, water area, velocity, and discharge are the same at each section of a channel reach. Whereas these conditions may be essentially correct for open channels in which roughness elements are small, relative to depth, they are hardly correct for channels having large roughness elements such as occur in mountain streams or in alluvial channels in which large dunes are formed. Existing formulas relating the gross variables of discharge, water area, depth, bed slope, and roughness that are based on the concept of uniform flow, could hardly be expected to apply in the latter case, especially if regions of supercritical flow form over the

Note.—Discussion open until April 1, 1961. To extend the closing date one month, a written request must be filed with the Executive Secretary, ASCE. This paper is part of the copyrighted Journal of the Hydraulics Division, Proceedings of the American Society of Civil Engineers, Vol. 86, No. HY 9, November, 1960.
[a] Presented to the Hydraulics Division, ASCE, July 1, 1959, Fort Collins, Colo.
[1] Prof. of Civ. Engrg. and Dean, Utah State Univ., Logan, Utha.
[2] Research Assoc., College of Engrg., Utah State Univ., Logan, Utah.

tops of the roughnesses. For this type of flow in nature, the basic variables can probably no longer be described by simple numbers, but become statistical.

The purpose of this study was to gain some insight into the basic dynamic relationships of flow in open channels, especially in steep channels, in which roughness is an appreciable portion of depth. Since conditions in nature are extremely complex, laboratory flume studies under idealized conditions of geometry were made as a first step in trying to understand the problem more fully.

The design of the experimental program and the apparatus was based, among other things, on consideration of many informal observations in the field, especially of Logan River located in northern Utah. This river is a typical, steep (50 to 75 ft per mile slope in its lower reaches), boulder-strewn mountain stream with discharge normally ranging annually from a minima of around 100 cfs to a maxima approaching 2000 cfs. The writers were impressed by the fact that the roughnesses commonly appeared to induce a "tumbling" phenomena whereby localized areas of supercritical flow followed by hydraulic jumps occurred. Fig. 1 shows this condition on the Logan River, that is typical of rough, steep streams observed at many other locations.

It seemed desirable that the flume be capable of rather large slopes, and that the roughness elements should be such as to induce large variations in depth and velocity. Since these latter effects were of primary importance, and because of a desire to separate them from other considerations and make them as simple as possible, two-dimensional roughness elements seemed appropriate. A second step could be to introduce three-dimensional roughnesses, and a third, to investigate similitude by using similar roughness elements of different size. As a fourth step, consideration was given to the introduction of roughness elements having a distribution of sizes, however, limitations on time precluded this.

A number of preliminary theoretical investigations were made utilizing dimensional and mechanical considerations. These indicated that some form of Froude number, together with slope, some description of roughness height, spacing, and intensity should be the important variables. These analyses could be developed to some degree for specialized ideal cases in the flume, but yielded little information regarding the general case.

This paper summarizes the principal results and conclusions reached by the study. More detailed information, including a complete tabulation of data are included in Mr. Mohanty's dissertation.[3]

Notation.—The letter symbols adopted for use in this paper are defined where they first appear, in the illustrations or in the text, and are arranged alphabetically, for convenience of reference, in Appendix II.

FLUME EXPERIMENTS

Flume.—Opportunities at hand dictated the design of the water supply, flume, and measuring devices. The installation was made in the out-of-doors at the site of the Utah Water Research Laboratory (Fig. 2). Water was siphoned from the reservoir above the 40-ft high State Power Dam to a 7-ft-by-

---

[3] "The Dynamics of Turbulent Flow in Steep, Rough, Open Channels," by P. K. Mohanty, thesis presented to Utah State Univ., at Logan, in 1959, in partial fulfilment of the requirements for the degree of Doctor of Philosophy.

FIG. 1.—TUMBLING FLOW IN NATURE

FIG. 2.—GENERAL LAYOUT OF FLUME

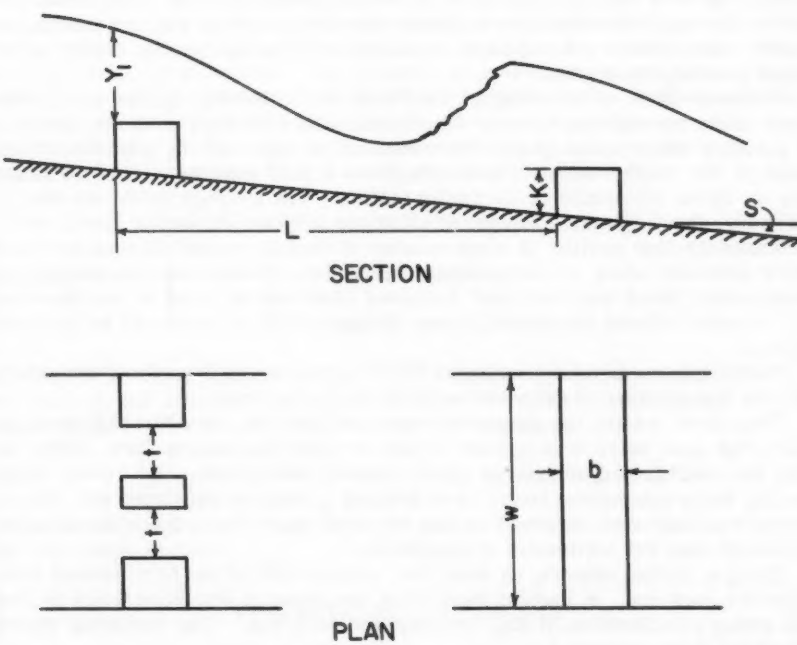

FIG. 3.—DEFINITION SKETCH

5-ft-by-7-ft headbox through a 10 in. pipe controlled by a gate valve at the headbox. A maximum discharge of 4 cfs was available.

The flume was 2 ft wide, 16 in. deep, and 64 ft long. It was constructed of plywood on longitudinal timber girders supported by a hinge at the center and by two differential chain hoists 9 ft from each end. It could be set on any slope between 0 and 8.5%. At the headbox connection, a sliding arrangement consisting of a non-stretchable piece of nylon cloth 16 ft-by-14 ft with a hinged and sliding door proved leak-proof and otherwise satisfactory. A sliding tail gate was provided at the discharge end of the flume.

The discharge from the flume spilled into a stilling pool excavated in the earth but lined with concrete. At the end of the pool, a V-notch weir was installed. Depth over the weir was measured at a stilling well with a micro-hook-gage. A floating slab of plywood served as a wave suppressor. As a check, a commercial flow-meter was installed in the siphon pipe. The weir measurements, however, were used in the analysis.

Two-dimensional roughness elements consisted of 0.3 ft-by-0.3 ft or 0.135 ft-by-0.135 ft square timber bars (or a combination of them). Three-dimensional elements were 0.3 ft-by-0.3 ft-by-0.3 ft timber cubes. These were machine planed and fastened to the flume bottom by toenailing. A template was used during installation to assure proper spacing. Roughness elements having finite width were chosen because of ease of attachment and because some closer resemblance to natural roughness, having finite width, could possibly be implied.

Measurements.—The slope of the flume was carefully checked at 2 ft stations using an engineers level. Depth measurements were made by means of a portable micro-point-gage. Measurement of the depth Y_1 over the leading edge of the roughness was repeated at from 5 to 10 roughness stations in order to check uniformity of the cyclic pattern. The average value was used in analysis. Depth was also measured along the longitudinal center line in order to obtain the flow profile. A large number of closely spaced piezometer holes were provided along the longitudinal center line. These were connected to a manometer board and recorded localized piezometric head at the boundary that usually differed appreciably from the depth of flow measured at the same station.

Discharge was measured using the 90° V-notch weir as described previously, and the temperature of the water was noted for each run.

Procedure.—After the roughness elements had been installed and the slope fixed, the gate valve was opened enough to allow the desired flow. After the flow was established, discharge measurements were made. The rubber tubes leading to the manometer board were drained to remove entrapped air. Manometer readings and observed values of depth were recorded after allowing sufficient time for attainment of equilibrium.

Using a reflex camera, at least two photographs of the flow pattern were taken for each run. A journal describing the physical characteristics of flow and noting peculiarities, if any, was kept for each run. The following shows the range of the variables:

Variable	Symbol	Range
Discharge	Q	0 to 4 cfs
Slope of channel	S	0.01 0.0246 0.05 0.083

Roughness height	K	0.3 ft-by-0.3 ft bars 0.135 ft-by-0.135 ft bars 0.3 ft-by-0.3 ft-by-0.3 ft cubes
Longitudinal spacing of roughness	L	5 K 10 K 15 K

A total of 163 runs were made.

Dimensional Analysis.—A number of possibilities for measuring and characterizing velocity and depth for the flume studies are apparent. Several of these were tried during the investigation. However, if a cyclically uniform steady state is established, a particular velocity and depth should serve as an index to which all other elements of the velocity-depth cycle may be referred. For the purpose at hand, the depth Y_1 and velocity at the front edge of the roughness element proved most satisfactory (Fig. 3). Letting the corresponding velocity V_1 serve as the dependent variable,

$$V_1 = \phi_1\left(Y_1, K, b, L, t, S, g, \nu, \lambda\right) \qquad (1)$$

in which K, b, L, and t are, respectively, the height, top width, longitudinal and transverse spacings center to center of the roughness elements, S is the channel slope, and g and ν are the acceleration of gravity and kinematic viscosity of water, respectively. The factor λ represents a roughness intensity factor. Since roughness elements with sharp edges were used, fixed lines of separation were anticipated, and thus the form drag, and consequently, V_1 should be nearly independent of Reynolds number. Choosing g and Y_1 as repeating variables and neglecting ν and b, Eq. 1 may be reduced to

$$V_1/\sqrt{g\,Y_1} = \mathbf{F}_1 = \phi_2\left(K/Y_1, L/Y_1, t/Y_1, S, \lambda\right) \qquad (2)$$

The roughness intensity factor λ may be expressed as

$$\lambda = \alpha K(1 - pt)/L \qquad (3)$$

in which p is the number of transverse roughness spacings per unit width of the channel, and α is a shape factor. For two-dimensional roughness, $p\,t = 0$ and $\lambda = \alpha\ K/L$. For the two-dimensional roughnesses,

$$\mathbf{F}_1 = \phi_3\left(K/Y_1, L/Y_1, S, \alpha\right) \qquad (4)$$

Since the roughness elements are of standard shape, α was not a variable for these experiments.

PRESENTATION OF RESULTS

Classification of Flow.—Early observations of natural streams focused the attention of the writers on a condition of flow dominated by scattered regions of alternate acceleration and deceleration through critical flow over the large roughness elements. This condition was termed tumbling flow because the water appeared to tumble over the roughnesses. At lower discharges, in reaches of lower slope or smaller roughness, however, the standing waves associated with the hydraulic jumps were no longer in evidence, and the flow

appeared to be in a tranquil state even over the tops of the roughness elements. At higher stages, the subcritical depth pools below the large roughnesses were swept out by the increased momentum, and the flow appeared to skim over the roughnesses at supercritical velocity. These observations were repeated in the flume experiments, and the flow was, accordingly, classified into three major regimes; (1) tranquil flow, which, essentially was maintained throughout, (2) tumbling flow—supercritical flow occurred over the roughness elements with hydraulic jumps and subcritical flow in the regions between, and (3) rapid flow—supercritical flow occurred generally throughout the streams.

In the flume, the flow could be readily classified into the principal regime by visual inspection. The depth Y_1 also helped distinguish the rapid and tranquil flow regimes because Y_1 was smaller than Y_c in the rapid flow regime and appreciably greater than Y_c in the tranquil flow regime. No hydraulic jump between roughness elements formed for either the rapid or the tranquil flow regimes.

In planning the program, the writers were quite preoccupied with the tumbling flow phenomenon and, accordingly, most of the experimental runs were consciously chosen to assure that tumbling flow was induced. Nevertheless, many runs occurred in the tranquil and rapid regimes. In presenting the results, the latter are presented first, even though they are not as extensive as for the tumbling problem.

Tranquil and Rapid Flow Regimes.—For flows in either of these regimes, successful correlations in the form of Eq. 4 were possible. Except for the basic difference of subcritical and supercritical velocities, the correlations obtained were similar for both regimes. Fig. 4 shows a plot of K/Y_1 versus $\mathbf{F}_1$ for tranquil flow over two-dimensional roughness elements. For this plot all roughness elements were 0.3 ft-by-0.3 ft except for those points represented by the triangles with the right half blacked, ($S = 0.01$, $L = 15$ K) that were 0.135 ft-by-0.135 ft. The curves in Fig. 4 are typical in shape to those for various slopes in both the rapid and tranquil flow regimes and for both the two-and three-dimensional roughness elements.

Study of Fig. 4 indicates that for intermediate values of roughness spacing, the Froude number is smallest, and that for low values of relative roughness the Froude number tends to increase. These observations are consistent with those made by Morris[4] in connection with pipe flow. Morris proposed the following classifications depending on roughness spacing:

1. Isolated roughness flow.—The roughness elements are sufficiently apart so that the wake and vortex generating zone at each element is completely dissipated before the next zone is reached.
2. Wake interference flow.—The roughness elements are close enough to interfere.
3. Quasi-smooth or Skimming Flow.—The roughness elements are sufficiently close that the flow essentially skims the crests of the elements.

The decrease in Froude number for the intermediate values of roughness spacing could be associated with wake interference, whereas, the increase associated with decreased height and spacing of roughness could indicate skimming. Similitude appears to exist as is indicated by the curves for $S = 0.01$

4 "Flow in Rough Conduits," by Henry M. Morris, Jr., Transactions, ASCE, Vol. 120, 1955, pp. 373-398.

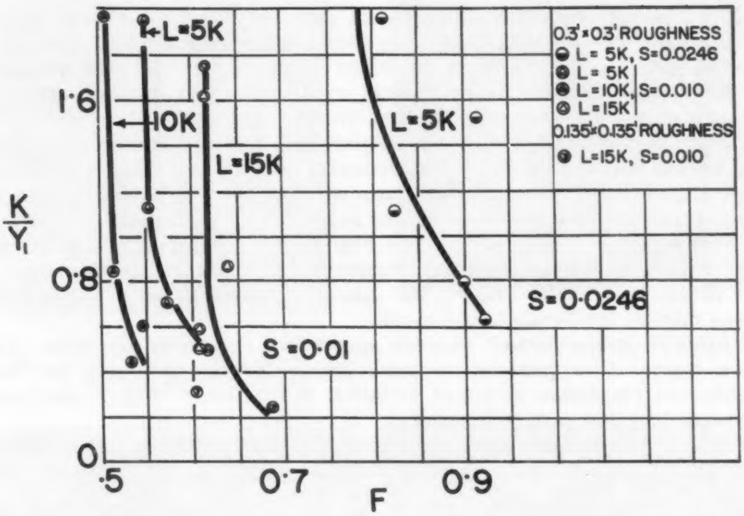

FIG. 4.—$\frac{K}{Y_1}$ VERSUS F_1 IN TRANQUIL FLOW

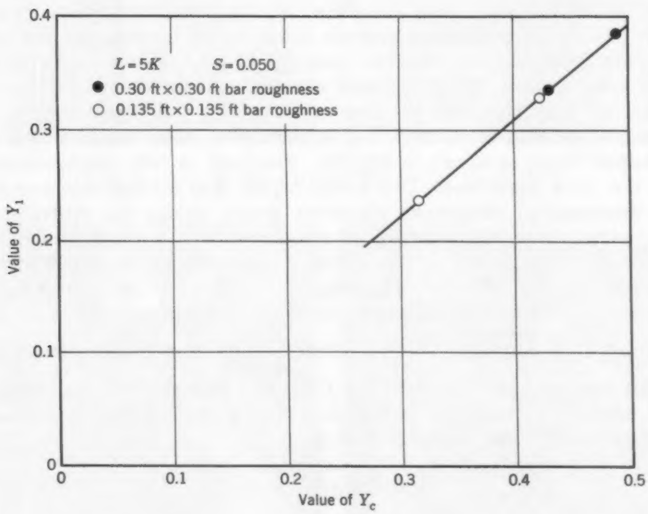

FIG. 5.—SIMILITUDE IN RAPID FLOW

and $L/K = 15$ in Figs. 4 and 5 that are drawn using similar roughness configurations of different size.

Fig. 6 shows occurrence of tranquil, quasi-smooth flow in a fairly rough, steep, natural stream. The roughness elements are of quite high intensity and their heights are estimated to be of the order of $0.15\ Y_1$. The velocity is probably approaching, but is less than $\mathbf{F}_1 = 1$. Fig. 7 shows natural rapid flow, also probably in the skimming region. The flow of Fig. 7 differs from that of Fig. 1 in that essentially it is completely supercritical; no hydraulic jumps are able to form between the roughness elements, and the magnitude and direction of velocity remains essentially the same over the roughness elements and between them. Fig. 8 shows tranquil and rapid flow in the flume.

Tumbling Flow.—The flow in this regime was characterized by alternate acceleration and deceleration from subcritical to supercritical velocities, and vice-versa, in a cyclic order. The spacing between two successive roughnesses marked the length of one cycle.

Hydraulic jumps formed between successive roughness elements. Fig. 9 shows typical flow patterns in this regime for the two- and the three-dimensional roughness elements installed in the flume. Fig. 1 illustrates a corresponding flow pattern in nature.

Based on considerations from dimensional analysis, a number of correlations were tried. Whereas some appeared to be successful, the simple relationship between critical depth $Y_c = \sqrt[3]{q^2/g}$ and Y_1 was most satisfactory. The flow characteristics were independent of K/L and S.

As in Figs. 1 and 9, it can be seen that each roughness element acts as an overfall control. In the two dimensional studies, the control extends entirely across the channel. For the three-dimensional arrangements, the extent of the control depends on the configuration of the roughness pattern and the lateral spacing of the roughness elements. In the latter case, the stream tends to flow at subcritical velocities between the roughness elements and at supercritical velocities over them. The flow, however, is carried by momentum both over and around the roughness elements and consequent acceleration causes a region of supercritical flow much larger than that actually occupied by the roughness (Fig. 9). A region of supercritical flow induced by a solitary rock in Logan River is shown in Fig. 10. The rock is only about one-third the width of the area disturbed. One would expect that a relatively low intensity of three-dimensional roughness elements would induce the equivalent of full overfall control in a rough reach of stream under tumbling flow. Thus, the discharge under conditions of fully developed tumbling flow would be independent of K, L and S. For this case, the depth Y_1 over the tops of the roughness elements would be less than critical depth computed on the basis of average q, that is, $Y_c = \sqrt[3]{q^2/g} = Y_1 + c$. For the tumbling regime, therefore, the formula for the critical flow weir, $q = C\sqrt{g\ Y_c{}^3}$ should form the basis for the discharge-depth relationship in which C and c are constants depending on roughness geometry and intensity; that is,

$$q = C\sqrt{g\left(Y_1 + c\right)^3} \quad \ldots\ldots\ldots\ldots\ldots\ldots (5)$$

In Fig. 11 is a plot showing $Y_c = \sqrt[3]{q^2/g}$ versus Y_1 for the 0.3 ft-by-0.3 ft bar roughnesses. The plots for the 0.135 ft-by-0.135 ft bar roughness (not shown) fall on exactly the same curve. From this figure $C = 0.83$ and $c = 0$,

FIG. 6.—NATURAL TRANQUIL QUASI-SMOOTH FLOW

FIG. 7.—NATURAL RAPID FLOW

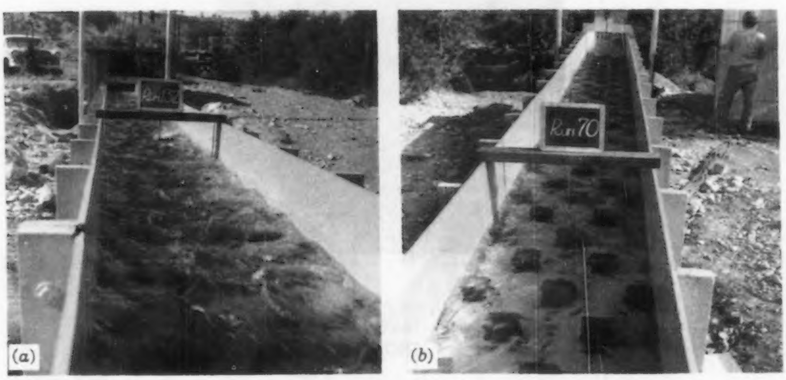

FIG. 8.—TRANQUIL AND RAPID FLOW IN FLUME

FIG. 9.—TUMBLING FLOW IN FLUME

therefore,

$$q = 0.83\sqrt{g\ Y_1^3} \quad \ldots\ldots\ldots\ldots\ldots\ldots (6)$$

Fig. 12 shows a similar plot for the 0.3 ft cube roughnesses. For this case, C = 1.0 and c = 0.09, thus,

$$q = \sqrt{g\left(Y_1 + 0.09\right)^3} \quad \ldots\ldots\ldots\ldots\ldots\ldots (7)$$

The foregoing hypothesis permits one to substitute the concept of an overfall weir for a reach of tumbling flow. The single overfall for natural streams, instead of being located at a particular cross section, is now divided into many smaller overfalls statistically distributed throughout the reach. Such a reach may be regarded as a statistical critical depth weir for which the discharge coefficients depend on the relative size, distribution, shape, and intensity of the roughness configuration. The depth-discharge relation depends on neither the overfall height for a weir, nor on the length and slope of a tumbling flow reach of channel.

FIG. 10.—EFFECT OF ISOLATED ROUGHNESS

In nature, in which roughness elements are variable in size and intensity, one still has the problem of deciding how to characterize the flow parameters of velocity and depth, that are now statistical. This foregoing concept of the virtual weir may furnish a means of approaching the problem. In such a weir, the crest elevation might be represented by the proper statistical function describing roughness distribution for a tumbling reach of stream corrected for separation and roughness intensity effects. Flow would be expected to occur at a minimum of total energy. In Fig. 13,

$$P = \int_0^W \left(z + y + V_x^2/2\,g\right)\gamma\ V_x\, y\, dx \quad \ldots\ldots\ldots\ldots (8)$$

with the condition that

$$Q = \int_0^W y\ V_x\, dx \quad \ldots\ldots\ldots\ldots\ldots\ldots (9)$$

in which Z, y and V_x are, respectively, the height of equivalent roughness, depth of flow and velocity at a vertical section of the virtual weir, and γ is

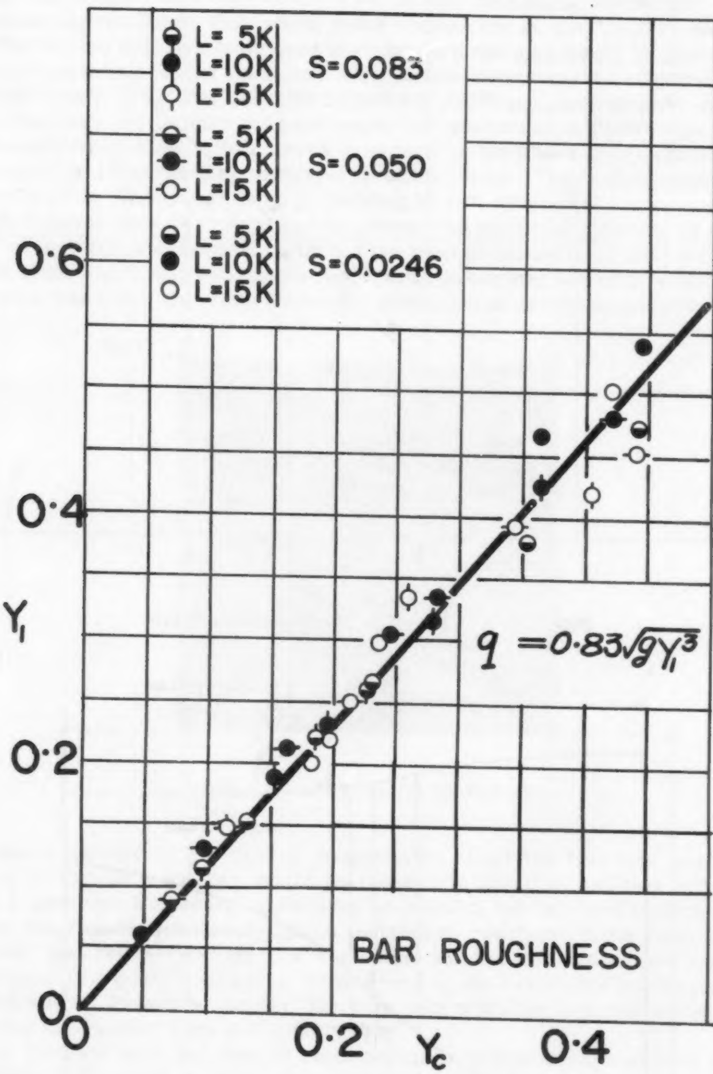

FIG. 11.—Y_1 VERSUS Y_c IN TUMBLING FLOW

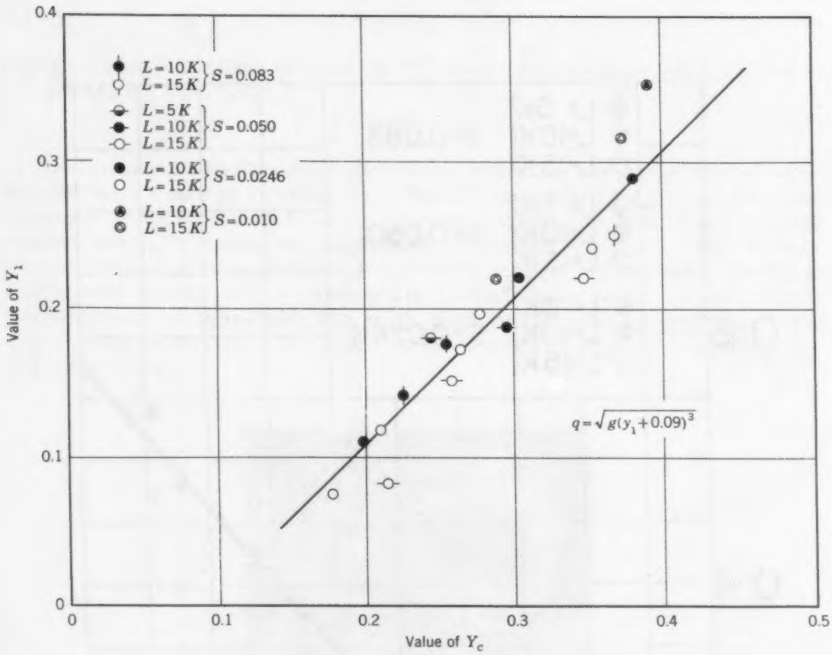

FIG. 12.—Y_1 VERSUS Y_c IN TUMBLING FLOW

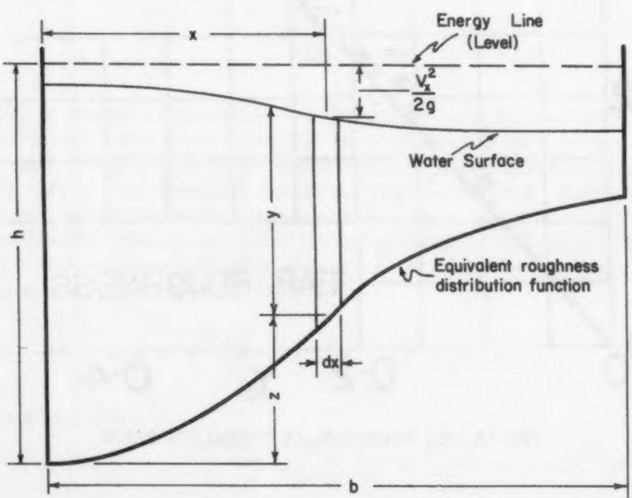

FIG. 13.—VIRTUAL WIER CROSS SECTION

the unit weight. P is the power and h is the elevation of the energy line. For a minimum, dp/dh = 0. The writers were unsuccessful in using this approach since V_x is an unknown function of x. However, it now appears that statistically within the reach $q_x = Q/w = V_x\ y\ dx$ may be a valid assumption. Using machine computations this would make evaluation of the integral possible.

The limited data available need to be supplemented by flume studies of flow over roughnesses having statistical distribution of size and spacing and by extensive study of natural streams in order to develop a generalized concept of tumbling flow and to infer the best means for describing it quantitatively.

Instability of Flow.—Roll waves occurred in the flume under certain conditions; Fig. 14 shows their occurrence in the flume. The leading crest of the wave is at A. The trough is at B, building up to a crest at C.

Roll waves have been reported in natural and artificial channels by a number of writers, and several criteria have been proposed to predict the conditions under which they will appear. Depending on whether Chezy's or Manning's formula was used, the most frequently presented criterion is a lower limit of

FIG. 14.—ROLL WAVES IN FLUME

Froude's number of 1.5 or 2.0, respectively, implying that flow above this value of Froude's number would be inherently unstable, and that roll waves would develop. Koloseus,[5] attempting to connect the Darcy-Weisbach resistance coefficient with free-surface instability, concluded from experimental studies that for $\mathbf{F} < 1.6$, the flow was stable and the resistance coefficient independent of Froude's number. When $\mathbf{F} > 1.6$, the resistance coefficient was dependent on Froude's number, the flow was unstable, and roll waves would form if the channel were sufficiently long.

In contrast with the results reported in the literature, the writers did not observe roll waves in rapid flow even though the Froude number frequently exceeded 1.6 and the flume should have been of adequate length. Rather, roll

[5] "The Effect of Free Surface Instability on Channel Resistance," by H. J. Koloseus, thesis presented to the State Univ., of Iowa, at Iowa City, in 1958, in partial fulfilment of the requirements for the degree of Doctor of Philosophy.

waves formed in the transition ranges between tranquil and tumbling flow or between tumbling and rapid flow. As reported by others, they formed only when the depth of flow was relatively shallow. No roll waves were observed using the cube roughness elements. Ordinarily, the large roughness elements damped out instabilities, and a stable condition was quickly established. However, in the transition region a delicate condition of stability evidently exists.

During the present investigation, data on roll waves were collected only incidentally and are, thus, too limited for systematic study. Two interesting observations were made: (1) For L/K = 5 roll waves occurred during the transition from tumbling to rapid flow only when $\mathbf{F}_1/\sqrt{S} \approx 6$, in which S is the channel slope, (2) For L/K = 10 or 15 roll waves occurred during the transition from tranquil to tumbling flow when $\mathbf{F}_1 \approx 0.9$.

Air Entrainment.—The writers had anticipated that air entrainment might create a problem, especially with regard to measurements. Except for the case of three-dimensional roughness under extreme conditions of slope and discharge, however, air entrainment did not affect the measurements significantly. For both tranquil and tumbling flow, the approach velocity to the roughness crests was, of course, subcritical.

ANALYSIS

Flow in Steep, Rough, Channels as Uniform Flow.—Uniform flow, as commonly defined, implies that depth does not change from section to section. This is a relative matter—truly uniform flow would be approached only in very smooth channels at low velocities, because any irregularities would cause some variation in depth, even though small. Where one draws the line is thus a matter of judgment. For example, the flow shown in Fig. 6 would ordinarily be classed as uniform. However, what about the flow in Figs. 1, 7, and 9?

In the flume studies under a regular roughness pattern, the water surface varied in a regular repetitive cyclic way throughout the length of the flume, once equilibrium was established. One might, therefore, regard such flow as uniform, at least in a macroscopic sense. Over a reach of natural channel one would suspect also that there would exist a statistical uniformity of flow, again in a macroscopic sense. Perhaps a more general concept of uniform flow would be more appropriate based on equilibrium between the weight component and the boundary drag (shear plus form drag of roughness elements) over a sufficiently long reach of channel so that statistical description would be constant. Under this definition, except for the runs where roll waves formed, macroscopically uniform flow was quickly established for all of the runs performed by the writers.

Delineation of Flow Regimes.—The relation between discharge, slope, and height and spacing of roughness elements determined the flow regime in the flume. This is, undoubtedly, also true in nature, although the description of the roughness may be quite complex. Since tumbling flow separates the regimes of tranquil and rapid flow, an understanding of the conditions under which this can occur should lead to criteria delineating the principal regimes.

The distinguishing characteristic of the tumbling regime is the occurrence of stationary hydraulic jumps. Thus, an understanding of the conditions leading to the formation of hydraulic jumps in sloping channels should be helpful. The common equation derived from consideration of conservation of momentum

and continuity between two successive cross sections,

$$\gamma\, d_1^2/2 - \gamma\, d_2^2/2 + W \sin\theta = \rho\, q \left(V_2 - V_1\right) \quad \text{.........(10)}$$

is difficult to solve because of the difficulty of determining the weight, W, of the water prism.

Hydraulic jumps in sloping channels have been studied by a number of researchers, and the results have been summarized by Bradley and Peterka.[6] The writers found that these data may be summarized by the generalized empirical formula,

$$d_2 = F_1\, d_1\, (S + 0.153)/0.133 \quad \text{..............(11)}$$

This is plotted in Fig. 15.

For hydraulic jumps to be maintained, slope S must be sufficient to accelerate all or part of the flow to supercritical velocities, and the height of the

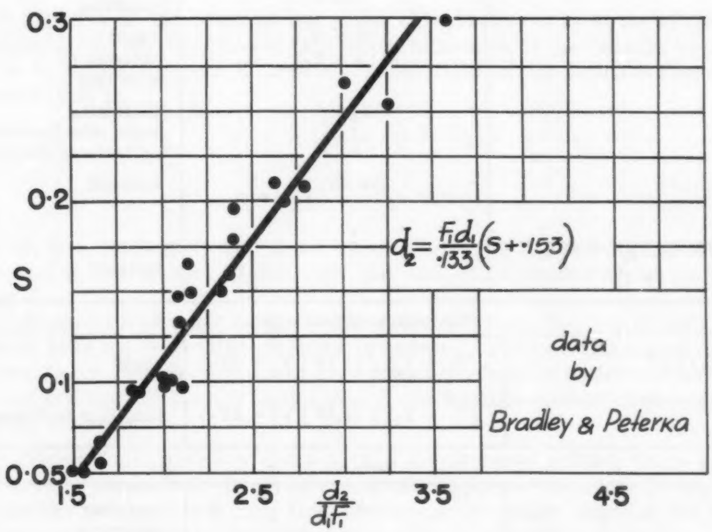

FIG. 15.—HYDRAULIC JUMP IN SLOPING CHANNELS

roughnesses must be sufficient to induce the required sequent depth. The slope must also be such that the form drag of the roughness elements and the shear on the channel bottom may be overcome by the component of the weight parallel to the bed. Form drag depends on the flow distribution around the roughness and, thus, on the flow regime. From rational considerations together with empirical evidence, tentative criteria delineating the various flow regimes in the flume are proposed (Table 1). Analysis leading to these criteria are included in Appendix I.

6 "Hydraulic Design of Stilling Basins: Stilling Basin with Sloping Apron (Basin V)," by J. N. Bradley and A. J. Peterka, Proceedings ASCE, October, 1957, Vol. 83, No. 10, pp. 1-32.

Flow Formula.—Open channel flow formulas in common use may be expressed in the general form,

$$V = C' g^{1/2} Y^m S^n \qquad (12)$$

in which m and n are constants and C' is a function of the channel roughness. Although these formulas were originally proposed for tranquil flow and com-

TABLE 1.—CRITERIA FOR FLOW REGIMES

Criterion	Condition	Type of Flow
	Two-dimensional bars	
$(F_1 Y_1/Y_2)^2$	$\tilde{>} 1/2$	rapid
	$\tilde{<} 1/2$	tranquil or tumbling
d_2	$>(K + Y_c)$	rapid
	$<(K + Y_c)$	tranquil or tumbling
L	$<F_1 Y_1$	Skimming
	$>F_1 Y_1$	wake interference or isolated roughness
$L/(Y_1-LS)$	>0.85	tranquil
$K < [1/2(Y_c/Y_a)^3 - 3/2(Y_c/Y_a) + 1]$		tranquil
	Three-dimensional cubes	
$(F_1 Y_1/Y_2)^2$	$\tilde{>} (Y_1 + Y_2) / (1.16\, j\, Y_1 + 2Y_2)$	rapid
	$\tilde{<} (Y_1 + Y_2) / (1.16\, j\, Y_1 + 2Y_2)$	tumbling or tranquil
	General	
l_j	$>L$	tumbling will not occur
$S-S_D$	$<S_{cr}$	tranquil
	$>S_{cr}$	tumbling or rapid

paratively low relative roughness, their use in the past has been extended to include supercritical flow as well.

In the tumbling regime, the depth of flow over the roughness crest tends to pass through the critical value regardless of S, L, and K. Thus, in Eq. 12 the values of C', m, and n would tend to become 1, 1/2, and 0, respectively. In the other regimes C', m, and n would approach those for a smooth channel. Within the transition zones, the values of C', m, and n apparently will vary depending on proximity of the flow balance to tumbling flow.

Due to the extremely rough channel bottom as compared to its sides, the channel should behave essentially as a very wide channel, and m should be very close to 1/2. This strongly suggests the possibility that a general open channel flow formula may be expressed as

$$V_1 = C'\sqrt{g\,Y}\;S^n \quad (13)$$

or

$$V_1/\sqrt{g\,Y_1} = \mathbf{F}_1 = C'\,S^n \quad (14)$$

in which both C' and n are functions of relative roughness geometry only.

The interdependence of $\mathbf{F}_1$, K/Y_1, and L/Y_1, discussed previously, also suggests that the most important parameter representing roughness geometry may be the roughness intensity λ expressed possibly in the form

$$\lambda = \alpha\,K(1 - p\,t)/L \quad (15)$$

In this form, λ is the ratio of the projected effective area of the roughness perpendicular to the direction of flow to the total area of tne channel bed.

It is believed that both C' and n are functions of the relative roughness geometry, that is

$$C' = f_1\left(\lambda,\ L/Y_1,\ K/Y_1\right) \quad (16)$$

and

$$n = f_2\left(\lambda,\ L/Y_1,\ K/Y_1\right) \quad (17)$$

However, lack of adequate data in all sub-regimes of flow prevents quantitative evaluation of Eq. 16 and 17 for even the simplified conditions of the flume studies.

Roughness in Hydraulic Design.—The writers believe that use of roughness elements have not been fully exploited in hydraulic design. With better understanding, their rational use could very possibly result in improved performance and economy of certain structures. Some specific possibilities might include the following:

1. Energy Dissipator.—A chute with a single large stilling basin is frequently very expensive. By proper use of roughness elements it might be practical to establish tumbling flow throughout the entire length of the chute. The energy would then be dissipated by a number of overfall sinks throughout its length rather than by a single large one. Velocities would never greatly exceed critical.
2. Use of Steeper Slopes in Channel Design.—In earthen channels steep slopes resulting in scouring velocities are usually undesirable. In lined channels of steep slope there is the danger of instability, impact waves, and formation of roll waves. Use of roughness elements to control the flow at a suitable velocity might permit the use of steeper slopes where this is desirable.
3. Increased Sediment Transport.—By using roughness to induce greater turbulence, the sediment carrying capacity of a designed channel may be increased. Benedict, Albertson, and Matejka[7] used roughness elements in a flume to develop sufficient turbulence to suspend the bed load of a stream, thus

[7] "Total Sediment Load Measured in Turbulence Flume," by P. C. Benedict, M. L. Albertson, and D. Q. Matejka, Transactions, ASCE, Vol. 120, 1955, pp. 457-484.

making possible the measurement of total transport. This same idea could be utilized to insure transport of sediment loads through channels.

4. Stream Measurement.—Through a thorough understanding of the role of extreme roughness elements in a natural stream, an inexpensive and yet satisfactory method of estimating discharge of mountain streams may be developed eventually. Also, because uniform flow is rapidly induced by large roughness elements, a roughness flume might be developed for water measurement. This would seem to be a promising device for intermittent streams transporting large quantities of sediment. A properly designed tumbling-flow flume might permit use of a flume having approximately the same natural slope and roughness as the stream, thus avoiding the problems inherent in providing a stilling pool and sediment drop out, but still having the desirable characteristics of an overfall weir.

5. Roughness Standard.—An artificial standard of roughness for flow in open channels comparable to that of Nikaradse for pipes is desirable, but has not been fully developed.

6. Flow Analysis.—Understanding of the pressure distribution around roughnesses in open channels under various flow conditions would permit dynamical analysis of many flow problems.

CONCLUSIONS

1. Flow in extremely rough steep open channels may be classified into three regimes: tranquil, tumbling, and rapid.

2. In the tranquil and rapid regimes, flow may possibly be described by an equation of the type $\mathbf{F}_1 = C' S^n$, in which C' and n depend on the roughness intensity and configuration.

3. In the tumbling regime, the hydraulic jumps form over the roughness elements to the degree that a reach of stream acts as a control. Such a reach may be regarded as analogous to a critical flow weir.

4. For shallow depths under certain conditions, roll waves may form at the transition zone between tranquil and tumbling flow and rapid flow.

5. Based on better understanding of their action, the use of large roughness elements could result in improved hydraulic design for energy dissipators, improved sediment transport, and stream measurement.

ACKNOWLEDGMENT

The studies reported herein were conducted through the Utah State Engineering Experiment Station, Logan, Utah, under a university research grant as part of a continuing project on flow in steep, rough channels.

APPENDIX I. CRITERIA FOR FLOW REGIMES

Dynamic.—In Fig. 16(a) assume

$$Y_2 = Y_1 + K \qquad (18)$$

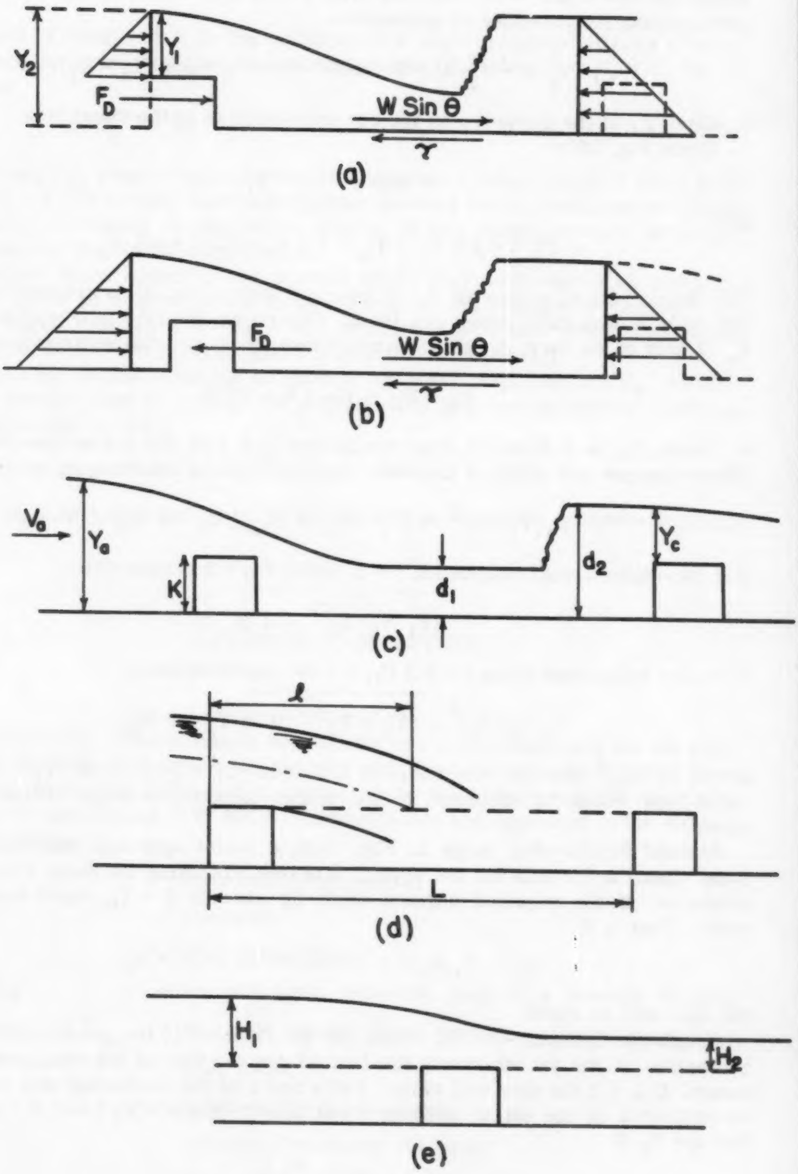

FIG. 16

From the observed data, this was true within 2%. Considering 1 ft of width and applying the principle of momentum,

$$\gamma\left(Y_1^2/2 - Y_2^2/2\right) + W \sin\theta - \tau + F_x = \rho\, q\left(V_2 - V_1\right) \ldots\ldots (19)$$

in which F_x is the pressure on the downstream face of the roughness.

From Fig. 16(b)

$$W \sin\theta = \tau - F_D \ldots\ldots (20)$$

and

$$\gamma\, Y_1^2/2 + \rho\, q\, V_1 + F_D + F_x = \gamma\, Y_2^2/2 + \rho\, q\, V_2 \ldots\ldots (21)$$

For supercritical values of V_1, if the right side of Eq. 21 is greater than the left side, a hydraulic jump can form. Otherwise, the flow will tend to skim. F_x is part of the form drag on the roughness; thus, one can summarize

$$F_x + F_D = C_D\, j\, K \rho\, V_2^2/2 \ldots\ldots (22)$$

in which C_D is a form of drag coefficient and j is the transverse width of roughness per unit width of channel. Substituting and rearranging yields

$$\mathbf{F}_1(Y_1/Y_2)^2 = \left(Y_1 + Y_2\right) / \left(C_D\, j\, Y_1 + 2\, Y_2\right) \ldots\ldots (23)$$

For two-dimensional roughness, j = 1, using $C_D = 2$ arbitrarily,

$$\left(F_1\, Y_1/Y_2\right)^2 \approx 1/2 \ldots\ldots (24)$$

For cube roughness using j = 0.3 C_D = 1.16, approximately,

$$\mathbf{F}_1\left(Y_1/Y_2\right)^2 \approx \left(Y_1 + Y_2\right) / \left(0.35\, Y_1 + 2\, Y_2\right) \ldots\ldots (25)$$

If $\left(F_1\, Y_1/Y_2\right)^2$ exceeds the value of 1/2 or of $\left(Y_1 + Y_2\right) / \left(0.35\ Y_1 + 2\ Y_2\right)$, rapid flow would be expected; if not, either tumbling or tranquil flow would occur.

Sequent Depth.—For large L, Fig. 16(c), d would approach that computed from Chezy's formula for the appropriate bed, excluding the large roughness elements. If the required sequent depth d_2 exceeds K + Y_c, rapid flow prevails. That is if

$$d_2 = \mathbf{F}_1\, d_1\, (S + 0.153)/0.133 > K + Y_c \ldots\ldots (26)$$

the flow will be rapid.

Roughness Spacing.—In Fig. 16(d), l is the distance to the point at which the centerline of the jet intersects the line joining the tops of the roughness elements. If L < l, the flow will skim. Let x and z be the horizontal and vertical co-ordinates of the jet of velocity V_1 at time t, then $x = V_1\, t$ and $Z = g\, t^2/2$. For $z = Y_1/2$

$$x = l = V_1 \sqrt{Y_1/g} \ldots\ldots (27)$$

Submergence.—Keutner[8] found that for $H_2/H_1 > 0.85$, Fig. 16(e), the nappe did not plunge, and the flow remained tranquil. Assuming $H_1 = Y_1$ and $H_2 = Y_1$

[8] "Neues Berchnungsverfahren fur den Akfluss anWehren aus der Geschwindegklitsverteilung des Wassers uber der Wehrkone," by C. Keutner, Die Bautechnik, p. 575, 1929.

- LS, Keutner's criterion reduces to $Y_1/(Y_1 - LS) > 0.85$ would imply tranquil flow.

Length of Jump.—If d is the uniform flow depth established for a channel excluding the gross roughness elements, and d_2 is replaced by $Y_c + K$, Eq. 10 becomes

$$\gamma\, d_1^2/2 + \rho\, q\, V_1 + W \sin\theta = \gamma \left(Y_c + K\right)^2/2 + \rho\, q\, V_2 \qquad (28)$$

Eq. 28 may be used to compute W. Assuming an average depth of jump to be $\left(d_1 + Y_c + K\right)/2$ (or any other appropriate average depth), compute the length of jump l_j necessary to provide the weight. If this length exceeds the roughness spacing, the flow cannot tumble.

Residual Slope.—Part of the channel slope may be thought of as providing gravity force to overcome the drag offered by the roughness element. Let this be designated S_D. If $S - S_D < S_{cr}$ in which S_{cr} denotes critical slope, the velocity cannot reach critical, and tranquil flow will prevail.

Roughness Height.—Let the velocity of approach, Fig. 16(c) be V_a. Assuming no energy loss, the equations of continuity and energy may be combined and rearranged to form

$$K = Y_c \left[1/2 \left(Y_c/Y_a\right)^3 - 3/2 \left(Y_c/Y_a\right) + 1\right] \qquad (29)$$

Values of K less than that given by Eq. 29 will be too small to induce tumbling flow.

APPENDIX II. NOTATION

The following letter symbols, adopted for use in the paper and for the guidance of discussers, conform essentially with American Standard Letter Symbols for Hydraulics (ASA-Z10.2), prepared by a committee of the American Standards Association, with ASCE representation, and approved by the Association in 1942:

b	= top width of roughness;
C, c	= constants;
C_d	= drag coefficient;
d_1, d_2	= sequent depth, hydraulic jump in a smooth channel;
$\mathbf{F}_1 = V_1/\sqrt{g\, Y_1}$	= Froude's number at the upstream crest of roughness;
F_d	= drag force;
g	= acceleration due to gravity;
H_1	= upstream head over the weir;
H_2	= downstream head over the weir;
j	= transverse width of roughness per unit width of channel;
K	= height of roughness;
L	= longitudinal roughness spacing;

l_j = length of jump;

L_{bwc} = length of backwater curve;

m = exponent of depth;

n = exponent of slope;

p = number of transverse roughness spacings per unit width of channel;

q = discharge per unit width of channel;

S = channel slope;

S_{cr} = critical slope;

S_d = slope used to provide gravity energy to overcome form drag;

t = transverse roughness spacing;

V_1 = velocity at upstream roughness crest;

V_a = velocity of approach;

V_c = critical velocity;

W = weight of small prism of water in hydraulic jump;

w = width of flume or channel;

x = horizontal distance;

Y_1 = depth of flow above upstream crest of roughness;

Y_2 = $K + Y_1$;

Y_a = depth of flow approaching the roughness;

z = vertical distance;

α = shape factor;

γ = specific weight;

ρ = density;

f_1, f_2, ϕ_1, ϕ_2, ϕ_3, = symbols denoting functions;

τ = shear;

θ = angle of slope;

ν = kinematic viscosity;

Journal of the
HYDRAULICS DIVISION
Proceedings of the American Society of Civil Engineers

TESTS ON PRESTRESSED CONCRETE EMBEDDED CYLINDER PIPE

By Hugh F. Kennison,[1] M. ASCE

SYNOPSIS

This paper presents the results of the first full-scale combined internal pressure and external load tests ever made on 60-in. prestressed concrete embedded cylinder pipe, designed according to AWWA Specification C301. The structural behavior of this pipe under combined loads is reported, based on the development of stress cracks in the concrete and on strain recordings from SR-4 strain gages.

INTRODUCTION

Prestressed concrete cylinder pipe has had world-wide acceptance since its introduction in 1942. In this original pipe, the prestressed wires are wrapped directly on the steel cylinder encasing the concrete core (Fig. 1). The pipe is manufactured in diameters from 16 in. to 48 in. In 1952 the first prestressed concrete embedded cylinder pipe was commercially produced. In this pipe, as distinguished from prestressed concrete cylinder pipe, the prestressed wires are wrapped about the concrete core in which the steel cylinder is embedded (Fig. 2). This pipe has been manufactured in diameters from 24 in. to 120 in. and is particularly applicable for large diameter and high pressure pipelines. Both types of pipe are described in the American Water Works Association (AWWA) Specification C301-58.

Prestressed concrete embedded cylinder pipe consists of a steel cylinder with bell and spigot joint rings welded to its ends. This steel membrane is

Note.—Discussion open until April 1, 1961. To extend the closing date one month, a written request must be filed with the Executive Secretary, ASCE. This paper is part of the copyrighted Journal of the Hydraulics Division, Proceedings of the American Society of Civil Engineers, Vol. 86, No. HY 9, November, 1960.

[1] Vice Pres., Engrg. and Research, Lock Joint Pipe Co., East Orange, N. J.

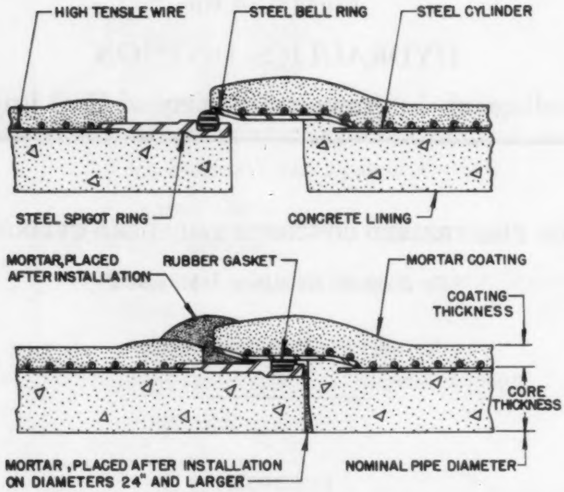

FIG. 1.—PRESTRESSED CONCRETE CYLINDER PIPE

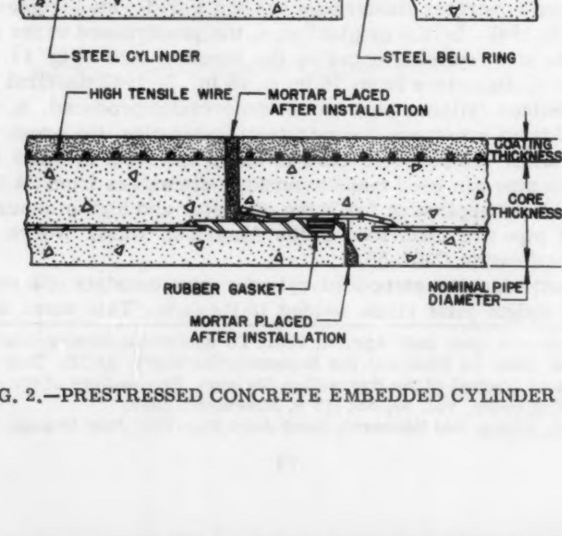

FIG. 2.—PRESTRESSED CONCRETE EMBEDDED CYLINDER PIPE

hydrostatically tested for water tightness and strength. The cylinder is then encased in a core of quality concrete consolidated by high frequency vibration. After the core has been properly cured, it is helically wrapped with prestressing wire under a high uniform tension. The wire is then protected with a concrete or mortar coating.

To obtain realistic information on the physical behavior of prestressed concrete embedded cylinder pipe, the American Concrete Pressure Pipe Association (ACPPA) sponsored a series of tests at a laboratory in Wharton, N. J. This three-day test program was witnessed by consulting engineers and major consumers from New York, N. Y., Philadelphia, Pa., Baltimore, Md., Kansas City, Mo., Dallas, Tex., Fort Worth, Tex., Ames, Ia., Denver, Col., Los Angeles, Calif., and San Francisco, Calif. These tests were designed to determine the structural behavior of 60-in. pipe when subjected to combinations of external loading and internal pressure, since under normal use these simultaneous conditions would be in effect.

PREVIOUS TESTS ON PRESTRESSED CONCRETE CYLINDER PIPE

Earlier combined load tests on small diameter prestressed concrete (lined) cylinder pipe have indicated a cubic parabola relationship between three-edge bearing load and internal hydrostatic pressure, as shown in Fig. 3.

The basic curves resulting from these earlier investigations are the "design" curve, and the "ultimate" curve. The "design" curve has been the principal control for a combined analysis of prestressed concrete (lined) cylinder pipe. The combination of normal operating pressure and dead load has been confined within a curve which is 90% of the "design" curve.

The "ultimate" curve represents the combinations of pressure and load which will cause failure. This curve is by far the least realistic of the curves and consequently seldom used. Under the three-edge type of loading this curve does not give an accurate representation of the pipe's performance under field conditions. As the pipe nears its ultimate capacity it behaves as flexible pipe, and under field conditions this capacity would be far greater than indicated, due to the extra side support given by passive earth pressures. In actuality, a much higher bedding factor should be applied with the ultimate curve, to obtain realistic results.

The terminal ordinate and abscissa values of these basic curves can be calculated and/or verified by relatively simple tests. These terminal values are: $W_{0.001\ in.}$ = three-edge bearing load producing the first 0.001-in. crack (incipient cracking); W_{ult} = three-edge bearing load producing ultimate failure of the pipe; P_0 = pressure causing zero concrete stress in the core; and P_b = bursting pressure of the pipe.

PIPE DESIGN FOR 60-IN. COMBINED LOAD TESTS

Class 160 psi, 60-in. prestressed concrete embedded cylinder pipe was selected for this test program, since it falls approximately in the middle of the range of sizes and pressures for this type of construction. Seven identical test specimens were constructed and tested at various combinations of internal pressure and external loads. These test pipe were 4 ft long, 60-in. internal diameter and designed for a combination of a working pressure of 160 psi

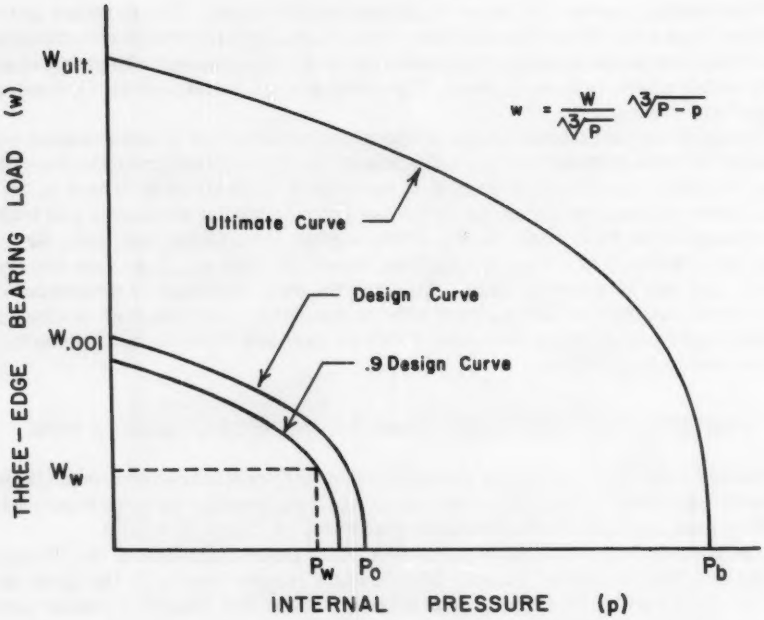

FIG. 3.—COMBINED LOAD CURVES FOR PRESTRESSED CONCRETE (LINED) CYLINDER PIPE

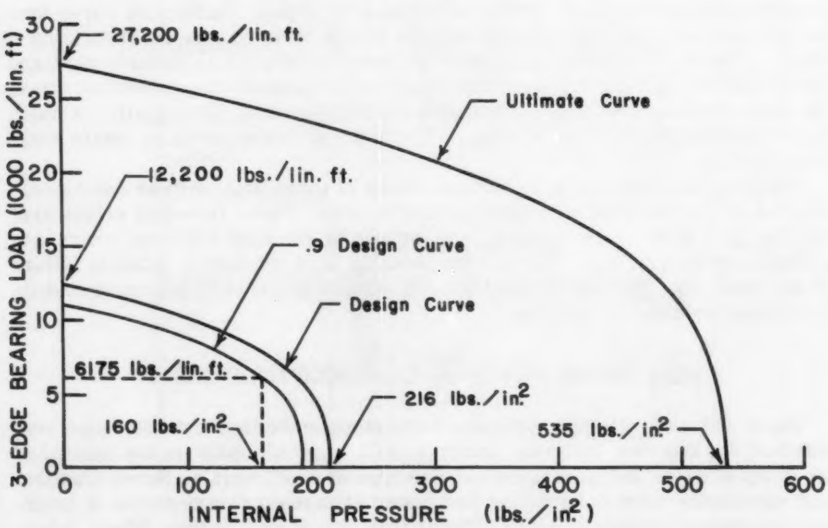

FIG. 4.—COMBINED LOAD DIAGRAM FOR TEST PIPE

and a three-edge bearing load of 6,175 lb per lin ft. A common design was chosen for all specimens to minimize the many variables which occur in such a series of tests. The design, consistent with AWWA Specification C301, is as follows:

Concrete core thickness = $4\frac{1}{2}$ in. (steel cylinder $1\frac{1}{2}$ in. from inside of core); concrete coating thickness = $1\frac{1}{2}$ in.; cylinder gage = #16 U.S.S. hot rolled (ASTM A245); prestress wire = #6, MB untempered (ASTM A227); steel cylinder area = 0.718 sq in. per lin ft; steel cylinder diameter = 63 in. (outside diameter); prestress wire spacing = 0.392 in., c. to c.; prestress wire area = 0.883 sq in. per lin ft; P_w = normal operating pressure = 160 psi; P_0 = zero compression pressure = 216 psi; P_b = bursting pressure = 535 psi; W_w = allowable three-edge bearing load at operating pressure = 6,175 lb per lin ft; W_{ult} = load to cause three-edge bearing failure at zero pressure = 27,200 lb per lin ft; gross wire wrapping stress = 140,000 psi; resultant wire stress = 105,000 psi; and wire stress at P_w = 111,570 psi.

Fig. 4 shows the design curve, the 0.9 design curve, the ultimate curve, the normal operating pressure, and the normal three-edge bearing load for these test specimens. These curves will be reproduced on all subsequent plots of the test results for reference purposes.

DESCRIPTION OF TESTING EQUIPMENT

For these tests the ASTM standard three-edge bearing load was chosen as the method of applying the external load because it was felt that this loading could be reproduced more consistently than a simulated trench condition. Extensive research work previously performed at Iowa State College (Ames, Ia.) by Anson Marston, W. J. Schlick, and M. G. Spangler provides the necessary

TABLE 1.—THREE-EDGE BEARING LOADS CONVERTED TO EQUIVALENT DEPTHS OF COVER

Three-Edge Bearing Load, in Pounds per Linear Foot (1)	Cover with Ordinary Bedding, in Feet			
	$B_d = D_o + 2$ ft, w = 100 pcf (2)	$B_d = D_o + 3$ ft, w = 100 pcf (3)	$B_d = D_o + 2$ ft, w = 120 pcf (4)	$B_d = D_o + 3$ ft, w = 120 pcf (5)
3,110	6.3	5.6	5.2	4.6
4,660	10.1	8.7	8.2	7.0
6,220	14.6	12.3	11.5	9.8
7,780	19.3	16.2	15.3	12.8
9,330	25.6	20.5	19.4	16.1
10,890	32.9	25.4	24.6	19.8
12,430	43.5	31.5	29.6	23.7
14,000	57.5	38.7	38.0	28.3
15,550	85.6	47.6	48.0	33.7
17,100	. . .	59.4	61.6	40.0
18,650	. . .	77.4	86.4	47.7

This table of equivalent depths of cover is based on the studies of Marston, et al, and assumed "ordinary" bedding (a bedding factor of 1.5 when compared with three-edge bearing loads) and soil constants of $K\mu$ and $K\mu'$ of 0.130, the ordinary maximum for clay soils.

information for converting the three-edge bearing loads to various types of trench conditions. The use of this excellent material eliminates the additional variable of evaluating a simulated trench condition and allows a reasonable interpretation of relatively simple and routine crushing tests. Table 1 has

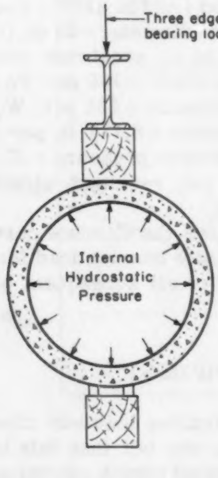

FIG. 5.—SYSTEM OF COMBINED LOADING

FIG. 6.—60-IN. PRESTRESSED CONCRETE EMBEDDED CYLINDER PIPE AND BULKHEAD ASSEMBLED FOR COMBINED LOAD TEST

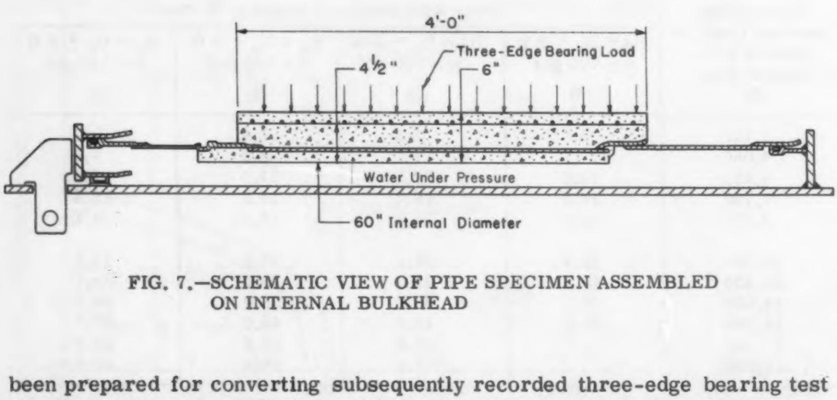

FIG. 7.—SCHEMATIC VIEW OF PIPE SPECIMEN ASSEMBLED ON INTERNAL BULKHEAD

been prepared for converting subsequently recorded three-edge bearing test results to the more realistic trench conditions, in feet of cover over the pipe; in Table 1 B_d is the trench width, D_o denotes the outside diameter of the pipe, and w is the specific weight of the soil.

The combined conditions of three-edge bearing external load and internal hydrostatic pressure under which these tests were carried out is illustrated in Fig. 5. The 60-in. test pipes, with 18-in. long thin steel cylinder extensions, were placed over a tubular internal bulkhead. The steel cylinder extensions reduced the supporting effect of the bulkhead on the three-edge bearing load. The test specimen completely assembled in the combined load testing facility is shown in Fig. 6. The arrangement of the test specimen mounted in the tubular bulkhead is illustrated in Fig. 7. The support which was provided by the hydrostatic bulkhead was carefully determined and all three-edge bearing loads

FIG. 8.—INTERIOR VIEW OF TUBULAR BULKHEAD WITH THICK GLASS WINDOW, SUBMARINE LIGHT HOUSING AND LONG FOCAL LENGTH MICROSCOPE

FIG. 9.—EXAMINATION OF THE CONCRETE COATING

were corrected by this amount. The tests and results for evaluating this supporting effect are presented subsequently.

Throughout the tests it was necessary to observe the inside concrete lining of the pipe to detect and measure the development of lining cracks. To accomplish this the tubular bulkhead was constructed with a thick glass window, through which the inside lining of the pipe could be surveyed with a 40X microscope. This window was placed opposite the bottom of the pipe, which would be the location of the maximum tensile stress in the concrete lining. A submarine lighting device was constructed within the bulkhead to illuminate the

inside bottom lining of the pipe over the area covered by the microscope. The arrangement of the glass window, the microscope, and the submarine light is shown in Fig. 8.

PROCEDURE USED TO OBSERVE TEST RESULTS

One of the major indications of adequacy of design in prestressed concrete, as in reinforced concrete, is the degree to which stress cracking of the concrete is controlled under load. Reinforced concrete pipe must necessarily have tensile stresses and resulting cracking of the concrete whenever the tensile strength of the concrete is exceeded. Prestressed concrete pipe was developed to prevent or reduce such stress cracking with resulting improved

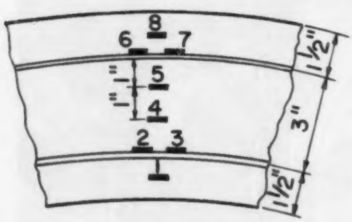

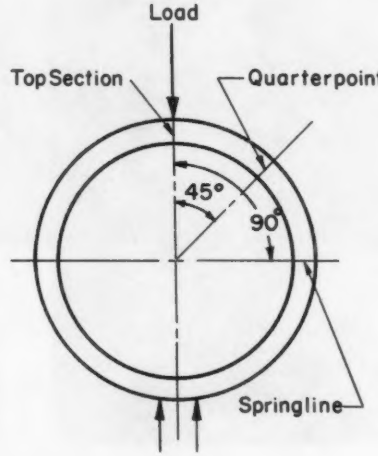

FIG. 10.—LOCATION OF SR-4 STRAIN GAGES

performance. A considerable margin exists between the load or pressure causing first visible stress crack, and that causing ultimate failure. Between these two points, lies the critical stress crack condition which many authorities consider to be in excess of 0.01 in. for conventionally reinforced pipe. In prestressed concrete pipe, the critical stress crack occurs in the exterior coating and is conservatively defined as having a sustained maximum width in excess of 0.005 in.

These tests report on the cracking of the lining and coating caused by the combined load application. The cracking behavior of the pipe was obtained by a careful examination of the concrete lining and coating with a 40X microscope equipped with a calibrated grid to accurately measure crack widths. The condition of "incipient" cracking or first tensile failure can be recorded by trained personnel through the use of such a microscope. This microscopic crack is

not readily visible to the naked eye and is defined as a crack, 0.001 in. in width and 12 in. long. The first visible crack is defined as a crack 0.002 in. wide and 12 in. long and can usually be observed with normal eyesight if a meticulous examination of the surface is made. The first visible crack supplies a consistent criterion of the stress cracking of the concrete and is so used in the recording and interpretation of the results of these tests. Fig. 9 shows the survey of the pipe coating by microscope to detect and measure stress cracks occurring in the coating while the pipe is under a combined load.

To further study the structural behavior of the pipe under combined loads, strain recordings were obtained through the use of SR-4 gages. These gages were installed in three test specimens at various locations as shown in Fig. 10(a). During the tests the pipe were placed with the strain gages at specified locations (Fig. 10(b)) relative to the points of application of the external load. Strain readings were then taken during combined load applications.

PRELIMINARY INFORMATION AND TESTS

The seven test specimens were numbered 1834 through 1840 for purpose of record. Table 2 gives the history of these seven test pipe.

TABLE 2.—MANUFACTURING AND TEST DATES (IN 1955) AND CONCRETE CYLINDER STRENGTHS

Pipe No.	Date Core Cast	Date Pre-stressed	Date Coated	Date Tested			Concrete Strengths, in Pounds per Square Inch			
				Combination Loading	Hydrostatic Test	Crushing Test	Core		Coating	
							7 Day	28 Day	7 Day	28 Day
(1)	(2)	(3)	(4)	(5)	(6)	(7)	(8)	(9)	(10)	(11)
1834	6/8	7/9	7/29	9/28	9/30	-	4,200	5,700	4,100	5,090
1835	6/14	7/23	7/25	-	-	11/7	4,150	5,400	4,000	5,180
1836	6/29	7/9	8/3	-	-	9/9 & 9/13	4,200	5,100	4,400	5,350
1837	6/23	7/9	8/1	9/29 & 11/8	-	-	4,650	5,625	4,000	5,350
1838	6/21	7/9	8/2	9/30	9/30	10/6	3,775	5,150	4,250	5,050
1839	6/27	7/9	7/26	-	9/29	-	4,400	5,750	3,800	4,800
1840	6/16	7/9	8/5	-	9/28	-	4,275	5,150	4,050	4,900

Pipe #1836 was used in the test conducted to evaluate the effect of the hydrostatic bulkhead in supporting external loads, as mentioned previously. In this test the pipe alone was subjected to increasing three-edge bearing loads in 2500 lb per lin ft; increments up to 19,000 lb per lin ft. Vertical deflections were measured to the nearest 0.001 in. at each increment of load. This test was repeated to record any effect of concrete tensile failure. The lower curve shown in Fig. 11 resulted from these two tests. The 18-in. long steel extension cylinders were then welded to the ends of pipe #1836 and the unit assembled in the hydrostatic bulkhead. The complete assembly was then subjected to the three-edge bearing test as before, the results of which appear as the upper

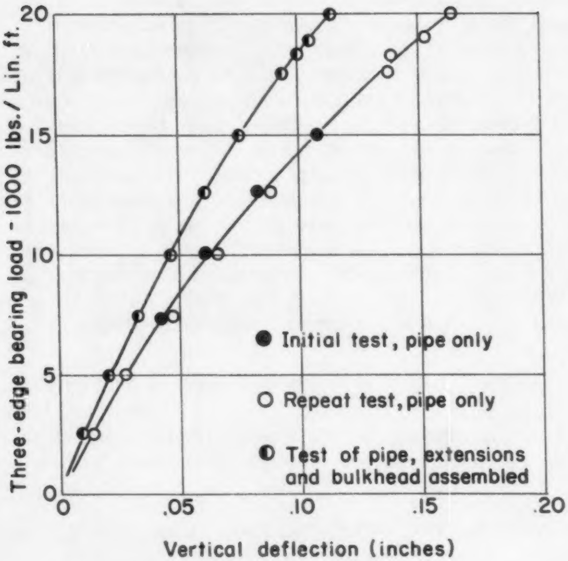

FIG. 11.—SUPPORTING EFFECT OF HYDROSTATIC BULKHEAD

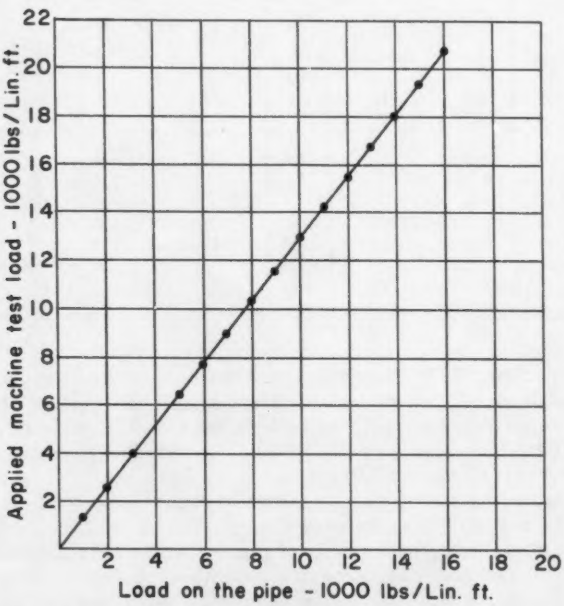

FIG. 12.—CORRECTION DUE TO BULKHEAD EFFECT

curve of Fig. 11. The difference in three-edge bearing load between the two curves, for a given deflection, is then taken as the supporting effect of the hydrostatic bulkhead at that load. Fig. 12 shows the resulting correction factor which was used to obtain the true three-edge bearing load.

TEST PROCEDURE AND RESULTS BASED ON CRACKING BEHAVIOR

The following discussion contains a separate section on the tests and resulting data, based on cracking behavior, for each of the individual test specimens. Results obtained through the use of the SR-4 strain gages will be presented separately following this section. A variety of test procedures was

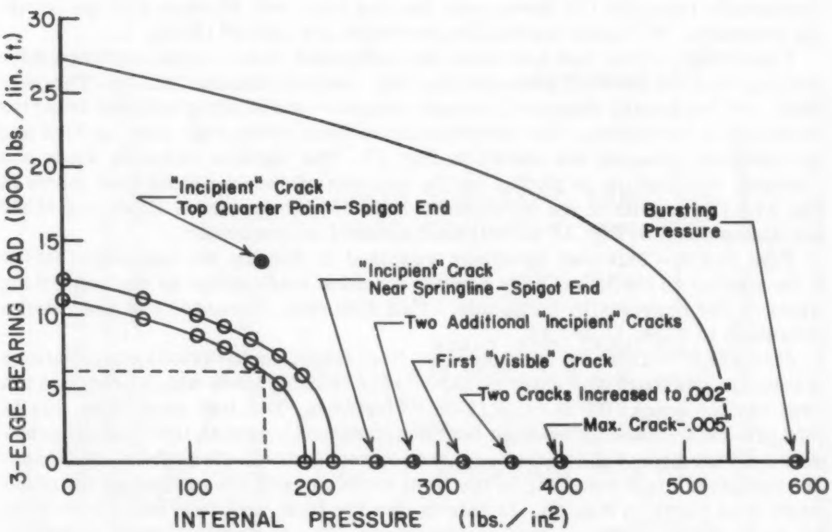

FIG. 13.—COMBINED LOADS ON TEST PIPE NO. 1834

carried out on each test pipe. These include: (1) subjecting the specimen to combined loadings that trace the 0.9 design curve and the design curve; (2) subjecting the specimen to a variety of combined loadings sufficient to produce "incipient" cracking (0.001-in. x 12-in. crack); (3) subjecting the specimen to combined loadings sufficient to produce the first visible crack (0.002-in. x 12-in. crack); (4) subjecting the specimen to combined loads in which both the internal pressure and three-edge load were increased by a predetermined amount; (5) subjecting the specimen to an increasing three-edge bearing load (no internal pressure) resulting in ultimate failure of the pipe; and (6) subjecting the specimen to an increasing internal pressure (no three-edge bearing load) resulting in ultimate bursting of the pipe. Each section will contain a description of the tests performed on the specimen along with a plot of the resulting data on a combined load curve for this design such as was shown in Fig. 4.

Figs. 13, 14, 15 and 16 show clearly the conservatism of the design method because of the very adequate margin between the theoretical design, or incipient crack, curve for the pipe tested and the actual pressure - load combinations which caused these cracks.

Pipe #1834.—Pipe #1834 was first subjected to a series of combined loads that traced the 0.9 design curve. These combined loads are plotted on Fig. 13. It was next subjected to a series of combined loads that traced the design curve. No microscopic cracking of the lining or coating was detected during these two series of combined loads. Following this the internal pressure was held at 160 psi (normal operating pressure) and the three-edge bearing load was increased until the first "incipient" crack (0.001-in. x 12-in.) formed. This first "incipient" crack appeared at the top quarter point of the spigot end. The last test consisted of recording the cracking behavior of the pipe as the internal hydrostatic pressure (no three-edge bearing load) was increased to the bursting pressure. All loads applied to pipe #1834 are plotted in Fig. 13.

Pipe #1835.—This test specimen was subjected to an increasing three-edge bearing load (no internal pressure) until it reached ultimate failure. The vertical and horizontal diameter changes were recorded along with the behavior of the crack formation. The relationship between three-edge bearing load and the diameter changes are shown in Fig. 17. The various cracking loads and cracking information is plotted on the ordinate of the combined load curve in Fig. 14. The results of the hydrostatic tests on test specimen #1839 and #1840 are also plotted in Fig. 14 as will be discussed subsequently.

Pipe #1836.—This test specimen was used to develop the correction factor to be applied to the three-edge bearing machine load caused by the supporting effect of the hydrostatic bulkheads. This test was discussed and the results presented in Figs. 11 and 12.

Pipe #1837.—This test specimen was first subjected to various combinations of internal pressure and external three-edge bearing loads which produced the first visible crack (0.002-in. x 12-in.) condition. The test procedure was to hold pre-established three-edge bearing loads and increase the internal pressure until the first visible crack occurred or reoccurred under subsequent loads. The combined loads resulting in the first visible crack are plotted on the combined load curve in Fig. 15. In this series the first visible crack occurred in the pipe coating under all load combinations. The controlling crack under internal pressure and no external load occurred at the top of the pipe while the controlling crack under external load and no internal pressure was located at the springline (90° from the top of the pipe).

Next this pipe was subjected to three combinations of internal pressure and three-edge bearing loads in which these loads were increased simultaneously to 2.0, 2.5, and 2.75 times the normal operating loads of 160 psi internal pressure and 6175 lb per lin ft three-edge bearing loads. The maximum crack width at each of these three combination loads was recorded. This information is recorded on the combined load curves of Fig. 15.

Pipe #1838.—As in pipe #1837 this specimen was first subjected to various combinations of internal pressure and three-edge bearing loads which produced the first visible crack (0.002-in. x 12-in.) condition. The procedure on this specimen was reversed so as to hold a predetermined internal pressure and increase the three-edge bearing load until the first visible crack formed. The combined loads resulting in the first visible crack are plotted on the combined load curve in Fig. 16. The controlling crack, in the case of pipe #1838, occurred in the coating and started at the upper quarter point (45° from the top of

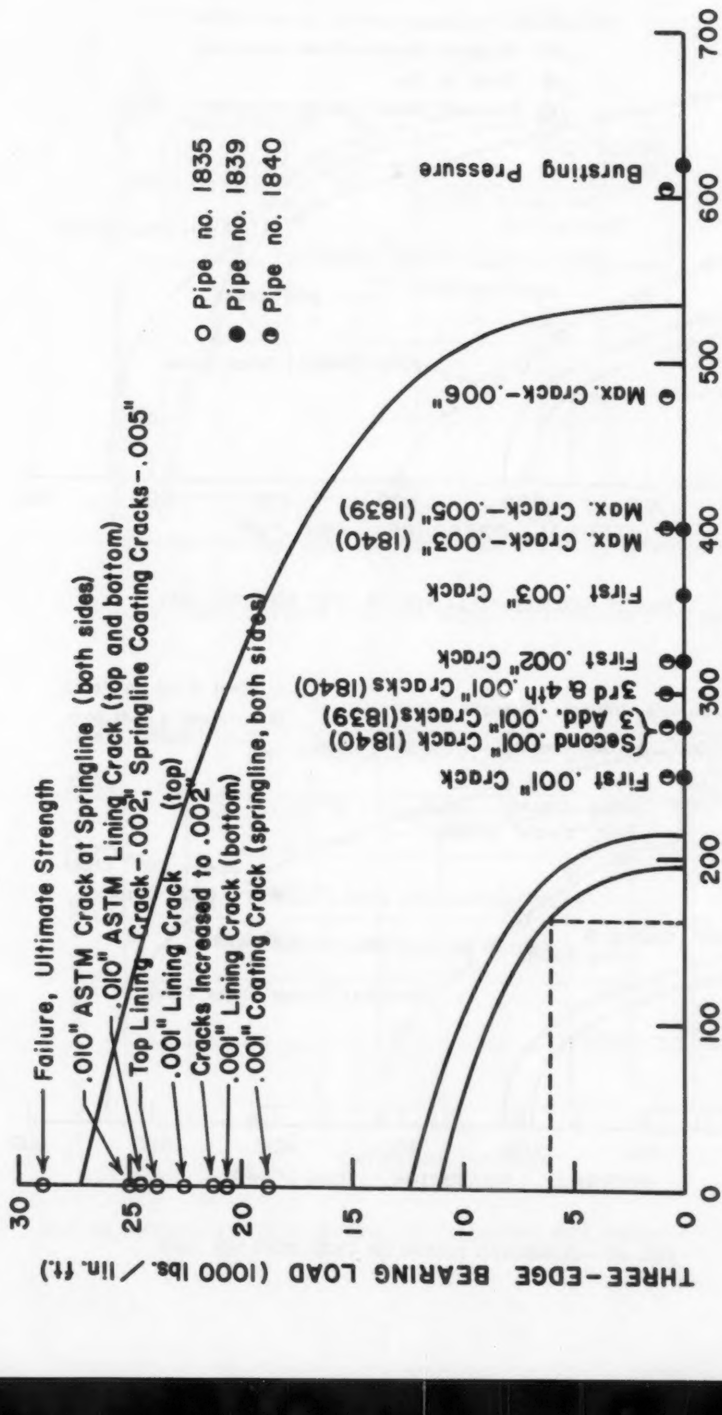

FIG. 14.—CRACKING BEHAVIOR OF TEST PIPES 1835, 1839 & 1840

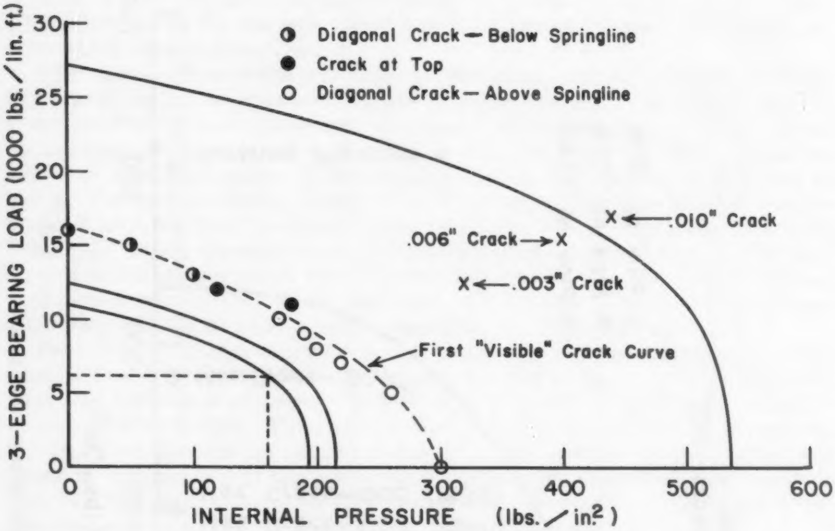

FIG. 15.—COMBINED LOADS ON TEST PIPE NO. 1837

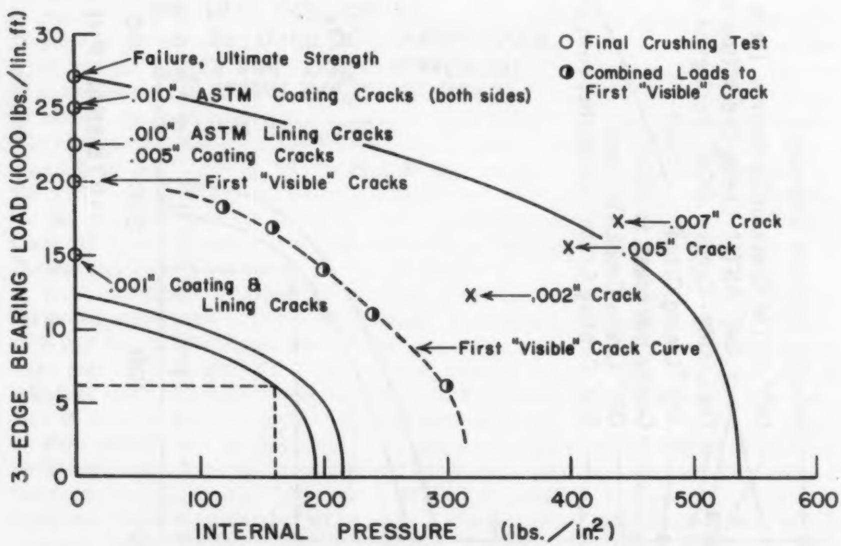

FIG. 16.—COMBINED LOADS ON TEST PIPE NO. 1838

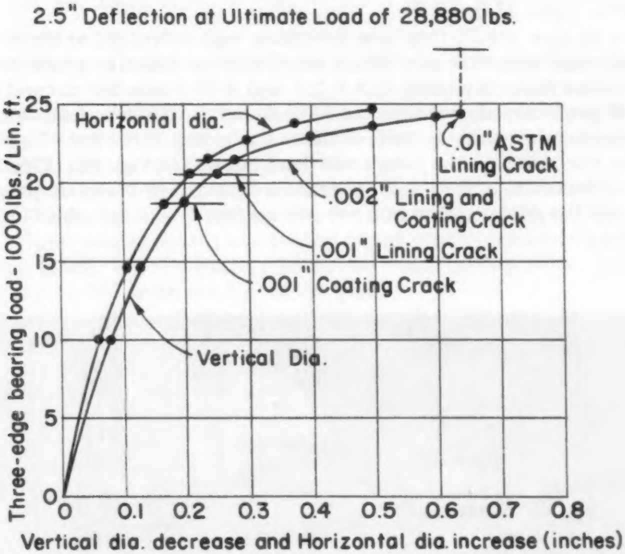

FIG. 17.—DEFLECTIONS AND CRACKING BEHAVIOR OF PIPE 1835

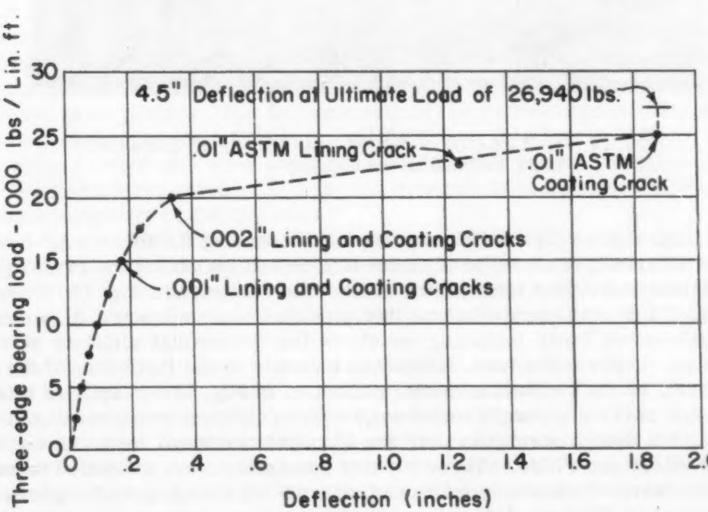

FIG. 18.—VERTICAL DEFLECTION AND CRACKING BEHAVIOR OF PIPE 1838

the pipe) and descended diagonally downward toward the springline (90° from the top of the pipe) of the pipe.

Next, as in pipe #1837, this test specimen was subjected to three combinations of internal pressure and three-edge bearing loads in which these loads were increased simultaneously to 2.0, 2.5, and 2.75 times the normal operating loads of 160 psi internal pressure and 6175 lb per lin ft three-edge bearing load. The maximum crack width at each of these loads was recorded. This information is also recorded on the combined load curves of Fig. 16. This specimen was then subjected to a series of increasing internal hydrostatic pressures up to 300 psi for the purpose of strain recordings, the results of which will be presented later.

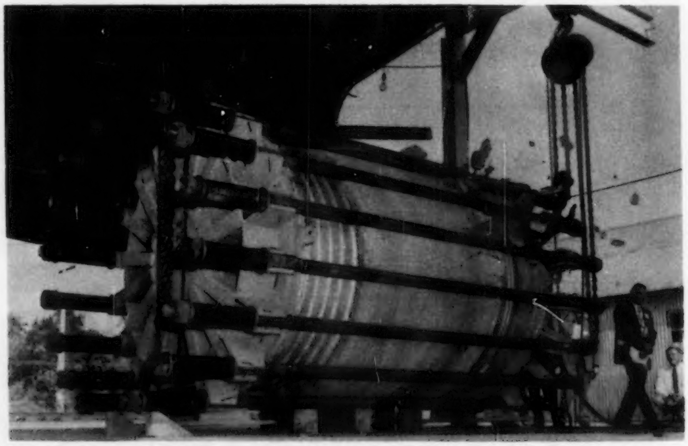

FIG. 19.—FAILURE OF PIPE NO. 1840 UNDER HYDROSTATIC TEST PRESSURE OF 605 PSI

The final test on pipe #1838 consisted of increasing the three-edge bearing load (no internal pressure) to ultimate failure and recording the cracking behavior throughout. This information is likewise recorded in Fig. 16. Previous to this last test to ultimate failure this pipe had been subjected to numerous high combination loads including one above the theoretical ultimate strength of the pipe. This resulted in a substantial increase in the flexibility of the pipe as is shown by the vertical diameter deflection in Fig. 18. In spite of this the three-edge bearing strength under each crack condition was greater than the conservative design strengths used for standard combined load calculations.

Pipes #1839 and #1840.—These two test specimens were subjected to an increasing internal hydrostatic pressure (no three-edge bearing load) up to bursting pressure of 620 and 605 psi respectively. The cracking behavior of the specimen was observed and is shown on the combined load curves of Fig. 14

along with the results of the three-edge bearing load tests on pipe #1835. Fig. 19 shows test specimen #1840 at the instant it failed under hydrostatic test.

TEST PROCEDURE AND RESULTS BASED ON STRAIN RECORDING

Pipe #1834.—Pipe #1834 was constructed with SR-4 strain gages distributed radially through the walls of the pipe at three different circumferential sections. The radial distribution of the SR-4 gages is shown in Fig. 10(a) and the spacing of the circumferential sections is shown in Fig. 10(b). The circumferential sections were spaced at 45° so that the strains recorded during the combined loads were those occurring at; (1) the top of the pipe directly under the three-edge bearing loads; (2) the quarter point, 45° from the top of the pipe; and (3) the springline or 90° from the top of the pipe.

The strains occurring at these locations in pipe #1834 were recorded during the combined load applications which traced the 0.9 design curve and the design curve as shown previously in Fig. 13. Since the strain recordings in the two series of combined loads were of essentially the same pattern but slightly displaced in magnitude, only the records obtained during the tracing of the design curve will be presented. Some of the gages were damaged during construction of the test specimen or for some other reason failed to record properly during the test. For this reason there is not a record for each of the SR-4 gages shown in Fig. 10(a). Fig. 20 shows a plot of the strains recorded during the application of the combined loads on pipe #1834 which traced the design curve. The letters on the abscissa of the strain curves denote the particular load application, as shown on the combined load curve.

The solid lines in Fig. 20 represent the strains as recorded by the SR-4 gages. The dotted lines are computed values of the strain obtained from a theoretical analysis of that particular section under a combined internal pressure and external three-edge bearing load. For the computed curves an elastic modulus of 28.5×10^6 psi was used for the steel and 3.7×10^6 psi for concrete. As seen on the curves of Fig. 20 the computed and recorded strains in general follow the same pattern. The displacement of the curves representing gage #7 at the top of the pipe is difficult to explain unless it is a zero shift of the recorder that occurs only when the pipe is loaded. The larger variation between the computed and recorded strains for the concrete is to be expected because of the non-homogenity of the material.

Pipe #1837.—Pipe #1837 had SR-4 strain gages mounted on the prestress wire and the concrete coating at the springline on both sides of the pipe. There were two gages on the prestress wire and two on the concrete coating at each location. Type A-7 SR-4 gages were used for mounting on the coating and Type A-9 for mounting on the prestress wire.

Strain recordings were taken on pipe #1837 during the combined loads to produce the first visible crack as was previously shown in Fig. 15. The strains resulting from this series of combined loads is shown in Fig. 21. The strains shown in the upper diagram of Fig. 21 are plotted directly above the combined loads, plotted in the lower diagram, which produced those strains. Since there was reasonable agreement between the four SR-4 gages on the prestress wire. the average strain recorded by these gages has been plotted. The average of the two coating gages on each side of the pipe have been plotted separately.

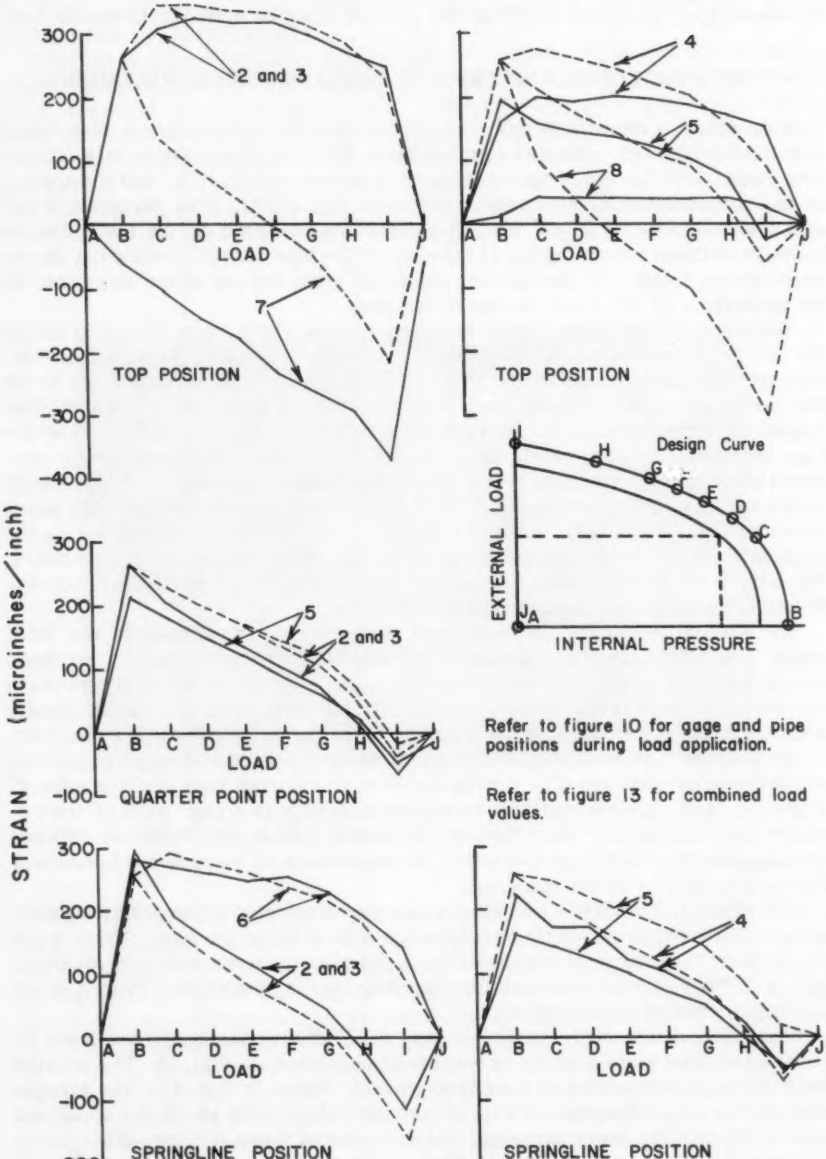

FIG. 20.—COMBINED LOAD STRAIN DATA FOR PIPE NO. 1834

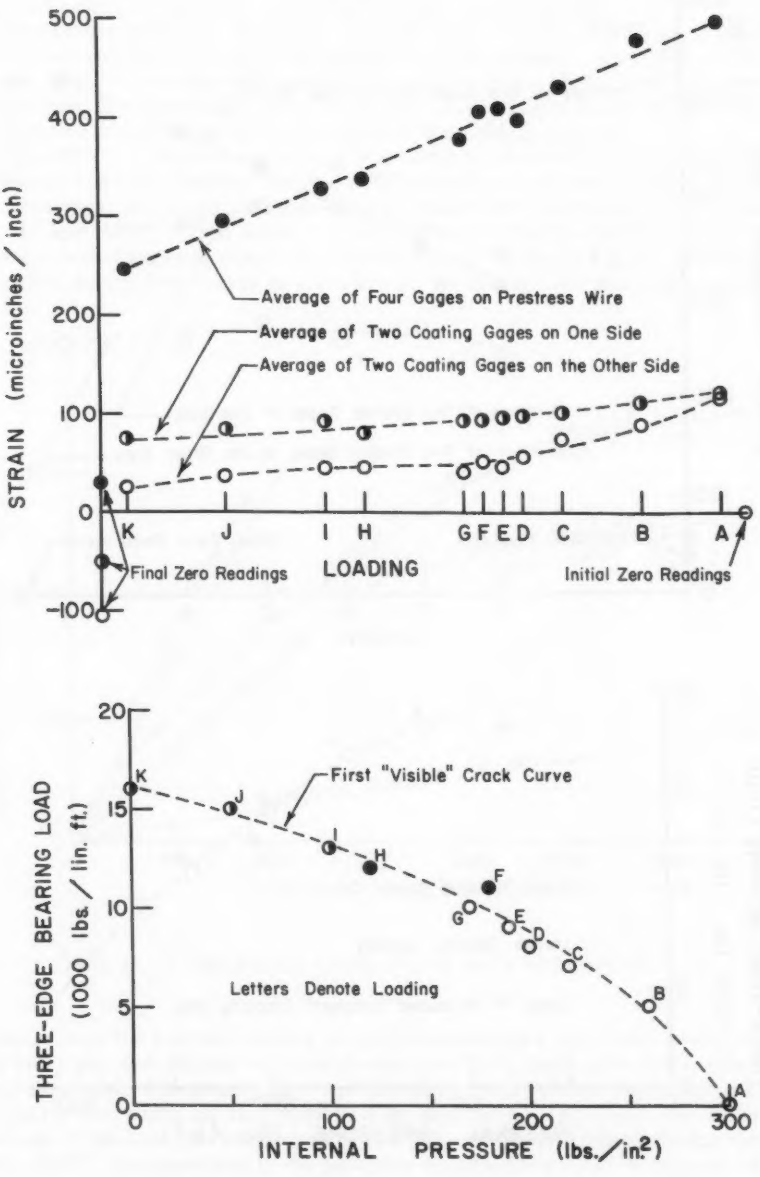

FIG. 21.—COMBINED LOAD STRAIN DATA FOR PIPE NO. 1837

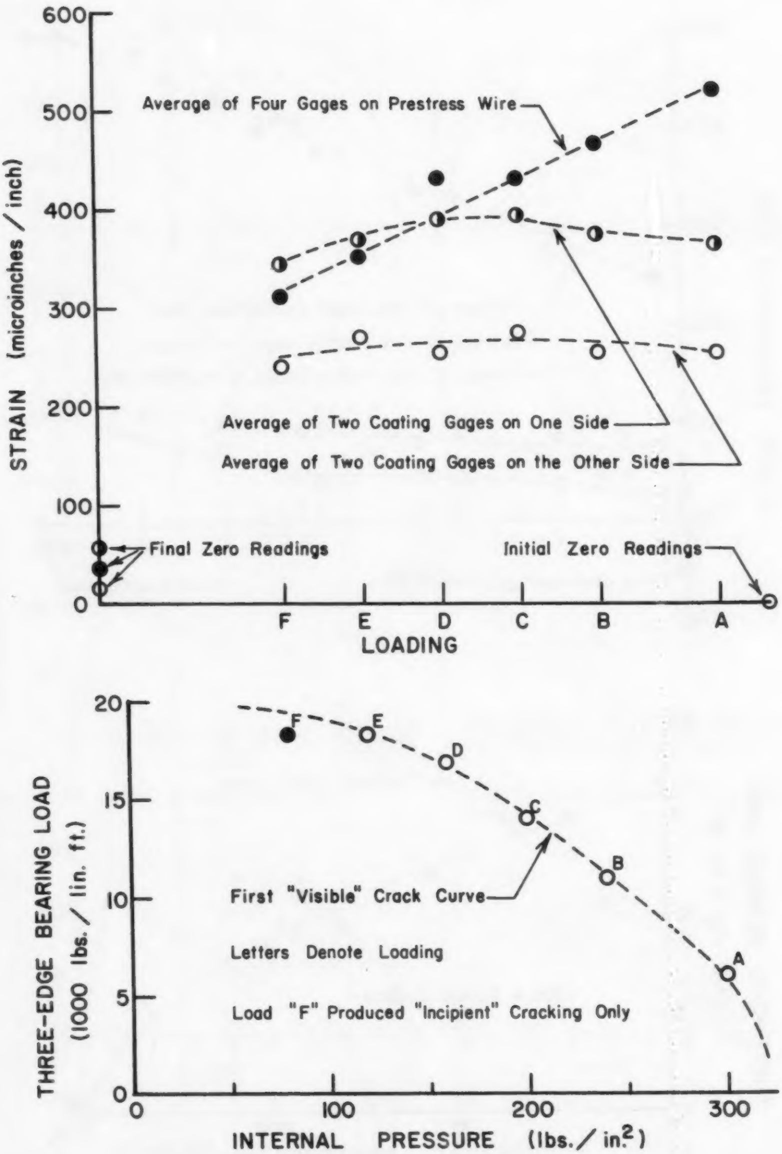

FIG. 22.—COMBINED LOAD STRAIN DATA FOR PIPE NO. 1838

Considerable shift in the zero readings of the coating gages is shown by the measured strain following removal of the last load (load K).

This strain data was recorded when the first visible (0.002-in. x 12-in.) crack formed, which, in all cases occurred in the coating. Since any cracking of the concrete coating will necessarily relieve some of the tensile stress in the coating, the strains as recorded by the coating gages would be affected by the location and general characteristics of the coating cracks.

Pipe #1838.—This test specimen was instrumented with SR-4 strain gages in exactly the same manner as pipe #1837 which has been discussed in the previous section. Again, as with pipe #1837, strains were recorded during the application of the combined loads to produce the first visible (0.002-in. x 12-in.) crack as was discussed previously and the results shown in Fig. 16. The strains recorded during this series of tests are shown in Fig. 22. Again the recorded

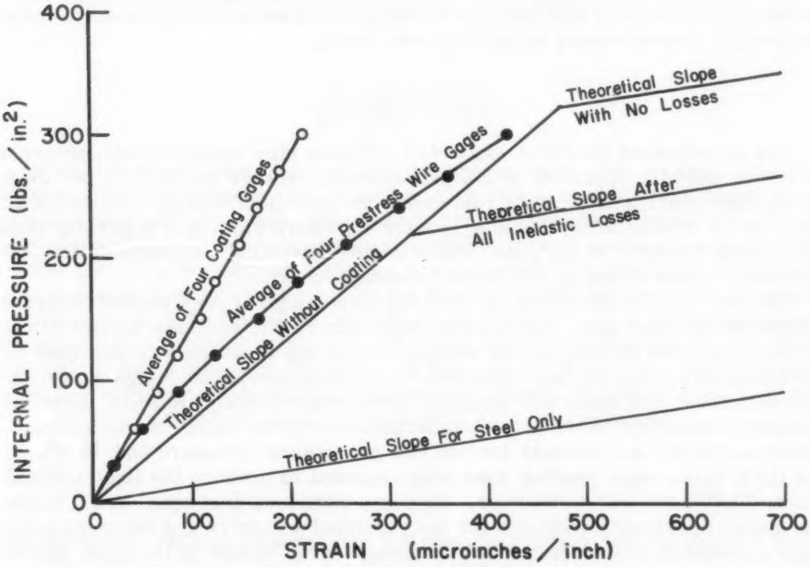

FIG. 23.—HYDROSTATIC LOAD STRAIN DATA FOR PIPE NO. 1838

strains from the four SR-4 gages on the prestress wire have been averaged and the two recorded strains on the concrete coating on each side of the pipe have been averaged. The strain pattern exhibited by the prestress wire in pipe #1838 is nearly the same as that exhibited by pipe #1837. However, the indicated strains of the concrete coating on pipe #1838 are considerably greater than on pipe #1837. As discussed in the previous section the strains measured by the coating gages could be affected by the cracking characteristics of the coating. This is a possible explanation for the large variation in strains indicated by the coating gages on the two pipe.

In both cases (pipe #1837 and #1838) the strain in the coating remains substantially constant while the prestress wire strain decreases with a decrease in internal pressure.

Following the increasing combination loads on pipe #1838 (shown in Fig. 16) strain recordings were taken on this specimen as the internal hydrostatic pressure was increased from 0 to 300 psi in 30 psi increments with no three-edge bearing load. The resulting strains are plotted in Fig. 23. Since there was good agreement between the various gages, the average, of the four prestress wire gages and the average of the four coating ggaes are plotted. Shown in Fig. 23 also are; (1) the theoretical strain - pressure relationship for the prestress wire with no coating effect with and without all the inelastic losses occurring after the core is prestressed; (2) the theoretical strain pressure relationship for steel only. The displacement of the coating strain curve to the left of the prestress wire strain curve can possibly be explained by the stress relief in the concrete coating caused by the cracking of the coating. It must be remembered that previous to this test pipe #1838 had been subjected to numerous loadings which caused cracks in the concrete coating.

CONCLUSIONS

The prestressed concrete embedded cylinder pipe tested in this program were designed for operation at 160 psi internal pressure and 6175 lb per lin ft three-edge bearing load. This represents an equivalent trench condition of 12 ft of cover with ordinary bedding in a trench whose width is 3 ft greater than the outside diameter of the pipe. These normal operating conditions fall on the 0.9 design curve which is 10% below the design curve.

The test results illustrate the conservative design of prestressed concrete embedded cylinder pipe, and clearly demonstrate the adequate stress crack control provided by the present design. No stress cracking was observed on the lining or coating for any combined load falling inside the design curve. In fact as pointed out under the heading "Test Procedure and Results Based on Cracking Behavior" there is a considerable margin of safety in the incipient crack condition. A combined load of 400 psi internal pressure and 15,400 lb per lin ft three-edge bearing load was required to produce the first critical cracks (0.005-in.) in the concrete. This is a combined load equal to 2.5 times the design operating conditions for both internal pressure and external load. Upon removal of the excessive loads, these cracks closed to the point where they were only visible through the 40X microscope. This illustrates that minor cracking as a result of stresses caused by live loads or water hammer which may temporarily exceed normal design conditions is not serious, since the stress crack will close when the excess load is removed.

Journal of the
HYDRAULICS DIVISION
Proceedings of the American Society of Civil Engineers

TRANSLATIONS OF FOREIGN LITERATURE ON HYDRAULICS

Third Progress Report of the Task Force on List of Translations of the Committee on Hydromechanics of the Hydraulics Division

INTRODUCTION

In an attempt to bring to hydraulic engineers an up-to-date listing of translations of foreign literature on hydraulics, it is the intent of the task force preparing this report to issue, from time to time, progress reports containing suitable items. Interested readers are urged to submit discussions to (a) add to this list, (b) offer suggestions for improvement, and (c) otherwise assist the task force in fulfiling its aims. The present list is the third issued since the publication, in 1957, of ASCE Manual 35, entitled "A List of Translations of Foreign Literature on Hydraulics." The first list appeared in the August 1959 Journal of the Hydraulics Division and the second in the June 1960 journal. This list is to be considered as an addendum to Manual 35 and will be included in a revision of that Manual when the time is deemed appropriate.

ANONYMOUS. "Model Experiments in Hydraulic Engineering." Statens Vattenfallsverk, pp. 75-76, 1951. (On file at Army Map Service.) Ref. No. TC 89, S97, Eng. Tr.

ANONYMOUS. "Model Experiments in Hydraulic Engineering." Statens Vattenfallsverk, pp. 73-74, 1952. (On file at Army Map Service.) Ref. No. TC 89, S97, Eng. Tr.

ANONYMOUS. "Model Experiments in Hydraulic Engineering." Statens Vattenfallsverk, pp. 80-81, 1953. (On file at Army Map Service.) Ref. No. TC 89, S97, Eng. Tr.

Note.—Discussion open until April 1, 1961. Separate discussions should be submitted for the individual papers in this symposium. To extend the closing date one month, a written request must be filed with the Executive Secretary, ASCE. This paper is part of the copyrighted Journal of the Hydraulics Division, Proceedings of the American Society of Civil Engineers, Vol. 86, No. HY 9, November, 1960.

ARMANET. L. "Genissiat (Power Station) Turbine Butterfly Valves" (Vannes-papillon des Turbines). From book entitled "Genissiat" published by La Houille Blanche, pp. 199-219. Tr. by P. J. Colleville. (On file at the Hydraulics Division, Fritz Engineering Laboratory, Department of Civil Engineering of Lehigh University.) Ref. Tr. No. 1, 1953.

BELOVA, M. N. "The Theory of Pneumatic Wave Damping" (K voprosu o teorii pnevmaticheskogo volnogasheniya). Gidrotekh. Stroit, Vol. 1956, No. 5, pp. 46-48. Tr. by Technical Information and Library Services, Minstry of Supply, London, England. (ASTIA Order No. AD 215819).

CHECHEĹ, N. S. "The Effect of the Number of Runner Blades on the Power Output of High Speed Variable Pitch Blade Turbines." Transactions of the Leningrad Polytechnical Institute of M. I. Kalinin, Ministry of Higher Education of the USSR, No. 193, pp. 38-50, 1958. (On file at DSIR, LLU.) Ref. RTS 1327.

CONSTANTINESCO, GOGU, AND HADDON, WALTER. "Means for Checking the Effect of Inertia in Fluid Columns." Tr. of Dutch patent 4,270, 16 pp, 22 July 1959. (On file at LC and SLA) Ref. 59-18792.

DECHEV, V. I. "An Investigation of Profile Cascades of a Reversible-flow Pump Turbine in a Cavitation Tunnel." Energetika, Vol. 1958, No. 10, pp. 130-143. (On file at DSIR, LLU) Ref. RTS 1346.

DREYER, A. A., AND SELITSKAYA, Ye. S. "USSR Oceanographic Research; Measurement of Wind-raised Waves During the Second Voyage of the Complex Antarctic Expedition (and) Study of Variations in Sea Level." Mezhdunarodnyy Geofizicheskiy God. Informatsionnyy Byulleten (USSR), Vol. 1959, No. 7, pp. 57-64. (On file at OTS) Ref. JPRS L-1166-N, 60-11164.

DUMOV, V. I. "Design of Centrifugal Pump Stages with Preconnected Axial Wheels Having Improved Anticavitational Characteristics." Teploenergetika, Vol. 6, No. 6, pp. 35-39, June 1959. (On file at U. S. Army Engineer Research and Development Laboratories, Fort Belvoir, Va.) Ref. T-703.

FILATOV, I. N. "Effect of Hub and Throat Ring Form on the Cavitation Properties of Variable Pitch Blade Hydraulic Turbines." Transactions of the Leningrad Polytechnical Institute of M. I. Kalinin, Ministry of Higher Education of the USSR, No. 193, pp. 66-74, 1958. (On file at DSIR, LLU) Ref. RTS 1328.

FRANKE, P. "Theoretical Considerations Concerning Jet Contraction in the Case of Flow Under Gates" (Theoretische Betrachtungen zur Strahlkontraktion beim Ausfluss unter Schützen). Die Bautechnik, Vol. 33, No. 3, pp. 73-77, March 1956. Tr. by J. C. Van Tienhoven, WES. (On file at WES) Ref. Tr. No. 60-2.

GIERS, I. V., AND SRETENSKI, L. M. "Influence of Varying the Principal Dimensions of a Ship on its Wave Resistance" (Vliianie izmeneniia glavnykh razmerov korablia na ego volnovoe soprotivlenie). Prikladnaia Matematika i Mekhanika, Vol. 10, pp. 21-32, 1946. Tr. by M. H. Brode, D. Fisher, and A. C. Thorpe, DTMB. (On file at DTMB) Ref. Tr. No. 282.

HASKIND, M. D. "The Oscillations of a Floating Form on the Surface of a Heavy Fluid" (Kolebaniia plavaiushchego kontura na poverkhnosti tiazheloi zhidkosti). Prikladnaia Matematika i Mekhanika, Vol. 17, pp. 167-178, 1953.

Tr. by M. H. Brode, D. Fisher, and A. E. Thrope, DTMB. (On file at DTMB) Ref. Tr. No. 283.

ILLARIONOV, V. I., AND BENDITSKY, N. D. "A Measurer of the Velocity and Direction of Flow (and) Measurement of the Temperature of the Surface Layer of Water in the Open Sea" (Struyemer - Izmeeritel' Skorosti i Napravleniya Techeniya (and) Ob Izmerenii Temperatury Poverkhnostnogo Sloya Vody v Otkrytom More). Meteorologiya i Gidrologiya (USSR), No. 6, pp. 49-54, 1958. (On file at LC and SLA) Ref. M168, M169; 59-19065.

INDRI, E. "Experimental Research on Models of Constrictions for Surge Tanks" (Ricerche sperimentali su modelli di strozzature per pozzi piezometrici). L' Energia Elettrica, Vol. XXXIV, No. 6, pp. 554-569, June 1957. Tr. by J. C. Van Tienhoven, U.S. Army Engineer WES. (On file at WES) Ref. Tr. No. 60-3.

IVANOV, A. A. "Some Conclusions from an Analysis of Observational Data on Windexcited Disturbances" (Nekotoryye Vyvody iz Analiza Dannykh Nablyudenii nad Vetrovym Volneyem). Akademiya Nauk SSSR. Morskoy Gidrofizicheskiy Institut. Trudy, Vol. 8, pp. 44-62, 1956. Tr. by Robinson. (On file at IC and SLA) Ref. 59-22613.

JAFFRY, P. AND HOURS, R. "The Study of Littoral Drift Using Radioactive Tracers." Cahiers Oceanographiques, pp. 475-498, 1959. (On file at Army Map Service) Ref. No. 339696.

KALIKHMAN, L. E. "Heat Exchange in the Vicinity of the Forward Stagnation Point in an Axially Symmetrical and Two-dimensional Gas Flow" (Teploobmen v okrestnosti perednei kriticheskoi tochki v osesimmetrichnom i ploskom potoke gaza). Akademiia Nauk SSSR, Izvestiia, Otdelenie Tekhnicheskikh Nauk, Vol. 8, pp. 11-16, 1955. (On file at the Ministry of Aviation, Gt. Brit.) Ref. N-45780X.

KOLMOGOROV, A. N. "The Breaking Up of Droplets in a Turbulent Stream." Akademiya Nauk SSSR., Doklady, Vol. 66, No. 5, pp. 835-838, 1949. (On file at ATS) Ref. ATS-07L37R.

KONONKOVA, G. Ye. "Measurement of Waves on the Surface of the Sea by Underwater Pressure Transmitters." Nauchaye Doklady Vysshey Shkoly. Fiiko-Matematicheskiye Nauki, No. 2, pp. 228-234, 1958. (On file at Ministry of Defense, Joint Intelligence Bureau, Division of Scientific Intelligence, London, England) Ref. Tr. No. 520.

KOSTERIN, S. I., SHEYNIN, B. I., AND KATABRZHIS, A. K. "Experimental Characteristics of Stratified Flow in a Steam-water Mixture in a Straight, Horizontal Pipe" (Opytnyye kharakteristiki razdelennogo techeniya parovodyanoy smesi v pryamoy gorizontalnoy trube). Teloenergetika (USSR), Vol. 3, No. 1, pp. 22-26, 1956. (On file at LC or SLA) Ref. 59-16543, CTS No. 345.

KOVALEV, N. N., et al. "Investigation of the Pressure and Stresses Acting on the Runner Blade of Hydraulic Turbines at the Narva Hydroelectric Power Station." Energomash, No. 1, pp. 29-32, 1959. (On file at DSIR, LLU) Ref. RTS 1113.

KRASSOV, I. M., AND TURBIN, B.G. "A Possibility of the Determination of the Axial Hydrodynamic Force in a Valve" (Ob odnoy vozmoshnosti opredeleniya osevoy gidrodinamicheskoy sily na zolotnike). Avtomatika i Telemekhanika (USSR), Vol. 19, No. 3, pp. 217-220, 1958. (On file at OTS) Ref. 59-11958, No. H-2056A.

KRISAM, F. "Influence of Volutes on Characteristic Curves of Centrifugal Pumps" (Der Einfluss des Leitvorrichtung auf die Kennlinien von Kreiselpumpen). VDI Zeitschrift, Vol. 94, No. 11-12, pp. 319-322, April 1952. Tr. by A. Ostapenko and J. B. Herbich. (On file at the Hydraulics Division, Fritz Engineering Laboratory, Department of Civil Engineering of Lehigh University.) Ref. Tr. No. T-5.

KRYANIN, I. R. "Cavitation Erosion in the Blades of High-power Hydraulic Turbines." Energomashin, No. 3, pp. 14-18, 1955. (On file at DSIR, LLU) Ref. M. 943.

LAMBOSSY, P. "Forced Oscillations of an Incompressible and Viscous Liquid in a Rigid and Horizontal Tube. Calculation of the Force of Friction" (Oscillations forcées d'un liquide incompressible et visqueux dans un tube rigide et horizontal. Calcul de la force de frottement). Helvetica Physica Acta (Switzerland), Vol. 25, No. 4, pp. 371-386, 1952. (On file at SLA) Ref. 59-17964, Tr. No. 192.

LAUCK, A. "The Nappe Over a Weir" (Der Ueberfall über ein Wehr). Zeitschrift fur angevandte Mathematik und Mechanik, Vol. 5, No. 1, pp. 1-16, Feb. 1925. (On file at WES) Ref. Tr. 59-6. Tr. by J. C. Van Tienhoven.

LAVRENTIEFF, V. M. "Theory of the Ideal Cavitating Propeller" (Teoriia ideal'nogo kavitiruiushchego dvizhitelia). Doklady Akademii Nauk SSSR, Vol. 50, pp. 89-93, 1945. Tr. by B. V. Nakonechny, DTMB. (On file at DTMB.) Ref. Tr. No. 279.

LETERRIER, G. "Behavior of Rock in Steel-lined Tunnels; Results of Measurements Made at Randens, Montpezat, Brévierès, and Serre-Ponçon" (Le comportement du rocher dans les galeries blindées; résultats des measures effectuées à Randens, Montpezat, Brévières, Serre-Ponçon). La Houille Blanche, Vol. 11, Special No. A, pp. 144-170, March-April 1956. Tr. by J. C. Van Tienhoven, U. S. Army Engineer WES. (On file at WES) Ref. Tr. 60-4.

MAMEDOV, G. A. "Crossflow of Fluids Between Two Adjacent Beds of Different Permeability." Izwestiya Vysshikh Uchebnykh Zavedeniy. Nefti Gaz (USSR), Vol. 2, No. 4, pp. 49-55, 1959. (On file at ATS) Ref. ATS-08L35R.

MEIXNER, J. "Flows of Fluid Media with Internal Transformations and Compression Viscosity" (Strömungen von fluiden Medien mit inneren Unwandlungen und Druckviskosität). Zeitschrift für Physik (West Germany), Vol. 131, No. 4, pp. 456-469, 1952. (On file at SLA) Ref. 59-17940, Tr. No. 188.

MIKHAYLOV, I. G., AND SHUTILOV, V. A. "A Simple Method of Detecting Cavitation in Liquids." Akusticheski Zhurnal, Vol. 5, No. 3, pp. 376-378, 1959. (On file at DSIR, LLU) Ref. M. 1504.

OBUKHOV, A. M. "Energy Distribution in the Spectrum of Turbulent Flow." Izv. AN SSSR Ser. geogr. i geofiz, Vol. 5, No. 4-5, pp. 453-463, 1941. (On file at DSIR, LLU) Ref. M. 1375.

OSTOSLAVSKII, I. V., AND GRUMONDZ, T. A. "On the Relation Between the Generation of a Lift Force on a Wing and the Character of the Flow in the Boundary Layer." Izvestiia Vysshikh Uchebnykh Zavedenii, Seriya Aviatsionnaiia Tekhnika, No. 1, pp. 27-36, 1958. (On file at NASA) Ref. NASA TT F-26.

RADIONOV, S. I. "Wave Dissipation by Compressed Air (Pneumatic Breakwater)." 47 pp, "Ocean Transport", Moscow, 1958. Tr. by Hildegard Arnesen, University of California, Dept. of Engineering Technical Report 104, Issue 9. (On file at U of C).

ROCHA, M. ,et al. "Observation of Dams. Methods and Apparatus Used in Portugal". Ministerio Das Obras Publicas, Laboratorio Nacional de Engenharia Civil, Lisbon, 28 pp, 1957. Technical Report No. 104. (On file at U. S. Army Research and Development Laboratories, Dept. of the Army Corps of Engineers, Fort Belvoir, Va.) Ref. Tr. No. T-646.

ROZIN, L. A. "An Approximation Method for the Integration of the Equations of a Nonstationary Laminar Boundary Layer in an Incompressible Fluid." Prikladnaia Matematika i Mekhanika, Vol. 21, pp. 615-623, 1957. (On file at NASA). Ref. NASA TT F-22.

SERGIENKO, A. A. AND GRETSOV, V. K. "Transition from a Turbulent to a Laminar Boundary Layer." Dokl. Akad. nauk SSSR, Vol. 125, No. 4, pp. 746-747, 1959. (On file at DSIR, LLU) Ref. R. A. E. 827.

STOPSKIY, S. B. "Hydroturbine Noise." Elek Stants, No. 4, pp. 22-25, 1958. (On file at DSIR, LLU) Ref. RTS 1300.

UVAROV, G. A. "Entrainment of Liquid by Gas or Steam" (Uvlechenie zhidkosti gazom ili parom). Sbornik Nauchniykh Trudov Kuibyshevskogo Industrial'nogo Instituta, Vol. 5, pp. 196-203, 1955. (On file at Ministry of Aviation, Gt. Brit). Ref. N-82289.

VLADIMIROV, A. N. "Submersion of a Ship's Bow Under Head-on Waves" (Zalivaemost'korablei pri khode na volnenii). Prikladnaia Matematika i Mekhanika, Vol. 10, pp. 75-92, 1946. Tr. by M. H. Brode, D. Fisher, and A. C. Thrope, DTMB. (On file at DTMB) Ref. Tr. No. 284.

VOLKOV, D. M. "Concerning Eact Solutions of a Class of Hyperbolic Equations Applicable in the Theory of the Water Hammer." Dokl. Akad. Nauk SSSR, Vol. 90, No. 1, pp. 49-50, 1953. (On file at DSIT, LLU) Ref. M. 886.

YEZSHOV, V. N. "The Principle of Minimum Drag and the Construction of the Characteristics of the Runner of an Axial-flow Fan" (Printsip Minimuma Soprotivleniya i Postroenie Kharakteristik rabochego Kolesa Osevogo Ventilyatora). Akademiya Nauk URSR, Kiev. Laboratoriya Hidravlichnykh Mashyn. Sbornik Trudov, Vol. 1956, No. 6, pp. 74-85. (On file at LC and SLA) Ref. 59-22672.

Respectfully submitted,
Jan C. Van Tienhoven, Chairman
Task Force on List of Translations of the
Committee on Hydromechanics of the
Hydraulics Division

Journal of the
HYDRAULICS DIVISION
Proceedings of the American Society of Civil Engineers

DISCUSSION

Note.—This paper is a part of the copyrighted Journal of the Hydraulics Division, Proceedings of the American Society of Civil Engineers, Vol. 86, No. HY 9, November, 1960.

[illegible]

[illegible]

[illegible]

[illegible]

[illegible]

[illegible]

RESISTANCE EXPERIMENTS IN A TRIANGULAR CHANNEL[a]

Closure by Ralph W. Powell and Chesley J. Posey

RALPH W. POWELL,[21] F. ASCE and CHESLEY J. POSEY,[22] F. ASCE.—The authors wish to express their appreciation for the contributions of the discussers. They also wish to take this opportunity to report on additional tests which have been made since the original paper was prepared. Table 3 gives the results of 19 more runs on the smooth channel and 27 runs on the channel with the walls coated with paraffin. This was a mineral wax with small polyethylene content, such as is used for waterproofing paper milk cartons, which was heated and rolled onto the inside surface of the flume with painting rollers. As the material solidified upon contact with the relatively cool surface of the flume, it became slightly tacky so that the rollers pulled it up into a pebbled surface much like that of fairly smooth concrete. Plaster casts of this surface were taken, and a method found whereby the casts could be hardened without distortion. Equipment, designed to measure this roughness and analyze the measurements, was built, but so far it has not been perfected.

The numeration of runs in Table 3 is not continuous with that of Table 1. For runs 158-174, a false bottom was installed in the channel, making it a trapezoidal channel. The results for the trapezoidal shape will be reported elsewhere.

Only one of the 19 runs on the smooth triangular channel had a Froude number over 0.85 (No. 202 with 0.88), and it showed no greater resistance than the others, so that these runs are all classed as tranquil flow. The average n by Manning's formula was 0.0092, the same as for the 23 runs already reported. The average discrepancy was slightly more, however, bringing the average for the entire 42 runs with tranquil flow up to 3.8%.

The Colebrook formula for circular pipes is

$$\frac{1}{\sqrt{f}} = 1.74 - 2 \log \left(\frac{\epsilon}{r_o} + \frac{18.7}{R \sqrt{f}} \right)$$

Substituting 2 R for r_o this reduces to

$$\frac{1}{\sqrt{f}} = - 2 \log \left(\frac{\epsilon}{14.83R} + \frac{2.52}{R \sqrt{f}} \right)$$

Mr. Ackers says that for the triangular channel a better fit is obtained if the 2 is changed to 2.2. (He also uses 14.8 instead of 14.83 and 2.51 instead of 2.52,

[a] May, 1959, by Ralph W. Powell and Chesley J. Posey.

[21] Prof. Emeritus of Engr. Mechanics, Ohio State Univ., Columbus, Ohio.

[22] Dir., Rocky Mountain Hydr. Lab. and Head, Dept. of Civ. Engr., State Univ. of Iowa, Iowa City, Iowa.

TABLE 3 - SUMMARY OF TEST RESULTS (CONTINUATION OF TABLE 1)

RUN NO.	DATE	TIME	ROUGHNESS	WEIR	AVER. HEAD	TEMP C°	SLOPE	y_n ft.	Q cfs	FROUDE No.	R $\times 10^{-3}$	CHEZY C	f	MANNING n
175	9-2-58	11:00-11:23	PARAFFIN	V	0.490	12.0	.0153	0.334	0.421	1.62	133.6	88.7	.0327	.0118
176	9-2-58	10:31-10:46	"	V	0.686	11.8	.0153	0.439	0.969	1.89	233	103.3	.0241	.0106
177	9-2-58	9:56-10:14	"	V	0.889	11.4	.0153	0.560	1.852	1.97	345	107.5	.0222	.0106
178	9-2-58	9:19- 9:35	"	V	1.084	10.6	.0153	0.694	3.04	1.89	446	102.8	.0243	.0114
179	9-2-58	8:46- 9:06	"	V	1.236	10.0	.0153	0.762	4.22	2.07	553	112.9	.0202	.0106
180	9-2-58	4:47- 4:59	"	⊔	0.311	14.5	.0152	0.776	4.55	2.14	663	117.2	.0187	.0102
181	9-2-58	4:23- 4:37	"	⊔	0.459	14.7	.0152	1.006	8.18	2.01	926	109.8	.0213	.0114
182	9-2-58	3:57- 4:13	"	⊔	0.600	14.9	.0152	1.165	12.27	2.09	1207	114.4	.0196	.0112
183	9-2-58	3:30- 3:44	"	⊔	0.740	15.0	.0152	1.296	16.89	2.20	1497	120.5	.0177	.0108
184	9-2-58	2:59- 3:16	"	⊔	0.898	14.9	.0152	1.434	22.72	2.30	1812	125.9	.0162	.0105
185	9-8-58	3:40- 3:58	"	V	0.349	14.6	.00874	0.313	0.1818	0.83	65.7	59.6	.0724	.0173
186	9-8-58	2:57- 3:16	"	V	0.500	14.4	.00874	0.405	0.442	1.06	123.3	76.3	.0442	.0141
187	9-8-58	1:25- 2:17	"	V	0.711	14.0	.00874	0.534	1.059	1.27	222	91.6	.0306	.0123
188	9-8-58	11:02-11:24	"	V	0.973	12.3	.00874	0.683	2.32	1.50	363	108.5	.0218	.0108
189	9-5-58	3:35- 3:55	"	⊔	0.301	13.5	.00875	0.886	4.33	1.46	540	105.5	.0231	.0116
190	9-8-58	10:08-10:30	"	V	1.275	11.3	.00875	0.891	4.56	1.52	532	109.3	.0215	.0112
191	9-5-58	2:49- 3:13	"	⊔	0.439	13.7	.00876	1.088	7.65	1.55	781	111.2	.0208	.0114
192	9-5-58	1:55- 2:32	"	⊔	0.623	13.7	.00876	1.335	13.00	1.58	1078	113.5	.0200	.0115
193	9-5-58	10:51-11:35	"	⊔	0.836	13.0	.00876	1.565	20.36	1.66	1415	119.4	.0180	.0113
194	7-30-59	11:20-11:26	SMOOTH	V	0.352	13.5	.00144	0.343	0.1856	0.67	59.8	119.4	.0180	.0087
195	7-30-59	10:41-11:00	"	V	0.549	12.8	.00144	0.516	0.556	0.73	117.0	128.9	.0155	.0087
196	7-30-59	9:39-10:05	"	V	0.708	11.8	.00144	0.649	1.049	0.77	170.1	137.0	.0137	.0085
197	7-29-59	4:22- 4:43	"	V	0.884	13.0	.00144	0.786	1.826	0.83	252	147.5	.0118	.0081
198	7-29-59	2:52- 3:54	"	V	1.228	13.2	.00144	1.106	4.15	0.81	410	143.0	.0126	.0089
199	7-17-59	10:20- 3:28	"	⊔	0.349	12.1	.00147	1.247	5.41	0.78	462	136.5	.0138	.0095
200	7-29-59	10:01-10:55	"	⊔	0.596	13.0	.00147	1.684	12.15	0.82	784	144.6	.0123	.0094
201	7-20-59	3:04- 4:24	"	⊔	0.814	12.2	.00150	2.01	19.55	0.85	1036	148.5	.0117	.0095
202	7-18-59	11:16-11:51	"	⊔	0.897	11.9	.00150	2.11	22.69	0.88	1139	152.2	.0111	.0093
	& 7-20-59	10:51- 2:29												
203	8-4-59	9:09- 9:44	"	V	0.288	11.0	.00068	0.330	0.1131	0.45	35.4	116.6	.0189	.0089
204	8-3-59	3:09- 3:51	"	V	0.447	12.7	.00068	0.509	0.335	0.45	71.2	116.9	.0188	.0096
205	8-3-59	2:18- 2:47	"	V	0.724	12.3	.00070	0.786	1.108	0.50	150.5	128.5	.0156	.0094
206	8-3-59	11:25- 1:34	"	V	1.011	12.3	.00071	1.070	2.55	0.54	255	136.2	.0139	.0093
207	8-1-59	11:21-11:46	"	V	1.139	11.8	.00071	1.208	3.44	0.54	301	135.6	.0140	.0095
	& 8-3-59	9:15-10:50												
208	8-1-59	9:55-11:05	"	V	1.301	11.3	.00071	1.362	4.80	0.55	367	140.1	.0131	.0094
209	8-10-59	11:39-12:11	"	⊔	0.480	13.5	.00074	1.704	8.75	0.58	567	142.7	.0126	.0096
210	8-10-59	9:09-11:18	"	⊔	0.564	11.8	.00074	1.878	11.17	0.58	628	142.8	.0126	.0097
211	8-4-59 8-5-59 8-5-59 8-8-59 8-12-59 8-19-59	4:19- 4:57 8:53-11:55 3:22- 3:36 9:30-10:00 2:49- 3:02 9:49-11:12	"	⊔	0.669	12.0	.00074	2.09	14.49	0.57	737	141.9	.0128	.0099
212	8-8-59	10:38-12:04	"	⊔	0.817	12.5	.00074	2.29	19.66	0.62	923	153.1	.0110	.0094
213	8-27-59	11:57- 3:15	PARAFFIN	V	0.590	13.6	.00074	0.699	0.665	0.41	104.9	100.6	.0254	.0117
214	8-27-59	10:40-11:30	"	V	0.801	12.5	.00074	0.904	1.426	0.46	169.6	113.4	.0200	.0108
215	8-27-59	9:14- 9:49	"	V	1.047	10.7	.00074	1.160	2.79	0.48	245	118.9	.0182	.0108
216	9-1-59	4:59- 5:37	"	⊔	0.313	13.2	.00074	1.396	4.60	0.50	361	123.4	.0169	.0107
217	8-26-59	2:01- 4:53	"	V	1.268	14.2	.00074	1.421	4.50	0.47	355	115.8	.0192	.0114
218	9-1-59	4:03- 4:45	"	⊔	0.469	13.7	.00077	1.752	8.45	0.52	534	126.1	.0162	.0109
219	8-27-59	4:35- 5:08	"	⊔	0.664	13.9	.00077	2.15	14.32	0.53	743	128.1	.0157	.0111
	& 8-28-59	8:05- 9:16												
220	9-1-59	3:26- 3:39	"	⊔	0.665	13.9	.00077	2.16	14.36	0.52	742	127.3	.0159	.0112

but this is not a significant difference.) Therefore we have called

$$\frac{1}{\sqrt{f}} = -\ 2.2 \log \left(\frac{\epsilon}{14.83\ R} + \frac{2.52}{R\ \sqrt{f}} \right)$$

Ackers' formula, and have recomputed much of our data by this formula. It should be noted that when 2 is changed to 2.2, the value of ϵ is automatically changed.

The 19 new runs in the smooth channel were computed by this formula with $\epsilon = 0.00030$ ft, which was the value Mr. Ackers found for the 23 runs we had already reported. The average discrepancy of the computed f from the observed f was 5.4%, which corresponds to an error of 2.7% in n or V. Combined with the 23 runs with an average error of 3.5% as found by Mr. Ackers, this makes a weighted average discrepancy of 3.1%. This is slightly less than the average discrepancy found by Manning's formula or the formula suggested by the authors under the heading "Discussion of Results," but the difference is hardly significant.

For the tranquil flow in the triangular channel with the rolled-on paraffin surface, the average value of n was 0.0111 with an average discrepancy of 0.0003 or 2.7%. Using Ackers' formula an average value of ϵ of 0.00269 ft is found. The f's computed with this value agree with the observed f's with an average discrepancy of 5.5% which is equivalent to a 2.7% discrepancy in n or V. This is just the same as found for Manning's formula, so it has no advantage. These data are for the 8 runs (Nos. 213-220) for which the Froude number did not exceed 0.53. No runs were made for this roughness with the Froude number between 0.53 and 0.83, but from the results with rectangular roughness it is assumed that tranquil flow would exist up to a Froude number of at least 0.70.

When fitted to Nikuradse's formula the ϵ for these 8 runs is 0.0014 ft and the average discrepancy of the computed from the observed value of f is 6.3% which corresponds to a 3.1% error in V. But it is not surprising that this formula does not give good results here, because the flow is in the transition rather than the rough-channel range. The expression $\frac{\epsilon\ R\ \sqrt{f}}{8\ \sqrt{2}\ R}$ had no value higher than 15.1 instead of 100 as it needs to have for "fully developed turbulence."[23]

The 16 runs (Nos. 175-184 and 188-193) for which the Froude number was more than 1.27 gave an average n of 0.0111, just the same as for the tranquil runs. The average discrepancy was 0.0004 or 3.7%. Ackers' formula gave an average ϵ of 0.00341 ft and the f's computed from this value agree with the observed f's with an average discrepancy of 6.9% which is equivalent to a 3.4% discrepancy in n or V, not significantly better than Manning's. The ratio of the observed f to the f as computed by Ackers' formula with $\epsilon = 0.00269$ ft was also investigated. The average of these ratios was 1.049 with an average discrepancy of 7.3% which is equivalent to 3.6% in n or V, not significantly better than Manning's formula. It is surprising however that the f's averaged 4.9% larger for rapid than for tranquil flow, while Manning's n remained the same.

Three of the runs (Nos. 185-187) had Froude numbers from 0.83 to 1.27. For these runs n varied from 0.0123 to 0.0173, ϵ by Ackers' formula varied from 0.00685 to 0.0332 ft, and the ratio of f to the f computed by Ackers' formula with $\epsilon = 0.00269$ ft varied from 1.32 to 2.61. If we can believe the results

23 "Hydraulic Laboratory Practice," Engineering Monograph No. 18, U.S. Bur. of Reclam., Denver, Colo., 1953.

of these three runs, the resistance to critical flow is much greater than for tranquil or rapid flow. Runs 21 and 22 also fall in this group. Considering the waves which form, this high resistance is perhaps not surprising. It was surprising however that the run at a Froude number of 0.83 gave more resistance than the one with a Froude number of 1.06. (These are the Froude numbers

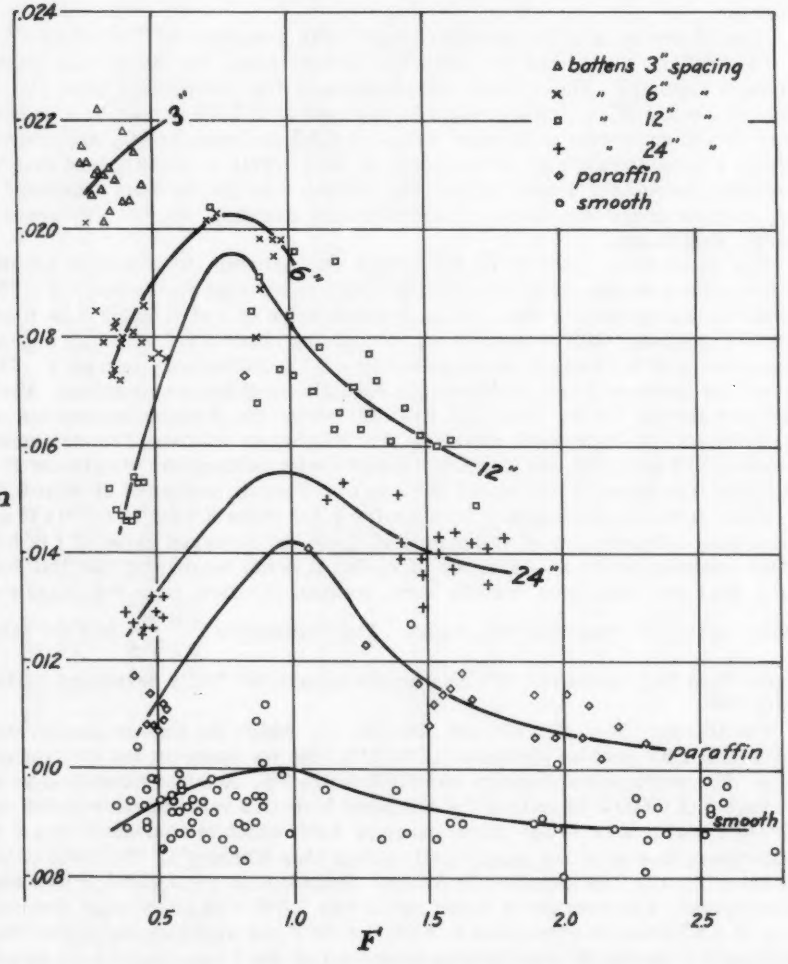

FIG. 17.—n AS A FUNCTION OF FROUDE NUMBER $\frac{V}{\sqrt{\frac{g\ A}{B}}}$

without the α term, but including it would not increase these values by more than about 3%.)

However, Mr. Ackers' Fig. 1 indicates that even dividing the runs into three catagories, tranquil, critical, and rapid, is not sufficient. Fig. 17 is a plotting

of Manning's n against the Froude number

$$\mathsf{F} = \frac{V}{\sqrt{\frac{gA}{B}}} = \frac{V}{\sqrt{\frac{g\,y_n}{2}}} = \frac{0.2495\ Q}{y_n^{2.5}}$$

While there is a great deal of scatter and the lines drawn are only tentative, it is evident that n is low at low Froude numbers, rises to a maximum as critical flow is approached, and then falls off gradually rather than suddenly as the Froude number becomes more than one. Similar curves would result from plotting ϵ against F as in Mr. Ackers' Fig. 1. We thank him for calling this to our attention.

In regard to his last question, the authors plan to study other types of roughness, but probably will make no further tests on rectangular batten roughness.

TABLE 4.—VALUES FOR a, b, AND c.

Author (1)	Date (2)	Shape (3)	a (4)	b (5)	c (6)
Zegjda	1938	Rectangular	2.00	2.125	-
Keulegan	1938	Wide	2.03	2.121	0.812
Keulegan	1938	Trapezoidal	2.03	2.210	0.993
Powell	1945	Wide	2.48	-	2.63
Bretting	1948		2.00	2.342	-
Thijsse	1949	Wide	2.03	2.205	0.981
Owen	1953	Triangular	1.902	-	0.1515
Sayre	1957	Wide	2.14	2.03	0.366
Waterways Experiment Station	1958	Actual concrete	2.2	-	3.056
Powell & Posey	1959	Triangular	2.074	-	0.797
Ackers	1959	Triangular	2.2	3.75	0.879

To answer Mr. Ackers' other question, let the Colebrook formula be written in the more general form

$\frac{1}{\sqrt{f}} = -\,a \log \left(\frac{\epsilon}{14.83\ R} + \frac{2.52}{\mathsf{R}\sqrt{f}}\right)$ and when R becomes very large $\frac{1}{\sqrt{f}} = a \log\left(\frac{R}{\epsilon}\right)$ + b and when $\epsilon = 0$, $\frac{1}{\sqrt{f}} = a \log \mathsf{R}\sqrt{f} - c$. In the literature we find the values given for a, b, and c in Table 4. It seems, therefore, that while the value of a may depend upon the shape of the cross section, it depends more on the judgment of the experimenter in fitting values of a, b, and c to his data, and, of course, also on the accuracy of his data. Also, it must be remembered that Colebrook's formula is at least partially empirical and that it still remains an open question as to whether it is the best formula to represent the facts.

From the purely empirical standpoint, it does not seem to us that Ackers' formula fits our data as well as some of the others. This is shown by the table of values of the average percentage discrepancy in the computed value of V

from the observed value for tranquil flow given in Table 5. For the smooth channel, Ackers' gives the best fit, and for the paraffin lining it ties with Manning's. But for the 12 in., 6 in., and 3 in. spacing of battens it gives the poorest fit. We have not tested the fit for rapid flow except for the paraffin lining. Here the average percentage discrepancy in the velocity by the three formulas was 3.7 by Manning, 3.6 by Nikuradse, and 3.4 by Ackers.

We will turn now to Mr. van Malde's discussion. He is very kind to refer to our work as accurate. We of course tried to be as accurate as we could, but the sources of error which we have already described must have had a sizable effect, as the scatter of points in Fig. 17 indicates.

Varying the slope while keeping the depth constant is a good way of varying the Froude number. Since we have shown above that the resistance to flow depends on the Froude number, we agree with Mr. van Malde that ψ is influenced by S. Unfortunately, we had not foreseen this effect so that we did not make a wide variation in our slopes for some of the roughnesses. We thank Mr. van Malde for calling attention to Kirschmer's papers. We had seen only the earlier one in its French form,[9] and that not until we had torn out our 3-in. batten spacing. Since none of Kirschmer's papers are widely available in the U.S. we are reproducing Fig. 14 from his French paper as our Fig. 18. The observations are by Varwick, a student of Kirschmer's. The ordinate λ^1 is our f/4 and

TABLE 5.—AVERAGE PERCENTAGE DISCREPANCY IN V

Formula	Smooth	Paraffin	Battens spaced, in inches			
			24	12	6	3
Manning	3.8	2.7	1.6	2.1	2.5	1.8
Prandtl-Nikuradse	3.3	3.1	1.3	1.7	1.8	3.2
Ackers	3.1	2.7	1.4	2.5	3.2	4.5

the abscissa is our R/4. With our apparatus it would have been very difficult to observe a large number of slopes with the same depth, but we are glad that Varwick was able to do it. Similar results had already been obtained in Russia by Zegjda.[24]

We agree with Mr. van Malde that these tests give no certain answer as to what formula for channel resistance is "best." About as far as we can go is to say that for the range covered by these experiments, Manning's formula with n constant for any given absolute roughness and any given Foude number, gives discrepancies no larger than might be expected due to experimental errors. Other formulas investigated do not fit the data well enough to warrant their use. This is especially striking since the authors had begun their study with the belief that a formula definitely better than Manning's could be found. The wide variation of n for rough channels with changes in the Froude number is perhaps the most important finding of this study.

9 "Pertes de charge dans les conduits forcees et les canaux decouverts," Revue Generale de l'Hydraulique, Paris, France, Vol. 15, No. 51 (May-June, 1949), pp. 115-138.

24 "Teoriia Podobiia i metodika rascheta gidroteknicheskikh modelei," (Theory of Similarity and Methods of Design of Models for Hydraulic Engineering,) by A. P. Zegjda, Leningrad, Union of Soviet Socialist Republics, 1938.

We believe one of Mr. van Malde's remarks in the first paragraph of his discussion might be misinterpreted. For tranquil flow in the smooth channel we found $\psi = 0.93$ which means that f averaged 7% less than by Prandtl's formula. This means that our observed V's averaged 3.5% greater than Prandtl's formula would give, or that if our data are correct, the average error in V by Prandtl's formula would be -3.5%. But for the rough channel, using the ϵ which gave the best fit, the average discrepancy in V was 2.18% or say 2.2%, with no minus sign, as this is the average of the absolute values of the discrepancies without regard to sign.

In a private communication to the authors, H. J. Koloseus, M. ASCE, has made a very thoughtful study of why the two equations given under the heading "Results from Rough Channel," seem to be about equally satisfactory while the first makes f depend only on the relative roughness ϵ/R (but with ϵ a function of the batten spacing λ), and the second makes it depend on λ and f_p which is a function of the Reynolds number. He introduces another dimensionless parameter which he calls $S_* = \frac{\sqrt{2\,g\,S}\,\epsilon^{1.5}}{\nu}$ (which by the way is the square root of twice the expression $X = g\,S\left(\epsilon^3/\nu^2\right)$ used by Bretting.[25] Koloseus shows that $f = \frac{(4R/\epsilon)\,S_*^2}{\mathbf{R}^2}$ so that f could be expressed in terms of **R** and S_* instead of $4R/\epsilon$. Then if in a given set of data S_* is approximately constant, f seems to be a function of **R** alone, or of ϵ/R alone. He points out that with the 12 in. batten spacing there was very little variation in S_*. The same was true with the 24 in. spacing. However with the 3 in. and 6 in. spacing there was quite a little variation in S_* and he submits Fig. 19 which shows an interesting relationship. He also points out that Nikuradse's formula for rough pipe with ϵ = 0.00040 ft fits the smooth channel tranquil data with an average discrepancy in f of 6.6% which is somewhat better than the 3.5% for V (7.1% for f) which Mr. Ackers reported for his modified Colebrook formula. It may be added that Mr. Koloseus[26] has made a very careful study of resistance to flow at high Froude numbers in a rectangular channel roughened by closely spaced cubes.

The authors wondered why Buckley called his formula Manning's formula. This matter has now been cleared up by one of the authors.[27]

The authors are sorry that there was no discussion of the "capillary rise" mentioned under the heading "Results from Rough Channel." It seems that this little known phenomenon may account in whole or in part for the apparent increase in roughness in critical and rapid flow.

During the summer of 1959 a very large number of pitot measurements of the velocity were made for uniform flow at a relatively large depth. In order to do this the flow had to be held steady for many hours at a time. This took less man-power than establishing new steady flow rates at frequent intervals. Advantage was taken of the long duration of the uniform flow condition and of the availability of personnel to determine water-surface and bottom profiles more thoroughly than before. Values were read every 2 ft along the length of

25 "A Set of Practical Formulas Based on Recent Experimental Research," by A. E. Bretting, Report, 2nd Meeting of the Internatl. Assn. for Hydr. Research, 1948, pp. 399-415.

26 Dissertation, by H. J. Koloseus, Presented to the State University of Iowa, Iowa City, Iowa, in partial fulfilment of the requirements for the degree of Doctor of Philosophy, August, 1958. Presented at the October, 1958, ASCE Convention.

27 "History of Manning's Formula," by Ralph W. Powell, Journal of Geophysical Research, Vol. 65, April, 1960, pp. 1310-1311.

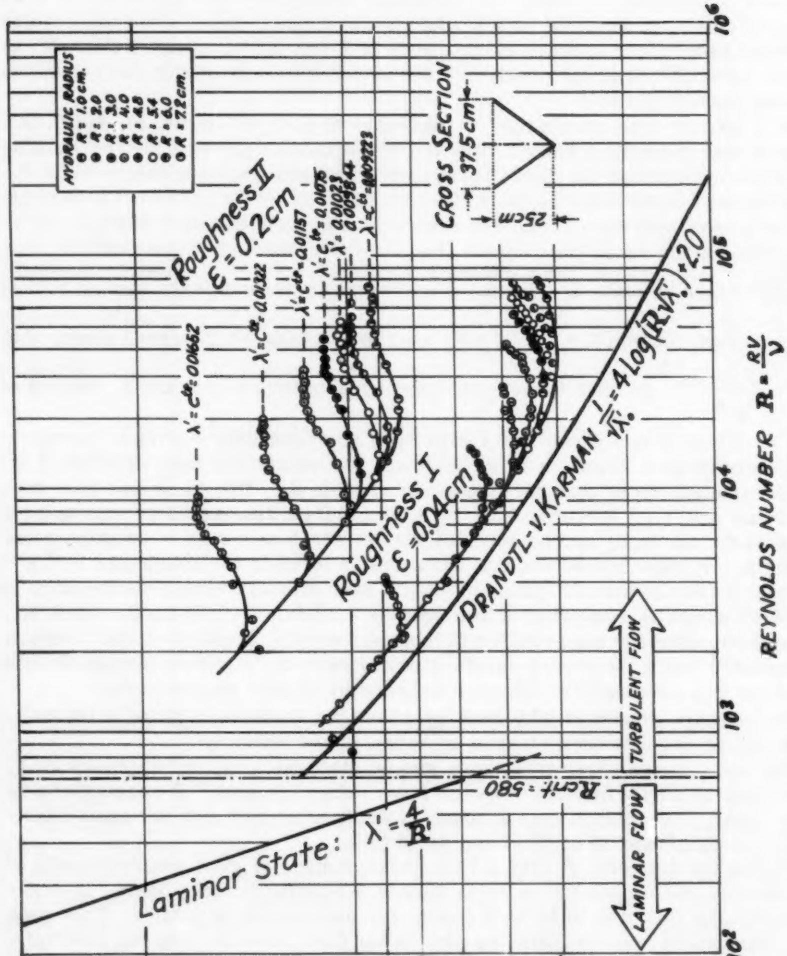

FIG. 18.—FRICTION COEFFICIENT λ^1 VERSUS REYNOLDS NUMBER R

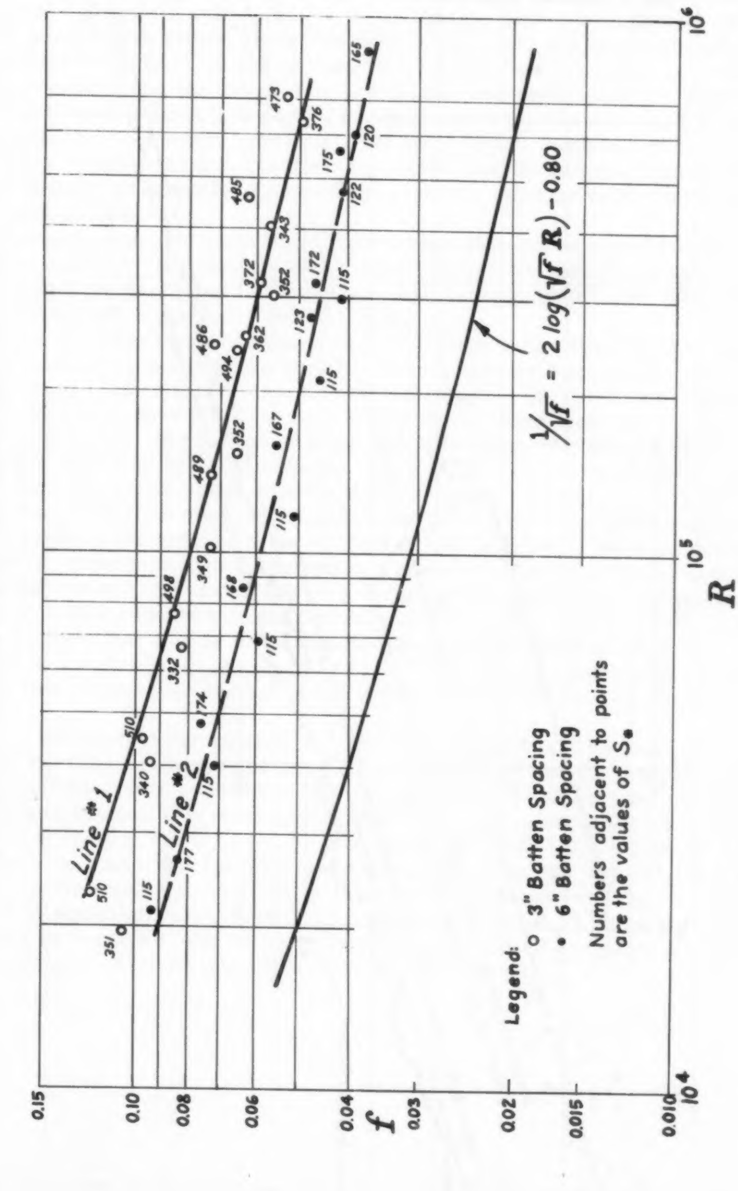

FIG. 19.—RESISTANCE COEFFICIENT VERSUS REYNOLDS NUMBER

from the observed value for tranquil flow given in Table 5. For the smooth channel, Ackers' gives the best fit, and for the paraffin lining it ties with Manning's. But for the 12 in., 6 in., and 3 in. spacing of battens it gives the poorest fit. We have not tested the fit for rapid flow except for the paraffin lining. Here the average percentage discrepancy in the velocity by the three formulas was 3.7 by Manning, 3.6 by Nikuradse, and 3.4 by Ackers.

We will turn now to Mr. van Malde's discussion. He is very kind to refer to our work as accurate. We of course tried to be as accurate as we could, but the sources of error which we have already described must have had a sizable effect, as the scatter of points in Fig. 17 indicates.

Varying the slope while keeping the depth constant is a good way of varying the Froude number. Since we have shown above that the resistance to flow depends on the Froude number, we agree with Mr. van Malde that ψ is influenced by S. Unfortunately, we had not foreseen this effect so that we did not make a wide variation in our slopes for some of the roughnesses. We thank Mr. van Malde for calling attention to Kirschmer's papers. We had seen only the earlier one in its French form,[9] and that not until we had torn out our 3-in. batten spacing. Since none of Kirschmer's papers are widely available in the U.S. we are reproducing Fig. 14 from his French paper as our Fig. 18. The observations are by Varwick, a student of Kirschmer's. The ordinate λ^1 is our f/4 and

TABLE 5.—AVERAGE PERCENTAGE DISCREPANCY IN V

Formula	Smooth	Paraffin	Battens spaced, in inches			
			24	12	6	3
Manning	3.8	2.7	1.6	2.1	2.5	1.8
Prandtl-Nikuradse	3.3	3.1	1.3	1.7	1.8	3.2
Ackers	3.1	2.7	1.4	2.5	3.2	4.5

the abscissa is our R/4. With our apparatus it would have been very difficult to observe a large number of slopes with the same depth, but we are glad that Varwick was able to do it. Similar results had already been obtained in Russia by Zegjda.[24]

We agree with Mr. van Malde that these tests give no certain answer as to what formula for channel resistance is "best." About as far as we can go is to say that for the range covered by these experiments, Manning's formula with n constant for any given absolute roughness and any given Foude number, gives discrepancies no larger than might be expected due to experimental errors. Other formulas investigated do not fit the data well enough to warrant their use. This is especially striking since the authors had begun their study with the belief that a formula definitely better than Manning's could be found. The wide variation of n for rough channels with changes in the Froude number is perhaps the most important finding of this study.

9 "Pertes de charge dans les conduits forcees et les canaux decouverts," Revue Generale de l'Hydraulique, Paris, France, Vol. 15, No. 51 (May-June, 1949), pp. 115-138.

24 "Teoriia Podobiia i metodika rascheta gidroteknicheskikh modelei," (Theory of Similarity and Methods of Design of Models for Hydraulic Engineering,) by A. P. Zegjda, Leningrad, Union of Soviet Socialist Republics, 1938.

We believe one of Mr. van Malde's remarks in the first paragraph of his discussion might be misinterpreted. For tranquil flow in the smooth channel we found $\psi = 0.93$ which means that f averaged 7% less than by Prandtl's formula. This means that our observed V's averaged 3.5% greater than Prandtl's formula would give, or that if our data are correct, the average error in V by Prandtl's formula would be -3.5%. But for the rough channel, using the ϵ which gave the best fit, the average discrepancy in V was 2.18% or say 2.2%, with no minus sign, as this is the average of the absolute values of the discrepancies without regard to sign.

In a private communication to the authors, H. J. Koloseus, M. ASCE, has made a very thoughtful study of why the two equations given under the heading "Results from Rough Channel," seem to be about equally satisfactory while the first makes f depend only on the relative roughness ϵ/R (but with ϵ a function of the batten spacing λ), and the second makes it depend on λ and f_p which is a function of the Reynolds number. He introduces another dimensionless parameter which he calls $S_* = \frac{\sqrt{2\,g\,S}\,\epsilon^{1.5}}{\upsilon}$ (which by the way is the square root of twice the expression $X = g\,S\left(\epsilon^3/\upsilon^2\right)$ used by Bretting.[25] Koloseus shows that $f = \frac{(4R/\epsilon)\,S_*^2}{R^2}$ so that f could be expressed in terms of R and S_* instead of $4R/\epsilon$. Then if in a given set of data S_* is approximately constant, f seems to be a function of R alone, or of ϵ/R alone. He points out that with the 12 in. batten spacing there was very little variation in S_*. The same was true with the 24 in. spacing. However with the 3 in. and 6 in. spacing there was quite a little variation in S_* and he submits Fig. 19 which shows an interesting relationship. He also points out that Nikuradse's formula for rough pipe with ϵ = 0.00040 ft fits the smooth channel tranquil data with an average discrepancy in f of 6.6% which is somewhat better than the 3.5% for V (7.1% for f) which Mr. Ackers reported for his modified Colebrook formula. It may be added that Mr. Koloseus[26] has made a very careful study of resistance to flow at high Froude numbers in a rectangular channel roughened by closely spaced cubes.

The authors wondered why Buckley called his formula Manning's formula. This matter has now been cleared up by one of the authors.[27]

The authors are sorry that there was no discussion of the "capillary rise" mentioned under the heading "Results from Rough Channel." It seems that this little known phenomenon may account in whole or in part for the apparent increase in roughness in critical and rapid flow.

During the summer of 1959 a very large number of pitot measurements of the velocity were made for uniform flow at a relatively large depth. In order to do this the flow had to be held steady for many hours at a time. This took less man-power than establishing new steady flow rates at frequent intervals. Advantage was taken of the long duration of the uniform flow condition and of the availability of personnel to determine water-surface and bottom profiles more thoroughly than before. Values were read every 2 ft along the length of

---

25 "A Set of Practical Formulas Based on Recent Experimental Research," by A. E. Bretting, Report, 2nd Meeting of the Internatl. Assn. for Hydr. Research, 1948, pp. 399-415.

26 Dissertation, by H. J. Koloseus, Presented to the State University of Iowa, Iowa City, Iowa, in partial fulfilment of the requirements for the degree of Doctor of Philosophy, August, 1958. Presented at the October, 1958, ASCE Convention.

27 "History of Manning's Formula," by Ralph W. Powell, Journal of Geophysical Research, Vol. 65, April, 1960, pp. 1310-1311.

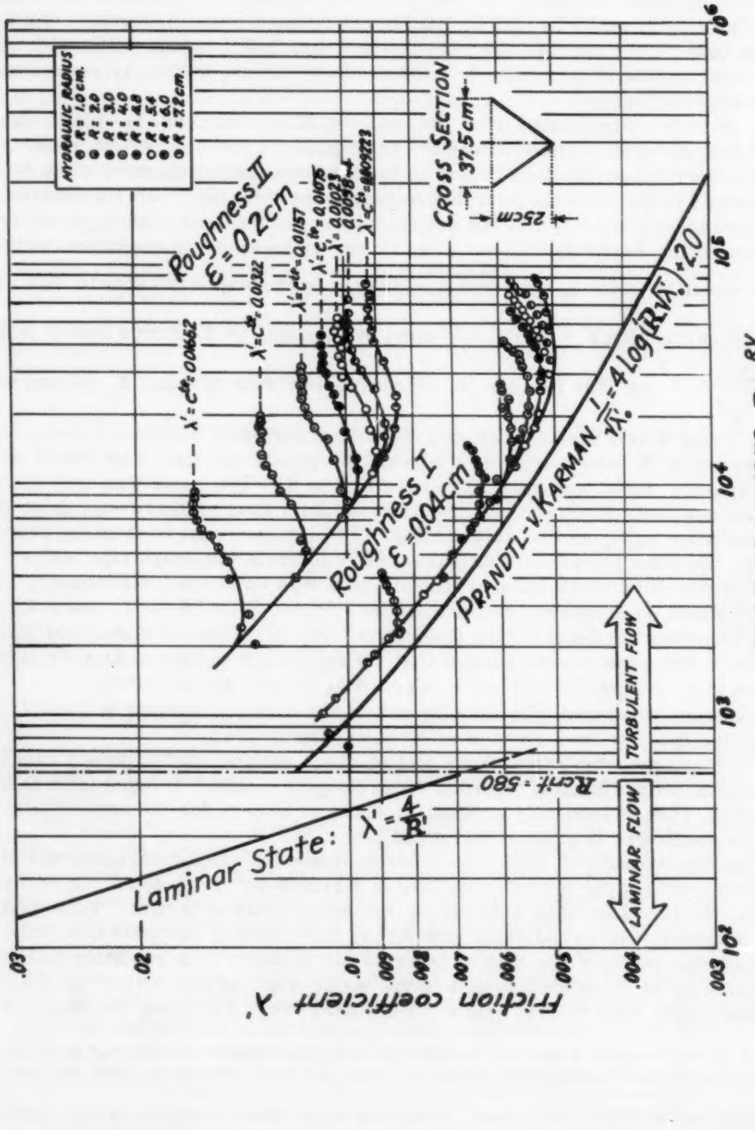

FIG. 18.—FRICTION COEFFICIENT λ^1 VERSUS REYNOLDS NUMBER R

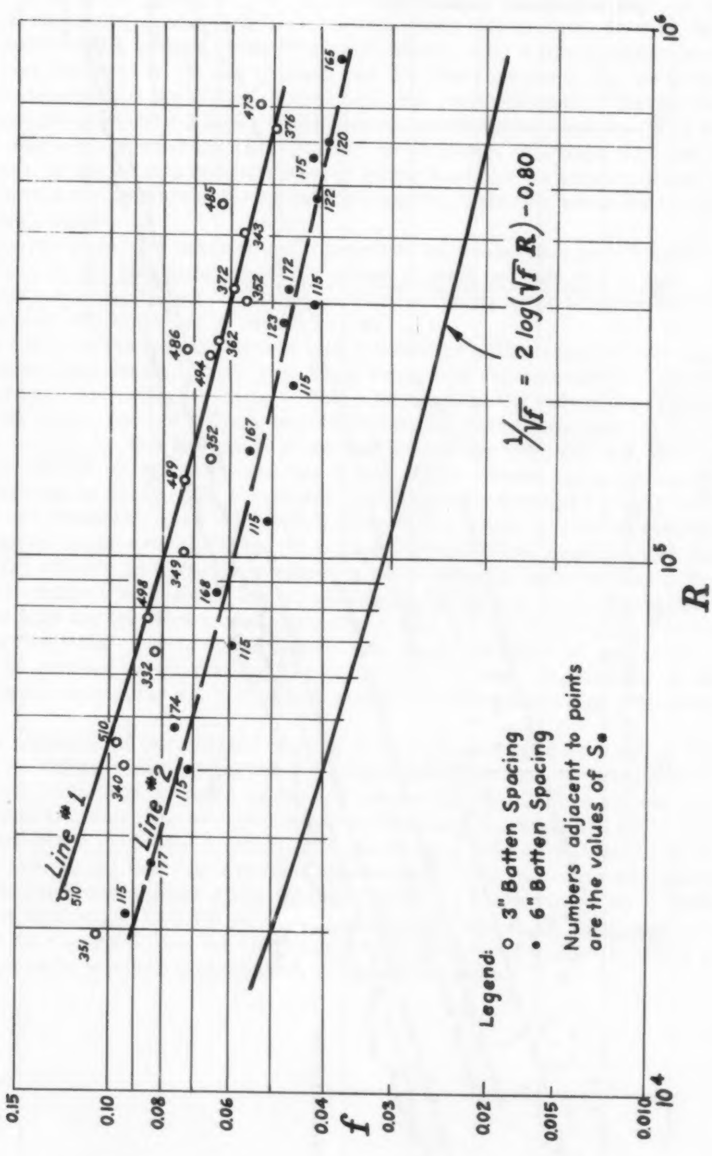

FIG. 19.—RESISTANCE COEFFICIENT VERSUS REYNOLDS NUMBER

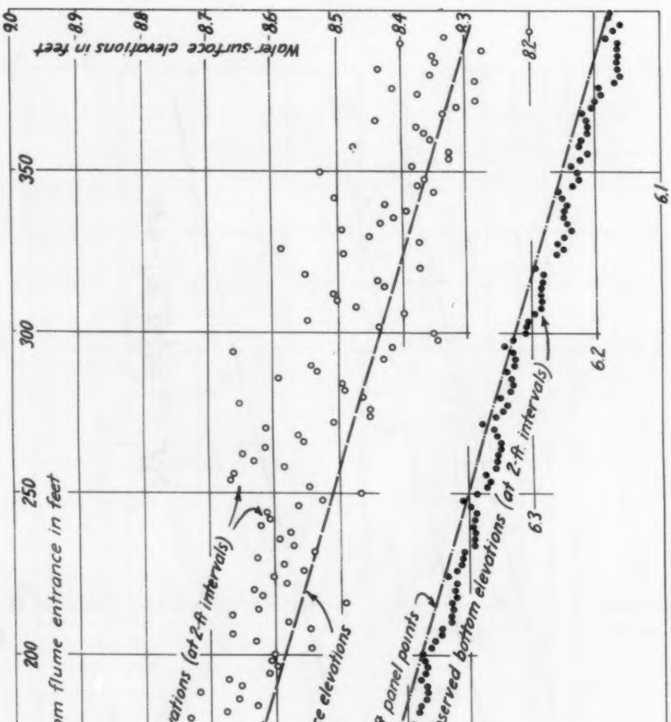

FIG. 20.—WATER-SURFACE AND FLUME-BOTTOM PROFILES

the flume with the exception of only a few points that could not be seen from the level stations.

The results are shown in Fig. 20 compared with the values for the mean water-surface and bottom profiles as ordinarily determined, that is, by the usual method with bottom elevations determined every 8 ft and water-surface elevations every 24 ft. It can be seen that for this flow condition the ordinary method determined the slopes fairly well, but underestimated the depths by perhaps 0.06 ft or about 2.85%. The Froude number for this run was 0.88 which meant that surface waves had a relatively large effect. Together with the large deflection of the bottom due to the heavy water load, the underestimation of the depth in this test undoubtedly represents nearly an extreme value for the present experiments.

Attempts were also made to get transverse water-surface profiles, but setting gages to the fluctuating water-surface proved too difficult a task. With the slight irregularities of the flume obviously causing much larger water-surface waves, they would be of doubtful value.

The fact that the channel showed less resistance to flow than the corresponding smooth pipe, has troubled both the authors and the discussers. However, Lansford and Robertson[28] reported that tests made at the University of Illinois, by W. M. Owen, showed f for a smooth triangular flume less than for the corresponding pipe. For values of $\mathbf{R}$ up to a little over 100,000, the tests gave $f = 0.295/\mathbf{R}^{0.25}$. It is well known that in this range of Reynolds numbers, Prandtl's formula is practically equivalent to the Blasius formula $f = 0.316/\mathbf{R}^{0.25}$. Therefore Owen's ψ would be 0.295/0.316 = 0.934 which is almost exactly the 0.936 given by the average of our 42 runs of tranquil flow in the smooth flume.

On the other hand Kirschmer[9] gives a graph showing tests on a smooth trapezoidal channel by Varwick and on a rectangular one by Raju. These indicate ψ about 1.04 for the trapezoidal channel and 1.12 for the rectangular one. Kirschmer feels that this is to be expected because the effect of secondary flow would be greater in the rectangular section than in the trapezoidal. It would seem that a triangular section should give ψ at least as great as a trapezoidal one.

The elevation of our channel bottom may have averaged as much as 0.01 ft below the values measured at the 8-ft panel points, so that the tabulated values of y_n may have been as much as 0.01 ft too small. The 42 runs for the smooth flume with tranquil flow were recomputed with each y_n increased 0.010 ft from the value given in Tables 1 and 3. The resulting ψ was 1.007 instead of 0.936. It was also found that the average discrepancy from the Prandtl-Nikuradse formula for smooth pipes given by these assumed values was only 5.4% for f, which is equivalent to 2.7% for V or n, compared with 3.3% using bottom elevations as recorded. But the close agreement with Owen's results leaves some question as to whether this adjustment should be made.

---

28 Discussion of "Open-Channel Flow at Small Reynolds Numbers," by Wallace M. Lansford and James M. Robertson, Transactions, ASCE, Vol. 123, 1958, p. 707.

THE SETTLING PROPERTIES OF SUSPENSIONS[a]

Discussion by N. Claes H. Fischerstroem

N. CLAES H. FISCHERSTROEM,[1] M. ASCE.—Mr. McLaughlin's paper is a valuable contribution to our knowledge of the sedimentation process, especially since it includes results from determinations of the settling of suspensions, as well as practical hints regarding the execution of the tests.

Although, according to the introduction, the paper is limited to the settling properties of suspensions and to the use of the results in computing removals, the author, in section 4, also discusses "practical engineering problems." He makes some statements regarding the influence of "other factors" on the design of a settling tank. The writer has some questions to ask regarding the author's opinions, and presents some further conclusions from the results.

In section 2 the author starts with an analysis of the settling, based on the amount of suspended solids which passes a certain plane, calculated by the mean concentration and mean velocity of the solids under non-disturbing flow conditions. The equation arrived at covers the settling in both the free and the hindered zone. The main value of the equation, according to the author, is to show what research and development are necessary for complete calculations. But are there really any new items of research mentioned in the paper which are not already known? However, the analysis is a good basis for the extensive discussion of the tube test procedure.

The flow of water ordinarily takes place mainly in the free settling zone and the equation is not very useful for the purpose of drawing conclusions regarding this part of the settling basin. Such an equation is still lacking.

In the end of section 2 the author discusses scale models. Settling studies in models cannot ignore the flow conditions. The writer believes that under most actual conditions it is more important to study the flow conditions in the scale model and the settling in the tubes. If the flow is satisfactory, and only then (not necessarily ideal) will the sedimentation in the prototype approximately confirm to that in the tube.

Section 3 gives valuable information regarding results and discussion of tests by the pipette and the multiple-depth analysis. The latter will be discussed here.

In Fig. 5 the settling in a tube is illustrated by a concentration diagram. If the dashed lines represent concentration at constant z/t, shouldn't they all start at ϕ (z,t) = 100%? Figs. 7 and 9 represents the settling in a tube of actual suspensions. Shouldn't the full lines (time curves) start at ϕ (z,t) = 0% and the dashed lines (z/t curves) start at ϕ (z,t) = 100%? As is seen from the figures, the shape of the upper part of the curves will be different if the limit values are taken into consideration. This first part of the curves can

[a] December, 1959, by Ronald T. McLaughlin.

[1] Chf. Cons. and Research Engr., Vattenbyggnadsbyran (VBB), Stockholm, Sweden.

never be vertical but will always be nearly horizontal or more or less sloped, which is important when drawing conclusions.

From Figs. 7 and 9 we can see that the settling properties of the suspensions are bad. If there has been no flocculation period there will be a chemical reaction and we are not studying a settling process alone. It is known that Fitch's sedimentation test is carried out after dosing of the (whiting and) ferrisul by a rapid mix, but without flocculation of any kind. Is the author's test with betonite clay and alum also carried out without preceding flocculation? Or if it is flocculated, what are the details (stirring, time etc)? Is the material tested really a suspension? Isn't it a suspension under formation by a process which is not only time-consuming but also influenced by turbulence, concentration, pH a.s.o. The writer does not mean to say that such suspensions would not occur, but nevertheless these tests might be too specific to allow conclusions regarding the settling laws.

In section 4, part b, the author states "This approximation will often be better than making an elaborate study of the hydraulics of the tank while ignoring the properties of suspension." Why ignore any of the important factors? The underestimation of the hydraulics seems to be not uncommon for the laboratory fellow. In contrast to the field engineer, he gets no experience from the disturbances from density currents, side currents, wind, turbulence etc. The settling properties are easily determined, but the hydraulic properties are not. That is perhaps why so many existing basins, and also so many basins under construction, are unsatisfactory in hydraulic respects.

In the same section, part d, the author states, "It will now be demonstrated that whether overflow rate or detention time should be used depends upon the nature of the suspension. Indeed, for a single tank the removal ratio may be closely related to overflow rate for one suspension, to detention time for a second, and to neither for a third." This sounds simple, but Mr. Fitch was perhaps nearer the truth when, in a discussion regarding influence on settling of Class II suspensions by the overflow rate, namely, the detention time, he wrote, "both are working." Will it ever be possible that a sedimentation only depends upon time? And what does the author mean by "neither for a third?"

To illustrate the preceding, the author starts with a theoretical discussion of the concentration diagram. Overflow rate, he says, is determining if z/t curves are straight and parallel to the z (depth) axis and detention time is determining if the concentration (time) curves are parallel to the same axis. If we deal with suspensions which settle, the latter will never be possible because all time curves but the one at $t = 0$ must start at the concentration ϕ (z,t) = 0. In the thin surface layer, sedimentation results immediately in a complete removal. In the surface layer there is no flocculation. Also in the next, shallow layers, clarification is more rapid than in the deeper layers. Take, for instance, the author's curve for T = 700 sec (Fig. 7). At a depth of 10 cm we have a removal of nearly 50%, at 20 cm of about 40%, and at a depth of 100 cm only 23% (at the same time or volume load). At the same detention time a shallow basin will always give a higher removal than a deeper basin. It is, consequently, even with a suspension with poor settling properties, more efficacious to use, for example, a 0.2 in. basin with 5 times as large surface than to use a 1.0 m basin. The shallow basin furthermore will have lower turbulence and higher stability than the deeper basin; when we alternatively insert 4 trays in the deeper basin, we also exclude disturbance from wind action in 4/5 of the basin.

To illustrate the relation between overflow rate and time for certain kind of suspensions we can study the writer's Fig. 1, based upon the results published by Fitch. This diagram, which is of the same type as the author's though rearranged for technical purposes, shows the residual after sedimentation:

a. at constant settling time (volume load) and variable depth (overflow rate, full lines)

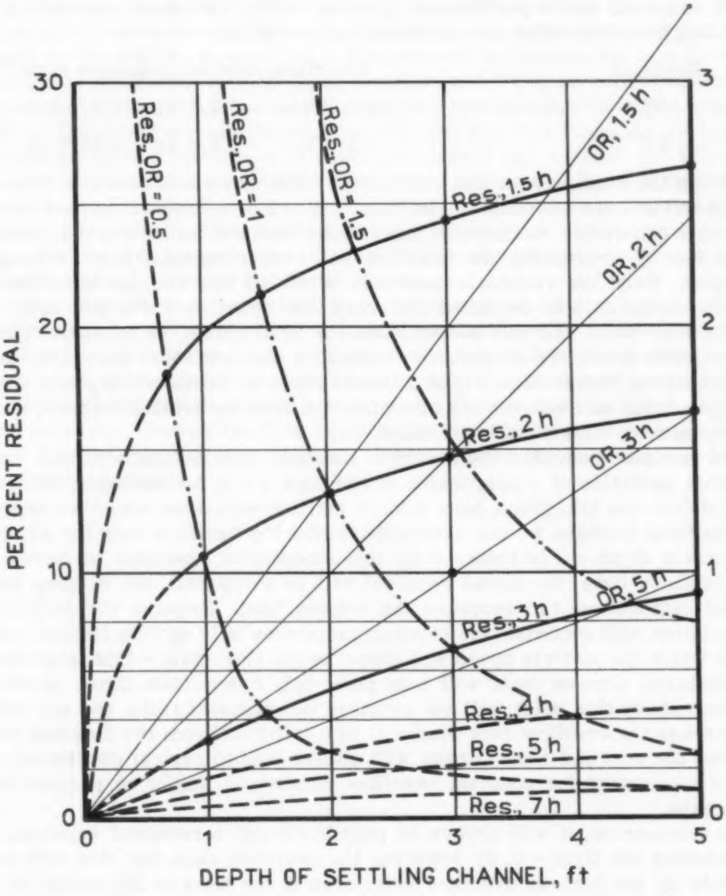

FIG. 1.—PERCENTAGE RESIDUAL VERSUS DEPTH OF SETTLING CHANNEL

b. at constant overflow rate and variable depth (settling time, dashed lines).

The time curves show us that at constant time, 1.5 hr, for example, the residual increases with the basin depth, or with a deeper basin with a smaller area. From these curves we may draw the conclusion that the best way -- from a sedimentation point of view -- to use a given volume is to give the basin as large an area as possible.

The overflow rate curves indicate that the residual decreases with increasing depth, which means with increasing time or a decreased volume load. The increased efficiency must be bought by a greater basin volume. The effect observed, which depends upon an accelerated settling because of flocculation, shows us, however, that there is a certain relation between the overflow rate and settling time for every required settling efficiency.

We can, for example, take a recovery process with 90% settling efficiency (10% residual) and a purification process with 2% allowed residual. Corresponding overflow rates and detention times will be.

Residual	Overflow rate per detention time		
10%	1.1/2.5 hr	0.4/2 hr	0.2/1.5 hr
2%	0.5/5 hr	0.2/3 hr	0.05/2 hr

From the examples we can confirm the often expressed relation: "the lower the overflow rate the shorter the time," in order to reach the same removal. The only possibility to increase the volume load and to reduce the basin size is in fact by decreasing the overflow rate, environmental factors being unchanged. Very low residuals, near 0%, which we now require in certain processes, seem only to be attained at very low overflow rates and very small depths with these extreme suspensions (or by flotation, of course). This can be achieved by shallow single story basins or multiple story basins of the type suggested by Camp. Which type of basin ought to be chosen depends upon the cost per basin unit volume and other factors, such as available space, stability requirements, wind conditions, and so on.

We can also consider the overflow rate and time influence in this way. If the free particles of a suspension at the time t = 0, for example, before any flocculation can take place, have certain settling velocities, which we represent in a settling diagram, we can always determine the overflow rate for a required removal at depth = 0 or time = 0 for this suspension. Because we have a certain depth or time, the actual removal will be increased, and to keep the required removal we can increase the volume load. Because the incluence of flocculation will increase the settling properties only up to a limited depth - above which the particle speed will disperse the floc again - this improvement by increased time or depth will take place only to a certain limit. Increasing the time above this point will not increase the removal ratio, and any attempt to increase the overflow rate load will be a failure. From the diagram we can see that the constant time curves will always lead to zero at decreased overflow rate; curves for constant overflow rate would finally be parallel to the depth axis.

To summarize, it will always be possible to get a required removal, even by reducing the time $\rightarrow 0$, by lowering the overflow rate, but this will not be possible by too high an overflow rate, even if the time is increased to $\rightarrow \infty$. Although both overflow rate and time can be said to be limiting factors, it follows that the overflow rate might be said to be of primary importance when an increased volume load is intended.

It seems most probable that the very shallow basin will have a future, provided it is designed on technically correct principles. Our knowledge regarding short-time settling is unsatisfactory. To determine the settling of a suspension in a very short water column in a short period will require new laboratory

methods. It does not seem to be possible to still the water and avoid turbulence rapidly enough in the "tube test." The writer believes that we perhaps must change to a continous flow method.

The investigations made by the author, Fitch, and others during recent years, have given us an idea of the relation between the overflow rate and time for some special types of suspensions. Further investigations regarding other types are desirable. What seems to be especially valuable is what has previously only been assumed or felt intuitively or possibly doubted or denied, that for flocculated suspensions of Class II A type, there is no direct proportionality in capacity to the settling surface area; the capacity increases, but at a slower rate, the speed depending upon the type of suspension. The investigations also confirm, however, that the conclusions regarding the extreme form of a basin, drawn from the overflow rate theory, are correct; the best basin for all types of suspensions is still the one with depth and time 0 and surface ∞. The investigations seem, in this respect, to have shown quite clearly, as mentioned, that the only constructional way to increase the volume load is to decrease the depth, not to increase it. The conclusion that a settling process can be dependent only upon the time, seems to be drawn from concentration curves lacking the important part just below the water surface.

The prior discussion is not meant as a criticism, only to give a more complete view on the conclusions drawn from the author's settling theories and experimental results. We must be grateful to the author for his excellent work and the writer agrees with his conclusions, with the exception possibly for No. 1. The writer believes, namely, that when a choice must be made, it may be more important to study the flow in the basin than the properties of the suspension. Finally such a choice depends, however, upon the knowledge and experience of the designer.

[illegible]

EARLY HISTORY OF HYDROMETRY IN THE UNITED STATES[a]

Discussion by Ivan J. Moskvitinoff

IVAN J. MOSKVITINOFF,[84] F. ASCE.—This paper is a valuable contribution to the history of engineering science in the United States in providing the collection and systematization of the information scattered in many publications and magazines. The author paid a tribute to the American pioneers in hydrometry and to the engineers and professors who built the scientific and technical base of modern hydrometry. The paper contains important information on the parallel development of the hydrometric methods and devices in some European countries.

Describing the investigation on velocity pulsation at Burlington, the author concludes: "The influence of pulsation cannot be eliminated by short observations at a great number of points as it is generally believed." The results of the writer's measurements of the velocity distribution in many irrigation channels of different sizes and in the Syr-Daria River, in Turkeston, Russia, in 1914-1915, led him to the following conclusion: the magnitudes of the rate of flow based on velocity measurements at many points in a cross section, with a short period of observation, were sufficiently accurate in comparison with the rates of flow obtained by two-point method with a long period of observation necessary to eliminate the influence of pulsation.

The writer vigorously supports the author's proposal to use a more logical terminology as indicated in Appendix I.

The writer hopes also that the author will be able to fulfil his intention to publish the history of the modern hydrometry after the First World War, for this would be a valuable contribution to engineering science.

---

[a] January, 1960, by Steponas Kolupaila.

[84] Civ. Engrg. Dept., The City College of New York, New York, N. Y.

GENERALIZED DISTRIBUTION NETWORK HEAD LOSS CHARACTERISTICS[a]

Discussion by F. P. Linaweaver, Jr., John C. Geyer, and Jerome B. Wolff

F. P. LINAWEAVER, JR.,[21] A. M. ASCE, JOHN C. GEYER,[22] F. ASCE, and JEROME B. WOLFF,[23] M. ASCE.—There are many problems that continually arise in the operation and planning of a water distribution system that require a hydraulic analysis. If the basic analyses of average daily, maximum daily, and peak hourly conditions are available for each pressure zone of a water distribution system, some of these problems can be answered by the use of proportional loads as presented by Mr. McPherson. For systems without storage or with storage at or near the pumping station, proportional load hydraulics accurately produces the desired answers. The author has used test data to show that for a single pumping station, and a reservoir elsewhere on the system, the head loss between the pumps and any given point in the system is a function of the ratio of pumping rate to demand rate. The discovery that such relationships exist should prove very useful, particularly when analyses are made by long hand methods or by use of digital computer.

The method appears to have usefulness for solving problems other than those involving pumping versus storage relationships. One recurring problem is to determine the effect of proposed housing developments on the distribution system. This would normally be a concentration of loading at a point and, therefore, would be a non-proportional load similar to a fire flow. The flows into or out of equalizing storage facilities are in effect non-proportional loads, and, therefore, a procedure might be determined whereby Eq. 2 can be used for applying fire flows, etc.

In making analyses involving a storage reservoir, the fact of discontinuity in the situation when pumps are changed or when the reservoir either fills or empties, must be dealt with. This requires, in particular, that the time of filling and of emptying the storage reservoir must be determined, because at these times there occur drastic changes in the hydraulic situation. Following of the cyclical variations in storage levels would appear to require the reverse application of Eq. 2, with appropriate accounting for pump operation and pumping station discharge curves.

In the case of a more complex system, as shown in Fig. 7, the determination of the appropriate Q_p/Q_d ratio to account for various pump curves of a particular pumping station, and the changes in levels of tanks and standpipes would appear to be very difficult. The author states that "The computations for the successive hourly balancing of pump-network-storage functions can now be performed much more simply using Eq. 2, . . ." In Eq. 2, Q_d, n and ϕ would be known; in order to determine Σh, Q_p must be determined. If there is more

[a] January, 1960, by M. B. McPherson.

[21] Asst. Civ. Engr., Bur. of Water Supply, Baltimore, Md.

[22] Prof. and Chmn. of Sanitary Engrg., Johns Hopkins Univ., Baltimore, Md.

[23] Asst. Dir. of Public Works, Baltimore County, Md.

than one pumping station or more than one tank or standpipe, the distribution of the quantities of water being supplied by each source would not be known. It would appear that in order to determine the ratios of Q_p/Q_d as shown in columns (3) and (10) of Table 4, an analysis of successive balancing would be required similar to the one described in another publication,[5] but accounting for the changes in levels of tanks and standpipes. Thus, a thorough analysis would still be required. It would be interesting to know the author's procedure for determining columns (3) and (10) of Table 4 especially in the Number 4 series of runs.

In analyzing complex systems on the Baltimore Analyzers, a procedure for balancing is used, whereby the operating levels of the storage tanks or reservoirs are determined on the initial test, and then the system is operated through the day just as the pump operator or an automatic station would operate. Instead of using an hour-to-hour balancing, the period between tests is varied as needed to obtain results within the desired accuracy.

The operating level is defined as the high water level during the early a.m. after several days of the same pattern and magnitude of demand. This level is obtained by setting the demand at the average for the day being analyzed, and by reading the difference in head between the sources and the storage facilities.

The question, "Is it not feasible to consider writing a design program for a digital computer which would permit direct determination of the best combination of pipes to satisfy prescribed conditions defined by means of Eq. 2?", is a very challenging one. It could be expanded to a determination of the best combination of pumps, pipes, and storage facilities by modifying Mr. McPherson's Eq. 2 to include the criteria presented by George G. Schmid.[24]

---

[5] "Distribution Design Considerations," by M. B. McPherson and J. V. Radziul, Journal, AWWA, Vol. 51, April, 1959, pp. 489-502.

[24] "Peak Demand Storage," by George G. Schmid, Journal, AWWA, Vol. 48, April, 1956, p. 378.

SCOUR AT BRIDGE CROSSINGS[a]

Discussion by D. V. Joglekar, W. J. Bauer, L. J. Tison, S. V. Chitale, A. Rylands Thomas, Mushtaq Ahmad, and Pier Luigi Romita

D. V. JOGLEKAR.[16]—It is agreed that each river and each reach must be studied to understand its individual, almost personalized, characteristics and that scour at bridge piers is closely related to (a) the river conditions upstream and downstream (such as indicated by flood hydrographs from year to year); (b) the meandering tendency of the river that, in turn, depends on the detritus load carried by the river during floods, (c) whether the river is flowing in its alluvial plain or has its sides and bed resistant to scour, (d) whether the river is flashy or has sustained floods, and (e) the constriction of the river section caused by the bridge. The reach of the river also has an important bearing on scour at bridge piers, for example, bridges on hill torrents, bridges on alluvial plains with mild slopes, and bridges on the tidal reaches of the river. In a braided river near a hilly region the river changes are so rapid that it is very difficult to estimate the waterway required for bridges across various streams of the braided river. An illuminating case of violent movement of Mànas River[17] in Assam can be cited. In 1909, three bridges were provided on the three tributaries of this river:

1. on the Manas River which had 10 spans of 100 ft,
2. on the Bholookadoba Branch - 2 spans of 75 ft,
3. on the Beki Branch - 4 spans of 12 ft.

Due to changes in river courses, the bridge had to be rebuilt several times on the Bholookadoba Branch between the period 1909 to 1945:

1. 2 of 75 ft,
2. 3 of 75 ft,
3. 1 of 250 ft and 2 of 150 ft.

Changes in the Beki Branch were more violent and larger waterways had to be provided during this period as follows:

1. 4 x 12 ft,
2. 4 x 20 ft,
3. 9 x 20 ft,
4. 1 x 50 ft, 1 x 30 ft, 6 x 19 ft,
5. 1 x 50 ft, 2 x 40 ft, 6 x 19 ft,
6. 2 x 40 ft, 3 x 100 ft,
7. 7 x 150 ft.

The river is still uncontrollable in spite of various training measures.

---

[a] February, 1960, by E. M. Laursen.
[16] Adviser, Central Board of Irrigation and Power, Poona, India.
[17] "River Training," Railway Board Technical Paper No. 334.

Experiments[18,19] were carried out at the Central Water and Power Research Station, Poona, India, in 1938 and 1939 for finding scour round a single pier placed in the center of a parallel sided flume, embedded in sand of mean diameter 0.29 mm. The following relation was worked out:

$$\frac{d_s}{b} = 1.70 \left(q_c^{\frac{2}{3}} \Big/ b\right)^{0.78} \qquad (14)$$

in which b is the width of the pier, q_c is the discharge per foot in the center of the flume upstream of the pier, and d_s is the maximum depth of scour at the pier below water level. As it was difficult to correlate this with the depth of scour at prototype piers, due to q (intensity of discharge per foot) depending upon the curvature of the river upstream - which varies from river to river, it was considered desirable to study cases of actual scour in prototypes and work out a general, empirical relationship. Besides, it has to be remembered that the angle of repose of bed material in the model and the prototype is the same, hence, the extent of scour in plan in the vertically distorted model is found always relatively greater than in the prototype. This in effect reduces the discharge intensity at the pier due to greater dispersion of flow and hence the depths of scour obtained in the model would be relatively less. Data[19] were, therefore, collected for scour round bridge piers of various bridges constructed in India and a general relationship[19,20] was worked out as follows:[21]

$$d_s = (2)\ 0.473(Q/f)^{\frac{1}{3}} = 2\ D(\text{Lacey}) \qquad (15)$$

in which Q is the maximum flood discharge in cu sec; d_s is the maximum depth of scour below highest flood level; f is = $1.76\sqrt{m}$, and m is the mean grade of bed material in millimeters. In Eq. 15, a representative f value has to be used. From bore data, values of f for each strata is to be worked out to ascertain that the anticipated depth is not based on the f value which is higher than that appropriate at that depth. Recent advances in foundation engineering have made it possible to take the pier foundation sufficiently below the maximum probable depth of scour to provide adequate grip length. Where this cannot be done, high level stone protection, though costly in the long run, has to be employed. Another advantage of deep foundation is that, because of increased side friction on the pier sides embedded in sand, the load bearing capacity of the pier increases considerably as compared to that of a pier with shallow foundation. Generally this additional load bearing capacity is not taken into consideration in the design but is kept as a margin of safety. The previous railway practice was to work out the depth of bridge foundations according to the observations made by Spring[22] and Gales.[23] In the case of shallow foundation, protection

---

18 Technical Annual Report, Central Water and Power Research Station, Poona, India, 1938-39.

19 "Behaviour and control of rivers and canals with the aid of models - part II," Research Publication No. 13, Chapter VIII, Central Water and Power Research Sta., Poona, India.

20 Technical Annual Report, Central Water and Power Research Station, Poona, India.

21 "Stable Channels in Alluvium," by G. Lacey, Journal of the Institution of Civil Engineers, Paper No. 4736, 1929.

22 "River Training and Control of the Guide Bank System," by F. J. E. Spring, Railway Board's Technical Publication No. 153.

23 "Principles of River Training for Railway Bridges and their Application to the Case of the Hardinge Bridge over the Lower Ganges at Sara," by R. Gales, Journal of the Institution of Civil Engineers, December, 1938, Paper No. 5167.

has to be provided by stone pitching and if this is at high level, a lot of the stone (stone used generally weighs 80 to 120 lb and is called one man stone) is washed away downstream due to turbulence and has to be replenished, even during floods, to ensure the safety of the bridge. Due to this turbulence very deep scour occurs downstream of the piers as in the case of Hardinge Bridge[24] on the river Ganges, depth of scour being of the order of 200 ft.

The current railway practice is to provide a grip length for the pier equal to half the depth of scoured bed below H.H.F.L. so that the total length of piers below H.H.F.L. is 3D(Lacey).

Experiments[25,26] were carried out at the Central Water and Power Research Station, Poona, India, for testing the design of training works, waterway, and length of piers of a railway bridge at Mokameh on the river Ganges near Patna (Bihar State). The pier foundation of this bridge has been taken to a depth of about 200 ft below H.H.F.L. which is equal to 3D(Lacey). As the foundations are deep enough, protection by way of stone pitching round piers is not provided.

Various cases of bridges, for which rivers had to be trained to ensure the safety of piers, have been experimented on. These experiments are described in the Technical Annual Reports of the Central Water and Power Research Station, Poona, India, for the year 1937-38, 1938-39, 1939-40, 1940-41, 1944 to 47, 1949 and 1952 to 1958.

In the case of flash flood type rivers, fixing the waterway is much more difficult. In such cases the flood rises and falls so rapidly that the river has no time to scour its bed with the result that the afflux (difference in water surface upstream and downstream of bridge) increases enormously; the bridge is likely to fail by outflanking. A railway bridge on Luni River in Rajasthan State[27] failed in this manner.

In the case of inerodible bed material, it is difficult to estimate the maximum depth of scour. Hydraulic model experiments are unable to reproduce this scour due to obvious limitations. Recourse has, therefore, to be taken to field data. In some cases, the maximum flood level is underestimated and the waterway provided is insufficient. If the bed is inerodible afflux increases beyond the safe limit, with the result that standing wave conditions prevail downstream of the bridge, which lead to undermining of bridge piers. The railway bridge on Yeshwantpur River[28] in Andhra Pradesh failed and collapsed for similar reasons.

The writer agrees with the author that afflux caused by a bridge depends so much on the erodibility of the bed material. Thus in the case of the railway bridge on the River Ganges[25] at Mokameh, the afflux caused by the bridge was only a couple of inches for a flood of 18,000,000 cu sec. This was because the flood was sustained and the river scoured its bed as the discharge increased.

---

24 Investigations carried out by means of models at the Khadakwasla Hydrodynamics Research Station, near Poona in connection with the protection of the Hardinge Bridge which spans the river Ganges near Paksey, by C. C. Inglis and D. V. Joglekar, East Bengal Railway, Public Works Department, Bombay, India, 1936, Technical Paper No. 55.

25 Technical Annual Report, Central Water and Power Research Sta., Poona, India, 1950.

26 "Manual on River behaviour, control, and training," Ch. VI, Pub. No. 60, Central Board of Irrigation and Power.

27 Technical Annual Report, Central Water and Power Research Station, Poona, India, 1954.

28 Technical Annual Report, Central Water and Power Research Station, Poona, India, 1955.

In the case of rivers with flash floods or with inerodible bed, full afflux has to be allowed for in the design according to standard formulas.

As emphasized by the author, more field experiments are necessary to improve our method of estimating scour at bridge piers.

W. J. BAUER,[29] M. ASCE.—The writer was in attendance at the University of Iowa, when the research described by Mr. Laursen was getting under way, and is, therefore, aware of its pioneering nature. The purpose of this discussion is to consider the application of the results presented by the author to a particular approach to waterway design.

The fundamental purpose of a bridge over a stream is to separate the human traffic and the flowing water. It is commonly accepted that provision for the passage of the maximum conceivable discharge through the waterway beneath the roadway is economically undesirable. It is good practice to provide for the safe, although infrequent, overtopping of the roadway by a rare flood. If the design is adequate, after the passage of such a flood, the highway is immediately ready for service with only minor repairs being required during subsequent routine maintenance.

In order to achieve this objective, the backwater produced by the structure must be small at the stage of incipient overtopping. The writer has used values of 0.5 ft to 1.0 ft as being reasonably small for the backwater at this stage. The design problem then becomes how to provide for the passage of the flood corresponding to the stage of incipient overtopping without exceeding an allowable backwater.

Some of the flow area required will exist beneath the elevation of the low-flow bed of the stream in accordance with the reasoning set forth by Mr. Laursen under the heading "Local Scour at Piers and Abutments: Backwater at Bridge Crossings." The extent to which such area is available to the flow during flood may be controlled by suitable scour protection.

At bridge sites in West Virginia, at which scour protection of broken rock is readily available, the writer has used a design velocity beneath the bridge of between two and three times the typical velocity in the stream during flood. This was accomplished without exceeding the allowable backwater at the stage of incipient overtopping. Such a relationship, between the velocity in the contracted section and that in the approach flow, gives sufficient assurance that the material deposited over the broken rock fill during low flow will be scoured out during flood, provided the depth of scour required is not excessive. Fig. 6 indicates the relationship between depth of scour at an encroaching abutment and a parameter dependent on the degree of contraction of the natural waterway by the structure. Fig. 6 indicates the attaining of depths of scour equal to the depth of flow at relatively minor amounts of contraction. It is, therefore, not difficult to imagine circumstances in which it would be possible to provide as much waterway area beneath the low-flow bed of the stream as above it.

In the instances that the writer has in mind, the waterway area provided beneath the low-flow bed of the stream was about 20% of the total waterway area at the stage of incipient overtopping. The depth of the waterway area beneath the low-flow bed was only about 40% of the nominal depth of flow at the stage of incipient overtopping. Nevertheless, significant cost savings were achieved compared to a longer bridge with equal waterway area entirely

[29] Cons. Engr., Chicago, Ill.

above the low-flow bed of the stream. It is possible to imagine circumstances in which the length of the bridge might be out in half, the waterway area remaining the same. This has obvious economic significance.

The natural filling of the scour hole during the recession of the flood tends to minimize the depth of the pool of water that might be left standing under

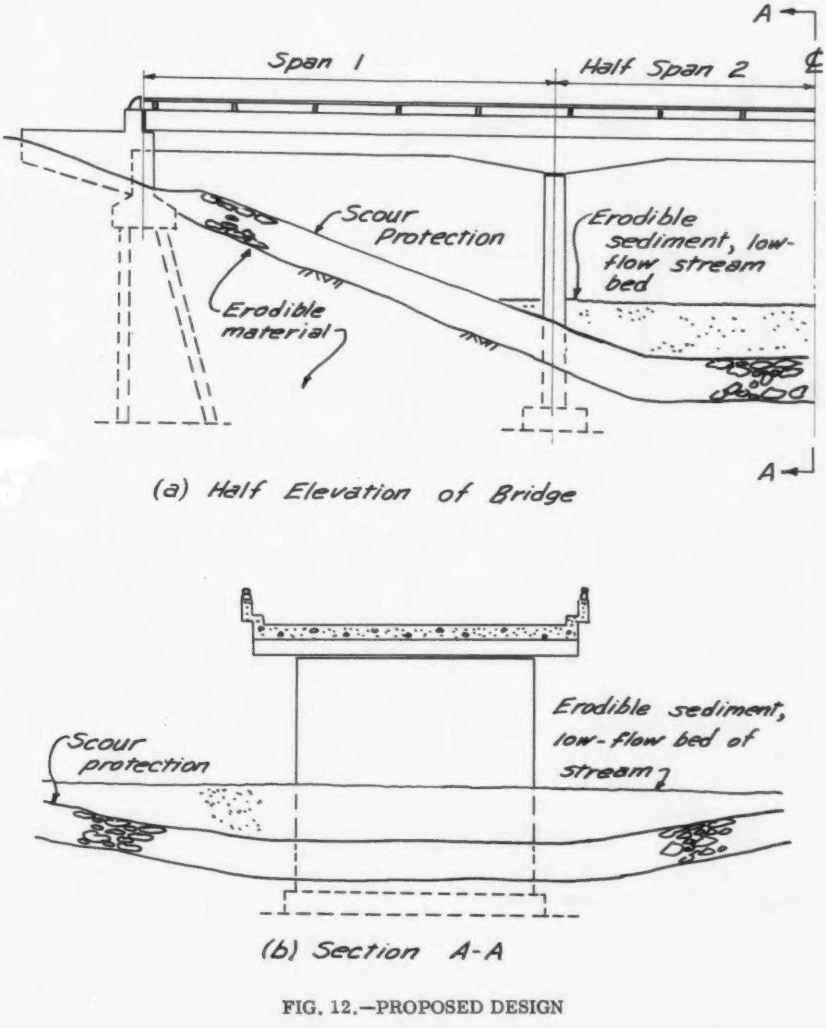

FIG. 12.—PROPOSED DESIGN

the bridge during low flow. As the beds of such streams are commonly made up of alternating pools and bars anyway, the addition of another small pool beneath the bridge is of little consequence. Fig. 12 shows the type of design proposed.

L. J. TISON.[30]—The relationship proposed by Mr. Laursen for the prediction of scour at piers and abutments for the case in which sediment is supplied to the scour hole, in extremely interesting.

The author presents an analysis in which he compares the flow without contraction and the flow due to a long contraction. He then uses, for both flows, an approximate form of the total sediment load relationship recently proposed by himself and consideres a bridge crossing as a long contraction, foreshortened in such an extreme that it has only a beginning and an end.

The writer has found that a scour at piers and abutments also took place when the contraction of the flow was without significance and introduced the idea that the scour at piers may be affected by the curvature of the streamlines around the piers.

When a pier with an arbitrary shape is placed in a stream, it produces (Fig. 13) a first curvature with a center 0_1 and a radius ρ_1, followed by a second curvature 0_2 ρ_2. In the neighborhood of the bank of the river, the pier exerts no action on the direction of the streamlines, cd. But, considering the region of the first curvature in the neighborhood of the surface, a line such AB, tangent in each point to the principal normals of the streamlines, the following relationship may be written:

$$z_B + \frac{p_B}{\gamma} + \frac{1}{g}\int_A^B \frac{v^2}{\rho}\, ds = z_A + \frac{\rho_A}{\gamma} \qquad (16)$$

in which z is the vertical height, p is the pressure, v is the velocity and γ is the specific weight of the liquid. The first supposition was that the motion is parallel to the bottom.

In the neighborhood of the bottom, another relationship of the same nature gives:

$$z_{B'} + \frac{p_{B'}}{\gamma} + \frac{1}{g}\int_{A'}^{B'} \frac{v'^2}{\rho}\, ds = z_{A'} + \frac{p_{A'}}{\gamma} \qquad (17)$$

B and B' are on a same line perpendicular on the bottom.

The variation of the pressure between B and B' follows the hydrosatic law, so that:

$$z_B + \frac{p_B}{\gamma} = z_{B'} + \frac{p_{B'}}{\gamma} \qquad (18)$$

From these three relationships

$$z_A + \frac{p_A}{\gamma} - \left(z_{A'} + \frac{p_{A'}}{\gamma}\right) = \frac{1}{g}\left[\int_A^B \frac{v^2}{p}\, ds - \int_{A'}^{B'} \frac{v'^2}{\rho}\, ds\right] \qquad (19)$$

with v greater than v' (v' is the velocity in the neighborhood of the bottom).

[30] Prof., Univ. of Ghent, Ghent, Belgium.

A consequence of Eq. 19 is that the motion cannot be parallel to the bottom, the trajectories must dive.

This diving motion will have another consequence : a local attack of the bottom under the influence of the first curvature $0_1 \rho_1$. Evidently, the importance of scour will depend on the value of the vertical component of the

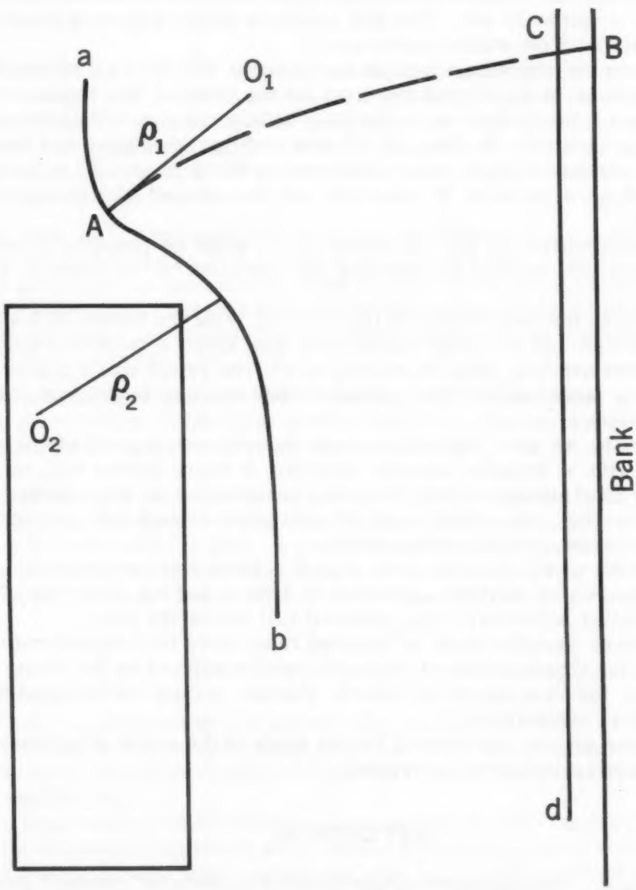

FIG. 13

diving motion, and this vertical component will depend on the value of the second member of Eq. 19.

For example, small values of ρ will increase the depth of scour. Experiments with different models of piers, with the same length and breadth and with the same discharges and heights, gave a confirmation of this result.

Rectangular piers (reduced values of ρ) produced a scour of 113 mm with a discharge of 301 per sec in a flume with a breadth of 70 cm and a height of 10.5 cm. The length of the pier was 24 cm and its breadth was 6 cm.

The simple rounding of the edges of the piers reduced the scour to 91 mm, whereas a triangular shape reduced it 70 mm.

An aerodynamic shape gave no further reduction, but the shape of a lens produced a reduced scour of 54 mm. (large values of ρ).

The protection realized by a single pile before the lens-shaped pier reduced the scour to 38 mm. This pile produced bigger values of ρ and worked as a reduction of the width-length ratio.

A change in the repartition of the velocity will have an influence on the second member of Eq. 19 and, therefore, on the value of the scour. A higher roughness of the bottom on a distance before the pier (with pebbles on the bottom) is realized. In Eq. 19, v' was reduced whereas v was increased, with the conclusion that the erosion had to be increased. That is what was found with an erosion of 71 mm with the lens-shaped pier (54 mm with the fine sand).

The consideration of Eq. 19 shows that it would be possible to considerably reduce the erosion by adapting the variation of the radius ρ with that of v^2.

Therefore, the repartition of the velocity from the bottom to the surface was measured and the lens-shaped pier was given a variable radii of curvature corresponding with the values of v^2. The result was a non-prismatic pier with a larger base. The erosion around this new model was reduced to 5 mm maximum.

It is easy to see that the second curvature $0_2 \rho_2$ will give a relation (Eq. 19) with a negative second member. A rising motion will, therefore, follow the first diving motion. This was observed on all the models. For the rectangular pier, the small radii of curvature around the upstream edges produced a quasi-vertical rising motion.

Behind the pier, with the lens-shaped section, the curvatures of the type 2 was followed by another curvature of type i, and the formation of a secondary smaller scour was to be observed just behind the pier.

Many other results could be deduced from three first considerations and also from the consideration of the spiral motion induced by the diving motion deviated by the reaction of the bottom. Further results can be found in some of the writers publications.

The same theory can be used for the study of the action of groynes and of the motion of sediments in derivations.

REFERENCES

1. Tison, L. J., "Affouillement autour de piles de ponts en riviere," Academie Royale de Belgique, Bulletin de la Classe des Sciences, 5e Serie XXIII, 1937.

2. Tison, L. J., "Recherches de Laboratoire sur l'Erosion dan les cours d'eau," Bulletin Société belge d'Etudes Géographiques, T. VIII, No. 2., 1938.

3. Tison, L. J., "Erosion autour de piles de ponts en riviere," Annales des Travaux Publics de Belgique, December, 1940.

4. Tison, L. J., "A u sujet du mode d'action des obstacles en saillie sur les rives et particulièrement des epis," Association Française pour l'Avancement des Sciences, Liege, Belgium, 1939.

5. Tison, L. J., "Erosion à l'aval des barrages," Association Internationale des Travaux hydrauliques, Stockholm, Sweden, 1948.

6. Tison, L. J., "Répartition du débit solide d'un cours d'eau se divisant en plusieurs bras naturels ou artificiels," Association Internationale des Congres de Navigation, Congrès de Rome, 1953.

S. V. CHITALE.[31]—In connection with estimation of scour at piers and abutments of bridges, Mr. Laursen has stated that comparison of model and prototype data indicated that the depth of scour could be treated as simply another length and that equilibrium depth of scour obtained in the field. This concept of equilibrium depth is due to the author and more clearly enunciated by the following quotation:[2]

> "At least as a first approximation the equilibrium scour depth, with certain qualifications as to the flow conditions, appears to be a function only of geometry, i.e. the relative depth of flow, the shape of the pier and the angle of attack. . . velocity of flow and sediment size (and, therefore, rate of transport and intensity of boundary shear) do not influence the equilibrium depth of scour. . . ."

Some investigations in models have been made on the subject of scour depth at bridge piers in India at the Central Water and Power Research Station, Poona which the writer thought would be of interest in context with the author's findings.

The first series of experiments were conducted in connection with the Hardinge Bridge over Ganga River and were reported in the Annual Reports of the Station for the years 1938 to 1942. A geometrically similar replica of Hardinge Bridge pier was embedded in Ganga sand of mean diameter of 0.29 mm in a parallel sided channel. The results of these experiments gave the relation

$$\frac{ds}{d} = 1.70 \left(\frac{q_c^{2/3}}{b}\right)^{0.78} \qquad \text{. . . . . (20)}$$

in which ds = maximum depth of scour below H.F.L.; d = depth of flow in the flume; b = width of pier; and q_c = discharge per foot run upstream of the piers. This relation is not dimensionally correct and cannot therefore be adopted for general application.

Basic experiments were subsequently conducted in 1941 with the object of testing the influence of upstream depth and sand diameter on scour round piers. The pier tested in these experiments was also 1/65 scale model of that of the Hardinge Bridge. It was rectangular in section, of length 1 ft, width 0.6 ft and semicircular cut and ease waters. The bed of the flume in these experiments

---

[31] Chf. Research Officer, Flood Control Div., Central Water and Power Research Station, Poona, India.

[2] "Scour Around Bridge Piers and Abutments," by E. M. Laursen and A. Toch, Iowa Highway Research Board Bulletin No. 4, May, 1956.

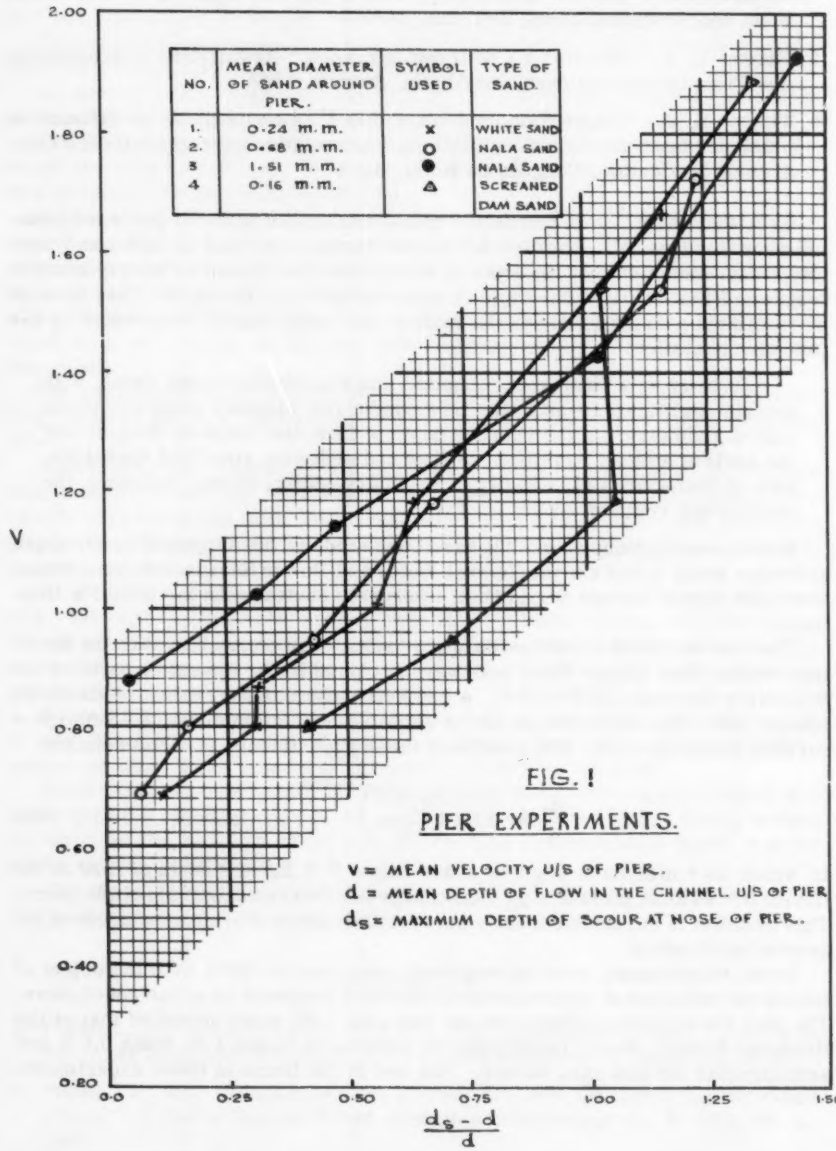

FIG. 14.—PIER EXPERIMENTS

was laid with sand of 0.32 mm while the following materials were used just around the pier in succession.

Sieve number	Type of sand	Mean size, in mm
1	screened dam sand	m = 0.16
2	White 'V' sand	m = 0.24
3	Nala sand	m = 0.68
4	Nala sand	m = 1.51

The sand round the piers was laid flush with the upstream bed level. A constant discharge of q = 1 cfs per ft was run and water level was adjusted to

TABLE 2.—RESULTS OF EXPERIMENT

Experiment No.	$V = \frac{q}{d}$ in ft per sec	ds in ft	d in ft	$\frac{V}{\sqrt{gd}}$	ds - d in ft	$\frac{ds - d}{d}$	Mean diameter of sand around pier, in mm
1	2	3	4	5	6	7	8
1	0.69	1.60	1.45	0.1005	0.15	0.103	0.24
	0.80	1.63	1.25	0.1261	0.38	0.304	
	0.87	1.51	1.15	0.1428	0.36	0.313	White
	1.01	1.55	0.99	0.1789	0.56	0.563	V
	1.18	1.40	0.85	0.2254	0.55	0.647	sand
	1.67	1.30	0.60	0.3799	0.70	1.170	
2	0.69	1.35	1.45	0.1005	0.10	0.069	0.68
	0.80	1.45	1.25	0.1261	0.20	0.160	
	0.95	1.50	1.05	0.1631	0.45	0.428	nala
	1.18	1.43	0.85	0.2254	0.58	0.682	sand
	1.54	1.41	0.65	0.3366	0.76	1.170	
	1.73	1.30	0.58	0.4002	0.72	1.240	
3	0.88	1.13	1.08	0.1490	0.05	0.046	1.51
	1.03	1.28	0.97	0.1841	0.31	0.320	
	1.14	1.30	0.88	0.2140	0.42	0.478	nala
	1.43	1.42	0.70	0.3012	0.72	1.030	sand
	1.93	1.28	0.52	0.4762	0.76	1.460	
4	0.80	1.77	1.25	0.1261	0.52	0.417	0.16
	0.95	1.80	1.05	0.1631	0.75	0.715	
	1.18	1.75	0.85	0.2254	0.90	1.060	
	1.54	1.33	0.65	0.3366	0.68	1.040	
	1.89	1.25	0.53	0.4575	0.72	1.360	

Pier experiments: In the 8 ft channel with sand of m = 0.32 mm

Scale of pier: 1/65 b = width of pier = 0.57 ft ≡ 37 ft
l = length of pier = 0.925 ft ≡ 63 ft
with constant discharge q = 1 cfs per ft
ds = maximum depth of scour round the pier
d = flow depth in the flume

get a particular depth, the depths varying from 0.5 to 1.45 ft. Each experiment was continued until final maximum scour was obtained round the pier.

In a few tests in which the upstream depth was less than stable depth the upstream bed scoured and blanketed the scour pit around the pier. In such cases,

the maximum depth of scour at the nose was measured just before deposition in the scour hole of sand from upstream occurred.

In experiments when sand around pier was coarser than the bed material upstream, the bed around the pier was laid higher than upstream level, to get scour round the pier for the upstream depth laid.

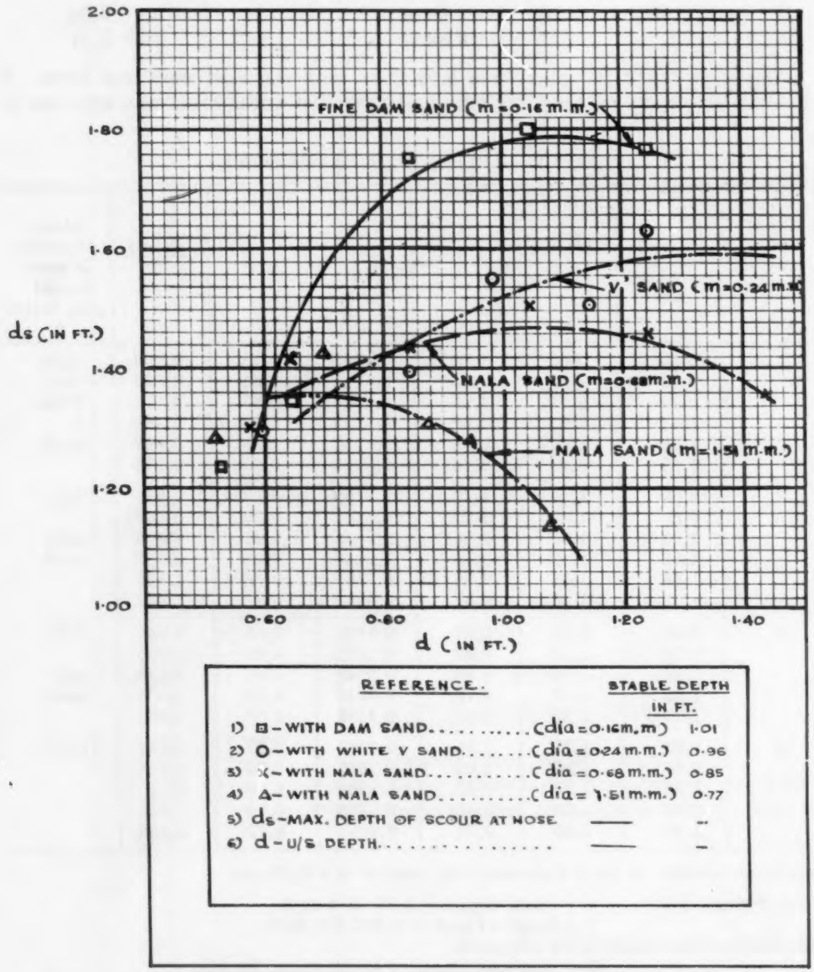

FIG. 15.—1/16 SCALE PIER EXPERIMENTS, ds : d FOR q = 1 cfs

Table 2 shows the results obtained important conclusions, as follows:

1. With axial flow, maximum depth of scour was always at the nose of the pier, scour at sides being less by 5 to 15%.

2. The ratio of scour at the nose and depth of flow in the channel bears a simple relation with the approach velocity in the channel (see Fig. 14).

3. The depth of flow on the upstream has also an influence on scour at the pier nose (see Fig. 15).

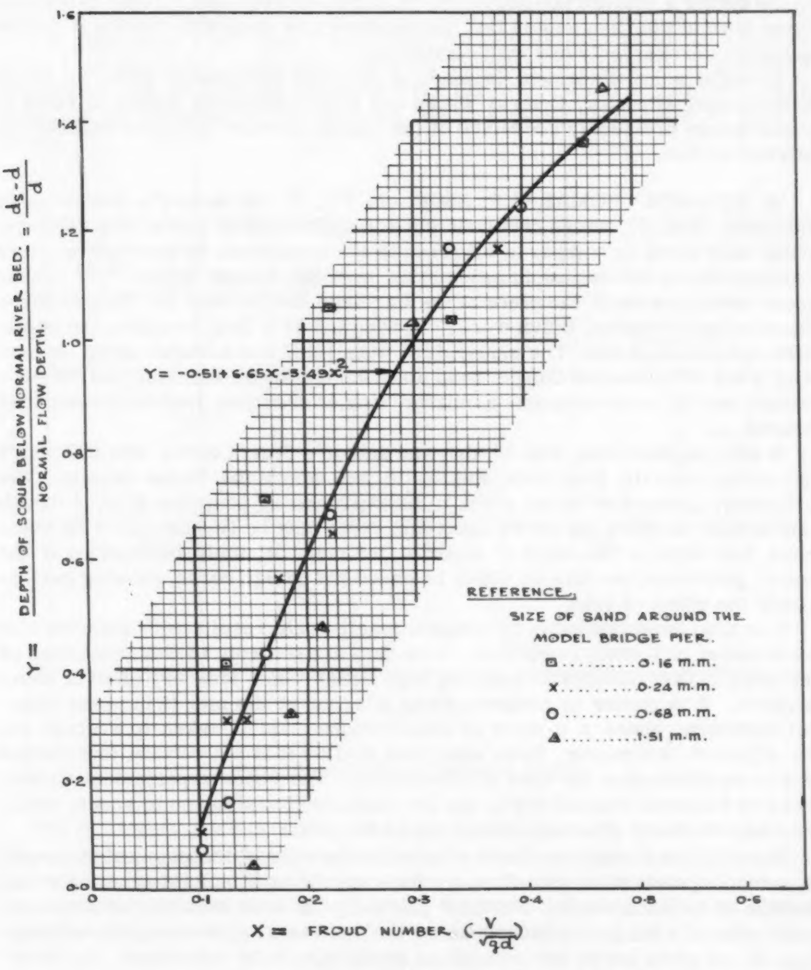

FIG. 16.—RESULTS OF BASIC EXPERIMENTS

It will be seen that correlation of depth of scour either with upstream depth (Fig. 15) does not appear to be satisfactory. The writer, therefore, further analyzed the experimental data and found that the Froud number provides a better criterion. Fig. 16 shows plot of depth of scour against the Froud num-

ber. Although some scatter of points is evident in this plot, the general trend is remarkable, statistical equation obtained over the range of experimental data being

$$y = -0.51 + 6.65\,x - 5.49\,x^2 \qquad (21)$$

It is thus seen that experiments at the Research Station do not lend support to the author's equilibrium scour theory, and it appears that further investigations both in the field and in the laboratories are desirable before it can be accepted unreservedly and with confidence.

Grateful acknowledgment is made of the kind permission given by M. G. Hiranandani, Director, Central Water and Power Research Station to refer to experiments previously conducted at the Station and also for useful suggestions offered by him.

A. RYLANDS THOMAS,[32] F. ASCE.—In Fig. 17, the author's design curve for piers (Fig. 9), with a factor of 0.9 for application to piers with semicircular nose form, is compared with results of experiments with models of piers carried out by the writer in association with Sir Claude Inglis.[33,34] These piers were models of the piers of the Hardinge Bridge over the Ganges River (now in East Pakistan) which were 37 ft wide and 63 ft long, including the semicircular nose and tail. The model piers were fixed in a parallel-sided channel with a bed of incoherent Ganges sand about 0.3 mm mean diameter and the procedure was to run a constant discharge without sediment load until scour had ceased.

It will be seen from Fig. 17 that the author's design curve, and still more his curve from the Iowa data, Fig. 3, lie well above the Poona results. The difference appears to be too great to be explained by sediment load,[21] though this cannot be ruled out as the upstream depth may be reduced more by sediment load than is the depth of scour at the pier. It would be of value if the author presented the data on which he based his design curve, showing particularly the effect of load.

It is also most desirable to compare small-scale results with observations made under full-scale conditions. Such data are difficult to obtain because of the need to take observations during high floods which are very often of short duration. It is easier to measure depth of scour at the pier than in the channel upstream, where a number of observations must be taken to average out the effect of bed waves. Even when this is done it is not certain that the bed was in equilibrium at the time of observation. The Poona experiments showed that a reduction in channel depth, due for example to resistence to scour, would increase the depth of scour at the nose of the pier.

The relationship between depth of scour at the nose of the pier and the depth of channel upstream is, therefore, perhaps not the most suitable one for comparison of full-scale data. Nor is it generally the most suitable for practical application of a design formula, because the upstream depth during a maximum flood is not often known beforehand and would have to be calculated. An error in assessing this depth would lead to a corresponding and greater error in estimating the level to which scour is liable to occur.

---

32 Cons. Engr., London, England.

33 Annual Reports (Technical), Central Irrigation and Hydrodynamic Research Station, Poona, India, 1938-39, p. 39; 1939-40, p. 33; 1940-41, p. 35.

34 "The Behaviour and Control of Rivers and Canals," by C. C. Inglis, Central Waterpower Irrigation and Navigation Research Station, Poona, India, 1949, p. 327.

A more basic relationship is that between depth of scour below water level, D_s, width of pier, b, and upstream discharge per unit width, q. The relationship indicated by the Poona results is

$$\frac{D_s}{b} = 1.70 \left(\frac{q^{2/3}}{b}\right)^{0.78} \qquad (22)$$

in ft-sec units, applicable to scour in fine sand within the limits of $q^{2/3}/b$ or y_o/b at least from 1 to 6 (see Fig. 17) and not greatly affected by the grade of sand. It is necessary to take into account the effect of obliquity of approach flow, which may be done by using for b the projected width of pier on a plane normal to the direction of approach. A factor of safety should also be used in design.

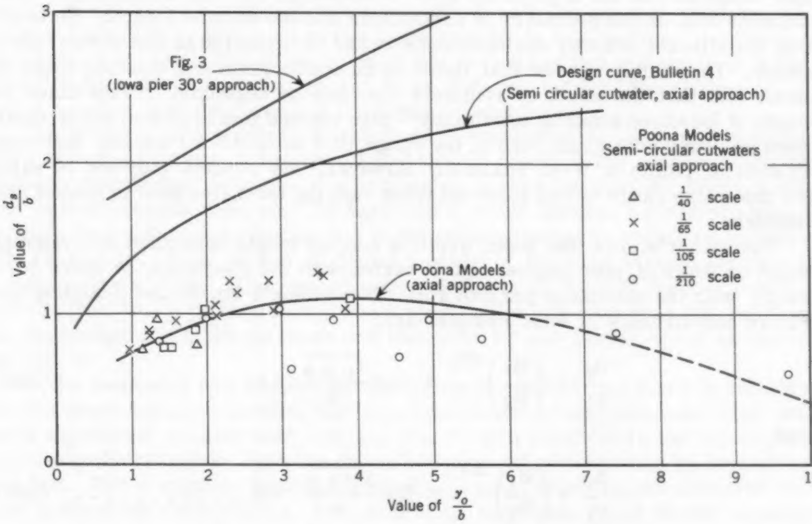

FIG. 17.—SCOUR AT BRIDGE PIERS

The discharge per unit width to be used for design must, in most cases, be greater than the mean value because in rivers the deep channel meanders from one bank to the other. It is therefore advisable to use, at least as a check, the relationship proposed by Inglis[34] giving the maximum depth of scour around a pier as approximately twice the Lacey regime depth, that is,

$$D_s = (Q/f)^{1/3} \qquad (23)$$

in which D_s is the depth of scour in feet below water surface, Q is the discharge in cu sec, and f is the Lacey silt factor (approximately $1.8\sqrt{m}$ where m = mean diameter of bed sand in mm). Eq. 23, derived from data of several bridges in India and Pakistan, takes into account obliquity of approach and concentration of discharge but not the width of pier, which is clearly an important factor. The data related to normal widths of pier and to depths of scour ranging from 25 ft to 117 ft.

MUSHTAQ AHMAD.[35]—The problem of correct estimation of depth, shape, and extent of localized scour is important from the point of view of establishing sound design practice and safety of hydraulic structures such as bridge piers, abutments, spur dikes, groins, or pitched islands. This problem is much more important for hydraulic structures in alluvial rivers of West Pakistan where fine sand is found for hundreds of feet in depth, and scour depths of 40 ft to 80 ft below water level are common. The author has, therefore, dealt with a subject of special importance and great utility to this region.

It is proposed to discuss the author's approach to the problem with special reference to field and laboratory experience in West Pakistan. The author has assumed the depth of scour as another length and has related it to the normal depth or the width of a pier, and maintains that the depth of scour does not depend on the degree of concentration until scour holes around neighboring obstructions overlap. He maintains that there is equilibrium or limiting depth and believes that for a given mode of sediment movement, the depth of scour depends only on the geometry of contraction and the approach depth. He holds that the effect of velocity and sediment size can be neglected as that of secondary order. The writer agrees that there is an equilibrium and limiting depth of scour and that the effect of sediment size can be neglected. Tests made on depth of localized scour at spur dikes[36] also showed that localized scour depth does not vary with grain size in the range (0.1 m to 0.7 m) usually met with in alluvial plains of West Pakistan. However, this concept may not be valid for the entire range of bed material sizes ranging from fine sand to gravel and boulders.

The author's view that scour depth is another length connected with normal depth or width of pier implies that it varies with the discharge, or more correctly with the discharge per foot run. The author's Eq. 8b and c holding for rivers and streams in West Pakistan are:

$$\frac{d_s}{y_1} = \left(\frac{B_1}{B_2}\right)^{.64} - 1 \text{ for } \frac{\sqrt{g\,y\,s}}{w} = 1 \ldots\ldots\ldots\ldots \quad (24a)$$

and

$$\frac{d_s}{y_1} = \left(\frac{B_1}{B_2}\right)^{.69} - 1 \text{ for } \frac{\sqrt{g\,y\,s}}{w} < 2 \ldots\ldots\ldots\ldots \quad (24b)$$

where the exponent varies between 0.64 to 0.69, or on the average the relation can be written as

$$\frac{d_s + y_1}{y_1} = \left(\frac{Q/B_1}{Q/B_2}\right)^{.64-.69} \sim \left(\frac{q_2}{q_1}\right)^{2/3} \ldots\ldots\ldots\ldots (25)$$

$$\frac{y_2}{y_1} = \left(\frac{q_2}{q_1}\right)^{.64-.69} \sim \left(\frac{q_2}{q_1}\right)^{2/3} \ldots\ldots\ldots\ldots\ldots (26)$$

and

$$\frac{y_2}{q^{2/3}} = \frac{y_1}{q^{2/3}} = K \ldots\ldots\ldots\ldots\ldots\ldots\ldots (27)$$

---

[35] Dir., Irrigation Research Inst., West Pakistan.

[36] "Experiments on Design and Behaviour of Spur Dykes," by Mushtaq Ahmad, Proceedings, Minnesota Internatl. Hydr. Convention, September 1-4, 1953.

in which K may be a function of boundary geometry of the contraction at the bridge, abutment shape and thickness and shape of the nose of the piers, and so forth. Because the depth is a dependent variable on discharge intensity, the latter may be used in preference to depth. Here only lies the difference in approach between the author and the writer in studying this problem. As shown previously the two approaches are not very different. The writer prefers to study the variation of $D_s/q^{2/3} = K$ as a function of boundary geometry, shape of pier nose, and abutment, characteristics of bed material, and distribution of velocity in the cross section at the piers representing the concentration of flow. The functional relation for study may be of the type:

$$\frac{D_s}{q^{2/3}} = K f \left(\theta, \frac{V^{1/2}}{V}, \frac{\sqrt{g\ y\ s}}{w}, S, \frac{B}{B_t - nt}\right) \text{ etc. } \ldots\ldots\ldots (28)$$

in which θ is the angle between the current and the spur dike, an abutment or a pier, $V^{1/2}/V$ is the ratio of mean velocity in half the channel width on the side of spur dike or abutment to the mean velocity in full section. It will be a measure of concentration of flow; W is fall velocity of bed material; B is the river width upstream of the bridge; B_t is distance between the abutments; n is the number of piers,; and t is thickness of each piers.

The writer does not agree that the depth of scour does not depend on the degree of concentration. It has been found that by changing the concentration or velocity distribution at bridge site by training works upstream, the scour depth can be considerably reduced. The variation of scour depth as a result of change in velocity and flow distribution due to the training works is explained in Figs. 18, 19, and 20. Figs. 19 and 20 depict a model of the Ling Stream showing a bridge below a curve. The concentration of flow near the left flank is noticeable in Fig. 19. A pitched island and a spur on the left bank fans out the flow at the bridge site to obtain more uniform velocity and lesser scour as shown in Fig. 20.

In the method of plot adopted by the author in which scour depth in relation to U/S depth has been studied, the non-dimensional scour perimeter may not have significant relation with velocity, for, in open channels as the velocity or discharge increases so does the depth, although not necessarily by erosion of the bed. For a uniform approach velocity, a mean depth can be assumed for use in the author's relations. But, generally, abnormal scour depths at piers or abutments are associated with concentration of flow resulting from the variation of velocity and depth in the approach section and the selection of representative approach depth for use in the author's relation and the estimation of discharge distribution in the channel and on the berm becomes very difficult. In fact, the author's term $(Q_c + Q_o)/Q_c$ in Eq. 9 is, also, a measure of concentration of flow. However, the estimation of Q_c, Q_o, or Q_w is difficult for practical use in the computation of maximum scour depth in case of a curved approach. The writer has shown[37] that change in flow concentration above a spur dike, can be depicted in terms of velocity distribution and common types are depicted in Fig. 21 by I, II and III. The type III velocity distribution gives the maximum concentration on the outside of a bend as due to negative velocity on the inside, a part of the water way is blocked by reverse flow. For the three types of velocity distribution depending on different types of approaches, the values of $V_{\frac{1}{2}}/V$ and K as determined from writer's studies on spur dikes (which may be applicable to abutments), are given in Table 3. Since maximum scour can occur on any one or a group of piers in a meandering alluvial channel, the

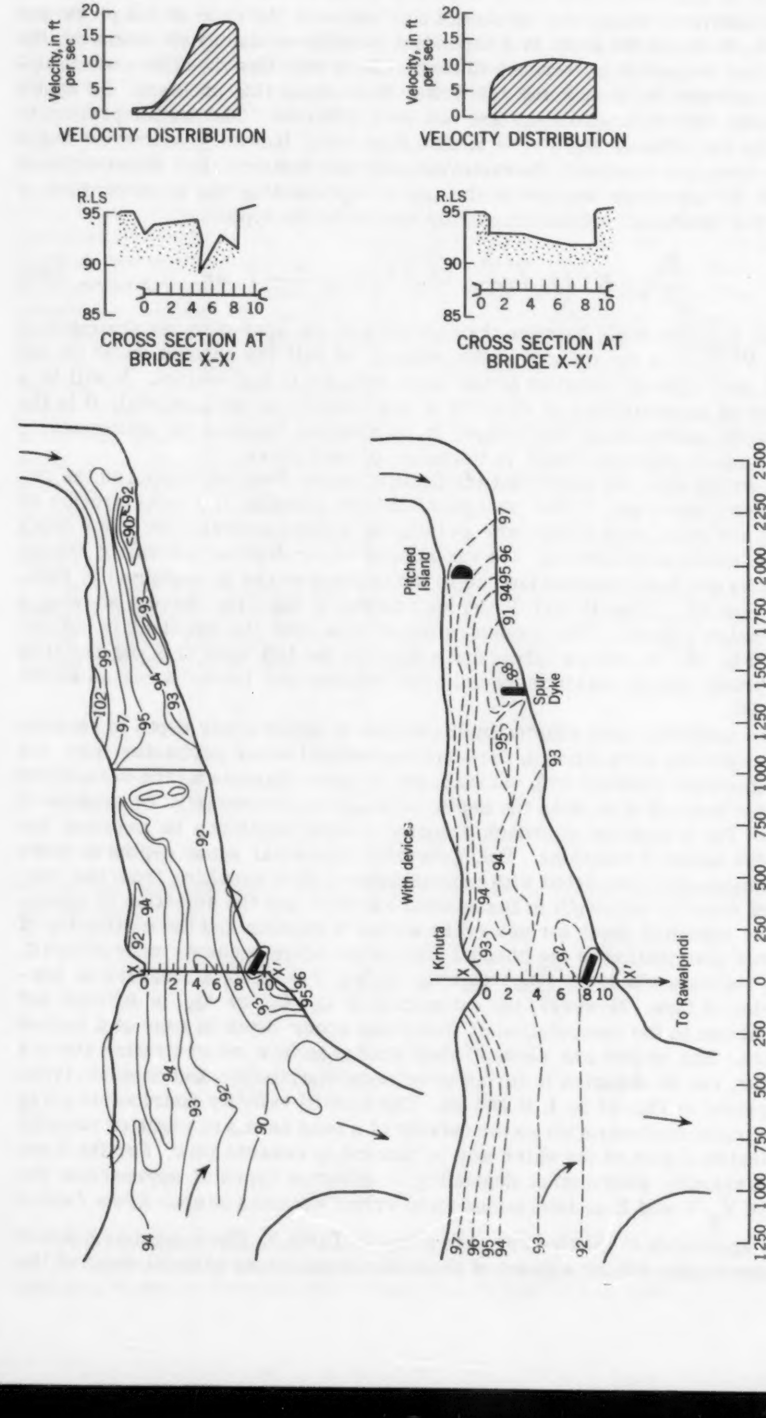

FIG. 18.—LING NALLAH BRIDGE

FIG. 19

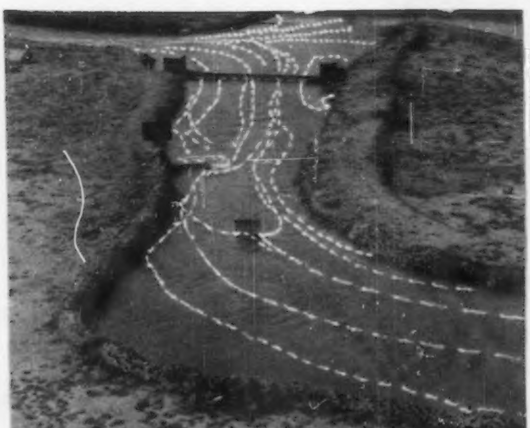

FIG. 20.—FLOW AT BRIDGE SITE

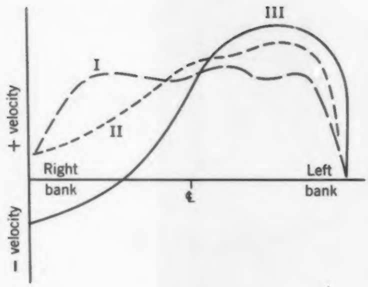

(*a*) VELOCITY DISTRIBUTION AT BRIDGE SITES I, II, AND III

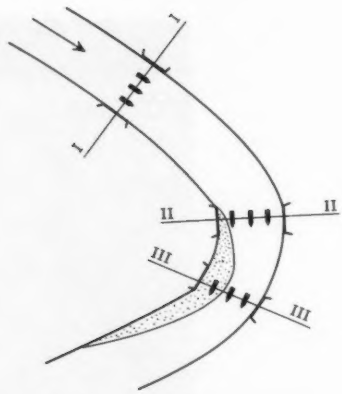

(*b*) THREE BRIDGE SITES IN A CURVE

FIG. 21.—THREE BRIDGE SITES IN A CURVE

FIG. 22.—ABNORMAL SCOUR AT A GUIDE BANK HEAD

depth of foundation of piers has to be computed from the values of K as fixed by the river curvatures likely to occur, keeping in view the restraints imposed on river by the upstream training works. The method commonly used in West Pakistan supported by Laboratory studies and field observations consists in working out $q = \frac{Qmax}{B}$.

TABLE 3.—VALUES OF $V_{\frac{1}{2}}/V$ AND K

Approach condition (1)	$V_{\frac{1}{2}}/V$ (2)	K (3)
Scour below a severe bend on the concave side accompanied by a swirl on the convex bend.	1.25	2 - 2.25
Moderate Bends.	1.15	1.5 - 1.75
Straight obstruction placed at any angle of 30° to 90°	1.0	1.2 - 1.5
Straight obstruction placed at an angle of 90° - 150° to the flow	1.0	1.5 - 1.75

TABLE 4.—MAXIMUM SCOUR DEPTHS OBSERVED AT BRIDGE PIER AND ABUTMENTS ON DIFFERENT MODEL STUDIES AT IRRIGATION RESEARCH INSTITUTE, LAHORE.[b]

River	Site	Q Max, in cu sec	q	Scour depth			$K = \frac{Ds}{q^{2/3}}$	Y_o	Thickness of pier (b)	$\frac{Y_o}{b}$	$\frac{ds}{b}$	$D_s = ds + Y_o$
				Observed	Scale distortion factor.	Corrected scour depth.						
(1)	(2)	(3)	(4)	(5)	(6)	(7)	(8)	(9)	(10)	(11)	(12)	(13)
Ravi	Shahdara Bridge	332,000	237	52	1.23	64.0	1.68	26.4	10	2.64	2.06	47
Jhelum	Jhelum bridge[a]	600,000	120	30	1.3	39	1.60	23	10	2.3	1.98	42.8
	Maagla New bridge	275,000	429	90	1.0	90	1.60	28	abutment	..	..	..
Deg	S-harakpur	40,000	200	34	1.34	45	1.34	21.5	6.25	3.45	2.22	35.5
Rohi	Kasur	35,000	147	30	1.3	39	1.4	14	6.25	2.25	1.97	26.3
Sohan	Dhok Pathan	150,000	172	36	1.17	42	1.36	18.6	9.0	2.07	1.94	36.1
Indus	Thatha Sujjawal proposed bridge.	1,100,000	275	52	1.31	68	1.6	25	7.0	3.57	2.25	40.8

[a] Computation from Fig. 9, Bulletin No. 4.
[b] Bed material - five sand.

At the bridge site, the value of K can be selected from the maximum curvature likely to occur. This will give scour depth below water level, and the depths below bed level can then be worked out. Maximum depth of scour from model studies at bridge piers and abutments of different rivers and streams, after

correcting the results for the effect of scale distortion on geometry of scour,[37] are summarized in Table 4. In this table, scour depth has been computed from the author's design curves of Bulletin No. 4, in Fig. 9. The scour depths obtained after correcting for the model scale distortion are generally higher than those of the author. In computing D_s value by his method, the actual mean value of Y_o has been taken from the cross section above the bridge. The value of K does not exceed 1.7 because severe bends are not possible in these cases due to the presence of guide banks.

TABLE 5.—SHAHDARA RAILWAY BRIDGE ON RIVER RAVI[a]

S. No.	Year	Q	H.F.L.	Gauge B	Water-way at the bridge B, in feet	q	Max. Scour R.L.	Max. Scour Ds	$K - \frac{DS}{q^{2/3}}$
(1)	(2)	(3)	(4)	(5)	(6)	(7)	(8)	(9)	(10)
1.[b]	1948	86000	688.0	11.7	12 x 90 = 1080	79.5	651.14	36.86'	1.989
2.[c]	1949	52000	686.0	9.7	8 x 90 = 720	72.2	657.14	28.86	1.664
3.[c]	1950	1,93000	692.0	15.7	15 x 90 = 1350	142.9	651.2	40.8	1.49
4.[c]	1951	44000	686.3	10.0	7 x 90 = 630	69.8	656.14	30.16	1.77
5.[c]	1952	56000	687.2	10.9	9 x 90 = 810	69.13	655.0	32.0	1.63
6.[c]	1953	83000	689.1	12.8	11 x 90 = 990	83.75	651.64	37.46	1.95
7.[c]	1954	1,72000	691.8	15.5	15 x 90 = 1350	127.5	655.0	36.8	1.453
8.[c]	1955	250,000	695.0	18.7	15 x 90 = 1350	105.18	660.0	35.0	1.078
9.[c]	1956	87000	688.3	12.0	12 x 90 = 1080	80.5	657.22	31.08	1.66
10.[c]	1957	1,92000	692.3	16.0	15 x 90 = 1350	142.2	654.54	37.66	1.383
11.[c]	1958	1,52000	691.2	14.9	14 x 90 = 1260	120.61	662.64	28.56	1.17

[a] Part of the water way is marked by a semi erodable island at the bridge and hence the difference in the water way for different years. [b] No training works a river bed u/s. [c] A spur constructed u/s to current approach.

Fig. 22 shows abnormal scour at a guide bank head. A heavy embayment is noticeable on the right and construction due to silting caused by roller on the left. The K value of 2.3 can be obtained in such a case.

The heavy embayment resulting in abnormal scours illustrated in Fig. 22 with K value greater than 2 are possible only on spur dikes or guide bank heads

[37] "Effect of Scale Distortion, Size of Model Bed Material and Time Scale on Geometrical Similarity of Localized Scour," by Mushtaq Ahmad, Proceedings, Internatl. Assoc. of Hydr. Research, The Hague, Netherlands, 1955.

and are not to be allowed on bridge piers or abutments. In fact, for alluvial rivers or streams of West Pakistan, guide banks at least equal to the length of the bridge, with curved heads and expanding water way on the upstream side, are provided to shift the maximum embayment and abnormal localized scour to the guide bank heads instead of allowing it to occur near the bridge with short abutments. Under these conditions, the values of K for estimating the maximum probable depth of scour can safely be taken between 1.7 and 2.0. In case of a short abutment length before the conditions for abnormal scour where K greater than 2 are obtained, the approach roads or railway will be threatened and cut by the embayment formed by an alluvial meandering river. It is therefor necessary to design pier and abutment depths for scour calculated from K 1.7 to 2.0 and provide proper guide bank to keep the road or railway approaches safe from embayment and to keep abnormal scour away from the main bridge crossing. Actual scour depths observed on the railway bridge on Ravi near Lahore and the computed values of K as recorded in Table 5 also supported the recorded values of K.

PIER LUIGI ROMITA.[38]—The author's long lasting efforts to cast light upon the phenomenon of scour around bridge piers and abutments are to be greatly commended because of the great practical importance of the problem. The clear and condensed presentation in this paper of the results of these efforts is a substantial step towards a generalized solution of the problem, and will be of great use to designers and to the administrations responsible for the construction and maintenance of roads and railways. To this end a coordinated effort should be made, in order to insure the necessary verification on prototypes of the proposed relationships.

There is no doubt that one of the most important factors of scour, when piers have a sufficiently high length per width ratio, is the angle of attack between the pier and the flow. Even small deviations of this angle from the zero value are responsible for fast increases of the scour; this usually represents a much greater danger to the stability of the pier than any underevaluation of the maximum possible flood. The collapse of many piers during floods is, in fact, to be ascribed more to the angles of attack, which may occur due to unusual cross-currents and deformations of the river bed, than to the unexpected entity of the discharge.

In view of all this, the writer carried out, some years ago, a systematic model investigation of the influence of the angle of attack upon the depth of scour. The experiments were carried out in a glass-flume of the Hydraulic Laboratory of the Polytechnic Institute of Milan, supplied with clear water, using uniform sand of 1 mm diam as bed material, and in such conditions that there was no general bed movement but only localized scour around the pier. The shape of the pier was not particularly studied, and it reproduced a rather widely used type of pier; its length per width ratio was about 5. Two series of tests were carried out with different values of the discharge, while the angle of attack was varied from 0° to 90°.

The data obtained at a zero angle of attack are in rather good agreement with the curve representing Eq. 11 Fig. 9, but for the fact that they consistently lie a little below this curve. An increase by 60% in the discharge (which corresponded to an increase by 20% in the average velocity of flow) brought around only a 20% increase in the maximum depth of scour, at the same angle of attack.

---

[38] Assist. Prof., Hydr. Structures, Politecnico di Milano, Milan, Italy.

The tests with varying angle of attack have shown the basic importance of this factor. For an angle of 15° the maximum depth of scour was 1.9 times that corresponding to a zero angle; for an angle of 30° the increase of scour depth was in the ratio 2.6:1 in respect to the zero angle, for an angle of 45° in the ratio 3.0:1, and for an angle of 60° in the ratio 3.3:1. Increases of the angle of attack beyond 60° and up to 90° did not bring around any further appreciable increase in the scour depth. These values are considerably in excess of those indicated by Fig. 10.

Another interesting observation was that the point of maximum scour depth always occurs very close to the pier wall, so that, if the depth of the foundation is not sufficient, the pier will easily be undermined, and collapse.

As a conclusion, the fundamental importance of avoiding any angle of attack between the pier and the flow should again be stressed. In order to obtain this, the river banks should be stabilized with adequate measures for a sufficiently long stretch upstream of every bridge crossing. In braided rivers, however, the possibility that an angle of attack occurs should always be taken into account, and the pier foundations designed accordingly.

CONSERVANCY DISTRICTS AS FLOOD CONTROL ORGANIZATIONS[a]

Discussion by Samuel A. Greeley

SAMUEL A. GREELEY,[5] F. ASCE.—This is an excellent and timely paper. In my opinion, it has important bearing not only on conservancy districts, but also on other forms of municipal organizations such as authorities, sanitary districts, water districts, and, in Michigan, refuse disposal districts. The importance of organizations of this kind, which may be generally referred to as Authorities, was emphasized in fine fashion by Mr. Robert Moses in his address before the American Public Works Congress in New York, on August 17, 1960. It is pertinent, therefore, to consider Mr. Chambers' paper as applying to more kinds of public works activities than flood control.

It is of interest to refer to the Progress Report dated January, 1945 of a Committee of the Society on Organization, Financing, and Administration of Sanitary Districts, of which the writer was Chairman. Relative to the organization and creation of sanitary districts (or authorities), the following is abstracted:

> In general, the Committee feels that the steps required to create, form, and organize a sanitary district should be taken within the locality which will comprise the district.
>
> The Committee favors the origination and creation of districts by local petition followed by a general vote by qualified persons within the designated boundaries.
>
> The Committee favors the determination of the extent of the district by a competent engineer or board of engineers after an adequate survey and investigation of the locality.
>
> The Committee favors, in general, the election locally of the members of the administrative board. The Committee recognizes, however, that many appointed boards have been eminently successful and suggests that the appointment of board members by some locally elected official may be an acceptable method.

In Item 3 of the Summary, Mr. Chambers refers to the needs of "such developments." The writer suggests that not only the need, but also the relative need as compared to other interests should be included in the original studies.

It is further suggested that the paper does not give sufficient weight to financing procedures. In two elections under the Illinois Conservation District Act, organizations of the districts have failed. The writer thinks one reason was that the enabling act limits all financing to taxes derived from assessed valuations. It seems likely that properties in different parts of the district will have different views relative to the need and validity of the proposed district or authority to be organized and financed. The obtaining of funds by the

---

[a] April, 1960, by Cloyde C. Chambers.

[5] Partner, Greeley and Hansen, Engrs., Chicago, Ill.

Miami Conservancy District which was organized shortly after 1913 provided for charges or assessments by zones carefully related to the resulting benefits or uses of the flood control works. This is a good example of an approach to fair financing. Having in mind the conception that the paper as a whole is useful in the consideration of other kinds of municipal organizations such as authorities and districts, reference should be made to the so-called two-part rate as developed by a Joint Committee of the Society and the American Bar Association with six other National organizations. The report of this group stated the following fundamental principle relative to a fair procedure in financing water, sewage, and other public works:

> "The needed total annual revenue of a water or sewage works shall be contributed by users and non-users (or by users and properties) for whose use, need and benefit the facilities of the works are provided approximately in proportion to the cost of providing the sue and the benefits of the works."

This statement means that the needed total annual revenue (operating and debt service costs) shall be derived from the users and properties in proportion to the amount which each causes to be spent.

COMPARISON OF STREAM VELOCITY METERS[a]

Discussion by Harold G. Golden and I. L. Trotter, Jr.

HAROLD G. GOLDEN,[10] A. M. ASCE and I. L. TROTTER, JR.[11]—In this most interesting paper, the authors concluded that the screw type and cup type current meters gave identical results in U. S. Lake Survey flow measurements.

TABLE 4.—COMPARISON OF DISCHARGE MEASUREMENTS OBTAINED BY PRICE AND OTT METERS

Date (1)	Measured discharge, in cubic feet per second: Price meter (2)	Measured discharge, in cubic feet per second: Ott meter (adjusted) (3)	Percentage variation of discharge obtained by Ott meter from discharge obtained by Price meter (4)
3-28-58	700,000	692,000	-1.14
4-16-58	796,000	774,000	-2.76
4-28-58	795,000	796,000	+0.13
5-23-58	1,178,000	1,184,000	+0.51
6- 9-58	475,000	474,000	-0.21
6-30-58	688,000	688,000	0
7-21-58	667,000	672,000	+0.75
8- 4-58	1,032,000	1,005,000	-2.62
8-25-58	624,000	624,000	0
9- 8-58	335,000	326,000	-2.69
9-26-58	399,000	397,000	-0.50
10-20-58	291,000	291,000	0
11-10-58	206,000	205,000	-0.49
Average percentage variation of 1958 measurements			-0.69
3-30-60	662,000	672,000	+1.51
4-18-60	1,047,000	1,059,000	+1.15
5-11-60	746,000	751,000	+0.67
6- 3-60	755,000	763,000	+1.06
6-17-60	546,000	547,000	+0.18
7- 6-60	720,000	731,000	+1.53
Average percentage variation of 1960 measurements			+1.02
Average percentage variation of all measurements			-0.15

[a] April, 1960, by F. Wayne Townsend and F. A. Blust.
[10] Hydr. Engr., U. S. Geol. Survey, Jackson, Miss.
[11] Engr. Tech., Hydr., U. S. Geol. Survey, Jackson, Miss.

Of particular interest was the comparison between the Price (cup-type) meter and the Ott (screw-type) meter.

The purpose of this discussion is to present additional data that indicate there are no significant differences between independent discharge determinations using Price and Ott meters. During 1958 and 1960 the U. S. Geological Survey obtained nineteen pairs of discharge measurements using the Price and Ott current meters at the stream-gaging station on the Mississippi River near Vicksburg, Miss. The results of these measurements are shown in Table 4. All measurements were made from the downstream side of the highway bridge near Vicksburg. In all cases, the Ott meter discharge measurements were made after the completion of the Price meter discharge measurements, with an average time lag of $4\frac{1}{2}$ hr. The cross sectional areas used for the Ott meter measurements were based on the soundings obtained during the Price meter measurements. For comparative purposes, The Ott meter discharge measurements were adjusted when a significant change in river stage occurred between the two measurements.

An equipment change was made between the measurements obtained in 1958 and in 1960. The measurements in 1958 were obtained using a 300 lb Vicksburg-type lead sounding weight and a single pin attaching the Ott meter to the hanging-bar. The measurements in 1960 were obtained a 150 lb Columbus-type lead sounding weight and two pins attaching the Ott meter to the hanging bar. The effect of this equipment change is not evaluated but is noted as a matter of record.

FRICTION LOSSES IN LINES WITH SERVICE CONNECTIONS[a]

Discussion by M. H. Diskin, Annabel L. Tong, M. B. McPherson and J. V. Radziul, and K. M. Yao

M. H. DISKIN.[5]—The author has presented a solution, based on the Hazen-Williams formula, for the problem of head losses in a pipe with a non-constant discharge along its length. The solution is based on a number of assumptions that should be critically examined before the solution can be adopted for general use. The main assumptions on which the analysis is based are:

1. The head losses per unit length of pipe, at any given discharge, are the same whether it is a constant discharge or whether it is variable along the pipe.
2. The local head losses in the main stream due to the side outlets are negligible.
3. There is no redistribution of energy content, per unit weight of fluid, between the main flow and the side flow.

The first two assumptions are mentioned or implied in the orginal paper and require no further explanations. The third assumption refers to the possibility that water arriving at a side outlet (Fig. 8) with a total head (energy per unit weight) H_1 and discharge Q_1 will be divided into two streams Q_2 and Q_3 in such a way that one of them will have a higher head $(H_2 > H_1)$ and the other a lower head $(H_3 < H_1)$ than the original head (H_1). The total energy balance will, of course, still be in accordance with the principle of conservation of energy:

$$\gamma Q_1 H_1 \geq \gamma Q_2 H_2 + \gamma Q_3 H_3 \quad \ldots\ldots\ldots\ldots\ldots \quad (21)$$

in which γ is the unit weight of the liquid.

That such a redistribution is possible can be demonstrated with a simplified analysis of the conditions at a side outlet using the momentum equation. It is assumed for simplicity that the side outlet is in a horizontal plane. The free body to which the momentum equation will be applied is defined by sections 1-1, 2-2, and 3-3 in Fig. 8. Section 1-1 is taken just before the side outlet, and the other two sections are taken sufficiently downstream for the velocities to be approximately uniform. The momentum equations for the free body previously defined, in directions parallel and perpendicular to the main pipe axis, and based on the usual assumptions for the momentum equation, are:

$$p_1 A_1 - p_2 A_1 = \frac{\gamma}{g} \left(Q_2 V_2 - Q_1 V_1\right) \quad \ldots\ldots\ldots \quad (22)$$

---

[a] April, 1960, by D. L. Muss.

[5] Acting Head of Hydr. Lab., Technion, Israel Inst. of Tech., Haifa, Israel.

and

$$p_4 A_3 - p_3 A_3 = \frac{\gamma}{g} \left(Q_3 V_3 - 0 \right) \qquad (23)$$

in which A_1 and A_3 are cross sectional areas of main pipe and side outlet respectively, p_1, p_2, p_3 are pressures; V_1, V_2, V_3 are velocities at the corresponding sections and p_4 is the pressure at the main pipe wall opposite the side outlet.

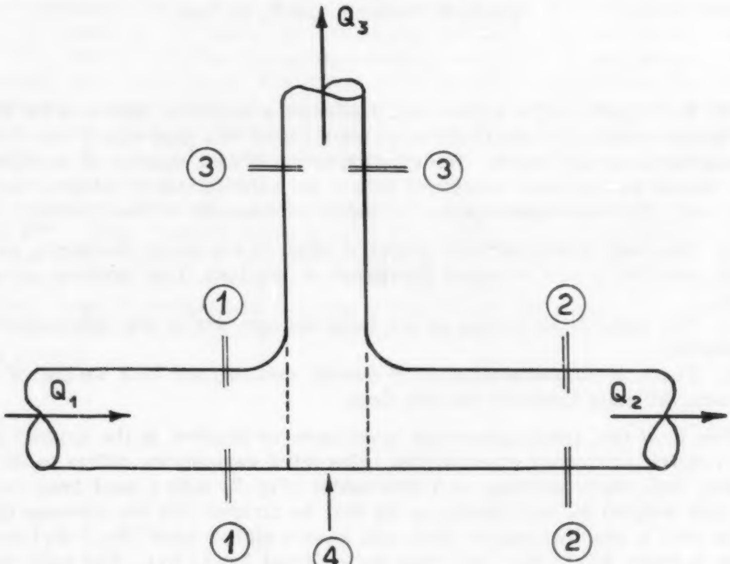

FIG. 8

Dividing Eq. 22 by γA_1, it is transformed to:

$$\frac{p_1}{\gamma} - \frac{p_2}{\gamma} = \frac{V_2^2}{g} - \frac{V_1^2}{g} \qquad (24)$$

or

$$\frac{p_1}{\gamma} + \frac{V_1^2}{g} = \frac{p_2}{\gamma} + \frac{V_2^2}{g} \qquad (25)$$

which may also be written as:

$$H_1 + \frac{V_1^2}{2 g} = H_2 + \frac{V_2^2}{2 g} \qquad (26)$$

Since the velocity at section 2-2 is smaller than that in section 1-1 $(V_2 < V_1)$, the total head at section 2-2 is higher than the total head at section 1-1:

$$H_2 > H_1 \qquad (27)$$

Dividing the second momentum Eq. 23 by γ A_3 and assuming that the pressure at the pipe wall opposite the side outlet (p_4) is approximately equal to the inlet pressure (p_1)

$$p_4 \approx p_1 \qquad (28)$$

the equation is transformed into:

$$\frac{p_1}{\gamma} - \frac{p_3}{\gamma} = \frac{V_3^2}{g} \qquad (29)$$

or

$$\frac{p_1}{\gamma} = \frac{p_3}{\gamma} + \frac{V_3^2}{g} \qquad (30)$$

that may also be written as:

$$H_1 - \frac{V_1^2}{2\,g} = H_3 + \frac{V_3^2}{2\,g} \qquad (31)$$

from which it is seen that:

$$H_3 < H_1 \qquad (32)$$

It is not claimed that the preceding analysis is exact; it was put forward rather to show that a redistribution of energy at a side outlet is possible and that it could influence the results. Evidence that such a distribution takes place can be seen in the experimental results reported by Jaeger[6] for head loss coefficients at side outlets that, at certain combinations of flows, assume negative values indicating a gain of head.

Consideration of the possibility of the energy redistribution, together with possible errors introduced by the other assumptions given previously, leads to the conclusion that more experimental work is desired on the subject of head losses in pipes with varying discharge, before the results presented in the paper can be accepted as describing the actual conditions in such pipes.

ANNABEL L. TONG,[7] M. ASCE.—The author's methods in determining the friction losses in pipelines with service connections will give exact solutions for single pipelines of uniform size and constant coefficient of friction in the pipe. In Tables 2 and 3, equivalent discharges Q_e are given for ideal cases of inifinite and finite numbers of connections versus (q/Q_t) and also versus number of connections "n" for the case of finite number of connections. But, in actual practice, water network systems in service are mostly constructed of enclosed loops and sometimes combined with a number of dead end lines. It would be interesting to know to what extent the author's methods are applicable to a network system.

In order to make use of his tables, one may convert a single loop system consisting of one source of supply into a single line by taking an equivalent length L_e to represent the complete system as a unit. When the pipelines in one system were built at the same period in an area of similar environment, their physical condition would be assumed alike and a constant c value would

---

6 "Engineering Fluid Mechanics," by C. Jeager, Blackie & Son Ltd., London, England, 1956, pp. 477–480.

7 Hydr. and Structural Engr., Stearns and Wheler, Cazenovia, N. Y.

be used for the entire system with sufficiently good accuracy. With these simplifications, the author's tables can be readily applied to a simple loop system without much computation.

An example is shown in Fig. 9 to illustrate the degree of accuracy of his methods applied to the loop systems. A water distribution network of 12 pipelines, forming four enclosed loops is shown and the size and length of each line are marked in parenthesis adjacent to the line. A frictional coefficient C of 100 is assumed for the entire system. Seven service connections and the corresponding discharge rates are indicated in junction points B, C, D, E, G, H, and I. If a hydrant test flow of 300 gpm (Q_1) was make at junction F, and the

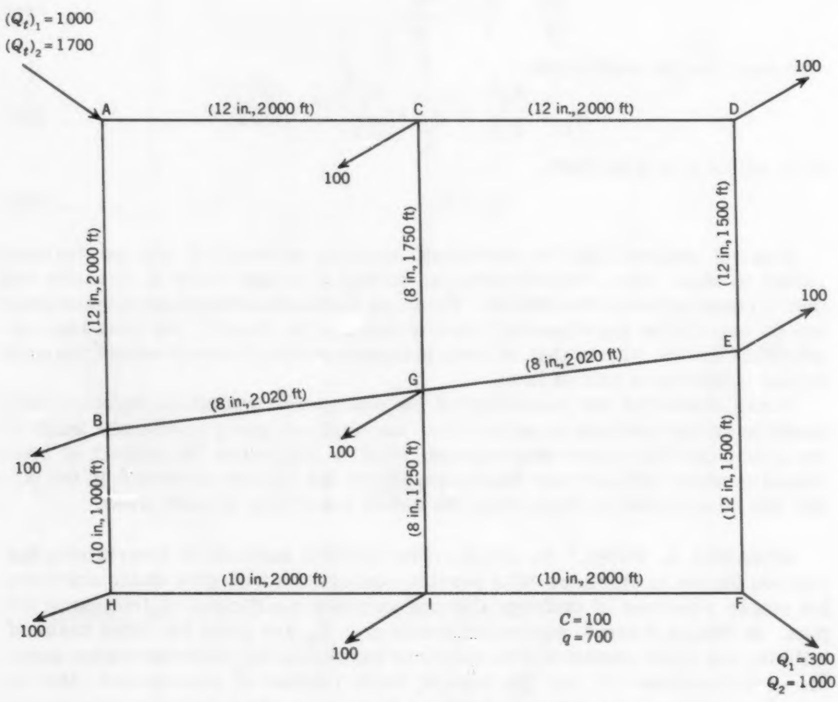

FIG. 9.—WATER DISTRIBUTION NETWORK

head loss (H_1) through the system during this flow is measured to be 4 ft, what will be the corresponding head loss (H_2) when the hydrant flow increases to 1000 gpm (Q_2)?

With the information obtained from the hydrant test the head loss (H_2) may be computed as follows:

Method 1.—The system is assumed to be a single line of infinite number of connections where q = 700 gpm and $(Q_t)_1$ = 1000 gpm. From Table 2, with q/Q_t = 0.7 and Q_e/Q_t = 0.676, one may find: $(Q_e)_1$ = 676 gpm. To determine L_e of the system, the Hazen-Williams formula in a simplified form, may be used.[8]

[8] "Nomograph For Equivalent Lengths of Water Pipelines," by Annabel L. Tong, Water and Sewage Works, February, 1960.

$$H = \frac{L_e Q_e^{1.85}}{119 \times 10^5} \qquad \text{. . . . . (33)}$$

where L_e is the length (in feet) of the equivalent pipe for the network. The unit for Q_e is gpm and the unit for H is linear feet.

Then

$$L_e = \frac{119 \times 10^5 \times 4}{(676)^{1.85}} = 280 \text{ ft}$$

When Q_t changes to 1700 gpm and q/Q_t to 0.41 from Table 2, $(Q_e)_2$ is computed as 0.087 × 1700 = 1370 gpm, and

$$H_2 = \frac{280 \times (1370)^{1.85}}{119 \times 10^5} = 14.8 \text{ ft}$$

Method 2.—If seven connections are assumed in the equivalent pipe, Table 3 can be used to compute Q_e. Using n = 7, q/Q_t = 0.7 then $(Q_e)_1$ = .734 × 1000 = 734 gpm. The equivalent length is computed as

$$L_e = \frac{119 \times 10^5 \times 4}{(734)^{1.85}} = 240 \text{ ft}$$

Similiarly $(Q_e)_2$ = .843 × 1700 gpm = 1430 gpm, and

$$H_2 = \frac{240 \times (1430)^{1.85}}{119 \times 10^5} = 13.7 \text{ ft}$$

Head loss H_2 is then computed by the Hardy Cross Distribution Method, the answer is found to be 14.0 ft. Using this value as a basis for comparison, the percentages of error from the preceding methods are approximately equal to +6% and -2%. If the number of service connections reduces to 3 by discharging 200 gpm at junctions H and D and 300 gpm at junction G only, the result by Method 1 is unchanged and by Method 2, H_2 equals to 13.0 ft. Again using the Hardy Cross Method, the head loss H_2 corresponding to 3 service connections is found to be 15 ft. The degrees of accuracy by Methods 1 and 2 are -2% and -15%. A change of location and rate of service discharges shall effect the value of the equivalent length for the system slightly, and subsequently shall effect the head loss under the same fire flow also. But both the methods are satisfactory to use for practical design problems.

For a complex system consisting of pumping facilities and two or more sources of water supply, the assumption of using an equivalent length to represent the system will not be correct, therefore, the above analysis should be limited to the simple networks only.

M. B. McPHERSON,[9] M. ASCE AND J. V. RADZIUL.[10]—Before commencing a discussion on the analyses presented in the paper, consideration of some overall design factors is necessary to place the limited scope of the subject in perspective.

In United States metropolitan municipal water works, it is common practice to supply the distribution system, or separated service districts, via an arte-

[9] Prof. of Hydr. Engrg., Civ. Engrg. Dept., Univ. of Illinois, Urbana, Ill.
[10] Water Distribution Design Engr., Water Dept., Philadelphia, Pa.

rial (or feeder) network. The smaller-pipe grid network is connected to the arterial system at relatively few points (about 1000-1500 ft apart). In a strong system a greater number of grid connections is not necessary while a minimum number is desireable to facilitate operations. Service connections into any arterial main grossly complicate operation, and are seldom tolerated. Service connections are normally made into grid mains. In small systems or districts, the arterial system and grid system are often inseparable or indistinguishable. Analysis of large systems is normally concentrated on the arterial network. Some of the major design considerations for arterial network analysis have been presented previously.[11,12] The author's paper is concerned principally with grid "water mains." In closing, the author states that his procedures are "particularly suitable for use in network analysis... ." While some of his procedures might be adapted to the skeletonizing of a grid network, they have no place in arterial network analyses.

Only the more progressive water works maintain a program of field measurements of pipe friction loss coefficients. Usually time and fund limitations restrict measurement programs to the arterial network; only scattered samplings of grid network mains can be made. In the city of Philadelphia, for example, there are over 2,600 miles of mains equal to or smaller than 12-in dia, but only about 360 miles of mains larger than 12-in. With few exceptions, the arterial mains are larger than 12-in. The author refers to the head loss "which actually exists" as a point of reference in defining a "range of error." It is seldom that a head loss coefficient is known to any resonable degree of exactitude for the grid mains with which the paper deals. In fact, one might ask how a flow test can be performed properly in the presence of active service connections.

Let m represent the power to which the flow rate is raised to compute head loss. The author has assumed m = 1.85 throughout his paper. Arguments advanced for the use of m = 2.00 for "old" pipes in arterial networks are not necessarily sound.[12] With the little information normally available on grid mains it would seem quixotic to argue whether m = 1.85 is more suitable than 2.00 for grid mains, and this discussion includes both powers in relations to be presented. For the low Reynolds numbers characterizing many grid mains, use of either 1.85 or 2.00 and assuming constancy of friction coefficient, regardless of Reynolds number magnitude and variation, are both unrealistic. Further, there are more local losses (fittings, valves, and specials) in grid mains than in arterial. Field flow coefficient values for arterial mains include the influence of all local losses over the reach of measurement. Although local losses in grid mains may be neglected, as in the paper, the consequent exactitude of the results is even further diminished.

While the paper implies that grid design is based on domestic demands, in the United States, fire flow requirements are often more severe. It is also implied that the local domestic demands, q, are known as a precise fraction of the imput to the local main, Q_t, which is not likely.

Retiring from the preceding reservations, the remainder of this discussion will be directed towards the development of the equations in the paper. As in the paper, a constant pipe coefficient (embodying friction coefficient and diameter) and equally spaced, equal-valued drawoffs will be assumed.

---

11 "Generalized Distribution Network Head Loss Characteristics," by M. B. McPherson, Proceedings, ASCE, Vol. 86, No. HY 1, January, 1960.

12 Discussion of "Relationships Between Pipe Resistance Formulas," by M. B. McPherson, Proceedings, ASCE, Vol. 86, No. HY 9, September, 1959, pp. 143-155.

The development of the equivalent of Eq. 9, has appeared in perhaps a dozen American hydraulics and fluid mechanics texts, but not in such general terms. One of the earlier presentations was by Dougherty.[13] Fair and Geyer[14] have used the same principle in describing the hydraulic losses in filter underdrain manifolds. These two references use m = 2.00. The author refers to the development of Eq. 9 as being for an "infinite number of connections" which is identical with the idealized uniformly decreasing flow (or velocity) assumed[13,14] along with constant diameter and friction coefficient. When the flow into the service connections is large and the number of services are few (for example, n less than 10, q/Q_t more than one-half), performance is more complex. It cannot be described properly by means of the simple pipe friction relations to which the paper is restricted because the hydraulic behavior of a manifold system[15] is being approached. It is not clear why the series comprising Eqs. 4 and 5 were introduced because Eqs. 1 and 6 are readily integrable, as shown in Eqs. 7 and 8.

In the section on a "finite number of connections" (n), there are typographical omissions and an error in Eq. 12. Eq. 12 has been corrected and expressed in terms of K' in Eq. 34.

$$K' = \frac{1}{n} \sum_{i=0}^{n-1} \left[1 - \frac{i\,q}{Q_t\, n} \right]^{1.85} \quad \ldots\ldots\ldots\ldots\ldots \quad (34)$$

Referring to the definition sketch of Fig. 10(a) it will be noted that for an idealized case the number of pipe lengths between cross-mains must be one plus the number of service locations (two services served at each location; there are thus six service locations in Fig. 10(a)). In Fig. 3 the author has either one too many connections or one too few pipe lengths. Eqs 10 through 14 and much of the remainder of the paper are based upon this error. Letting the number of service locations be n' (that is a differentiation from n of the paper), the corrected, general expression for K is given by Eq. 35.

$$K' = \frac{1}{n' + 1} \sum_{i=0}^{n'} \left[1 - \frac{i\,q}{Q_t\, n'} \right] \quad \ldots\ldots\ldots\ldots\ldots \quad (35)$$

Table 9(a) lists values of K' for Eq. 35 using n' and m = 1.85. Eq. 9 was, therefore, used for an infinite n'. Curves which should replace those in Fig. 6 are given in Fig. 10(b). It should be noted that for a realistic number of service locations, K' is practically constant, as opposed to the large variation indicated in Fig. 6 or Table 4. The most divergent case is for a q/Q_t of one, which would be for a dead-end main or a main in which flow was supplied from both ends. Eq. 35 is not proper for this case because one too many lengths would be used—this is the only instance in which Fig. 3 and Eq. 34, would apply.

---

13 "Hydraulics," by R. L. Dougherty, McGraw-Hill Book Co., Inc., New York, N. Y., 1950, pp. 244-245.

14 "Water Supply and Waste-Water Disposal," by G. M. Fair and J. C. Geyer, John Wiley and Sons, New York, N. Y., 1956, p. 687.

15 "Engineering Hydraulics," Hunter Rouse, ed., John Wiley and Sons, New York, N. Y., 1950, p. 436.

Values from Eq. 35 for m = 2.00 appear in Table 9(b) for comparison. Note that there is little difference in the values of K' from those in Table 9(a) for an m of 1.85. For m = 2.00 Eq. 9 becomes Eq. 36.

$$K' = \frac{1}{3\,q/Q_t}\left(1 - \left(1 - \frac{q}{Q_t}\right)\right)^3 \quad \ldots\ldots\ldots\ldots\ldots (36)$$

The most partinent section of the paper deals with the "ratio removed at the beginning of the line," r. Eq. 19 is not affected by the error in the development of Eq. 34, and has been expressed in terms of K' in Eq. 37.

$$r = \frac{1 - (K')^{0.54}}{q/Q_t} \quad \ldots\ldots\ldots\ldots\ldots (37)$$

Eq. 38 is for the case where m = 2.00.

$$r = \frac{1 - \sqrt{K'}}{q/Q_t} \quad \ldots\ldots\ldots\ldots\ldots (38)$$

Values of r for Eq. 37 using K from Table 9(a) appear in Table 10(a) and from Table 9(b). While the author's error leads to a large dependence of r on n,

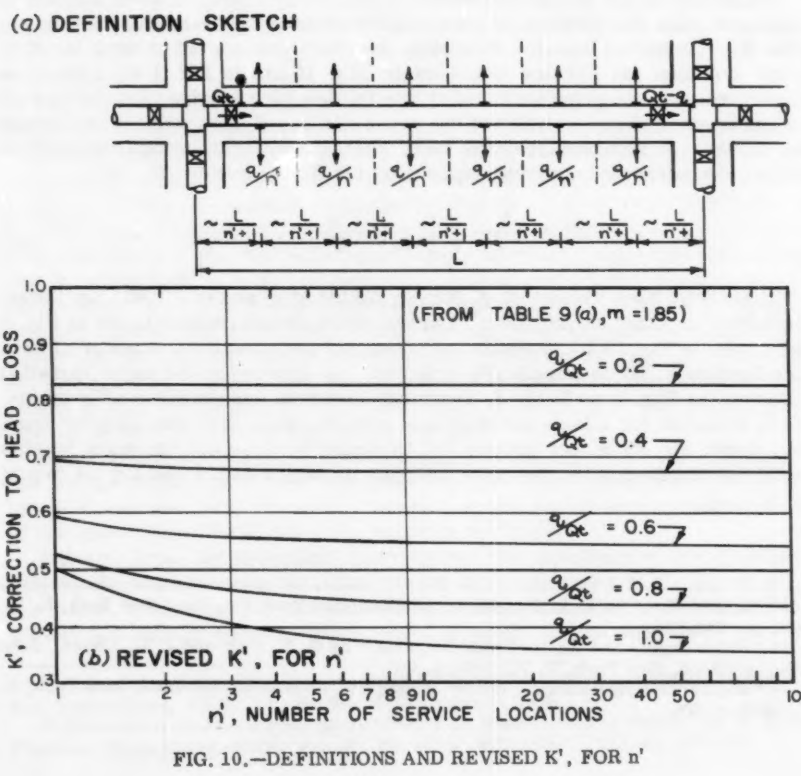

FIG. 10.—DEFINITIONS AND REVISED K', FOR n'

Fig. 7 and Table 8, the values of r in Tables 10(a) and 10(b) indicate an approximate value of about 45% for most of the realistic combinations. The author says that "European practice has been to assume...45%...", which appears reasonable. On the few occasions in which this type of problem has arisen, the writers have used a 50-50 division, partly to allow for flow from either direction but mostly because further refinement could not be justified. This practice, to the best knowledge of the writers, is common in water and gas works practice; the writers are not aware of any utility where "a single quantity at the end of the line" is used.

The assumptions leading to Eq. 35 are little better than those leading to Eq. 34. In Fig. 10(a), it may be seen that the assumption of equally spaced loads involves a series of premises: building lots must be equal in frontage, services must be located in the center of each lot, distance from center of side street to property line of corner lot must equal spacing of services, or lot frontage. In the opinion of the writers these are negligible assumptions compared with the assumption that the design peak q, equally distributed among

TABLE 9.—VARIATION OF K' FOR EQ. 35 VERSUS NUMBER OF LOCATIONS n'.

n', No. of Locations	Ratio of Quantity Withdrawn (q) to Total Inlet Flow (Q_t)					
	0.0	0.2	0.4	0.6	0.8	1.0
(a) m = 1.85						
1	1.000	0.831	0.694	0.592	0.526	0.500
3	1.000	0.828	0.680	0.558	0.464	0.404
9	1.000	0.826	0.675	0.548	0.442	0.368
∞[a]	1.000	0.826	0.673	0.541	0.434	0.351
(b) m = 2.00						
1	1.000	0.820	0.680	0.580	0.520	0.500
3	1.000	0.816	0.662	0.540	0.449	0.390
9	1.000	0.814	0.656	0.527	0.425	0.352
∞[b]	1.000	0.813	0.653	0.520	0.414	0.333

[a] Via Eq. 9. [b] Via Eq. 36.

services in the bargain, is known to an exactness consistent with the numerical values which issue from its use.

If elegance is desired, a paper by Brown and Markel[16] should be consulted. They have mathematically treated the case of varying diameter, varying flow coefficient, unequal service flows, unequal lengths between services, illustrated for an m of both 1.85 and 2.00. Their development leads to a two-load equivalent. The only assumption for an m of 1.85 is "that the sum of a MacLaurin's series (of a specified form) can be nearly approximated by the sum of the first three terms of the series." No assumptions are involved for an m of 2.00. Further, their development leads to a pair of equivalent loads which give identical losses regardless of direction of flow from one end or the other. Of the several discussions of their paper, the one by Malcolm S. McIlroy, inventor of

16 "A Fluid Network Reduction Method for Accurate Representation of the Nonlinear Characteristics," by Wilmer T. Brown and Robert A. Markel, AIEE Miscellaneous Paper 52-334, September, 1952 (Presented at Toledo Meeting, October, 1952).

the McIlroy Network Analyzer, is germane to this discussion. Because his discussion is not generally available, it is reproduced here without deletion or change:

"The authors are to be congratulated for deriving the method presented in the subject paper and for conceiving that it might exist. The method should often permit studies of pipeline networks to be carried out accurately on linear or non-linear electric calculating boards that would otherwise have inadequate capacity, and it should be generally helpful in studies conducted on paper. The opportunity of representing all the loads and pipeline sections between two adjacent network junctions by means of two pipeline elements, one intermediate load, and one terminal load is a very significant contribution to the art of pipeline-network analysis.

"The suitability of the method for flow in either direction, subject to the stated limitations, and for exponents of any value encountered in fluid-flow problems, gives it wide usefulness.

"In some studies of pipeline networks, exact values cannot be assigned to loads at definite locations along the pipelines. In these instances, the assumption is often made that the total load delivered to

TABLE 10.—VALUES OF r

n', No. of Locations	Ratio of Quantity Withdrawn (q) to Total Inlet Flow (Qt)				
	0.2	0.4	0.6	0.8	1.0
(a) Via Eq. 37 using K' from Table 9 (a), m = 1.85					
1	0.475	0.448	0.412	0.365	0.312
3	0.485	0.470	0.448	0.424	0.386
9	0.490	0.478	0.462	0.445	0.417
∞	0.490	0.482	0.470	0.456	0.432
(b) Via Eq. 38 using K' from Table 9 (b), m = 2.00					
1	0.470	0.438	0.397	0.348	0.293
3	0.485	0.468	0.440	0.412	0.376
9	0.490	0.475	0.457	0.435	0.406
∞	0.490	0.480	0.463	0.446	0.422

users along the pipeline is uniformly distributed between network junctions and may be represented by two half loads at the ends of the section. This rough equivalence is false, as the authors point out, but under many common operating conditions causes an error no greater than that inherent in the nature of known data. The error is not significant whenever the flow delivered to other network elements at the downstream terminal of the pipeline equals or exceeds the total load distributed along it. Wherever reasonable doubt exists regarding the ratio of distributed load to terminal load, or wherever definite values are known for loads at specific locations along a pipeline, the authors' method is a powerful and accurate tool for reducing the number of quantities to be considered in an analysis. The procedure is a technical contribution of lasting value."

While some of McIlroy's statements would appear to refute several arguments in the present discussion, it should be noted that the development by

Brown and Markel was phrased in terms of gas network analysis. The magnitudes and variation in local gas loads are normally known to a much closer tolerance than with water services (namely, the major share of the design load often comprises the winter heating load which fluctuates rather predictably with temperature). McIlroy's discussion was, therefore, directed principally towards gas applications.

In summary, the common practice of splitting the service connection loads evenly between the two ends of a grid main is entirely consistent with the degree of accuracy to which other hydraulic factors can be evaluated. If grid main connections to an arterial network cannot be consolidated in an obvious and equitable manner, the procedure developed by Brown and Markel is preferred, but can be applied only between arterial main junctions.

Some of the major design considerations for grid mains and networks in modern residential developments have been reviewed by the writers.[17]

In Fig. 2, the term Q_e is incorrect; perhaps Q_x was intended.

K. M. YAO.[18]—The arrangement of service connections as shown in Fig. 3 is a bit different from the actual pictures. Usually, pipelines in a pipenet run from one street intersection to another and it is unlikely to have service connection at both ends with possible exception of dead end lines, generally not considered in pipenet analysis. Therefore, one service connection on the pipeline would mean a service connection at the midpoint of the line instead of at the end of the line as assumed by the author. If this is the case, Eq. 10 will be:

$$h_f = K\left[\frac{L}{n+1}\left(Q_t\right)^{1.85} + \frac{L}{n+1}\left(Q_t - \frac{q}{n}\right)^{1.85} + \ldots\ldots + \frac{L}{n+1}\left(Q_t - \frac{n\,q}{n}\right)^{1.85}\right] \quad \ldots\ldots(39)$$

and Eq. 12 will be:

$$h_f = \frac{K\,L}{n+1}\,Q_t^{1.85}\sum_{i=o}^{i=n}\left[1 - \frac{i\,q}{Q_t\,n}\right]^{1.85} \quad \ldots\ldots\ldots\ldots\ldots(40)$$

17 "Distribution Design Considerations," by M. B. McPherson and J. V. Radziul, Journal, AWWA, Vol. 51, April, 1959, pp. 489-502.

18 Lecturer, Civ. Engrg., Univ. of Canterbury, Christchurch, New Zealand.

SEDIMENT PROBLEMS OF THE LOWER COLORADO RIVER[a]

Discussion by T. Blench

T. BLENCH,[14] F. ASCE.—It is suspected that the authors, like the writer, acquired most of their knowledge of river behavior without the aid of formal instruction, for the simple reason that, even now, practically no colleges provide any for engineers. Accordingly, it is hoped that they will not misunderstand when the writer expresses the opinion that the knowledge required to forsee and arrange for the general trend of the events they have described existed before Hoover and Parker Dams were built, but was not available to civil engineers generally; and he hopes they will agree with him that the absence from North American college curricula of some form of instruction on regime behavior of rivers and canals is as deplorable as would be the absence of soil mechanics. Actually, there is a little college activity in the matter already. The University of Alberta has given river and canal instruction at postgraduate level since 1949, and is now (1960) introducing it in the Hydraulics, Soils, and Municipal Engineering options at undergraduate level. The University of Saskatchewan has introduced a postgraduate course. The writer is aware of a few colleges in the United States that have given postgraduate instruction for some time. A Canadian of Indian extraction "drew attention to the value of teaching river and canal engineering, as is done in India, and . . . recommended . . . in the July issue of the Engineering Institute of Canada Journal" at the 1959 Congress of the International Association for Hydraulic Research.

That article[15] is relevant to the present paper because it (1) gives six hypothetical typical situations in which civil engineers could make major errors (including lack of foresight), because they lack the knowledge of specialized colleagues and geologists, (2) draws attention to official figures of the cost of sedimentation troubles in the United States, (3) discusses the magnitude of errors that can be made with the aid of modern construction equipment, (4) gives the opinion that "ignorance of river behavior is not universal; the trouble is that it is the prerogative of the civil engineers who build and plan water projects," (5) argues that the only effective method of removing this ignorance is to "offer civil engineering students the opportunity to study appropriately designed courses in river engineering, just as they now study soil mechanics," (6) discusses the need for suitable textbooks and refers to the writer's own,[16] (7) emphasizes that the geologic nature of river phenomena prevents any single

---

[a] April, 1960, by Whitney M. Borland and Carl R. Miller.

[14] Prof., Civ. Engrg., Univ. of Alberta, and Pres., T. Blench and Assoc. Ltd., Cons. Hydr. Engrs., Alberta, Canada.

[15] "River Engineering as a College Course for Civil Engineers," by T. Blench, Engineering Institute of Canada Journal, July, 1959.

[16] "Regime Behavior of Canals and Rivers," by T. Blench, Butterworth's Scientific Publications, London, England and Toronto, Canada, 1957.

person from acquiring expertness in terms of nothing but the experiences of his own short life, and (8) discusses the feasibility of college instruction.

The paper necessarily condenses theory and the authors' extensive field information without which, of course, even the most satisfying theory cannot be applied satisfactorily. The writer, therefore, would appreciate further elucidation of the following points:

1. In view of the facts that (a) Fig. 5 shows the bed material (median size about 0.3 mm) to follow closely the logarithmic Gaussian distribution of particle size that sedimentary petrologists seem to have found general for sandy sediments,[17] and that the writer himself has found in river bed sands;[18] and (b) the bed material is following this distribution even after several years of retrogression has occurred, what is the factual or theoretical justification for believing differentiation will now occur as implied in the statement "It was determined that bed stability would occur when a 6-in. armor layer of 4 to 10 mm material was obtained." Also, assuming that this differentiation of coarse material is possible, in general, can a computation and description of transport mechanism be produced to show how 6 in. of it could differentiate out of the particular sand in the depth estimated as yet to be degraded? Does the All-American canal show such differentiation, and is its behavior relevant?

2. How were channel widths found in Fig. 7 from Leopold and Maddock's work[7] when they did not propose any design formulas there, but instead recorded relationships with very different constants found for very different rivers whose bed-material sizes were generally not observed? How were widths found by any of the methods when none of them concerned erodibility of banks? Why is the width for Q = 15,000 cfs and 0.3 mm material about 2,500 ft when the All-American Canal and a figure shown elsewhere[19] for 20,000 cfs in the river at Yuma show that nature is satisfied with about 450 ft?

3. Why was canalization adopted as a solution to the difficulties in degrading reaches when the effect of straightening a meandering channel is to reduce its regime slope radically and shorten its length, thereby causing it to degrade more?

4. Is the canalized channel expected to meander? If so, what amount of stone protection is foreseen for the sides?

5. Is the proposed section in Fig. 9 related to the channel dimensions observed by Leopold and Wolman[19] to have developed at Yuma since about 1940? Their work seems to show that the channel is incised at discharges as high as 20,000 cfs and had acquired, for that discharge, a breadth of about 450 ft from 1940 to 1950, and a somewhat fluctuating depth that changed from 11 ft in 1940, to 13.5 ft in 1943, and back to about 10.5 ft in 1949.

6. Considering that the section just mentioned is for an appreciable bed-load, obtained by dumping the total sediment of the All-American Canal into the river (whose discharge is probably less than that of the canal), would the section needed for vanishing bed-load not be considerably narrower and deeper?

7. By what computations was "dominant discharge" decided?

---

17 "Size Frequency Distribution of Sediments and the Normal phi Curve," by W. C. Krumbein, Journal of Sedimentary Petrology 8, 1938, pp. 84-90.

18 "Normal Size Distribution Found in Samples of River-bed Sand," by T. Blench, Civil Engineering, February, 1952. (Answers to discussion, February, 1953).

19 "The Hydraulic Geometry of Stream Channels and Some Physiographic Implications, by Luna B. Leopold and Thomas Maddock, Jr., Geological Survey, Professional Paper 252, 1953, Fig. 28.

8. Do the authors attribute any significance to the following results from regime theory[16] taking a bed factor 1.05 for 0.3 mm sand with vanishingly small charge, and a side-factor of 0.20 for moderately cohesive sides:

(a) Regime slope of straight canal of 15,000 cfs = 1/11,000. (So regime slope of meandering canal approximately = 1/5,500.)
(b) Regime breadth for 20,000 cfs = 310 ft
(c) Regime depth for 20,000 cfs = 16 ft

Note that slope is very insensitive to discharge and side factor but roughly proportional to bed-factor. Breadth varies as the square root of the bed-factor divided by the side-factor, and depth as the cube root of side-factor and inversely as the 2/3 power of bed-factor, so b and c are not intended to be more than a guide.

9. Why was the problem not solved by model originally? The reasons favoring a model include (a) there would be no bed-load injection, (b) field data of every kind are available, or easy to collect, (c) models using natural bed-sand have been used satisfactorily for decades in India, and (d) regime theory provides the means for scaling such models rapidly. (e) Friedkin[20] demonstrated at the U.S. Waterways Experiments Station that the meandering of rivers, including degradation and aggradation, could be reproduced qualitatively using even artificial sediment. (f) Leopold has reproduced the details of braiding by using a model with suitably chosen sand.[21] The conditions seem remarkably favorable for a quick accurate model solution, provided regime principles were used to eliminate unnecessary trial-and-error with scales.

In the present state of river engineering, the writer feels that the publication of quantitative field information in accessible and discussable form is of high value, and he congratulates the authors on presenting so much information on a major project within the space available for a single paper.

---

20 "A Laboratory Study of the Meandering of Alluvial Rivers," by J. F. Friedkin, U. S. Waterways Experiment Station, Vicksburg, Miss., 1945.

21 "River Channel Patterns; Braided, Meandering and Straight," by Luna B. Leopold and M. Gordon Wolman, U.S.G.S. Professional Paper 282-B, 1957.

[illegible]

[illegible]

[illegible]

[illegible]

[illegible]

[illegible]

TOLKMITT'S BACKWATER AND DROPDOWN CURVE TABLES[a]

Discussion by Praxitelis A. Argyropoulos

PRAXITELIS A. ARGYROPOULOS,[21] F. ASCE.—The writer will comment on the formulas and tables by G. Tolkmitt for the computation in the actual practice of backwater and dropdown curves and to give practical and theoretical supplementary information on this method.

The Tolkmitt's method is well known in many countries of Europe as well as in Greece. On the other hand, the Tolmitt's formulas and tables for the uniform prismatic channel of broad parabolic cross section form are not only found in the German texts.[22]

It is very usual and important in Hydraulic Engineering to determine the stage at which, in a given artificial or natural channel, the flow takes place. On the other hand, it is well known that when a certain point of the channel is obstructed by a dam, sluice gates, weir, or other construction the raising of the latter will cause the water to set back up the stream. In this case, the water depth is increasing, and a new surface is formed.

Usually, in the case of a backwater curve, two questions arise: how much the water is raising at a given distance upstream from the point of obstruction and what is the distance for which the influence of the curve is felt. The questions, in the case of dropdown curve, are analogous.

Formulas, based on the assumption of channels possessing regularity in shape of cross section and having a uniform and constant bed slope, have been formulated. Also, in these formulas the roughness of the lining is assumed to remain constant. On the other hand, to facilitate the practical computations, tables were prepared.

Generally, in the case of a prismatic channel, the methods of computing backwater and dropdown curves can be divided into the following categories:

a. Analytical methods;
b. Graphical or semigraphical methods; and
c. Methods by nomograph.

The methods of Rühmann, Bresse Schaffernak, Tolkmitt, Bakmeteff, Dupuit, Jansen, Chow, Von Seggern,[23] Mononobe,[24] Ming Lee,[25] and Francesco

[a] May, 1960, by R. D. Goodrich.

[21] Dr. of Civ. Engrg., Special Scientific Researcher, Athens, Greece.

[22] "Hydraulics," by P. A. Argyropoulos, Ed. of the Technical Chamber of Greece, 1951, pp. 354-361.

[23] "Integrating the Equation of Non-Uniform Flow," by M. E. Von Seggern, Proceedings, ASCE, Vol. 75, No. IR 1, January, 1949.

[24] "Backwater and Dropdown Curves for Uniform Channels," by Nagaho Mononobe, Transactions, ASCE, Vol. 103, 1938.

[25] "Steady Gradually Varied Flow in Uniform Channels on Mild Slopes," Univ. of Illinois, Urbana, Ill.

Ramponi,[26] are noted. The method of Flavio Scano[27] and Escoffier-Raytchine-Chatelain[28] are graphical methods, while the Silber's method[29] is a method using a nomograph.

On the other hand, in the case of an irregular natural stream with varying slopes of bed and different cross sections along its length, the solution of the problem of backwater and dropdown curves is more difficult and delicate. In this case, except for the tedious trial methods, there are the Krivoshein method,[30] the Grimm[31] method, the Erza method, a simple method of the writer,[32] the Leach diagram[33] method and others.

Also, the methods for computing backwater and dropdown curves for the artificial channels of trapezoidal, parabolic, and other cross-sectional forms can be divided in two categories whether the effect of the change in kinetic energy owing the accelerated or delated flow of water is considered or not. Therefore, the methods of Bresse, Struckel, Kozény, and others consider the effect of velocity-head $V^2/2g$ (in which, V is the mean velocity of flow and g the gravitational acceleration) whereas, the Tolkmitt's method, the Rühmann's, the Schaffernak's method, and others, do not consider it.

Tolkmitt, who was particularly interested in natural watercourses, assumed in his method a constant value of friction factor C throughout the whole range of depths. Tolkmitt chose as an "idealized" profile, a parabolic channel (Fig. 3). Let T_o be the top width and A_o the cross sectional area.

The raising z the width T_o will be

$$T = T_o\sqrt{\frac{d+z}{d}} \quad \ldots\ldots\ldots\ldots\ldots\ldots \quad (17)$$

and the wetted area:

$$A = \frac{2}{3}\,T\,(d+z) = \frac{2}{3}\,T_o\sqrt{\frac{d+z}{d}}\,(d+z) \quad \ldots\ldots\ldots \quad (18)$$

On the other hand, the hydraulic radius:

$$R = \frac{A}{P} = \frac{2/3\,T\,(d+z)}{T} = \frac{2}{3}\,(d+z) \quad \ldots\ldots\ldots\ldots \quad (19)$$

---

26 "Determination approchée de la grandeur du remous dans les canaux rectangulaires à faible pente," Energie Electrice, December, 1951.

27 "Procédé graphique rapide pout tracer la courbe de remous de l'ecoulement permenent dans les canaux prismatiques," Energie Electrice, July, 1952.

28 "Determination graphique de la ligne d'eau et calcul des remous," La Houille Blanche, No. 3, 1950.

29 "Etude et tracé des ecoulements permenents en canaux et rivières," Ed., Dunod, Paris, France, 1954.

30 "Méthode naturelle de calcul des courbes de remous," Rev. Universidad, National de Plata, December, 1951.

31 "Blackwater Slopes Above Dams," Engineering-News Record, Vol. 100, 1928.

32 "Computation of the Backwater and Dropdown Curves in Natural Streams," Technical Records, Technical Chamber of Greece, No. 401-402, 1957.

33 "New Methods of the Solution of Backwater Problems," Engineering-News Records, Vol. 82, 1919.

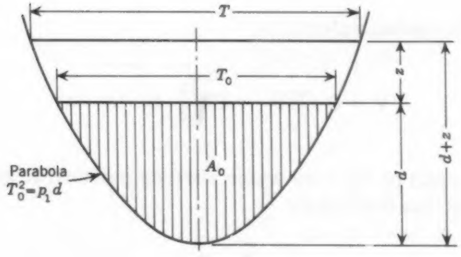

FIG. 3

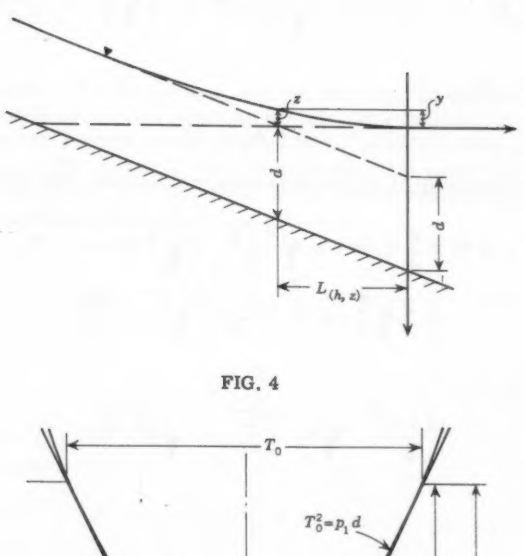

FIG. 4

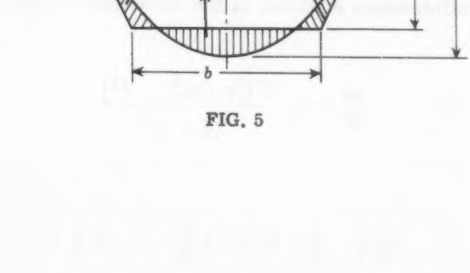

FIG. 5

where, $P = \sim T = T_o \sqrt{\frac{d+z}{d}}$, is the wetted perimeter.

In this case, the mean velocity

$$V = C\sqrt{RS} = C\sqrt{\frac{2}{3}(d+z) \quad S} \quad \ldots\ldots\ldots\ldots \quad (20)$$

in which, S is the fall of the free water surface per unit length.
On the other hand, the discharge:

$$Q = A \; V = \frac{2}{3}\sqrt{\frac{2}{3}} \; C \; T_o \; \frac{(d+z)^2}{\sqrt{d}} \; \sqrt{S} \quad \ldots\ldots\ldots\ldots (21)$$

Before the raising of the water (owing the obstruction), the discharge

$$Q_o = A_o \; V_o = \frac{2}{3} \; T_o \; d \; C\sqrt{\frac{2}{3} \; d \; S} = - \frac{2}{3}\sqrt{\frac{2}{3}} \; T_o \; d^{3/2} \; C \; \sqrt{S} \; \ldots (22)$$

But (from Fig. 4)

$$S = S_o - \frac{dz}{dx} \quad \ldots\ldots\ldots\ldots\ldots\ldots \quad (23)$$

if, S_o is the longitudinal slope of the channel bottom. The discharge will be:

$$Q = A \; V = \frac{2}{3} \; T \; (d+z)\sqrt{\frac{d+z}{d}} \quad C\sqrt{\frac{2}{3}(d+z) \quad \left(S_o - \frac{dz}{dx}\right)}$$

$$= \frac{2}{3}\sqrt{\frac{2}{3}} \; C \; T_o \; \frac{(d+z)^2}{d}\sqrt{S_o - \frac{dz}{dx}} \quad \ldots\ldots\ldots\ldots (24)$$

But, as $Q=Q_o$,

$$\frac{(d+z)^2}{\sqrt{d}} \quad \sqrt{S_o - \frac{dz}{dx}} = \sqrt{d^3 \quad S_o} \quad \ldots\ldots\ldots\ldots \quad (25)$$

or,

$$\frac{(d+z)^4}{d}\left(S_o - \frac{dz}{dx}\right) = d^3 \quad S_o \quad \ldots\ldots\ldots\ldots\ldots (26)$$

The general differential equation of the backwater curve is:

$$\frac{dz}{dx} = S_o \quad \frac{\left[(d+z)^4 - d^4\right]}{(d+z)^4} \quad \ldots\ldots\ldots\ldots\ldots \quad (27)$$

Eq. 27 may take the form

$$S_o\ dx = \left[1 + \frac{d^4}{(d+z)^4 - d^4}\right] dz \quad \ldots\ldots\ldots\ldots (28)$$

or

$$S_o\ dx = \left[1 - \frac{d}{4}\left(\frac{1}{z+2\ d} - \frac{1}{z} + \frac{2\ d}{(2+d)^2 + d^2}\right)\right] dz \quad \ldots\ldots (29)$$

The integration of Eq. 29 leads to Eq. 1. the procedure to find the formula for the dropdown curve, whose correct writing is:

$$L_{(h,z)} = \frac{d}{S_o}\left[f\left(\frac{d-z}{d}\right) - f\left(\frac{d-h}{d}\right)\right]\left(1 - S_o\ \frac{C^2}{g}\right) - \left(\frac{h-2}{S_o}\right) \quad \ldots (30)$$

is analogous.

In actual practice, the Tolkmitt's method can also be applied in the case of artificial channels or natural streams having other than parabolic form. In this case, the cross section of the channel must be deformated in equivalent parabolic profile of the same to the given channel top width T_o (Fig. 5) and cross sectional area A_o. For instance, if the given channel is of a regular trapezoidal cross section (Fig. 5),

$$A_o = \frac{T_o + b}{2}\ t_o = \frac{2}{3}\ T_o\ d \quad \ldots\ldots\ldots\ldots (31)$$

or

$$d = \frac{3}{2}\,\frac{A_o}{T_o} \quad \ldots\ldots\ldots\ldots (32)$$

On the other hand,

$$A = \frac{T+b}{2}\ t = \frac{2}{3}\ T\ (d+z) \quad \ldots\ldots\ldots\ldots (33)$$

That is,

$$(d+z) = \frac{3}{2}\,\frac{A}{T} \quad \ldots\ldots\ldots\ldots (34)$$

Also

$$T_o = \sqrt{p\ d} \quad \ldots\ldots\ldots\ldots (35)$$

and,

$$A_o = \frac{2}{3}\ T_o\ d = \frac{2}{3}\ d\ \sqrt{p\ d} = \frac{2}{3}\ \sqrt{p\ d^3} \quad \ldots\ldots\ldots\ldots (36)$$

in which

$$p = \frac{T_o^2}{d} = \frac{2}{3} \frac{T_o^3}{A_o} \quad \dots\dots\dots\dots\dots\dots \quad (37)$$

Example 1.—A rectangular channel, 98 ft wide and 4.6 ft in depth, has a slope of 1 in 2,000 (= .0005). The discharge is 1,483 cfs. By constructing a weir, the original water level has been raised 2.6 ft. Estimate (by the Tolkmitt's method): (1) at which distance upstream from the point of the obstruction the water is raised 7 ft, and (2) what is the total length of the backwater curve?

The depth of the equivalent parabola will be,

$$d = \frac{3}{2} \frac{A_o}{B_o} = \frac{3}{2} t = \frac{3}{2} 4.6 = 6.9 \text{ ft}$$

$$d + h = 6{,}9 + 2{,}6 = 9.5 \text{ ft and, } d + z = 6{,}9 + 1{,}0 = 7{,}9 \text{ ft}$$

$$\frac{d+h}{d} = \frac{9{,}5}{6{,}9} = 1{,}38 \text{ and, } \frac{d+z}{d} = \frac{7{,}9}{6{,}9} = 1.14$$

From the Tolkmitt's table, for $\frac{d+h}{d} = 1{,}38$ $f\left(\frac{d+h}{d}\right) = f(X) = 1{,}235$

when, $f\left(\frac{d+z}{d}\right) = f(1{,}14) = 0.818$

So,

$$L_{(h,z)} = \frac{6{,}9}{.0005} (1{,}235 - 0.818) = 5{,}755 \text{ ft}$$

On the other hand, as

$$f\left(\frac{d+z}{d}\right) = f\left(\frac{6{,}9 + 007}{6{,}9}\right) = f(1{,}001) = -\ 0{,}507$$

and,

$$L_{(h,z)} = \frac{6{,}9}{.0005} (1{,}235 + .507) = 24{,}040 \text{ ft}$$

Summarizing the present discussion, we note that, in Europe, the Tolkmitt's method for computation of backwater and dropdown curves, is considered valuable and satisfactory. European engineers feel a special confidence in this method. By Goodrich's paper, the Tolkmitt's formulas and tables, slightly enlarged by the addition of twenty items in each table (thus in many cases obtaining intermediate values by interpolation will be avoided), will be available to American engineers.

HOOD INLETS FOR CLOSED CONDUIT SPILLAYS[a]

Discussion by Bernard L. Golding

BERNARD L. GOLDING,[11] M. ASCE.— Mr. Blaisdell and the engineers of the Agricultural Research Service are to be congratulated for recognizing the potentialities of, and fully developing, the hood inlet culvert discovered by Karr and Clayton at Oregon State College, in 1954.

In the writer's opinion, the very simple hood inlet is the answer to the problem of making culverts on steep (supercritical) slopes flow full (prime). This could result in the saving of many dollars on the cost of culverts of the yet-to-be built portions of the Federal Interstate Highway System as well as other highways. It is the intention of the writer to discuss this paper as far as its application to the design of culverts under highway fills.

In the determination of a culvert size under a highway fill, the headwater depth upstream from the culvert entrance and the exit velocity of the flow from the culvert are the two principal factors that must be considered. The headwater depth upstream from the culvert entrance must be limited so that extensive flooding of upstream property does not occur. The exit velocity of flow must not be so great as to cause excessive scour of the stream bed and banks which could conceivably cause a washout of the highway embankment.

Generally, up to the present time, engineers in the writer's office have felt obligated to assume that a culvert would not flow full (an entrance control or orifice condition existed) in computing the headwater depth caused by culverts on hydraulically steep (supercritical) slopes, even though the normal depth of flow in the culvert was "greater" than the height of the culvert, and the actual headwater depth was greater than 1.5 times the height of the culvert. This design assumption was based on the many observations and reports of others as well as our own field and laboratory observations.

Making the assumption that the culvert would not flow full, resulted in the headwater depth being greater than that which would have occurred if the same pipe was to flow full, or for a particular allowable headwater depth, that is the usual design situation. The full flow condition would result in a smaller culvert size than the entrance control condition. An example of the possible reduction in culvert size that would result from the use of the hood inlet to insure full pipe flow will be shown subsequently.

The use of a smaller culvert flowing full will not necessarily mean that the exit velocity will be any greater than in the case of the larger pipe size with entrance control. Generally, the cross sectional areas occupied by the flow in each case will probably be the same. In the past, engineers in the writer's office have made the reasonable assumption that culverts with entrance con-

[a] May, 1960, by F. W. Blaisdell.

[11] Head, Hydr. Dept., Howard, Needles, Tamen and Bergendoff, New York, N. Y.

trol will flow two-thirds full at the exit and have placed rip-rap, stilling basins, and so forth, at culvert outlets based on this assumption.

In computing the headwater depth for culverts acting as orifices (entrance control condition), nomographs of the Bureau of Public Roads[12] have been used. These nomographs have been reproduced in two publications.[13,14]

In order to compute the head H over the invert of the culvert entrance for the full flow condition, the writer has simplified the Eqs. 4, 5, and 6 as follows:

$$H = H_t + D - S_o\, l \quad \text{(19a)}$$

in which

$$H_t = \left(1 - K_e\right) \frac{V_p{}^2}{2\,g} + \frac{184.5\, n^2\, l}{D^{4/3}}\, \frac{V_p{}^2}{2\,g} \quad \text{(19b)}$$

or

$$H_t = \frac{2.52\left(1 - K_e\right)}{D^4} + \frac{466.18\, n^2 l}{D^{16/3}}\, \frac{Q^2}{10} \quad \text{(19c)}$$

In deriving Eqs. 19a to c, the following simplifications and substitutions were made:

1. The term $\cos(\sin^{-1} S)$ has been completely dropped from Eq. 5b as being a neglible quantity.
2. $S_o l$ has been substituted for Z, where S_o is the slope of the culvert in ft per foot and l is the length of the culvert (not including the length of the hood).
3. Manning's roughness coefficient "n" has been substituted for the Weisbach friction factor "f."

In order to further simplify the computation of the head H over the culvert entrance, a nomograph is given in Fig. 16 that enables an immediate solution of Eq. 19c. In the solution of Eq. 19a, the reasonable assumption can also be made that the hydraulic gradient pierces the plane of the outlet end of the conduit at a distance above the invert equal to 0.75 times the diameter of the culvert (B = 0.75) that enables the complete solution of the head H over the invert of the culvert entrance.

Generally, the standard state highway department headwall is equal to the Headwall Type Anti-Vortex Wall shown in Fig. 8(e), so that no other special device to inhibit vortices seems necessary. However, the writer would appreciate more discussion by the author concerning the effectiveness of this type of anti-vortex device.

When a conduit flows full, it is usually a good idea for the designer to compute the subatmospheric pressure at the entrance of the conduit to make sure that it is not less than the vapor pressure or cavation that will occur at the

---

12 "Highway Drainage Manual," Bur. of Public Roads, Div. Two, Hagerstown, Md., July, 1953 (Preliminary).

13 "Highway Engineering Handbook," K. B. Wood, ed., McGraw-Hill Book Co. Inc., New York, N. Y., 1960.

14 "Design of Small Dams," Bur. of Reclam., Gov. Printing Off., Washington, D. C., 1960.

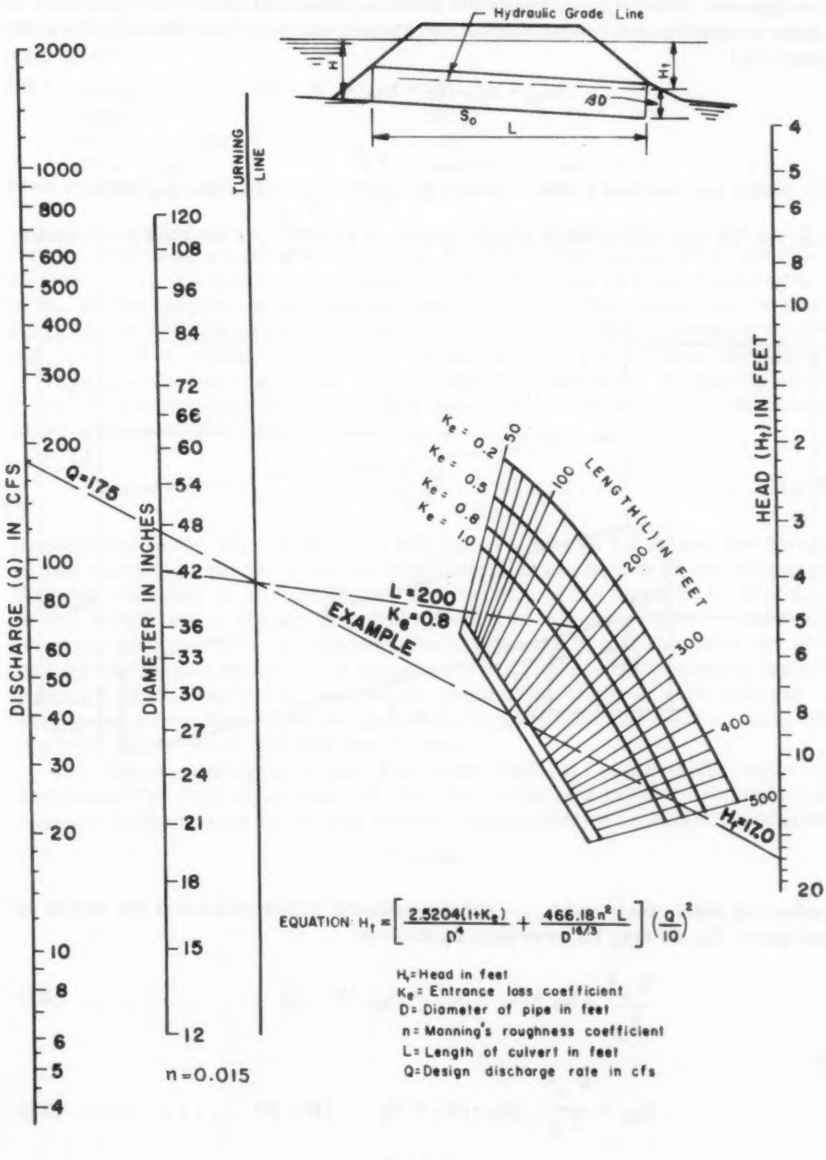
Hydraulic Grade Line
H
H_t
S_o
.8D
L
DISCHARGE (Q) IN CFS
2000
1000
800
600
500
400
300
200
100
80
60
50
40
30
20
10
8
6
5
4
Q=175
DIAMETER IN INCHES
120
108
96
84
72
66
60
54
48
42
36
33
30
27
24
21
18
15
12
n=0.015
TURNING LINE
L=200
K_e=0.8
EXAMPLE
K_e = 0.2
K_e = 0.5
K_e = 0.8
K_e = 1.0
LENGTH (L) IN FEET
50
100
200
300
400
500
H_t=17.0
HEAD (H_t) IN FEET
4
5
6
8
10
2
3
4
5
6
8
10
20
EQUATION: $H_t = \left[\frac{2.5204(1+K_e)}{D^4} + \frac{466.18 n^2 L}{D^{16/3}}\right]\left(\frac{Q}{10}\right)^2$
H_t= Head in feet
K_e= Entrance loss coefficient
D= Diameter of pipe in feet
n= Manning's roughness coefficient
L= Length of culvert in feet
Q=Design discharge rate in cfs

FIG. 16

pipe entrance. When the conduit entrance is of the re-entrant type, such as the hood inlet, the computation of the subatmospheric at the entrance should never be ignored. The actual computation of the pressure at the conduit entrance is quite simple once the head H at the entrance is known. From Fig. 17, it can be seen that

$$h_{vp} + h_e + h_r = h_{sa} + (H - D) \quad \ldots\ldots\ldots\ldots \quad (20)$$

in which h_e = entrance loss in feet = $K_e \dfrac{V_p{}^2}{2\,g}$; h_r = reduction in pressure head caused by the contraction at the entrance = $K_r \dfrac{V_p{}^2}{2\,g}$, in which K_r = pressure

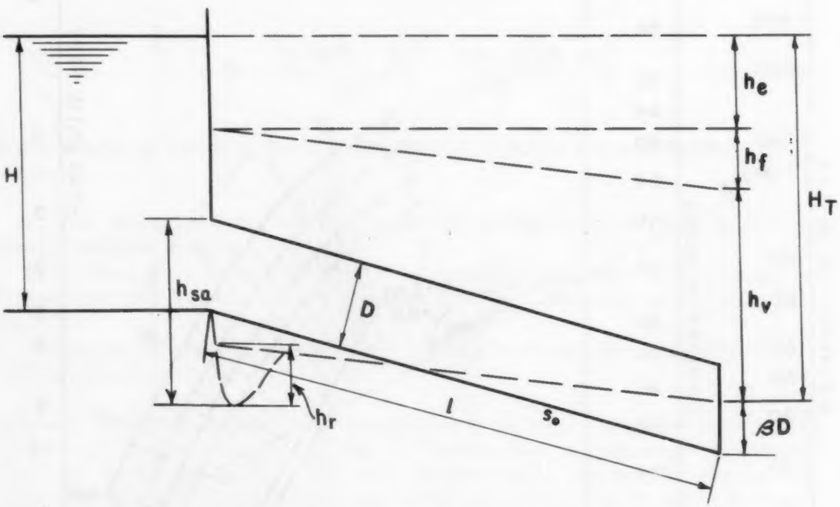

FIG. 17

reduction coefficient; and h_{sa} = subatmospheric pressure head at the crown of entrance. Eq. 20 may be rewritten as follows:

$$\frac{V_p{}^2}{2\,g}\left(K_e + K_v + K_r\right) = h_{sa}\,(H - D) \quad \ldots\ldots\ldots\ldots \quad (21)$$

or

$$h_{sa} = \frac{V_p{}^2}{2\,g}\left(K_e + K_v + K_r\right) - (H - D) \quad \ldots\ldots\ldots\ldots \quad (22)$$

For streamlined entrances, the pressure reduction coefficient K_r is quite low, but for the re-entrant type of entrance, the pressure reduction coefficient may

approach unity. Generally, a subatmospheric pressure of 25 ft at mean sea level is considered allowable in hydraulic design.

For purposes of comparsion between the sizes and costs of culverts arrived at under the two design assumptions, the typical field conditions are set forth as follows:

Design flow	175 cfs
Length	200 ft
Slope of culvert	6%
Pipe Type	Reinforced concrete (n = 0.015)
Maximum Allowable Headwater	8 ft

Full Flow Condition.—(Hood Inlet, $K_e = 0.8$) Substituting in Eqs. 19a and c, a 42 in. pipe flowing full will cause a head H = 7.9 ft over the invert of the culvert entrance. The exit velocity from the culvert will be 18.2 fps. Substituting in Eq. 22, the subatmospheric pressure at the crown of the culvert entrance is 9.0 ft that is well within the minimum subatmospheric of 25 ft allowed at mean sea level, if a pressure reduction coefficient $K_r = 0.8$ is used in design.

Entrance Control Condition.—(Square edged entrance) Eq. 23 may be used in lieu of a nomograph for orifice flow square edged concrete pipe entrances under low heads ($H > 1.0\ D$, $H < 3.0\ D$)

$$\frac{H}{D} = \frac{0.55\ Q}{D^{5/2}} - 0.60 \quad \ldots\ldots\ldots\ldots\ldots\ldots \text{(23)}$$

Substituting in Eq. 23, a 54 in. pipe will cause a head of 7.2 ft over the invert of the culvert entrance. If the depth of flow is assummed to be two-thirds of the pipe diameter at the outlet, the exit velocity of the flow will be 20.0 fps. In the northeastern states, the cost differential between a 42 in. reinforced concrete pipe and a 54 in. reinforced concrete pipe in place is about ten (10) dollars per ft, that would result in a savings of $2,000 in the preceding typical culvert installation. If the reasonable assumption of three such culverts in each mile of roadway is made, a cost saving of $6,000 per mile or $600,000 for each 100 miles of roadway would result.

The writer earnestly hopes that state highway departments will take cognizance of the advantages of the hood inlet as a culvert entrance, will sponsor further tests of it, and rapidly incorporate it into their standards.

ERRATA

Journal of the Hydraulics Division

Proceedings of the American Society of Civil Engineers

May, 1959

p. 31, 6 lines from bottom "Varwich" should be "Varwick"

p. 45, 12 lines from the bottom, the word "to" is omitted after "formula"

p. 45, 11 lines from the bottom, the symbol for Reynolds number should be R, not IR

p. 45, bottom line and page 64, IR should be R.

p. 46, Table I in headings, $R.10^{-3}$ should be $R.\ 10^{-3}$

p. 50, 6 lines above the Table, whole line should be omitted.

p. 66, "Chintu Lai" should be "Lai, Chintu"

CIVIL ENGINEERS

ERS FOR 196

PRESIDENT

GLENN W. HOLCOMBE

VICE-PRESIDENTS

Term expires October 1962:

LD H. ...TERN

...AM J. ...DLEY

DIRECTORS

Term expires October 1962:	Term expires October 1963:
... E. ...EBY	ROGER ... C...
... L. S. BA...ER	HENRY ... BUG...
... ... NILES	EARLE T. ANDREWS
... R. DAMES	JOHN B. SCALZI
WOODROW W. BAKER	JOHN D. WATSON
BERNHARD DORNBL...	HARMER E. DAVIS

PAST PRESIDENTS

Members of the Board

...A. FIDDLER...

TREASURER

... CHANDLER

ASSISTANT TREASURER

... E. ...

OFFICERS OF THE SOCIETY

...A. ... Editor of Technical Publications

...N J. SCHWARTZ ... Editor of Technical Publications

COMMITTEE ON PUBLICATIONS

... NILES, Chairman

...RA, Vice-Chairman

J... WATSON

...MES, ...

PART 2

NOVEMBER 1960 — 39 NO. HY 9
VOLUME 86 PART 2

Your attention is invited

NEWS OF THE HYDRAULICS DIVISION OF ASCE

AMERICAN SOCIETY OF CIVIL ENGINEERS
FOUNDED 1852

JOURNAL OF THE HYDRAULICS DIVISION
PROCEEDINGS OF THE AMERICAN SOCIETY OF CIVIL ENGINEERS

DIVISION ACTIVITIES
HYDRAULICS DIVISION
Proceedings of the American Society of Civil Engineers

NEWS

November, 1960

THE PURPOSE OF THE HYDRAULICS DIVISION

"The advancement and dissemination of scientific and engineering knowledge in all branches of hydraulics, hydrology, hydraulic engineering and water resources. In particular this shall embrace meteorology and hydrology as the sciences dealing with the occurrence of water in the atmosphere, on the earth surface and in the ground, fluid mechanics for the understanding of all flow phenomena, applied hydraulics for the design and planning of hydraulic structures and of comprehensive systems, and those social, economic and administrative aspects basic to the conservation and utilization of water as an essential natural resource."

COMMITTEES

This is the time of year when senior members retire, new members are added, and new chairmen take over. The memberships of the various committees of the Division will be somewhat as follows for the 1960-61 Society Year.

Executive Committee

M. L. Dickinson, Chairman
E. P. Fortson, Jr., Vice-chairman
A. T. Ippen
H. S. Riesbol, new member
Arno T. Lenz, Secretary

Publications Committee

Wallace M. Lansford, Chairman
James Smallshaw
Maurice L. Dickinson
Arno T. Lenz

Newsletter Editor

Fred A. Bertle

Water Resources Coordinator

Herbert S. Riesbol

J. C. Stevens Award

Jacob H. Douma, Chairman
Victor L. Streeter
S. K. Jackson, new member

Note.—No. 1960-39 is part 2 of the copyrighted Journal of the Hydraulics Division, Proceedings of the American Society of Civil Engineers, Vol. 86, No. HY 9, November, 1960.

Karl Emil Hilgard Hydraulic Prize

William E. Hiatt, Chairman
Joseph W. Howe
Joseph N. Bradley

Research

Clarence F. Wicker, Chairman
Vito A. Vanoni
Walter B. Langbein
Jacob H. Douma
Harold M. Martin, new member

Sessions Programs

Eugene P. Fortson, Jr.
Herbert S. Riesbol
Francis G. Christian
Norman H. Brooks
Harold K. Pratt
Robert B. Banks
Irvin M. Ingerson
Albert S. Fry
Roy K. Linsley, Jr.
H. Alden Foster
David K. Todd

Standards

Norbert Leupold
Frank B. Campbell
Carl E. Kindsvater, new member

Flood Control

Francis G. Christian, Chairman	1962
Joseph I. Perrey, term extended	1961
Arthur R. Luecker	1963
Walter G. Schulz	1964
Max L. Mitchell, new member	1965

Ground Water Hydrology

David K. Todd, Chariman
Paul Baumann
William Guyton
M. I. Rorabaugh
Harris McDonald

Hydraulic Structures

Harold K. Pratt, Chairman
Alvin J. Peterka
Rex A. Elder
Marvin J. Webster
Clifford H. McConnell, new member

Hydromechanics

Norman H. Brooks, Chairman
Emmett M. Laursen
Frederick R. Brown
W. Douglas Baines
E. Roy Tinney, new member

Hydrometeorology

Ray K. Linsley, Chairman
G. Earl Harbeck, Jr.
William E. Hiatt
Arvi O. Waananen
W. J. Roberts, new member

Sedimentation

Robert B. Banks, Chairman
Enos J. Carlson
Paul C. Benedict
Peter S. Eagleson
A. S. Harrison, new member

Surface Water Hydrology

H. Allen Foster, Chairman
William C. Ackermann
Stifel W. Jens
Victor A. Koelzer
Charles C. McDonald

Tidal Hydraulics

Irvin M. Ingerson, Chairman
Lindsay P. Disney, term extended
Raymond Boucher
Charles L. Bretschneider
C. P. Lindner, new member

Water Resources Planning

Albert S. Fry
R. L. Smith
Harold E. Hedger
Gordon Williams
Edward Kniper

The technical committees have many active task forces. New task forces are formed as the need arises, and old ones are dismissed as they complete their missions.

A new task force on Salt Water Intrusion (in ground-water aquifiers) has been formed under the Ground Water Hydrology Committee. Membership is to be determined.

Executive Committee Meets

The meeting of the Executive Committee was held on forenoons of Thursday, Friday, and Saturday, August 18, 19, and 20, 1960. The Committee Chairman, Professor Arthur T. Ippen, presided. Those in attendance were:

Dr. Arthur T. Ippen, Chairman
Mr. Maurice L. Dickinson, Vice-chairman
Professor Carl E. Kindsvater
Mr. Eugene P. Fortson, Jr.
Mr. Herbert S. Riesbol, Water Resources Coordinator
Mr. Samuel S. Baxter
Mr. Harold M. Martin, Secretary
Mr. Don P. Reynolds, Assistant Secretary, ASCE

The following are excerpts from the minutes of this meeting:

Adminsitrative Committees

Publications. Chairman W. M. Lansford gave an oral report to the Executive Committee. Some 50 papers have been received this year and 10 or more declined. A composite rating of seven is required for publication in the Journal. It is the feeling of the Executive Committee that rating of papers by more than three reviewers is desirable in order that adequate and fair rating may be measured; also, that the chairman of the committee on publications should receive all reviews, and assess them before sending them on the Manager of Publications.

Research. Dr. Vito A. Vanoni, Chairman, reviewed the minutes of the Washington, D. C. April 25-26, 1960 meeting of the Committee which summed up the activities and program of the past 4 years. The Committee is preparing an outline of eight typical basic research projects which may serve as examples of the kind of research which the Committee feels should be undertaken by civil engineers.

One important action favored by the Committee is to raise the annual dues of the Society about $5 and to reserve these additional funds for increasing research activities. Such serious action on the part of the civil engineering profession would indicate to the public and to prospective sponsors that research is important in the eyes of those most intimately acquainted with recent needs. The effect of this would be to increase the availability of funds for research from both public and private sources.

This and other conclusions and recommendations were endorsed by the Executive Committee with the request that Dr. Vanoni prepare the report of the Hydraulics Division Committee on Research for reproduction in order that the Executive Committee may recommend it to the Society Committee on Research. Furthermore, the report will be sent to all other Society Division

Research Committees; will be presented for publication in Civil Engineering; comments will again be requested from the Society Committee on Research.

The question whether the Hydraulics Division Committee on Research should review and endorse research proposals was discussed. It was agreed that it should for the technical aspects in assistance to the Society Research Committee. It can also advise an applicant on preparing proposals.

Sessions Programs. The Committee prepared Hydraulics Division programs for the following conventions held during the year 1960:

New Orleans	3 sessions--11 papers
Reno	3 sessions-- 9 papers
Seattle Conference	6 sessions--23 papers
Boston	5 sessions--18 papers

Number of Sessions Proposed for 1961 Meetings
(Sponsor shown in parenthesis)

Committee	Phoenix 10-15 April	Urbana 16-18 August	New York 16-20 October
The Five Committees on Water Resources	2-1/2 (Riesbol) *	3 (Riesbol)	None
Hydraulic Structures	1 (Elder)	1 (Webster)	1 (Peterka)
Sedimentation	1 (Carlson)	1 (Eagleson)	1
Hydromechanics		1 (Baines)	2 (Laursen)
Tidal Hydraulics	None		1 (Bretschneider)
Totals	4-1/2	6	5

Report on Water Resources Activities of Hydraulic Division. Herbert S. Riesbol, Water Resources Coordinator, presented a brief report on activities of the five water resources committees of the Hydraulics Division during the past year. Four of the committees were activated during the year while the Committee on Flood Control had been active and productive for many years.

The committees on hydrometeorology, ground water hydrology, and surface water hydrology were activated in late January while the Committee on Water Resources Planning was authorized in late March. The Committee on Ground Water Hydrology met in Denver with the Water Resources Coordinator on February 19-20, and the Committees on Hydrometeorology and Surface Water Hydrology, and the Chairman of the Committee on Flood Control met with the Coordinator in Chicago, Illinois, on April 21 and 22. The Committee on Flood Control held a meeting in Seattle on August 18 during the Hydraulics Division Conference. With the exception of the Committee on Water Resources Planning, which got off to a late start, all the committees have been very active during the year in the planning and execution of their activities. As a result, the following recommendations were approved by the Executive Committee:

1. The following six-point outline of committee functions was approved:

   a. To seek out oan encourage the presentation of papers pertinent to all phases of objectives and purpose.

   b. To seek out areas of needed research and to promote and encourage the initiation and conduct of such research.

c. To review and appraise on a continuing basis the availability of basic data in meteorology and hydrology and related physical data, as needed for the long-range planning of water resource development.
d. To review and appraise standards of data compilation, analysis, publication and distribution in terms of technical adequacy and uniformity.
e. To review and appraise standards of project design and to state recommended standards on the basis of safety, dependability, and economic feasibility.
f. To focus the attention of the profession on water resources problems and bring them to the attention of the Society.

2. The new emphasis on water resources in the organizational structure of ASCE should enable the Society to become the dominant professional organization dealing with water resources in the United States. This would quite properly focus attention on civil engineers as the professional leaders in this important area of national development.
3. The ASCE policy and program for publication of papers should be carefully reexamined as it relates to water resources to be certain that it is designed to give best service to the profession.
4. The water resources committees will sponsor 2-1/2 sessions at the Phoenix Convention, April 10-14, 1961. This was a reduction from the four sessions originally proposed by the water resources committees.
5. The committees will not sponsor sessions at the New York Convention (October 16-20, 1961).
6. The water resources committees will sponsor three sessions (9 to 12 papers) at the Hydraulics Division conference to be held in Urbana, Illinois, in August 1961.
7. The Task Force on Spillway Design Floods will complete its assignment as a task force of the Committee on Surface Water Hydrology. Mr. Joseph Paulus will represent the Committee on Hydrometeorology on this task force.
8. The Committee on Ground Water Hydrology will establish a Task Force on Salt Water Intrusion. The Task Force will carry out such activities as will enable it:

a. To be aware of the status of salt water intrusion in the United States.
b. To recognize sources and causes of intrusion.
c. To analyze methods for control of intrusion.
d. To keep abreast of an encourage research on intrusion.
e. To encourage presentation of papers relating to intrusion at society meetings.

9. The five water resources Committees will, if possible, hold a joint meeting in Chicago during the same week that the Executive Committee meets.

Future Hydraulic Division Conferences. The Hydraulics Division has been invited to have its 1961 conference (Tenth National Conference) at Champaign-Urbana, Illinois, August 16, 17, 18, 1961. Host will be the Central Illinois Section, ASCE, and the University of Illinois. Mr. W. J. Roberts, representing the Illinois local committee, made announcements for the 1961 conference at the Seattle meeting.

The Eleventh Conference was tentatively schedulted for Sacramento, California, in 1962, since the Sacramento Section issued an invitation 2 years ago.

Hydraulics Division Conference. University of Washington, Seattle, August 17-19, 1960, had a registration of over 200; in addition, approximately 50 women and young people attended.

The local committee arranged excellent housing facilities and the social program was unusually attractive. Two busloads took advantage of the preconvention Skagit tour. The banquet was well attended, and the program was interesting.

Lecture Tour. Engineers Joint Council is sponsoring a lectureship financed by the National Science Foundation. Dr. Thijsse of Delft, Holland, has been approached to determine whether he would be available in view of the limited funds available. Dr. Ippen will firm up an itinerary if Dr. Thijsse is willing to come and will supervise this project next year.

Note by Retiring Secretary. After 6 years' service on the Executive Committee, 2 years as Secretary, Harold M. Martin is to retire at the end of this Society year. He greatly appreciates the opportunity he has had for service to the Society and the pleasant relationship with so many in the profession during this experience in the Hydraulics Division.

Phoenix Meeting

Early correspondence indicates that sessions of extreme interest to the hydraulic engineer are being planned for this meeting. Better plan to go South in April. More about this in subsequent issues of the Newsletter.

The following news item comes from the Hydraulics Division of the Colorado Section. No doubt other sections have similar activities which would be of interest to members of the Hydraulics Division. We always welcome news from the local sections.

Colorado Hydraulic Division Activities

Officers elected for the 1960-61 year are:

Chairman	Claude R. Hunter (Soil Conservation Service)
Vice-chairman	W. P. Simmons, Jr. (Bureau of Reclammation)
Secretary-treasurer	Kenneth R. Wright (Wheeler and Wright Consultants)

Meetings are held regularly in the Denver Public Library Building on the 4th Thursday of every month, September through May at 7:30 p. m. Illustrated talks are presented by men prominent in engineering fields related to, or of interest to, the membership. The schedule of programs outlined at a recent planning meeting of the officers is studded with interesting speakers and subjects, and is expected to draw capacity crowds.

For Your Calendar

ASCE Meetings

April 10-14, 1961	ASCE, Phoenix Convention
August 16-18, 1961	Hydraulics Division Conference, Urbana, Illinois
October 16-20, 1961	ASCE, New York Convention
February 1962	ASCE, Houston Convention
May 1962	ASCE, Omaha Convention
October 15-19, 1962	ASCE, Detroit Convention

Non-ASCE Meetings

October 29-November 2, 1960	Annual Meeting Geological Society of America, Division of Engineering Geology, Denver, Colorado
June 26-July 2, 1961	Seventh Congress International Committee on Large Dams, Rome, Italy
September 3-7, 1961	Ninth IAHR Convention, Belgrade, Yugoslavia
September 6-8, 1961	Seventh Midwestern Conference on Fluid Mechanics and Soil Mechanics, Michigan State University, East Lansing, Michigan
June 18-21, 1962	Fourth National Congress of Applied Mechanics, University of California, Berkeley, California

Much credit for the success of the Newsletter the past year is due to you who contributed timely news items and to the promptness of the Executive Committee and other committee members in furnishing pertinent information on Hydraulics Division participation at ASCE Conventions. Your editor for 1960 expresses deep appreciation for the many timely items furnished, for these make the Newsletter worthwhile and lighten the workload of the editor.

James W. Ball

Use of the Hydraulics Division Newsletter

You are urged to use the Division Newsletter for announcements, inquiries, personnel news, committee reports, surveys and other items of interest to Division members. A short note summarizing the highlights of committee meetings is particularly requested. Suggestions for improvement of the Newsletter will be appreciated. All contributions are appreciated.

Deadline dates for Newsletter contributions: January 1961 issue--November 20; March 1961 issue--January 20.

Please direct all future contributions to your new Editor.

Mr. Fred A. Bertle
4475 Carr Street
Wheatridge, Colorado

NEW DIRECTORY IS AVAILABLE TO MEMBERS

The 1960 Directory is now available to members on request. The Directory lists the entire membership of the Society, giving the membership grade, position, and mailing address of each. In addition, there is a complete listing of the Honorary Members, past and present, and the Life Members. A useful geographical listing of the members is also included.

It goes without saying that the information contained in the Directory is of value to every member, and every member can obtain this valuable information. To receive your free copy of the Directory simply fill out the coupon below. Prompt delivery depends on prompt return of the coupon.

The Society publishes the membership Directory every other year. The next edition will be issued in 1962.

DIRECTORY 1960

ASCE members are entitled to receive, free of charge, the 1960 ASCE Directory. To obtain the directory simply clip this coupon and mail to: American Society of Civil Engineers, 33 West 39th Street, New York 18, N. Y.

Please make the mailing label legible—correct delivery depends on you.

------------------------------CUT HERE------------------------------

Print Name

Address

City Zone State

1960-Dir.

ASCE-WPCF JOINT SEWER MANUAL ISSUED

A major addition to the ASCE series of Manuals of Engineering Pracitice is now available in a new volume entitled "Design and Construction of Sanitary and Storm Sewers." Identified as No. 37, this publication is the result of serveral years of joint effort by the Sanitary Engineering Division of ASCE and the Water Pollution Control Federation (formerly the Federation of Sewage and Industrial Wastes Associations).

The twelve-chapter sewer manual contains 283 pages, over 100 illustrations, 24 tables, and more than 100 references. As the first extended collection of information on the subject, it will make a valuable reference in an important phase of wastewater technology. Individual subjects covered include organization and administration of sewer projects, surveys and investigations, quantity of sanitary sewage and storm water, hydraulics of sewers, design of sewer systems, appurtenances and special structures, materials for sewer construction, structural requirements, construction plans and specifications, construction methods, and pumping stations.

The manual may be ordered with the coupon herewith. The list price is $7.00 per copy. However, ASCE members may order the manual for $3.50

per copy. The price to members of the Water Pollution Control Federation is the same upon application to their organization.

-----------------------------CUT HERE-----------------------------

American Society of Civil Engineers
33 West 39th Street,
New York 18, N. Y.

Please send me . . . . . . copy(s) of Manual 37. Enclosed is my remittance of $. . . . . . My ASCE membership grade is . . . . . . List price: $7.00.

Print Name

Address

City Zone State

. . . of M37

[illegible]